Title
Sources, Physicochemical Transformations, and Inhalation Exposures of Indoor Organic Chemicals

Author
Lunderberg, David Matthew

Publication Date
2022

Peer reviewed|Thesis/dissertation

Sources, Physicochemical Transformations, and Inhalation Exposures of Indoor Organic Chemicals

by

David Matthew Lunderberg

A dissertation submitted in partial satisfaction of the

requirements for the degree of

Doctor of Philosophy

in

Chemistry

in the

Graduate Division

of the

University of California, Berkeley

Committee in charge:

Professor Allen H. Goldstein, Co-chair
Professor Ronald C. Cohen, Co-chair
Professor Evan R. Williams
Professor John R. Balmes

Summer 2022

Sources, Physicochemical Transformations, and Inhalation Exposures of Indoor Organic Chemicals

Abstract

Sources, Physicochemical Transformations, and Inhalation Exposures
of Indoor Organic Chemicals

by

David Matthew Lunderberg

Doctor of Philosophy in Chemistry

University of California, Berkeley

Professor Allen H. Goldstein, Co-chair

Professor Ronald C. Cohen, Co-chair

Modern human populations spend ∼90% of their time indoors. Moreover, concentrations of well-studied organic chemicals in indoor air are often orders of magnitude higher than equivalent outdoor concentrations. Considering that airborne organic pollutants can impact human and environmental health, it is critical to understand the sources, physicochemical behavior and modes of exposure of airborne organic chemicals in the indoor environment. This dissertation improves scientific understanding of these topics via analysis of time-resolved measurements of organic pollutants acquired in three normally-occupied residences and test houses over several months.

Until recently, researchers have largely used offline measurement approaches to study indoor air quality. Time-averaged samples are collected over a period spanning hours to weeks and then returned to the laboratory for subsequent analysis. While this approach is well-suited for survey-based analyses where pollutant concentrations are measured at many different sampling sites, the limited time-resolution inhibits study of dynamic processes that influence indoor air quality. Recent advances in instrumentation permit continuous monitoring of airborne organic chemicals with high chemical specificity on minute-by-minute and hourly time-scales over extended observation periods. This dissertation reports key findings from several months of time-resolved measurements of volatile organic compounds (VOCs) as measured by proton-transfer reaction time-of-flight mass spectrometry (PTR-ToF-MS) and semivolatile organic compounds (SVOCs) as measured by semivolatile thermal desorption aerosol gas chromatography in two normally-occupied residences (H1, H2) and a test house with scripted experiments (HOMEChem).

In Chapter 2, time-varying concentrations and gas-particle phase partitioning of phthalate diesters, a class of compounds of public-health interest, are reported at the H2 site. The

dynamic behavior of four reported phthalates is observed to be related to their vapor pressure and physicochemical parameters such as temperature and particle mass concentration. These findings are generalized in Chapter 3 where it is suggested that volatility-dependent partitioning processes are the principle drivers of SVOC dynamic behavior. As part of this analysis, observations are connected to a theoretical model that assumes kinetic equilibrium with organic surface films commonly found indoors. Furthermore, it is observed that certain SVOCs can be deposited on surfaces during large emission events and then re-emitted into bulk air during future particle-emission events. In these scenarios, particles were inferred to enhance mass transport from condensed-phase reservoirs to bulk air. A high-resolution exposure assessment is conducted for VOCs in Chapters 4 and 5. Source apportionment analysis, a risk-based prioritization analyses and experimental estimates of intake fractions are reported for >200 VOCs. In contrast to expectations, a key finding suggests that for most VOCs, time-averaged exposure are attributable to the building and its static contents rather than episodic emission-events like cooking related to occupants or outdoor-to-indoor transport.

Contents

List of Figures

List of Tables

Acknowledgments

In any challenging endeavor, particularly one that approaches half a decade in span, one accrues an inordinate amount of debt towards those who have provided the guidance, support, and camaraderie that make the endeavor possible. This case is no exception.

I am deeply grateful to my advisor, Dr. Allen Goldstein. When we first met, you mentioned that your research lab was quite full and that you were not expecting to add additional students. Still, you kindly offered to meet and give general advice about atmospheric chemistry at Berkeley. Thank you for somehow including a five-year dissertation, four field-based research campaigns, and thousands of miles of travel under the scope of "general advice." The voyage has been challenging, rewarding, and fun. I am also deeply grateful to Dr. William Nazaroff. Your guidance always suggested paths towards a higher standard of scholarship and I took great joy in observing the difference in quality between the first and final manuscript drafts after responding to your reviews. Thank you for your substantial feedback, both specific and general, about the scientific research process. I also need to thank my undergraduate research mentors, Drs. Graham Peaslee and Paul DeYoung. It is a rare week that an adage, aphorism, or anecdote from you about the research process fails to cross my mind.

I also extend thanks to the members of the H2, HOMEChem, and H3 research teams. Kasper, Becca, Caleb, Yilin, and Yingjun, I greatly appreciated learning from you in the research lab, out in the field, and during research meetings (even when research meetings extended well past their allotted time, a tradition we have continued). Thank you Kasper for providing the base of my hands-on scientific training at Berkeley. And thank you Caleb for your unparalleled culinary palate (and culinary deliveries), particularly when the tribulations of field-research stretched into the wee hours of the Texan night. Thank you to Nathan K. and Becca for your help with TAG and not marking my number and email address as "spam." And concerning the PTR-quad, thank you to Nathan S. for your unbridled enthusiasm when working together and to Eva for your help and wisdom. Dr. Brett Singer, Caleb, Betty, Jennifer, and Erin, I'm glad we were able to work together on the H3 campaign. Thank you to Robin for never failing to give wisdom and help whenever I knocked on your door. Thank you to the rest of the Goldstein research group, past and present, including Arthur, Coty, Deep, Ellyn, Emily, Jeremy, Lindsay, Michael, Mike, and Yutong. And thank you to all co-authors and collaborators. It has been good.

I thank my graduate cohort, including Bryan, Abdul, and Jonathan for suggesting great places to eat. I thank Rolando, Mike, Ryan, and David – it was a pleasure living with and learning from you. I thank Jess for trekking to redwood groves, traversing ragged granite, and teetering on the edges of river gorges with me across the Bay, the Sierra, and beyond. Finally, thank you to my parents, Jon and Marla, and to my siblings, Mark, Eric, and Anna, for decades of fun dinner table conversations about the world we live in.

The data ***is*** in. This work would not have been possible without those mentioned above, among countless others unnamed but not forgotten. I have much for which to be grateful.

Chapter 1

Introduction

1.1 Motivation

The average American is expected to spend roughly 90% of his or her lifespan, more than 70 years, indoors.[1] Considering that releases of pollutants indoors are often up to 1,000× more impactful to human exposures than equivalent outdoor releases (Figure 1.1.1), it is critical to understand the physical and chemical processes controlling airborne concentrations of indoor pollutants.[2] What are the principal sources of organic chemicals in indoor air? How long do emitted chemicals persist and what are the dominant removal mechanisms? What fraction of these chemical emissions enter into a person's lungs and are these exposures important for health? This dissertation considers gas- and particle-phase concentrations of semivolatile organic compounds (SVOCs) and volatile organic compounds (VOCs) in indoor air to answer these questions.

1.1.1 What are SVOCs?

Exact definitions vary, but SVOCs can be roughly defined as organic chemicals with boiling points between 240 and 400 °C.[3] SVOCs constitute a diverse class of organic compounds presenting diverse indoor dynamic behavior, and can be found in dust, surface films, airborne particles, and the gas phase. The dynamic behavior of indoor SVOCs is expected to be influenced by chemical- and volatility-dependent partitioning between these reservoirs. SVOCs in the indoor environment originate from static indoor sources, episodic source events related to occupant activity, outdoor-to-indoor transport, and chemical transformations. Many indoor SVOCs are of relevant health interest[4] and exposure to particulate matter, composed in part by SVOCs, is one of the world's leading mortality risk factors, causing >4 million premature deaths in 2015.[5]

Airborne SVOCs may be observed indoors for months and even years after original source events as SVOCs partition onto indoor surfaces.[6] Some SVOCs such as pentachlorophenol (PCP), dichlorodiphenyltrichloroethane, (DDT), polychlorinated biphenyls (PCPs), certain

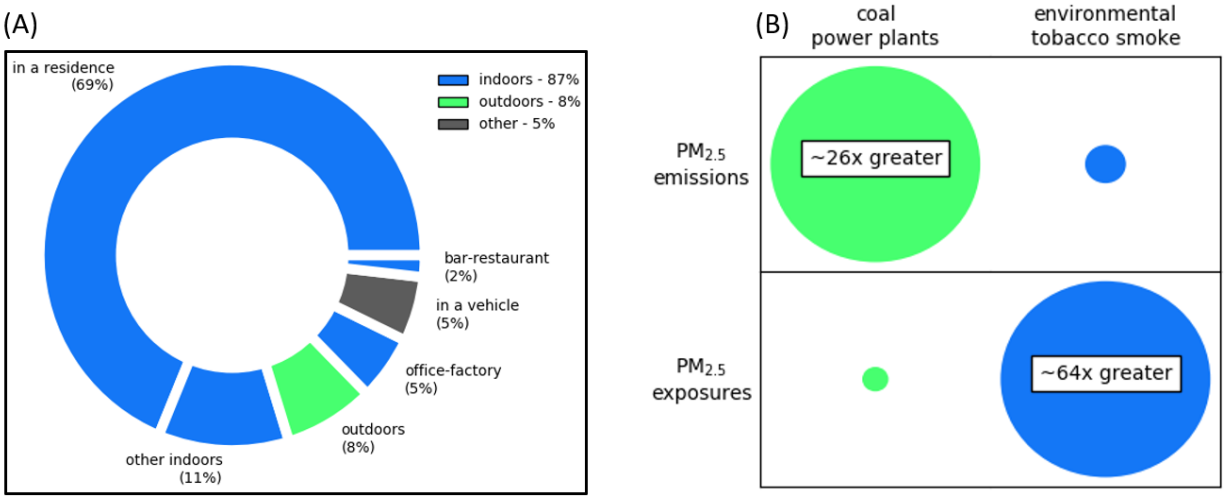

Figure 1.1.1: In Panel A, time-activity patterns as reported by Klepeis et al. (2001) are presented.[1] In Panel B, emissions and exposure data for particle concentrations as reported by Smith (1988) are presented.[2] Estimated particle emissions from coal power plants are >26 times greater than particle emissions from environmental tobacco smoke. In contrast, estimated population-level exposures to particles are >64 times greater for environmental tobacoo smoke than for coal power plants. These values roughly conform to the "Rule of 1,000" where indoor pollutant releases are ∼1000 times more likely to be inhaled than equivalent outdoor releases.

flame retardants, and certain perfluoroalkyl substances are legacy compounds that have not been used for decades and are still commonly found in indoor air.[4, 5, 8, 9]

1.1.2 What are VOCs?

VOCs are higher in vapor pressure than SVOCs and can similarly be roughly defined as organic chemicals with boiling points between 50 and 240 °C.[3] Thousands of VOCs have been observed indoors, each attributable to unique source profiles which include static indoor sources such as building materials or furnishings,[10] episodic activities such as cooking,[11, 12] outdoor-to-indoor transport,[13] and indoor chemistry.[14] The relative contributions from each source are not well understood for most VOCs in most buildings. VOC concentrations are modulated by physicochemical parameters such as the ventilation rate,[15] temperature (via interactions with condensed-phase reservoirs[16] and temperature-dependent emissions from building materials[12]), and humidity.[17] Unlike SVOCs, airborne VOCs are generally expected to be found in the gas phase. Exposures to many specific VOCs are associated with adverse health outcomes, including impaired cognitive function, asthma, and cancer.[18–22]

1.1.3 Knowledge Gaps and Opportunities

Historically, time-averaged measurements have been used in studies of VOCs and SVOCs in indoor air.[4, 7, 13] Under these study designs, indoor air is captured on filters or sorbent tubes and returned to the lab for subsequent analysis, often by gas chromatography mass spectrometry. These analytical methods yield concentration measurements with high chemical specificity and low temporal resolution, limited by practical limitations of sampling. The methods are often applied in survey-based study designs where time-averaged measurements of indoor air are acquired over sampling periods ranging from hours to weeks at singular locations in hundreds of buildings. While these study design can be used to understand pollutant concentrations at the population-level, they are not well suited to studying indoor dynamic processes.

Advancements in available analytical instrumentation now permit time-resolved measurements with high chemical specificity over extended monitoring periods. Chemical-ionization mass spectrometers can be used to quantify VOCs on timescales of seconds to minutes. Online thermal-desorption mass spectrometers can be used to quantify SVOCs on timescales of tens of minutes. When applied to singular residences, it is now possible to report time-resolved measurements of hundreds of unique chemicals in air at multiple locations. Together, these advancements in analytical capabilities can be used to study the many dynamic processes that occur indoors.

1.2 Methods

This dissertation interprets measurements of indoor air quality gathered at three separate locations. Measurements were collected at two normally occupied California residences, designated H1 and H2.[23, 24] At H1, measurements were collected in both the summer (∼10 weeks) and winter (∼5 weeks) seasons. At H2, measurements were collected in the winter season (∼10 weeks). Both residences are wood-framed single-family homes constructed in the first half of the 20th century. Two regular occupants were present at the H1 site and three regular occupants were present at the H2 site. A third monitoring campaign was conducted at the UTest House during the HOMEChem campaign in Austin Texas.[25] At HOMEChem, researchers conducted a series of controlled experiments simulating typical household events such as cooking and cleaning.

At each location, the composition of indoor and outdoor air was analyzed (Figure 1.2.1). Concentrations of VOCs were monitored in six different locations every 30 minutes as quantified by proton-transfer reaction time-of-flight mass spectrometry (PTR-ToF-MS).[23] The PTR-ToF-MS measurement cycle dedicated 5-minutes to each location with the first few minutes excluded to allow for sampling line equilibration. Concentrations of two key oxidative species, ozone and nitrate, were also quantified via spectroscopic methods. Particle concentrations were quantified by an ultraviolet aerodynamic particle sizer (UV-APS) and a series of optical particle counters (OPCs). Inert tracer gases were intentionally released

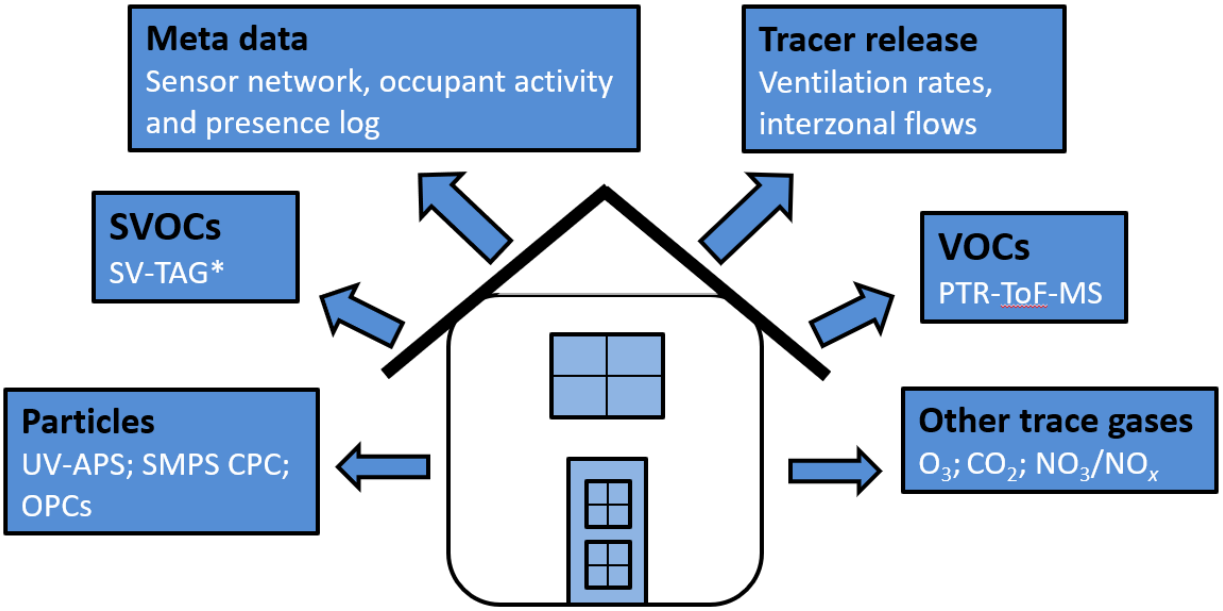

Figure 1.2.1: Experimental study design during residential monitoring campaigns

throughout the residences to estimate the ventilation rates and intrazonal mixing flow. A network of >50 wireless sensors was used to evaluate temperature, humidity, occupant activity, appliance-usage, and door and window position throughout each residence or test house.

During the H2 winter campaign, additional measurements were collected. Concentrations of indoor SVOCs were quantified every hour by semivolatile thermal desorption aerosol gas chromatography (SV-TAG). Concentrations of outdoor SVOCs, indoor gas-particle phase partitioning, and outdoor gas-particle partitioning were also quantified every four hours by SV-TAG.[24] A scanning mobility particle sizer was used to measure particle size distributions of fine-mode particles. During the HOMEChem campaign, additional measurements of indoor air quality were collected by >13 collaborating research groups.[25]

1.3 Map

This dissertation is divided into two parts. The first half of the dissertation investigates the physicochemical behavior of SVOCs. In Chapter 2, concentration and gas-particle partitioning data of four phthalate diesters at the H2 site are presented as an initial case study. Findings from the phthalate case study are generalized in Chapter 3, where SVOC concentrations from H2 are aggregated into bins defined by volatility and then compared against physicochemical parameters including temperature and particle mass. Additional study of phthalate diesters and cyclic siloxanes observed during the HOMEChem campaign are used

to support findings from the H2 campaign, namely that SVOCs interact with surfaces in a volatility-dependent manner.

The second half of the dissertation investigates human exposure to VOCs using time-resolved concentration and activity data collected during the H1 summer, H1 winter, and H2 winter monitoring campaigns. In Chapter 4, a source-apportionment analysis and risk-based prioritization are presented for exposures to >200 VOCs at the H1 summer, H1 winter, and H2 winter campaigns. In Chapter 5, experimental estimates of inhalation intake fractions are presented for individual occupants during the same monitoring periods. In Chapter 6, key results are summarized and suggestions for future research are presented.

1.4 References

[1] Klepeis, N. E.; Nelson, W. C.; Ott, W. R.; Robinson, J. P.; Tsang, A. M.; Switzer, P.; Behar, J. V.; Hern, S. C.; Engelmann, W. H. The National Human Activity Pattern Survey (NHAPS): a resource for assessing exposure to environmental pollutants. *J. Expo. Anal. Environ. Epidemiol.* **2001**, *11*, 231–252.

[2] Smith, K. R. Fuel Combustion, Air Pollution Exposure, and Health: The Situation in Developing Countries. *Annu. Rev. Energy Environ.* **1993**, *18*, 529–566.

[3] USEPA. Technical Overview of Volatile Organic Compounds. USEPA. https://www.epa.gov/indoor-air-quality-iaq/technical-overview-volatile-organic-compounds (accessed 2022-05)

[4] Rudel, R. A.; Camann, D. E.; Spengler, J. D.; Korn, L. R.; Brody, J. G. Phthalates, alkylphenols, pesticides, polybrominated diphenyl ethers, and other endocrine-disrupting compounds in indoor air and dust. *Environ. Sci. Technol.* **2003**, *37*, 4543–4553.

[5] Cohen, A. J.; Brauer, M.; Burnett, R.; Anderson, H. R.; Frostad, J.; Estep, K.; Balakrishnan, K.; Brunekreef, B.; Dandona, L.; Dandona, R.; Feigin, V.; Freedman, G.; Hubbell, B.; Jobling, A.; Kan, H.; Knibbs, L.; Liu, Y.; Martin, R.; Morawska, L.; Pope III, C. A.; Shin, H.; Straif, K.; Shaddick, G.; Thomas, M.; van Dingenen, R.; van Donkelaar, A.; Vos, T.; Murray, C. J. L.; Forouzanfar, M. H. Estimates and 25-year trends of the global burden of disease attributable to ambient air pollution: an analysis of data from the Global Burden of Diseases Study 2015. *Lancet* **2017**, *389*, 1907–1918.

[6] Weschler, C. J.; Nazaroff, W. W. Semivolatile organic compounds in indoor environments. *Atmos. Environ.* **2008**, *42*, 9018–9040.

[7] Rudel, R. A.; Perovich, L. J. Endocrine disrupting chemicals in indoor and outdoor air. *Atmos. Environ.* **2009**, *43*, 170–181.

[8] Weschler, C. J. Changes in indoor pollutants since the 1950s. *Atmos. Environ.* **2009**, *43*, 153-169.

[9] Blanchard, O.; Glorennec, P.; Mercier, F.; Bonvallot, N.; Chevrier, C.; Ramalho, O.; Mandin, C.; Bot, B. L. Semivolatile organic compounds in indoor air and settled dust in 30 French dwellings. *Environ. Sci. Technol.* **2014**, *48*, 3959–3969.

[10] Wolkoff, P. How to measure and evaluate volatile organic compound emissions from building products. *A perspective. Sci. Total Environ.* **1999**, *227*, 197–213.

[11] Farmer, D. K.; Vance, M. E.; Abbatt, J. P. D.; Abeleira, A.; Alves, M. R.; Arata, C.; Boedicker, E.; Bourne, S.; Cardoso-Saldana, F.; Corsi, R.; DeCarlo, P. F.; Goldstein, A. H.; Grassian, V. H.; Hildebrandt Ruiz, L.; Jimenez, J. L.; Kahan, T. F.; Katz, E. F.; Mattila, J. M.; Nazaroff, W. W.; Novoselac, A.; O'Brien, R. E.; Or, V. W.; Patel, S.; Sankhyan, S.; Stevens, P. S.; Tian, Y.; Wade, M.; Wang, C.; Zhou, S.; Zhou, Y. Overview of HOMEChem: House Observations of Microbial and Environmental Chemistry. *Environ. Sci.: Processes Impacts* **2019**, *21*, 1280–1300.

[12] Liu, Y.; Misztal, P. K.; Xiong, J.; Tian, Y.; Arata, C.; Weber, R. J.; Nazaroff, W. W.; Goldstein, A. H. Characterizing sources and emissions of volatile organic compounds in a northern California residence using space- and time-resolved measurements. *Indoor Air* **2019**, *29*, 630–644.

[13] Edwards, R. D.; Jurvelin, J.; Koistinen, K.; Saarela, K.; Jantunen, M. VOC source identification from personal and residential indoor, outdoor and workplace microenvironment samples in EXPOLIS-Helsinki, Finland. *Atmos. Environ.* **2001**, *35*, 4829–4841.

[14] Weschler, C. J.; Carslaw, N. Indoor Chemistry. *Environ. Sci. Technol.* **2018**, *52*, 2419–2428.

[15] Rackes, A.; Waring, M. S. Do time-averaged, whole-building, effective volatile organic compound (VOC) emissions depend on the air exchange rate? A statistical analysis of trends for 46 VOCs in U.S. offices. *Indoor Air* **2016**, *26*, 642–659.

[16] Wang, C.; Collins, D. B.; Arata, C.; Goldstein, A. H.; Mattila, J. M.; Farmer, D. K.; Ampollini, L.; DeCarlo, P. F.; Novoselac, A.; Vance, M. E.; Nazaroff, W. W.; Abbatt, J. P. D. Surface reservoirs dominate dynamic gas-surface partitioning of many indoor air constituents. *Sci. Adv.* **2020**, *6*, eaay8973.

[17] Xiong, J.; Zhang, P.; Huang, S.; Zhang, Y.; Comprehensive influence of environmental factors on the emission rate of formaldehyde and VOCs in building materials: Correlation development and exposure assessment. *Environ. Res.* **2016**, *151*, 734–741.

[18] Wieslander, G.; Norbäck, D.; Björnsson, E.; Janson, C.; Boman, G. Asthma and the indoor environment: the significance of emission of formaldehyde and volatile organic compounds from newly painted indoor surfaces. *Int. Arch. Occup. Environ. Health* **1997**, *69*, 115–124.

[19] Guo, H.; Lee, S. C.; Chan, L. Y.; Li, W. M. Risk assessment of exposure to volatile organic compounds in different indoor environments. *Environ. Res.* **2004**, *94*, 57–66.

[20] Logue, J. M.; McKone, T. E.; Sherman, M. H.; Singer, B. C. Hazard assessment of chemical air contaminants measured in residences. *Indoor Air* **2011**, *21*, 92–109.

[21] Logue, J. M.; Price, P. N.; Sherman, M. H.; Singer, B. C. A Method to Estimate the Chronic Health Impact of Air Pollutants in U.S. Residences. *Environ. Health Perspect.* **2012**, *120*, 216–222.

[22] Allen, J. G.; MacNaughton, P.; Satish, U.; Santanam, S.; Vallarino, J.; Spengler, J. D. Associations of Cognitive Function Scores with Carbon Dioxide, Ventilation, and Volatile Organic Compound Exposures in Office Workers: A Controlled Exposure Study of Green and Conventional Office Environments. *Environ. Health Perspect.* **2016**, *124*, 805–812.

[23] Liu, Y.; Misztal, P. K.; Xiong, J.; Tian, Y.; Arata, C.; Nazaroff, W. W.; Goldstein, A. H. Detailed investigation of ventilation rates and airflow patterns in a northern California residence. *Indoor Air* **2018**, *28*, 572–584.

[24] Kristensen, K.; Lunderberg, D. M.; Liu, Y; Misztal, P. K.; Tian, Y.; Arata, C.; Nazaroff, W. W.; Goldstein, A. H. Sources and dynamics of semivolatile organic compounds in a single-family residence in northern California. *Indoor Air* **2019**, *29*, 645–655.

[25] Farmer, D. K.; Vance, M. E.; Abbatt, J. P. D.; Abeleira, A.; Alves, M. R.; Arata, C.; Boedicker, E.; Bourne, S.; Cardoso-Saldaña, F.; Corsi, R.; DeCarlo, P. F.; Goldstein, A. H.; Grassian, V. H.; Hildebrandt Ruiz, L.; Jimenez, J. L.; Kahan, T. F.; Katz, E. F.; Mattila, J. M.; Nazaroff, W. W.; Novoselac, A.; O'Brien, R. E.; Or, V. W.; Patel, S.; Sankhyan, S.; Stevens, P. S.; Tian, Y.; Wade, M.; Wang, C.; Zhou, S.; Zhou, Y. Overview of HOMEChem: House Observations of Microbial and Environmental Chemistry. *Environ. Sci.: Processes Impacts* **2019**, *21*, 1280–1300.

Chapter 2

Characterizing Airborne Phthalate Concentrations and Dynamics in a Normally Occupied Residence

This chapter is adapted from:

Lunderberg, D.M.; Kristensen, K.; Liu, Y.; Misztal, P.K.; Tian, Y.; Arata, C.; Wernis, R.; Kreisberg, N.; Nazaroff, W.W.; Goldstein, A.H. Characterizing Airborne Phthalate Concentrations and Dynamics in a Normally Occupied Residence. *Environ. Sci. Technol.* **2019**, *53*, 337–7346.

2.1 Abstract

Phthalate esters, commonly used as plasticizers, can be found indoors in the gas phase, in airborne particulate matter, in dust, and on surfaces. The dynamic behavior of phthalates indoors is not fully understood. In this study, time-resolved measurements of airborne phthalate concentrations and associated gas-particle partitioning data were acquired in a normally occupied residence. The vapor pressure and associated gas-particle partitioning of measured phthalates influenced their airborne dynamic behavior. Concentrations of higher vapor pressure phthalates correlated well with indoor temperature, with little discernable influence from direct occupant activity. Conversely, occupant-related behaviors substantially influenced the concentrations and dynamic behavior of a lower vapor pressure compound, diethyl hexyl phthalate (DEHP), mainly through production of particulate matter during cooking events. The proportion of airborne DEHP in the particle phase was experimentally observed to increase under high particle mass concentrations and lower indoor temperatures in correspondence with theory. Experimental observations indicate that indoor surfaces of the residence are large reservoirs of phthalates. The results also indicate that two key factors influenced by human behavior – temperature and particle mass concentration – cause

short-term changes in airborne phthalate concentrations.

2.2 Introduction

Past indoor measurements of semivolatile organic compounds (SVOCs) have generally utilized sample collection methods that yield time-averaged results over sampling periods on the order of a day to a week.[1–3] Higher time-resolution measurements of indoor SVOCs are needed to investigate indoor dynamic processes relevant to understanding emissions, concentrations, and exposures. A few studies have explored the dynamic behavior of phthalates directly in real residential settings or in test houses.[4–6] In this study, we report an extensive sequence of phthalate diester measurements with hourly resolution in a normally occupied residence. Phthalate diesters are SVOCs of anthropogenic origin whose metabolites have been found in more than 95% of the US population.[7,8]

Several known and suspected adverse health effects are associated with phthalate exposures, including impaired reproductive development,[9, 10] infertility,[11, 12] asthma,[13, 14] and obesity.[15, 16] Phthalates are industrially produced and utilized on large scales. Phthalates are found broadly throughout the environment: in soil,[17, 18] in sediment,[17, 19] in wastewater,[17, 20] in indoor and outdoor air,[21, 22] in the Arctic,[23] and in biota.[24, 25] Certain phthalates are commonly found at elevated concentrations indoors and have been reported on surfaces, in settled dust, in airborne particles, and in the gas phase.[1, 22, 26] The abundance of airborne indoor phthalates indicates potentially important contributions to human exposure.[27] Ingestion, dermal uptake from direct contact, air-to-skin dermal absorption, and inhalation represent major modes of phthalate exposure, with relative strengths that are related to compound volatility. Exposure to lower volatility species, such as diethyl hexyl phthalate (DEHP), occurs primarily by ingestion. Higher volatility species, such as dibutyl phthalate (DBP), are subject to additional non-dietary modes of exposure, and exposure to the highest volatility phthalates, such as diethyl phthalate (DEP) and dimethyl phthalate (DMP), is expected to be dominated by nondietary routes such as inhalation and dermal absorption.[28–33] Because, on average, people spend 90% of their time indoors and 60% of their time in their own residence,[34–36] it is important to understand and characterize the processes driving indoor airborne phthalate dynamic behavior, especially in residences.

Chemical properties of phthalates are related to their industrial uses and affect their physical behaviors. Phthalates with higher vapor pressures, such as DMP, DEP, and DBP, can be found in high abundance in certain cosmetics, personal care products, and medications.[31, 37–40] Phthalates with lower vapor pressures, such as DEHP, butyl benzyl phthalate (BBzP), and diisononyl phthalate (DINP), are widely used as plasticizers, constituting large mass fractions of certain building materials.[41, 42]

Increased temperature should favor partitioning of phthalates into the gas phase. However, prior field studies comparing phthalate concentrations across similar indoor environments have yielded mixed results regarding the role of temperature. Some survey-based

studies did not find correlations between temperature and gas-phase phthalate concentrations.[26, 43, 44] Gaspar et al. noted that concentrations of three higher vapor pressure phthalates, DEP, diisobutyl phthalate (DIBP), and DBP, correlated with temperature while two lower vapor pressure phthalates, BBzP and DEHP, did not.[32] Conversely, an in-depth study in a test-house demonstrated that a 9 °C temperature difference could change concentrations of two lower vapor pressure phthalates, BBzP and DEHP, by 300%.[6] Qualitatively, these results corroborate findings from laboratory studies.[45, 46]

Particle concentration is known to affect the airborne abundances of lower volatility SVOCs, including lower vapor pressure phthalates such as DEHP and BBzP. Liu et al. developed a model characterizing how airborne particulate matter affects SVOC fluxes between indoor surfaces and indoor air, predicting that elevated particle concentrations could markedly increase SVOC emission fluxes from surfaces.[47] Total airborne SVOC abundances are expected to increase with elevated particle concentrations as SVOC material partitions from reservoirs such as dust or surfaces onto airborne particulate matter. However, full equilibrium partitioning of SVOCs to particles may not be reached for lower volatility species when the ventilation timescale (reciprocal of the air-exchange rate) is less than the timescale to approach equilibrium.[48–50]

Chamber studies have been undertaken to explore the role of particle concentration and composition on SVOC behavior. Benning et al. showed that the emission rate of DEHP is enhanced in the presence of ammonium sulfate particles.[51] Similarly, Lazarov et al. demonstrated that increased particle concentrations enhanced the emission rate of organophosphate flame retardants from materials.[52] Recent experiments by Wu et al. found DEHP particle/gas partition coefficients are higher in the presence of organic particles (squalane and oleic acid) than in the presence of inorganic particles (ammonium sulfate).[53] Weschler and Nazaroff described an equilibrium model of indoor SVOC partitioning between the gas phase and settled dust using the octanol-air partitioning coefficient (K_{oa}); that model can also be applied to airborne particles.[49] In Equation 2.1, the particle-gas partition coefficient, K_{p}, is determined where $f_{\mathrm{om\_part}}$ refers to the volume fraction of organic matter in airborne particles, and ρ_{part} refers to the density of particles.

$$K_p = \frac{K_{\mathrm{oa}} \times K_{\mathrm{p}}}{\rho_{\mathrm{part}}} \tag{2.1}$$

Now, let C_{p} refer to the particle-phase SVOC concentration, let C_{g} refer to the gas-phase SVOC concentration, and let TSP refer to the mass concentration of airborne particles. Then, the particle fraction of airborne SVOCs can be estimated using Equation 2.2.

$$F_{\mathrm{p}} = \frac{C_{\mathrm{p}}}{C_{\mathrm{g}} + C_{\mathrm{p}}} = \frac{TSP \times K_{\mathrm{p}}}{1 + TSP \times K_{\mathrm{p}}} \tag{2.2}$$

Weschler and Nazaroff describe how gas-phase SVOC abundances are expected to decrease with increased particle concentration, while total airborne (gas-plus-particle) SVOC concentrations are expected to increase. The magnitude of these effects increases with increasing

particle concentration.[48] This study presents a more detailed investigation of a subset of SVOCs reported by Kristensen et al.[54] Here, we report hourly measurements of four phthalates – DEP, DIBP, DBP, and DEHP – in a normally occupied northern California residence over a two-week monitoring period. We examine their dynamic behavior and explore the factors controlling their concentrations, emissions, and gas-particle partitioning. We investigate how the physicochemical properties of phthalates – specifically their vapor pressure and octanol-air partition coefficient – affect dynamic behavior. This work has relevance for modeling efforts assessing indoor SVOC exposure as there are limited experimental data available for model evaluation.[55–58] The results also have potentially important implications for better understanding human phthalate exposure and opportunities for exposure mitigation.

2.3 Methods

2.3.1 Field Site

Measurements were conducted at a normally occupied single-family residence in Contra Costa County, California, from 7 December 2017 to 4 February 2018. The single-story California ranch style wood-framed house was built in 1951, with 180 m^2 (1970 ft^2) of living space. The house temperature was controlled by a forced air gas-furnace with the thermostat programmed to operate only during morning (6:45 – 7:15 AM) and evening (5:45 – 10:00 PM) hours. Occasional variations in the baseline heating cycle were applied by manual occupant override, or by operating a vented gas-fireplace situated in the family room. A MERV 13 filter in the central-heating system efficiently removed particulate matter from recirculated indoor air when the furnace fan was on. The house contained a kitchen, living/dining room, family room, three bedrooms, and two bathrooms. Regular household activities included cooking, social gatherings, and professional house cleanings, as reported by Kristensen et al.[54] Data analyses presented here focus on the period 16 – 27 December 2017, the longest interval of SVOC monitoring with consistently high data quality and well characterized experimental parameters. Phthalate behavior trends were characterized during two distinct periods in this interval differentiated by house occupancy status. The house was regularly occupied (the "occupied period") from 16 to 21 December. The house was unoccupied (the "vacant period") from 22 to 27 December.

2.3.2 Instrumentation and Measurement Methods

The semivolatile thermal desorption aerosol gas chromatograph with in-situ derivatization (SV-TAG) is a two channel GC mass spectrometer instrument that quantifies gas-plus-particle or particle only concentrations of organic species and their associated gas-particle partitioning with hourly time resolution. Organic compounds with vapor pressures ranging from C14 to C30+ alkanes are routinely measured, with limits of detection varying from high

parts-per-quadrillion to low parts-per-trillion depending on the compound of interest.[59–63] SV-TAG was housed in a temperature-controlled shed adjacent to the house and sampled air from the dining room and from the outdoors. Indoor concentrations were acquired hourly. Outdoor concentrations, outdoor-gas particle partitioning, and indoor gas-particle partitioning were acquired every four hours on a rotating sampling basis. Three phthalate species (DEP, DBP, and DEHP) were identified and quantified using authentic external standards and a fourth (DIBP) was identified referencing mass spectra available in the NIST/EPA/NIH Mass Spectral Library. Detailed descriptions of SV-TAG operation, including instrumental positioning, instrumental sampling schedules, potential biases, and method quality assurance, are contained within the SI.

2.3.3 Supporting Measurements

Metadata collected in the house were used during source apportionment. A series of SmartThings motion sensors (temperature/motion; $n = 8$), SmartThings position sensors (door and window position/temperature; $n = 34$), SmartThings appliance sensors ($n = 5$), Netatmo weather stations (temperature/relative humidity/pressure/noise/CO2; $n = 10$), and HOBOTM sensors (temperature/humidity; $n = 10$) were used to characterize household state, indoor environmental parameters, and occupant activities. In this report, "indoor air temperature" refers to the temperature measured in the family room. Temperature sensors throughout the house strongly covary with the house heating cycle with small differences observed between main living spaces and the hallway. Occupants also kept detailed activity logs recording the timing of their presence/absence within the house and general activities, including cooking, cleaning, and sleeping. A Grimm 11-A aerosol spectrometer sampled continuously to quantify particle number concentrations in 31 diameter bins between 0.25 and 32 μm. Mass concentrations were calculated using an assumed particle density of 1.67 g cm^{-3} based on densities commonly used in the literature for characterizing ambient PM2.5.[64, 65]

2.4 Results and Discussion

Airborne concentrations of four phthalates (DEP, DIBP, DBP, and DEHP) were quantified with hourly time resolution throughout the normally occupied (Dec 16–21) and vacant (Dec 22–27) periods. Key characteristics of these phthalates and overall measurement results are summarized in Table 2.4.1. Other phthalates commonly reported in indoor air studies – including DMP, BBzP, DINP, and diisodecyl phthalate (DIDP) – were not identifiable above the background chromatographic signal, suggesting that their concentrations were much lower than those of the four reported phthalates. The three higher-vapor pressure phthalates, DEP, DIBP, and DBP, were present at median concentrations of 196 ng m^{-3}, 133 ng m^{-3}, and 93 ng m^{-3}, respectively, for the occupied period. These concentrations are generally consistent with past surveys of indoor environments; for example, median

concentrations of DEP (330, 590, 180; ng m^{-3}), DIBP (130, N/A, N/A; ng m^{-3}), and DBP (140, 220, 310; ng m^{-3}) were reported in surveys of (1) northern California residences, (2) Cape Cod MA residences, and (3) Boston MA indoor environments, respectively.[1, 22, 66]

Throughout the occupied period, concentrations of higher vapor pressure phthalates displayed remarkably small temporal variance. Maximum and minimum concentrations of DIBP and DBP differed by $\leq 32\%$ from the mean (RSD $\leq 11\%$), and concentrations of DEP fluctuated by no more than 47% (RSD = 15%). In contrast, indoor concentrations of DEHP were highly variable, ranging from 1.6 to 112 ng $m^{-}3$ during the occupied period (RSD = 183%) and from 2.3 to 8.8 ng m^{-3} during the vacant period (RSD = 34%). The median DEHP concentration during the occupied period (4 ng m^{-3}) was considerably lower than median residential concentrations reported in the surveys mentioned previously (77 ng m^{-3}, 68 ng m^{-3}, N/A).

In a recent study of the dynamic behavior of volatile organic compounds in an occupied residence, Liu et al. used measured mean-to-median ratios (MMR) to classify indoor species emissions as being primarily from static contents (MMR < 1.06) or primarily related to episodic occupant activities (MMR > 1.5).[67] In Table 2.4.1, we show that MMR < 1.06 for all three higher volatility phthalates, during both the occupied and unoccupied periods. These low values are strongly suggestive of the importance of ongoing emissions from static sources in the residence. In contrast, for DEHP during the occupied period, MMR = 2.1, indicating the importance of episodic events controlling the release of DEHP into indoor air.

Concentrations of DEP, DIBP, and DBP were significantly higher indoors than outdoors at all times. On average, phthalate concentrations were 3 times higher indoors than outdoors for DEP and 3.5 times higher for DBP and DIBP. Average concentrations of DEHP during the occupied period were 2.5 times higher indoors than outdoors, and were roughly equivalent between the indoors and outdoors during the vacant period. Outdoor time series for the analysis periods are displayed in Figures 2.7.3 and 2.7.4.

2.4.1 Dynamic Phthalate Concentrations

Figure 2.4.1 presents time series of phthalate concentrations and indoor air temperature. Diel plots of concentrations and temperature are shown in Figures 2.7.5 and 2.7.6. Concentrations of the primarily gaseous species (DEP, DIBP, and DBP) are characterized by a stable background with small perturbations associated with the indoor air temperature. Temperature profiles were regulated by wintertime home heating applied in mornings (6:45-7:15 AM) and evenings (5:45-10 PM) and, accordingly, DEP, DIBP, and DBP concentrations were higher on average during the warmer waking hours and lower during cooler sleeping hours. By contrast, concentrations of DEHP were much lower at baseline levels but exhibited substantial episodic enhancements during the occupied period. Multiple factors are expected to influence indoor phthalate concentrations. Among these are ongoing background emissions from static building materials and furnishings, episodic primary emissions from product usage, and dynamic phase-partitioning flows between indoor air and reservoirs including surface films and dust. Reversible sorptive interactions would be sensitive to dynamic changes in

Table 2.4.1: Characteristics of observed phthalate species along with major measurement results.

		DEP diethyl phthalate	DIBP diisobutyl phthalate	DBP dibutyl phthalate	DEHP diethylhexyl phthalate
Properties	**Log Saturation Vapor Pressure**[b]	-6.83	-8.30	-8.47	-11.85
	Log K_{oa}[b]	8.21	9.62	9.83	12.89
	CAS Number	84-66-2	84-69-5	84-74-2	117-81-7
	Chemical Formula	$C_{12}H_{14}O_4$	$C_{16}H_{22}O_4$	$C_{16}H_{22}O_4$	$C_{24}H_{38}O_4$
	Mol. Weight (g/mol)	222.24	278.35	278.35	390.56
Indoor[a]	**Occupied Conc.**	201 ± 30	133 ± 15	91 ± 8	9 ± 16
	Mean-to-median Ratio	1.03	1.00	0.99	2.13
	Vacant Conc.	200 ± 16	135 ± 17	93 ± 10	4.1 ± 1.4
	MMR	1.01	1.01	1.00	1.15
	Occupied Fp	0.05 ± 0.03	0.12 ± 0.01	0.16 ± 0.04	0.74 ± 0.22
	Vacant Fp	0.04 ± 0.01	0.11 ± 0.01	0.14 ± 0.02	0.68 ± 0.17
Outdoor[a]	**Occupied Conc.**	36 ± 21	44 ± 10	31 ± 5	3.4 ± 0.4
	Vacant Conc.	54 ± 17	45 ± 6	32 ± 4	3.9 ± 0.8
	Occupied Fp	0.16 ± 0.08	0.19 ± 0.03	0.21 ± 0.04	0.79 ± 0.18
	Vacant Fp	0.11 ± 0.02	0.16 ± 0.02	0.19 ± 0.02	0.59 ± 0.20

[a] All values are reported as mean ± standard deviation. Total (gas-plus-particle) concentrations are reported in ng m^{-3}. Fraction in particle phase (F_p) is defined as the measured SVOC concentration associated with particles divided by the total (gas-plus-particle) concentration. Mean F_p is reported as the average of calculated values in the analysis window. Variability of F_p is reported as the standard deviation of the population.

[b] Phthalate saturation vapor pressures vary by orders of magnitude among published measurements, but generally decrease with increasing molecular weight. Values of the saturation vapor pressure in atm and the octanol-air partition coefficient (K_{oa}) as determined by theory are reported by Salthammer et al. at T = 298 K.[68]

physical conditions, such as temperature and airborne particle concentrations, which would alter equilibrium partitioning between condensed and gaseous phases. Static emissions may contribute to a stable background, whereas episodic emissions of sufficient strength would be readily apparent from the time series of concentrations. Cosmetics, personal care products and medication are commonly reported sources of DEP, DIBP, and DBP.[31, 37–40] Strikingly, although multiple residents applied multiple personal care products throughout the campaign, no episodic concentration enhancements were observed for the three higher volatility phthalates.

SVOCs may interact with the envelope of household occupants at meaningful rates, such as during uptake on clothing or dermal absorption.[48] However, no associations were observed between occupancy and DEP concentrations. Weak associations between (increased) occupancy and (decreased) concentrations of two phthalates, DIBP and DBP, were observed during the occupied period (Figure 2.7.2).

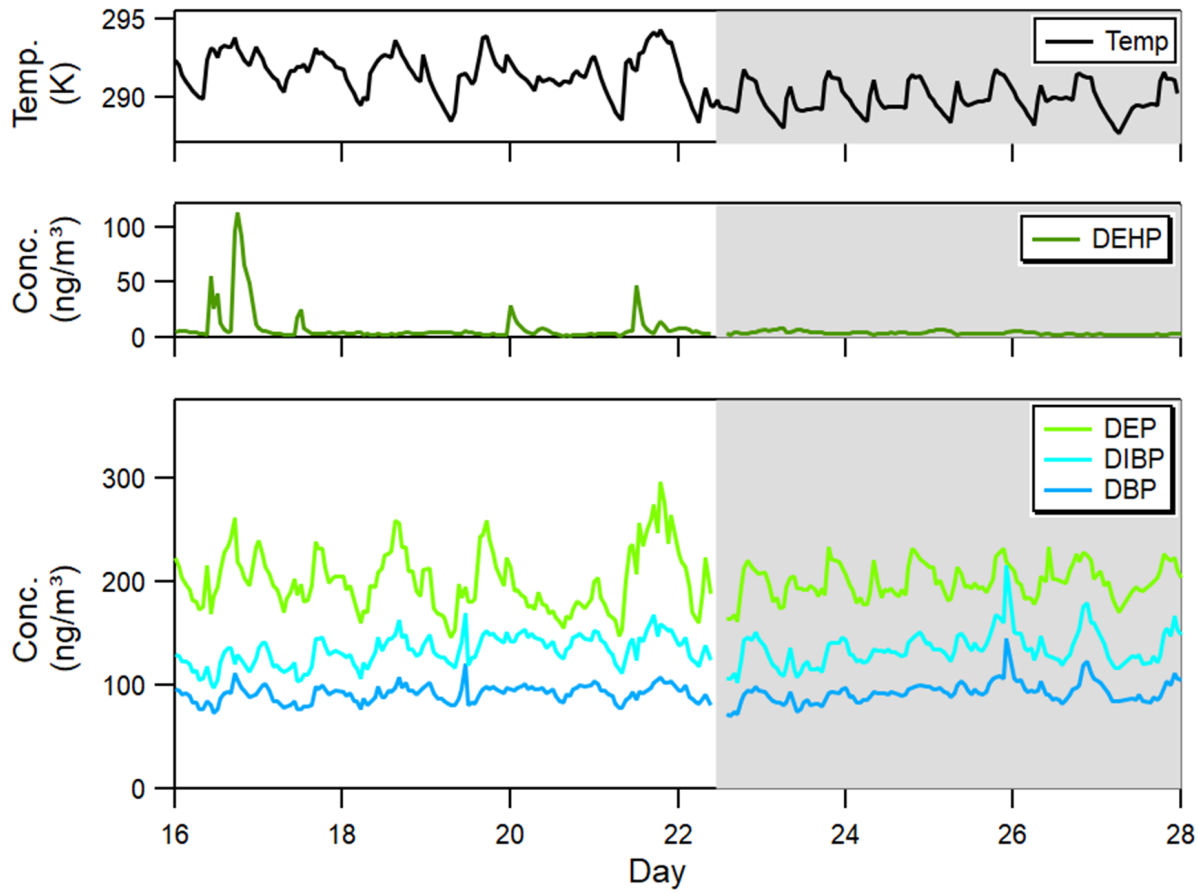

Figure 2.4.1: Total (gas-plus-particle) concentration time series of four phthalates over the occupied (left) and vacant (right, in gray) periods. Indoor air temperature is displayed in the upper panel. The horizontal axis is labeled with day of the month, December 2017.

2.4.2 Temperature and Surface-Air Equilibration

The hourly-averaged concentrations of the four measured phthalates are compared with indoor air temperature in Figure 2.4.2. The extent to which concentrations correlate with temperature diminishes with increasing molecular weight and decreasing vapor pressure. Specifically, DEP concentrations exhibited strong temperature dependence during both the vacant and occupied periods, whereas DBP and DIBP concentrations exhibited only moderate temperature dependence. Average DEP concentrations were essentially equivalent between the occupied (201 ng m^{-}3) and vacant (200 ng m^{-}3) periods and strongly correlated with the house heating cycle. Overall, however, indoor air temperatures were slightly colder ($\sim$2 K) during the vacant period than the occupied period. It is possible that the measured air temperature was not fully representative of reservoir surface temperatures throughout the

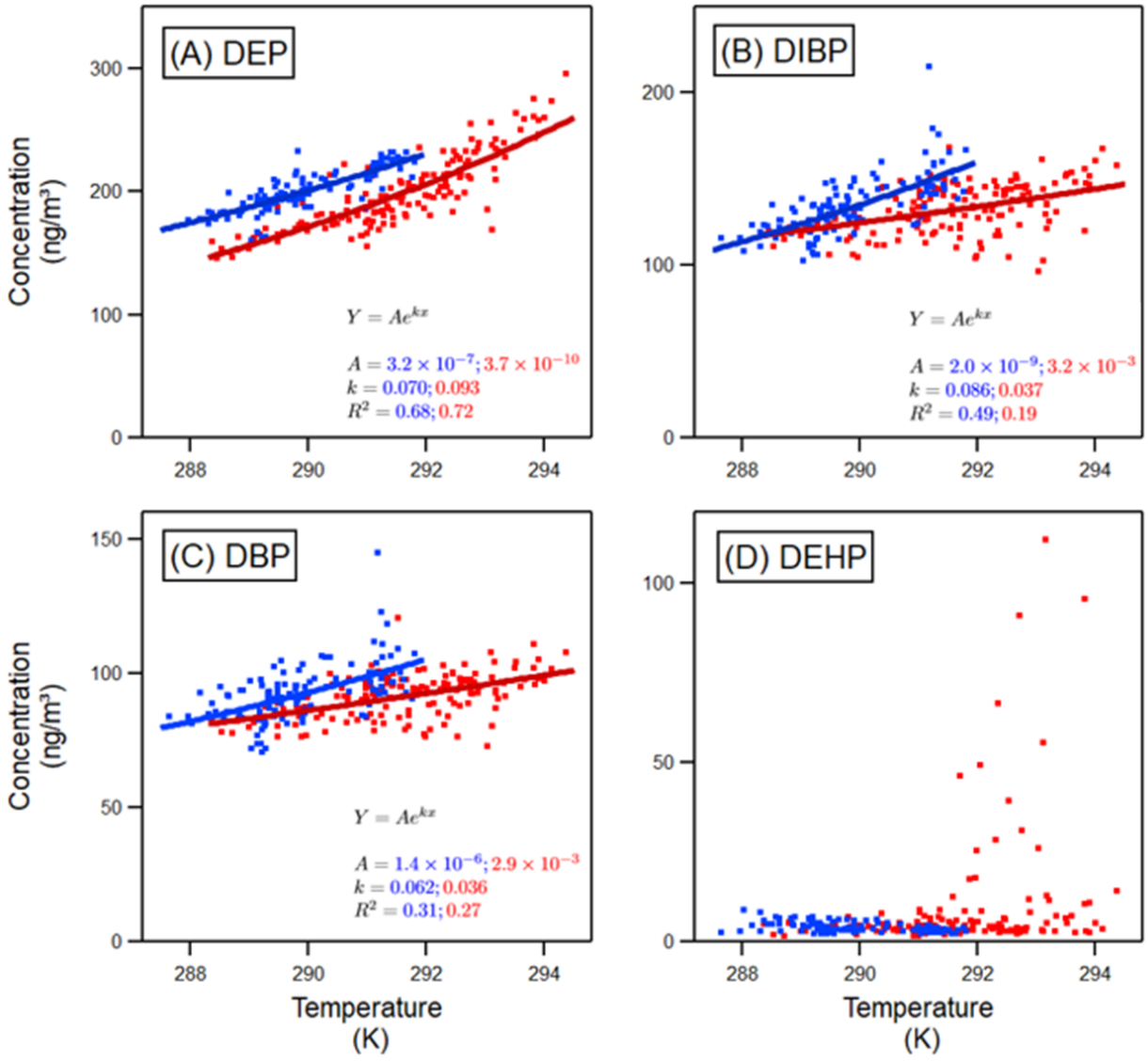

Figure 2.4.2: Total (gas-plus-particle) indoor-air concentrations of DEP, DIBP, DBP, and DEHP versus temperature. Data are differentiated by color between the occupied (red) and vacant (blue) periods, and regression lines correspond to an exponential fit. Units of measure on the fit parameters are inverse temperature for k (1/K) and concentration for A (ng m^{-3}).

residence and that the air-surface temperature relationship was different between occupied and vacant periods.

Conversely, DEHP was characterized by a low baseline concentration punctuated by episodic spikes unrelated to temperature. It is well known that the emissions of DEHP, which can be a major constituent of certain types of materials such as vinyl flooring, in-

crease strongly as temperature increases.[46] Remarkably, airborne DEHP concentrations displayed no observable correlations with temperature in the occupied period in this study. Furthermore, concentrations were weakly anticorrelated with temperature during the vacant period. Evidence suggests that airborne DEHP, which is primarily a particle-phase compound, was effectively removed by filtration during the morning and evening house-heating intervals (Figure 2.7.6).

Observed concentrations of DEP, DIBP, and DBP, were several orders of magnitude below their respective gas-phase saturation concentrations. DEHP was roughly one order of magnitude below its gas-phase saturation concentration. (Vapor pressure values are as reported in Salthammer et al.; substantial variation in vapor pressures exists throughout the literature.[68]) Interactions between organic surface films and the bulk air may influence airborne SVOC concentrations and these interactions have been modeled using octanol-air partition coefficients.[69] Observed median concentrations of each phthalate species strongly correlate with the octanol-air partition coefficient (log-log plot, $R^2 = 0.94$, Figure 2.7.7), a parameter describing the strength of interactions between air and a model organic film. Furthermore, the dynamics associated with the observed heating cycle may be tied to thermodynamic changes in the octanol-air partition coefficient. Temperature dependence of the saturation vapor pressure, which is anticorrelated with the octanol-air partition coefficient, has been experimentally determined for DIBP and DBP.[70] In Figure 2.7.8, the concentrations of DIBP and DBP are plotted against their saturation vapor pressures as a function of indoor air temperature, revealing a strong positive correlation ($R^2 = 0.71$). Together, these factors suggest that substantial condensed-phase reservoirs exist throughout the residence and that K_{oa} could be a key controlling variable related to both dynamics and observed airborne concentrations with additional contributions possible from static sources. Additionally, these factors suggest that the decreasing abundance of larger phthalate homologues ($C_{DEP} > C_{DIBP} > C_{DBP} > C_{DEHP}$) may be coupled to their physical parameters such as their respective vapor pressures and octanol-air partition coefficients.

2.4.3 Particle Loading Influences DEHP Concentrations

Indoor particle mass concentrations strongly correlated with total (gas-plus-particle) DEHP concentrations during the vacant and occupied periods. Occupant activities like cooking can markedly influence indoor particle concentration, composition and size distribution. Particle resuspension also can occur during occupant activities, but this process is more important for coarse particles and less important for particles smaller than 2.5 μm that are sampled by SV-TAG.[71] The effects of occupant-associated particle sources are explored in Figure 2.4.3, which displays DEHP concentrations against PM2.5 concentration and activity type during the occupied period. Notwithstanding diversity among particle sources, a linear relationship between particle mass concentration and total airborne phthalate concentrations is observed with DEHP accounting for about 0.3% of indoor PM2.5 by mass. DEHP concentrations are strongly associated with particle emission events from cooking. The absence of cooking events over the vacant period affected average DEHP concentrations. While concentrations

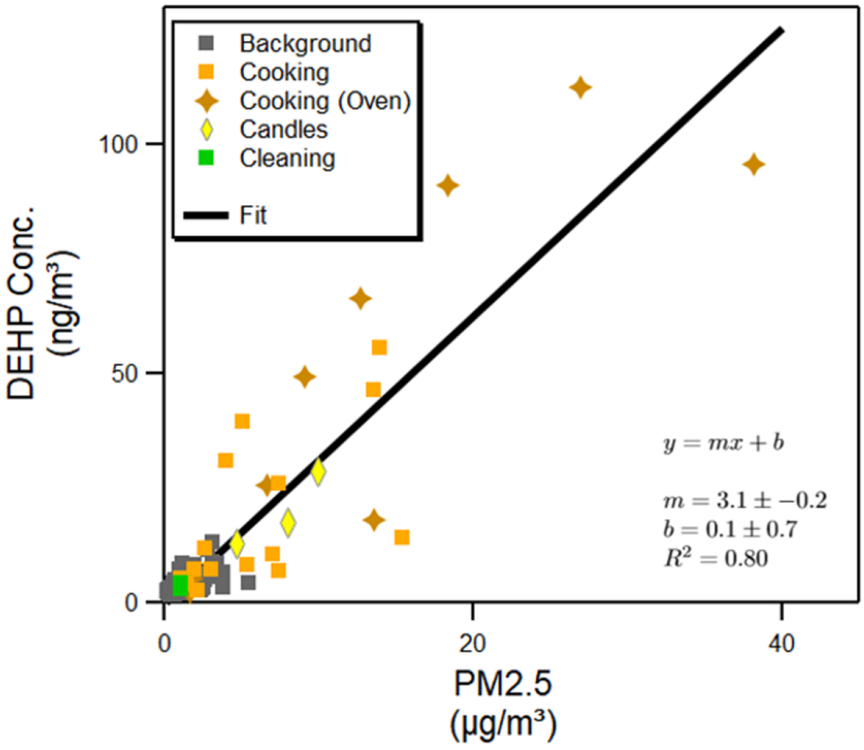

Figure 2.4.3: Total (gas-plus-particle) DEHP concentrations during the occupied period are compared against PM2.5 concentration. Concurrent indoor activities with the potential to influence airborne SVOC concentrations are highlighted: cooking, candle combustion, and cleaning. Units of measure on the fit parameters are ng μg^{-1} (parts per thousand) for the slope, m, and ng m^{-3} for the intercept, b.

of DEP, DIBP, and DBP were similar between the occupied and vacant periods, the average concentration of DEHP over the occupied period was nearly two times greater than during the vacant period.

It has been demonstrated in both modeling and chamber studies that the presence of airborne particles can enhance DEHP emissions from surfaces.[51, 72] Particles enhance surface mass transfer by increasing the gas-phase concentration gradient in the near-surface boundary layer. Particles act as an airborne sink, sorbing SVOCs from the gas-phase, thereby depleting gas-phase SVOCs in the bulk air and effectively increasing SVOC flux from surfaces. Similarly, total airborne concentrations of species with high K_p values are expected to increase with particle mass concentration, with minimal effect on low K_p species that are predominantly in the gas-phase.

It is worthwhile to consider whether direct cooking emissions of DEHP might account for episodic concentration enhancements. Food-borne DEHP has been reported at low ppb to low ppm concentrations. When oily food has been stored in jars with PVC gaskets, DEHP

can approach upper ppm concentrations.[73] We considered a hypothetical emission event where food-borne DEHP was fully transferred into residential air and assumed a food-borne phthalate concentration of 10 mg kg^{-}1, a typical upper bound. Assuming one kg of food cooked, a cooking event could release an upper bound of 10 mg of DEHP from food, which, when diluted throughout the house volume of 380 m^3, would yield a transient peak DEHP concentration of up to 25 ng m^{-3}. However, this value is below the measured concentrations associated with many cooking events, suggesting that direct DEHP emission from food was not a dominant contributor to airborne DEHP enhancements during major source events. Instead, we infer that the increased airborne particle concentrations enhanced the net rate of transfer of DEHP from static sources and/or from indoor surface films to indoor air.

PM2.5 concentrations strongly correlated with airborne DEHP concentrations under vacant conditions (Figure 2.4.4). Total (gas-plus-particle) concentrations of DEHP were comparable between the indoors and outdoors over the vacant period (Figure 2.7.4). However, outdoor DEHP-bearing particles are not expected to penetrate the building envelope with full efficiency. For the duration of the vacant period, indoor PM2.5 was always less than or (approximately) equal to outdoor PM2.5 concentrations with an average indoor:outdoor particle mass ratio of 1:4 for the duration of the vacant period. Because no occupants were present and because indoor particles were intermittently removed in association with the filter in the house's forced air heating system, nearly all indoor particles are believed to have originated from outdoor intrusion through the building envelope. Over the vacant period, outdoor DEHP constituted 0.10% of outdoor PM2.5 by mass on average. Together, these observations suggest that particulate matter entering the house rapidly acquires DEHP from indoor dust, surfaces, and the gas-phase such that DEHP comprises 0.24% of indoor PM2.5 by mass with contributions from both indoor and outdoor sources. Similar relations between airborne DEHP concentrations and PM2.5 are observed during the occupied period (event-driven spikes excluded), albeit with greater variability.

2.4.4 Gas-Particle Partitioning

The higher vapor-pressure phthalates (DEP, DBP, DIBP) were present primarily in the gas-phase (Table 2.4.1). Their particle fractions, while small, consistently increased as their molecular size and associated octanol-air partition coefficients increased (F_{p} values follow this order: DEP < DBP < DIBP). The particle-phase fraction of these species was largely independent of particle mass concentration and temperature in the ranges encountered in the studied residence. Observed particle fractions for DEP, DIBP, and DBP (5%, 12%, 16%,) were qualitatively similar yet quantitatively higher than those estimated by Weschler and Nazaroff who reported expected particle fractions to be 0%, 3%, and 5%, respectively.[49] Increasing particle mass concentration can drive gas-particle partitioning towards the particle phase. Airborne gas-particle partitioning of DEHP is associated with both PM2.5 concentration and indoor air temperature as revealed in Figure 2.4.5. At PM2.5 concentrations above 3 μg m^{-3}, airborne DEHP concentrations were predominantly in the particle phase.

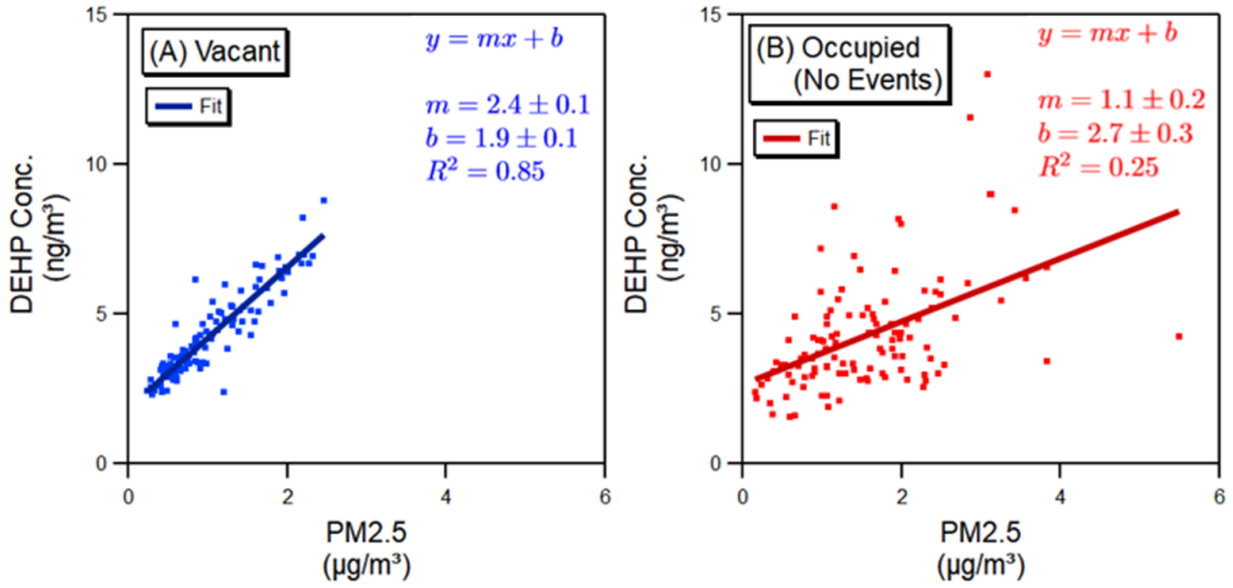

Figure 2.4.4: The gas-plus-particle concentration of DEHP is compared against PM2.5 concentration during the vacant period (A) and the occupied period when no cleaning, cooking, or combustion events were occurring (B). Units of measure on the fit parameters are ng μg^{-1} (parts per thousand) for the slope, m, and ng m^{-3} for the intercept, b.

Similar effects are observable with cooler temperatures promoting partitioning into particles and an increased F_p.

Using the model described in Equation 2 an apparent partition coefficient K_p^* was evaluated to be 2.4 ± 0.3 m^3 μg^{-1} under observed conditions. This empirically-derived partition coefficient is affected by assumptions about equilibrium conditions, the temperature, and by the experimental approach. Time-scales to approach gas-particle phase equilibrium vary depending on K_{oa} values and particle size.[48, 50] For DEHP, gas-particle equilibration time scales may approach hundreds of hours for particle diameters in the vicinity of 2.5 µm and would be minutes to hours for particle sizes near 100 nm. Considering the residence's average air-exchange period of 2.2 h, the DEHP phase-partitioning system may be far from equilibrium for larger particles but is expected to be at or near equilibrium for smaller particles.[48, 50, 54] Experimentally, the F_p values were determined only for particles smaller than 2.5 µm, the SV-TAG particle-size cutoff. In addition, the stated PM2.5 concentrations do not include particles with diameters smaller than 250 nm that were not quantified by the Grimm 11-A OPC.

Using the van't Hoff equation, and assuming equilibrium conditions, K_p^* is expected to change by roughly 3× over the observed indoor temperature range (288 – 294 K).[74] After normalizing each particle fraction measurement from the measured indoor air temperature to the standard state temperature, the best-estimate K_p^{*298} value at T = 298 K

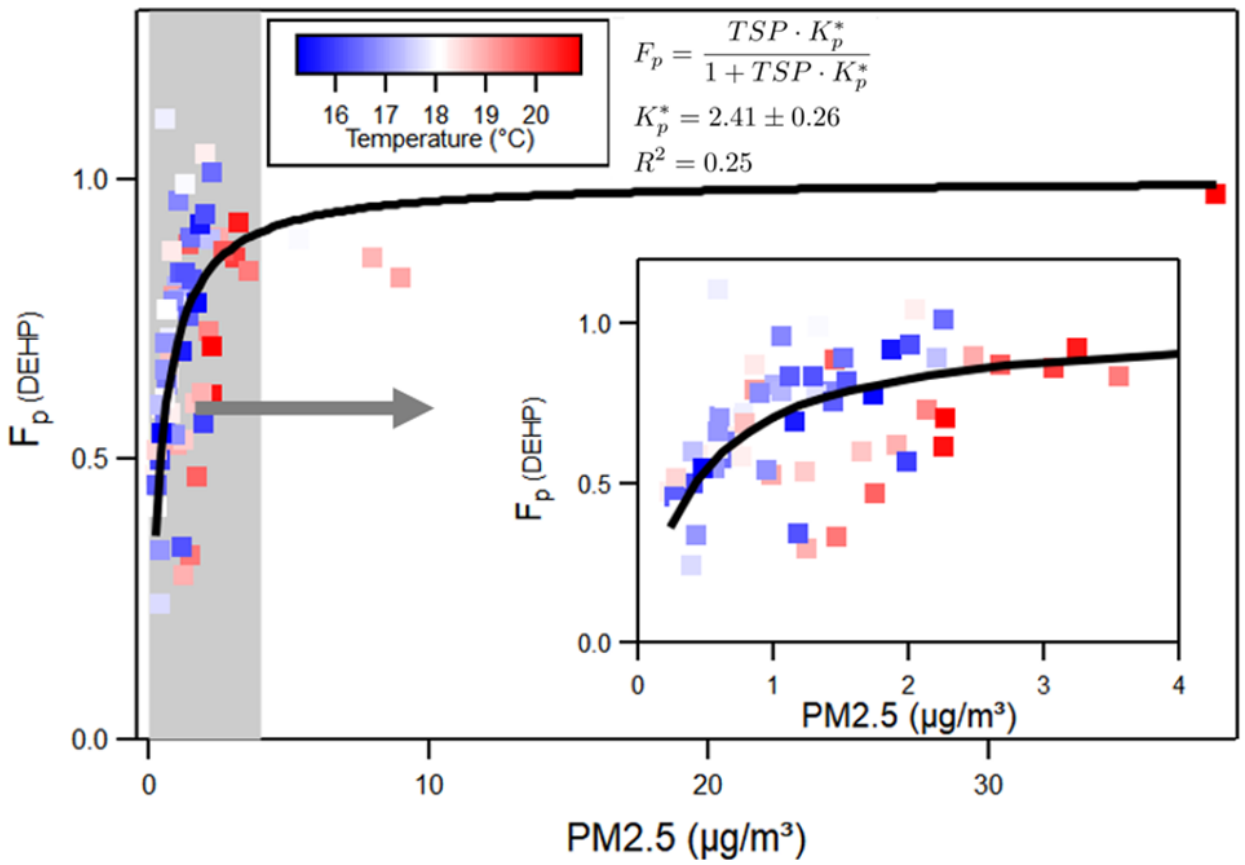

Figure 2.4.5: The particle fraction of DEHP is compared against PM2.5 concentration, with points colored by indoor air temperature. The lower right panel highlights the low PM2.5 concentration region between 0 and 4 µg m^{-3}.

is 0.80 ± 0.09 m^3 μg^{-1} (Figure 2.7.9). This value can be compared to the partition coefficient calculated using the model developed by Weschler and Nazaroff (3.2 m^3 μg^{-1}), which assumed equilibrium conditions, a log K_{oa} value of 12.9, a particle density of 1 × 10^6 g m^{-3}, and a volume fraction of organic matter associated with airborne particles (f_{om_part}) of 0.4.[49] The particle partitioning coefficient determined from this field-monitoring campaign is larger than has been reported in laboratory studies where Kp = 0.032 m^3 μg^{-1} for ammonium sulfate particles, 0.23 m^3 μg^{-1} for oleic acid particles, and 0.11 m^3 μg^{-1} for squalene particles.[51, 70] A recent theoretical prediction yielded Kp = 0.19 m^3 μg^{-1}.[74] Given the order of magnitude variability in K_p depending on literature source, particle composition, and ambient temperature, determinations of the apparent partition coefficient in real indoor environments are valuable. As the relative gas-particle abundance can influence consequent exposures and potential health risks, such observations and inferences are relevant for improving our understanding of the nature and significance of human phthalate encounters in

indoor environments.

2.4.5 Implications

Among the four quantified phthalates, concentrations of three higher-volatility species (DEP, DIBP and DBP) were found to be influenced mainly by indoor air temperature, whereas the lower volatility species (DEHP) varied with systematic and episodic indoor airborne particle mass concentrations. Ultimately, factors observed to affect airborne phthalate concentrations were indirectly related to human behavior. Spikes in DEHP concentrations were associated with particles generated by episodic emission events related to occupant activities such as stovetop cooking, oven usage, and candle combustion. Dynamic changes in gas-phase phthalate concentrations largely followed the occupant-influenced indoor temperature cycle. Overall gas-phase abundances may be related to factors external to the indoor temperature cycle such as the octanol-air partition coefficient and the presence of static sources in the residence. Perturbations affecting DEHP concentrations were also observed in association with particle removal by filtration during the operation of the central forced-air heating system.

Increased understanding of the factors that control airborne phthalate concentrations is important to gain insight into human phthalate exposure. The complex partitioning behavior exhibited in the case of DEHP suggests that human exposure assessments relying on static measures of concentrations and gas-particle partitioning are incomplete. In this residence, increasing PM2.5 concentrations from 0.5 $\mu g\ m^{-3}$ to 3 $\mu g\ m^{-3}$ could drive DEHP completely into the particle phase, thereby altering the inhalation mode of occupant exposure. This level of PM2.5 perturbation was regularly encountered during cooking events. These results illustrate that variable particle mass concentrations may influence occupant uptake by altering both DEHP concentrations and gas-particle partitioning. This finding points to the potential utility of particle reduction techniques as a means of reducing indoor airborne exposure to low-volatility phthalates and related SVOCs.

2.5 Acknowledgements

This work was supported by the Alfred P. Sloan Foundation Program on Chemistry of Indoor Environments via Grant 2016-7050. David Lunderberg acknowledges support from the National Science Foundation (Grant No. DGE 1752814). Kasper Kristensen acknowledges support from the Carlsberg Foundation (Grant No. CF16-0624). The occupants gave informed consent for this study, which was conducted under a protocol approved in advance by the Committee for Protection of Human Subjects for the University of California, Berkeley (Protocol #2016-04-8656). The authors extend thanks to Robin Weber for technical assistance. The authors wish to recognize and thank the house residents for allowing their home to be studied, and for their patience and geniality.

2.6 References

[1] Rudel, R. A.; Camann, D. E.; Spengler, J. D.; Korn, L. R.; Brody, J. G. Phthalates, alkylphenols, pesticides, polybrominated diphenyl ethers, and other endocrine-disrupting compounds in indoor air and dust. *Environ. Sci. Technol.* **2003**, *37*, 4543–4553.

[2] Saito, I.; Onuki, A.; Seto, H. Indoor organophosphate and polybrominated flame retardants in Tokyo. *Indoor Air* **2007**, *17*, 28–36.

[3] Blanchard, O.; Glorennec, P.; Mercier, F.; Bonvallot, N.; Chevrier, C.; Ramalho, O.; Mandin, C.; Bot, B. L. Semivolatile organic compounds in indoor air and settled dust in 30 French dwellings. *Environ. Sci. Technol.* **2014**, *48*, 3959–3969.

[4] Sukiene, V.; Gerecke, A. C.; Park, Y. M.; Zennegg, M.; Bakker, M. I.; Delmaar, C. J. E.; Hungerbuhler, K.; von Goetz, N. Tracking SVOCs' transfer from products to indoor air and settled dust with deuterium-labeled substances. *Environ. Sci. Technol.* **2016**, *50*, 4296–4303.

[5] Sukiene, V.; von Goetz, N.; Gerecke, A. C.; Bakker, M. I.; Delmaar, C. J. E.; Hungerbuhler, K. Direct and air-mediated transfer of labeled SVOCs from indoor sources to dust. *Environ. Sci. Technol.* **2017**, *51*, 3269–3277.

[6] Bi, C.; Liang, Y.; Xu, Y. Fate and transport of phthalates in indoor environments and the influence of temperature: A case study in a test house. *Environ. Sci. Technol.* **2015**, *49*, 9674–9681.

[7] Centers for Disease Control and Prevention (CDC). Fourth National Report on Human Exposure to Environmental Chemicals. 2018. Atlanta, Georgia.

[8] Zota, A. R.; Calafat, A. M.; Woodruff, T. J. Temporal trends in phthalate exposures: Findings from the National Health and Nutrition Examination Survey, 2001–2010. *Environ. Health Perspect.* **2014**, *122*, 235–241.

[9] Swan, S. H.; Main, K. M.; Liu, F.; Stewart, S. L.; Kruse, R. L.; Calafat, A. M.; Mao, C. S.; Redmon, J. B.; Ternand, C. L.; Sullivan, S.; Teague, J. L.; Study for Future Families Research Team. Decrease in anogenital distance among male infants with prenatal phthalate exposure. *Environ Health Perspect.* **2005**, *113*, 1056–1061.

[10] Martino-Andrade, A. J.; Chahoud, I. Reproductive toxicity of phthalate esters. *Mol. Nutr. Food Res.* **2010**, *54*, 148–157.

[11] Duty, S. M.; Silva, M. J.; Barr, D. B.; Brock, J. W.; Ryan, L.; Chen, Z.; Herrick, R. F.; Christiani, D. C.; Hauser, R. Phthalate exposure and human semen parameters. *Epidemiology* **2003**, *14*, 269–277.

[12] Tranfo, G.; Caporossi, L.; Paci, E.; Aragona, C.; Romanzi, D.; De Carolis, C.; De Rosa, M.; Capanna, S.; Papaleo, B.; Pera, A. Urinary phthalate monoesters concentration in couples with infertility problems. *Toxicol. Lett.* **2012**, *213*, 15–20.

[13] Bornehag, C.-G.; Sundell, J.; Weschler, C. J.; Sigsgaard, T.; Lundgren, B.; Hasselgren, M.; Hägerhed-Engman, L. The association between asthma and allergic symptoms in children and phthalates in house dust: A nested case-control study. *Environ. Health Perspect.* **2004**, *112*, 1393–1397.

[14] Callesen, M.; Bekö, G.; Weschler, C. J.; Sigsgaard, T.; Jensen, T. K.; Clausen, G.; Toftum, J.; Norberg, L. A.; Høst, A. Associations between selected allergens, phthalates, nicotine, polycyclic aromatic hydrocarbons, and bedroom ventilation and clinically confirmed asthma, rhinoconjunctivitis, and atopic dermatitis in preschool children. *Indoor Air* **2014**, *24*, 136–147.

[15] Buser, M. C.; Murray, H. E.; Scinicariello, F. Age and sex differences in childhood and adulthood obesity association with phthalates: Analyses of NHANES 2007–2010. *Int. J. Hyg. Environ. Health* **2014**, *217*, 687–694.

[16] Harley, K. G.; Berger, K.; Rauch, S.; Kogut, K.; Claus Henn, B; Calafat, A. M.; Huen, K; Eskenazi, B.; Holland, N. Association of prenatal urinary phthalate metabolite concentrations and childhood BMI and obesity. *Pediatr. Res.* **2017**, *82*, 405–415.

[17] Fromme, H.; Kuchler, T.; Otto, T.; Pilz, K.; Müller, J.; Wenzel, A. Occurrence of phthalates and bisphenol A and F in the environment. *Water Res.* **2002**, *36*, 1429–1438.

[18] Zeng, F.; Cui, K.; Xie, Z.; Wu, L.; Luo, D.; Chen, L.; Lin, Y.; Liu, M.; Sun, G. Distribution of phthalate esters in urban soils of subtropical city, Guangzhou, China. *J. Hazard. Mater.* **2009**, *164*, 1171–1178.

[19] Yuan, S. Y.; Liu, C.; Liao, C. S.; Chang, B. V. Occurrence and microbial degradation of phthalate esters in Taiwan river sediments. *Chemosphere* **2002**, *49*, 1295–1299.

[20] Zolfaghari, M.; Drogui, P.; Seyhi, B.; Brar, S. K.; Buelna, G.; Dubé, R. Occurrence, fate and effects of Di (2-ethylhexyl) phthalate in wastewater treatment plants: A review. *Environ. Pollut.* **2014**, *194*, 281–293.

[21] Rudel, R. A.; Perovich, L. J. Endocrine disrupting chemicals in indoor and outdoor air. *Atmos. Environ.* **2009**, *43*, 170–181.

[22] Rudel, R. A.; Dodson, R. E.; Perovich, L. J.; Morello-Frosch, R.; Camann, D. E.; Zuniga, M. M.; Yau, A. Y.; Just, A. C.; Brody, J. G. Semivolatile endocrine-disrupting compounds in paired indoor and outdoor air in two northern California communities. *Environ. Sci. Technol.* **2010**, *44*, 6583–6590.

[23] Xie, Z.; Ebinghaus, R.; Temme, C.; Lohmann, R.; Caba, A.; Ruck, W. Occurrence and air-sea exchange of phthalates in the Arctic. *Environ. Sci. Technol* **2007**, *41*, 4555–4560.

[24] Mayer, F. L.; Stalling, D. L.; Johnson, J. L. Phthalate esters as environmental contaminants. *Nature* **1972**, *238*, 411–413.

[25] Giam, C. S.; Chan, H. S.; Neff, G. S.; Atlas, E. L. Phthalate ester plasticizers: A new class of marine pollutant. *Science* **1978**, *199*, 419–421.

[26] Fromme, H.; Lahrz, T.; Piloty, M.; Gebhart, H.; Oddoy, A.; Rüden, H. Occurrence of phthalates and musk fragrances in indoor air and dust from apartments and kindergartens in Berlin (Germany). *Indoor Air* **2004**, *14*, 188–195.

[27] Otake, T.; Yoshinaga, J.; Yanagisawa, Y. Exposure to phthalate esters from indoor environment. *J. Expo. Anal. Environ. Epidemiol.* **2004**, *14*, 524–528.

[28] Wormuth, M.; Scheringer, M.; Vollenweider, M.; Hungerbühler, K. What are the sources of exposure to eight frequently used phthalic acid esters in Europeans? *Risk Anal.* **2006**, *26*, 803–824.

[29] Wittassek, M.; Koch, H. M.; Angerer, J.; Brüning, T. Assessing exposure to phthalates – The human biomonitoring approach. *Mol. Nutr. Food Res.* **2011**, *55*, 7–31.

[30] Bekö, G.; Weschler, C. J.; Langer, S.; Callesen, M.; Toftum, J.; Clausen, G. Children's phthalate intakes and resultant cumulative exposures estimated from urine compared with estimates from dust ingestion, inhalation and dermal absorption in their homes and daycare centers. *PLoS ONE* **2013**, *8*, e62442.

[31] Guo, Y.; Kannan, K. A survey of phthalates and parabens in personal care products from the United States and its implications for human exposure. *Environ. Sci. Technol.* **2013**, *47*, 14442–14449.

[32] Gaspar, F. W.; Castorina, R.; Maddalena, R. L.; Nishioka, M. G.; McKone, T. E.; Bradman, A. Phthalate exposure and risk assessment in California child care facilities. *Environ. Sci. Technol.* **2014**, *48*, 7593–7601.

[33] Weschler, C. J.; Bekö, G.; Koch, H. M.; Salthammer, T.; Schripp, T.; Toftum, J.; Clausen, G. Transdermal uptake of diethyl phthalate and di(n-butyl) phthalate directly from air: experimental verification. *Environ. Health Perspect.* **2015**, *123*, 928–934.

[34] Jenkins, P. L.; Phillips, T. J.; Mulberg, E. J.; Hui, S. P. Activity patterns of Californians: use of and proximity to indoor pollutant sources. *Atmos. Environ.* **1992**, *26A*, 2141–2148.

[35] Klepeis, N. E.; Nelson, W. C.; Ott, W. R.; Robinson, J. P.; Tsang, A. M.; Switzer, P.; Behar, J. V.; Hern, S. C.; Engelmann, W. H. The National Human Activity Pattern Survey (NHAPS): a resource for assessing exposure to environmental pollutants. *J. Expo. Anal. Environ. Epidemiol.* **2001**, *11*, 231–252.

[36] Schweizer, C.; Edwards, R. D.; Bayer-Oglesby, L.; Gauderman, W. J.; Ilacqua, V.; Jantunen, M. J.; Lai, H. K.; Nieuwenhuijsen, M.; Künzli, N. Indoor time–microenvironment–activity patterns in seven regions of Europe. *J. Exposure Anal. Environ. Epidemiol.* **2007**, *17*, 170–181.

[37] Koo, H. J.; Lee, B. M. Estimated exposure to phthalates in cosmetics and risk assessment. *J. Toxicol. Env. Heal. A* **2004**, *67*, 1901–1914.

[38] Koniecki, D.; Wang, R.; Moody, R. P.; Zhu, J. Phthalates in cosmetic and personal care products: Concentrations and possible dermal exposure. *Environ. Res.* **2011**, *111*, 329–336.

[39] Kelley, K. E.; Hernández-Díaz, S.; Chaplin, E. L.; Hauser, R.; Mitchell, A. A. Identification of phthalates in medications and dietary supplement formulations in the United States and Canada. *Environ. Health Perspect.* **2012**, *120*, 379–384.

[40] Guo, Y.; Wang, L.; Kannan, K. Phthalates and parabens in personal care products from China: Concentrations and human exposure. *Arch. Environ. Contam. Toxicol.* **2014**, *66*, 113–119.

[41] Liu, Z.; Little, J. C. Semivolatile organic compounds (SVOCs): Phthalates and flame retardants. In Toxicity of Building Materials; Pacheco-Torgal, F.; Jalali, S.; Fucic, A.; Eds. Woodhead Publishing: Oxford, 2012, 122–137.

[42] Shi, S.; Cao, J.; Zhang, Y.; Zhao, B. Emissions of phthalates from indoor flat materials in Chinese residences. *Environ. Sci. Technol.* **2018**, *52*, 13166–13173.

[43] Bergh, C.; Åberg, K. M.; Svartengren, M.; Emenius, G.; Östman, C. Organophosphate and phthalate esters in indoor air: a comparison between multi-storey buildings with high and low prevalence of sick building symptoms. *J. Environ. Monit.* **2011**, *13*, 2001–2009.

[44] Bergh, C.; Torgrip, R.; Emenius, G.; Östman, C. Organophosphate and phthalate esters in air and settled dust – a multi-location indoor study. *Indoor Air* **2011**, *21*, 67–76.

[45] Fujii, M.; Shinohara, N.; Lim, A.; Otake, T.; Kumagai, K.; Yanagisawa, Y. A study on emission of phthalate esters from plastic materials using a passive flux sampler. *Atmos. Environ.* **2003**, *37*, 5495–5504.

[46] Clausen, P. A.; Liu, Z.; Kofoed-Sørensen, V.; Little, J.; Wolkoff, P. Influence of temperature on the emission of di-(2-ethylhexyl)phthalate (DEHP) from PVC flooring in the emission cell FLEC. *Environ. Sci. Technol.* **2012**, *46*, 909–915.

[47] Liu, C.; Morrison, G. C.; Zhang, Y. Role of aerosols in enhancing SVOC flux between air and indoor surfaces and its influence on exposure. *Atmos. Environ.* **2012**, *55*, 347–356.

[48] Weschler, C. J.; Nazaroff, W. W. Semivolatile organic compounds in indoor environments. *Atmos. Environ.* **2008**, *42*, 9018–9040.

[49] Weschler, C. J.; Nazaroff, W. W. SVOC partitioning between the gas phase and settled dust indoors. *Atmos. Environ.* **2010**, *44*, 3609–3620.

[50] Liu, C.; Shi, S.; Weschler, C.; Zhao, B.; Zhang, Y. Analysis of the dynamic interaction between SVOCs and airborne particles. *Aerosol Sci. Technol.* **2013**, *47*, 125–136.

[51] Benning, J. L.; Liu, Z.; Tiwari, A.; Little, J. C.; Marr, L. C. Characterizing gas-particle interactions of phthalate plasticizer emitted from vinyl flooring. *Environ. Sci. Technol.* **2013**, *47*, 2696–2703.

[52] Lazarov, B.; Swinnen, R.; Poelmans, D.; Spruyt, M.; Goelen, E.; Covaci, A.; Stranger, M. Influence of suspended particles on the emission of organophosphate flame retardant from insulation boards. *Environ. Sci. Pollut. Res.* **2016**, *23*, 17183–17190.

[53] Wu, Y.; Eichler, C. M. A.; Cao, J.; Benning, J.; Olson, A.; Chen, S.; Liu, C.; Vejerano, E. P.; Marr, L. C.; Little, J. C. Particle/gas partitioning of phthalates to organic and inorganic airborne particles in the indoor environment. *Environ. Sci. Technol.* **2018**, *52*, 3583–3590.

[54] Kristensen, K; Lunderberg, D. M.; Liu, Y; Misztal, P. K.; Tian, Y; Arata, C; Nazaroff, W. W.; Goldstein, A. H. Sources and dynamics of semivolatile organic compounds in a single-family residence in northern California. *Indoor Air* **2019**, *20*, 645–655.

[55] Guo, Z. A framework for modelling non-steady-state concentrations of semivolatile organic compounds indoors–I: Emissions from diffusional sources and sorption by interior surfaces. *Indoor Built Environ.* **2013**, *22*, 685–700.

[56] Guo, Z. A framework for modelling non-steady-state concentrations of semivolatile organic compounds indoors–II. Interactions with particulate matter. *Indoor Built Environ.* **2014**, *23*, 26–43.

[57] Shi, S.; Zhao, B. Modeled exposure assessment via inhalation and dermal pathways to airborne semivolatile organic compounds (SVOCs) in residences. *Environ. Sci. Technol.* **2014**, *48*, 5691–5699.

[58] Wei, W.; Mandin, C.; Ramalho, O. Influence of indoor environmental factors on mass transfer parameters and concentrations of semi-volatile organic compounds. *Chemosphere* **2018**, *195*, 223–235.

[59] Zhao, Y.; Kresiberg, N. M.; Worton, D. R.; Teng, A. P.; Hering, S. V.; Goldstein, A. H. Development of an in situ thermal desorption gas chromatography instrument for quantifying atmospheric semi-volatile organic compounds. *Aerosol Sci. Technol.* **2013**, *47*, 258–266.

[60] Kreisberg, N. M.; Worton, D. R.; Zhao, Y.; Isaacman, G.; Goldstein, A. H.; Hering, S. V. Development of an automated high-temperature valveless injection system for online gas chromatography. *Atmos. Meas. Tech.,* **2014**, *7*, 4431–4444.

[61] Isaacman, G.; Kreisberg, N. M.; Yee, L. D.; Worton, D. R.; Chan, A. W. H.; Moss, J. A.; Hering, S. V.; Goldstein, A. H. Online derivatization for hourly measurements of gas- and particle-phase semi-volatile oxygenated organic compounds by thermal desorption aerosol gas chromatography (SV-TAG). *Atmos. Meas. Tech.* **2014**, *7*, 4417–4429.

[62] Isaacman-VanWertz, G.; Yee, L. D.; Kreisberg, N. M.; Wernis, R.; Moss, J. A.; Hering, S. V.; de Sá, S. S.; Martin, S. T.; Alexander, M. L.; Palm, B. B.; Hu, W.; Campuzano-Jost, P.; Day, D. A.; Jimenez, J. L.; Riva, M.; Surratt, J. D.; Viegas, J.; Manzi, A.; Edgerton, E.; Baumann, K.; Souza, R.; Artaxo, P.; Goldstein, A. H. Ambient gas-particle partitioning of tracers for biogenic oxidation. *Environ. Sci. Technol.* **2016**, *50*, 9952–9962.

[63] Yee, L. D.; Isaacman-VanWertz, G.; Wernis, R. A.; Meng, M.; Rivera, V.; Kreisberg, N. M.; Hering, S. V.; Bering, M. S.; Glasius, M.; Upshur, M. A.; Gray Bé, A.; Thomson, R. J.; Geiger, F. M.; Offenberg, J. H.; Lewandowski, M.; Kourtchev, I.; Kalberer, M.; de Sá, S.; Martin, S. T.; Alexander, M. L.; Palm, B. B.; Hu, W.; Campuzano-Jost, P.; Day, D. A.; Jimenez, J. L.; Liu, Y.; McKinney, K. A.; Artaxo, P.; Viegas, J.; Manzi, A.; Oliveira, M. B.; de Souza, R.; Machado, L. A. T.; Longo, K.; and Goldstein, A. H. Observations of sesquiterpenes and their oxidation products in central Amazonia during the wet and dry seasons. *Atmos. Chem. Phys.* **2018**, *18*, 10433–10457.

[64] Zhou, J.; Chen, A.; Cao, Q.; Yang, B.; Chang, V. W.-C.; Nazaroff, W. W. Particle exposure during the 2013 haze in Singapore: Importance of the built environment. *Build. Environ.* **2015**, *93*, 14–23.

[65] Hu, M.; Peng, J.; Sun, K.; Yue, D.; Guo, S.; Wiedensohler, A.; Wu, Z. Estimation of size-resolved ambient particle density based on the measurement of aerosol number, mass, and chemical size distributions in the winter in Beijing. *Environ. Sci. Technol.* **2012**, *46*, 9941–9947.

[66] Dodson, R. E.; Bessonneau, V.; Udesky, J. O.; Nishioka, M.; McCauley, M.; Rudel, R. A. Passive indoor air sampling for consumer product chemicals: a field evaluation study. *J. Expo. Sci. Environ. Epidemiol.* **2019**, *29*, 95–108.

[67] Liu, Y.; Misztal, P. K.; Xiong, J.; Tian, Y.; Arata, C.; Weber, R. J.; Nazaroff, W. W.; Goldstein, A. H. Characterizing sources and emissions of volatile organic compounds in a northern California residence using space-and time-resolved measurements. *Indoor Air* **2019**, *29*, 630–644.

[68] Salthammer, T.; Zhang, Y.; Mo, J.; Koch, H. M.; Weschler, C. J. Assessing human exposure to organic pollutants in the indoor environment. *Angew. Chem. Int. Ed.* **2018**, *57*, 12228–12263.

[69] Weschler, C. J.; Nazaroff, W. W. Growth of organic films on indoor surfaces. *Indoor Air* **2017**, *27*, 1101–1112.

[70] Wu, Y.; Eichler, C. M. A.; Chen, S.; Little, J. C. Simple method to measure the vapor pressure of phthalates and their alternatives. *Environ. Sci. Technol.* **2016**, *50*, 10082–10088.

[71] Thatcher, T. L.; Layton, D. W. Deposition, resuspension, and penetration of particles within a residence. *Atmos. Environ.* **1995**, *29*, 1487–1497.

[72] Xu, Y; Little, J. C. Predicting emissions of SVOCs from polymeric materials and their interaction with airborne particles. *Environ. Sci. Technol.* **2006**, *40*, 456–461.

[73] Cao, X.-L. Phthalate esters in foods: sources, occurrence, and analytical methods. *Compr. Rev. Food Sci. F.* **2010**, *9*, 21–43.

[74] Salthammer, T.; Goss, K.-U. Predicting the gas/particle distribution of SVOCs in the indoor environment using poly parameter linear free energy relationships. *Environ. Sci. Technol.* **2019**, *53*, 2491–2499.

2.7 Supporting Information

2.7.1 SV-TAG Operation

In this study, the SV-TAG resided in an external temperature-controlled shed built specifically to contain instrumentation throughout the campaign. The SV-TAG unit was situated approximately 0.5 m from the residence. The SV-TAG instrument is equipped with two sampling cells that are operated in parallel. One sampling cell was dedicated to measuring indoor gas-plus-particle concentrations. It sampled through a 1.6-m stainless steel inlet extending from the house's dining room. The inlet was positioned approximately 30 cm from the exterior room wall and 1.5 m above the floor. A second cell alternately collected indoor air from the same indoor inlet or from a separate outdoor air sampling port through a 2.0-m stainless steel tube extending outside the shed. The second cell was switched hourly among four states: indoor gas-plus-particle, indoor particle only, outdoor gas-plus-particle, and outdoor particle only, with a complete cycle occurring every four hours. Gas-phase removal for the particle-only measurements was accomplished by passing sample air through a carbon monolith denuder (500 channels, 30 mm OD $\times$ 40.6 cm; MAST Carbon) thereby removing all gas-phase organic compounds from the air stream before collection. Particle-only measurements (and corresponding gas-particle partitioning measurements) determined by the denuder method have, if any, a negative bias due to repartitioning and loss within the denuder.[1] Gas-particle partitioning of phthalates may be influenced by sorption of gas-phase species to sampling lines; however, past investigations indicate that such biases are minimal for the experimental conditions of this study.[2,3] Concurrent gas-plus-particle measurements in the two cells were used to normalize any cell differences when quantifying gas-particle partitioning. This cell-correction factor was adjusted downwards in the case of DEHP such that gas-particle partitioning maximized at 100% in the particle phase.

Both cells sampled air at 10 L min^{-1} through a PM2.5 cyclone (BGI, Inc.; SCC 2.654) for the first 15 minutes of each hour for the duration of the campaign. During sampling, the cell temperatures were controlled at 30 °C. After sample collection, the captured organic mass was thermally desorbed by raising the collection cell temperature to 320 °C. The organic mass was carried by helium gas saturated with a derivatization agent, MSTFA (N-methyl-N-(trimethylsilyl)trifluoroacetamide, > 98.5%, Sigma Aldrich), towards a concentrating trap before valveless injection into an Agilent 7890A gas chromatograph. Separation was achieved by linearly ramping the temperature (50 °C to 330 °C, over 14 minutes) with helium flow (0.5 standard cm^3 min^{-1} to 1.0 standard cm^3 min^{-1} through minute 12, then 1.0 standard cm^3 min^{-1} to 3.0 standard cm^3 min^{-1} to the end) through the column (Restek, Rtx-5Sil MS, 20 m $\times$ 0.18 mm $\times$ 0.18 μm). Species exited from the column into an Agilent 5975C quadrupole mass spectrometer (MS) for subsequent electron impact (EI) analysis. Mass spectral interpretation and quantification used a single-ion peak fitting approach via the TERN software.[4]

Time-resolved measurements of DEP, DIBP, DBP, and DEHP were acquired hourly. Peak areas were normalized by deuterated internal standards to account for cell-loading matrix

effects and a general ion source decline over the duration of the field campaign. DBP, DIBP, and DEHP were normalized to dibutyl phthalate-3,4,5,6-d4 (Sigma Aldrich), a deuterated analogue of DBP. DEP was normalized to a deuterated isotopologue of pentadecanol, considering similarities in retention time. Absolute concentrations were determined by multipoint linear calibration curves with a zero-point intercept that were generated every four days during the campaign. Calibration standards from the EPA 525 update phthalate esters mix were added to a 50/50 methanol/chloroform solution with other relevant chemical standards. Limits of detection (LODs), set at 3× the background chromatographic signal, are analyte dependent and variable depending on acquisition parameters, instrument status, chromatographic coelutions, and matrix interferents. These same factors affect uncertainties, which are typically less than 20% on a relative scale.[5] Typical LODs for DEP, DIBP, and DBP were on the order of 10 ng m^{-3}. Typical LODs for DEHP were on the order of 1 ng m^{-3}.

Throughout the campaign, three phthalate species (DEP, DBP, and DEHP) were identified by authentic external standards and a fourth (DIBP) was identified referencing mass spectra available in the NIST/EPA/NIH Mass Spectral Library.[6, 7] Major phthalate species, excluding dimethyl phthalate, have a prominent characteristic ion at $m/z = 149$. This characteristic ion was used to search for other phthalate species during periods with high temperature and high particle mass concentrations, when phthalate concentrations are expected to be highest. No additional species above background chromatographic signal were identified as phthalates; see Figure 2.7.1 of the Supporting Information.

2.7.2 SV-TAG Quality Assurance and Quality Control

Method blanks were conducted at the beginning, middle, and end of the sampling campaign by injecting pure solvent containing only deuterated internal standards onto the thermal desorption collection cells via an automated liquid injection system. Possible contamination of blanks by phthalates could occur from incomplete desorption of the collection cells, or from release of plastic components within the SV-TAG system. Such artifacts were minimally observed. Measured phthalate signals during method blank measurements relative to the prior gas-plus-particle measurement were: DEP: $< 0.5\%$; DIBP: $<3\%$; DBP: $<4\%$; DEHP: $<5\%$.

The primary purpose of the internal standard was to account for any changes in the efficiency of the analytical system as a function of time during the experiment. A solvent solution containing 45 deuterated internal standards was injected onto the thermal desorption collection cell on top of each ambient air sample by an automated injection system. These internal standards encompassed a broad range of chemical functionalities and volatilities. All internal standards qualitatively showed similar trends, with decreased responses being observed as the campaign progressed owing to degraded performance of the mass spectrometer's ion-source as it become dirtier. Internal standard responses were restored after an ion-source cleaning. Some variability in response was also observed, presumably because of sample matrix effects; these were corrected based on the internal standard response.

External standards were run every 25 hours such that a three-point calibration curve was generated every three to four days. After internal standard normalization to account for changes in the mass spectrometer's ion-source and sample matrix effects, calibration curves did not significantly differ over the course of the measurement period.

Although particle densities are known to vary, such as during different types of source events, we assume a constant particle density of 1.67 g cm^{-3} in congruence with past studies.[8,9] Sensitivity testing was conducted by renormalizing particle mass concentrations using densities of 1 and 2 g cm^{-3}, approximately spanning the range of expected values. Using these extrema, the slope of Figure 2.4.3 could vary between 1.9 and 3.8 ng μg^{-1} (parts per thousand), the slope of Figure 2.4.4A could vary between 1.4 and 2.8 ng μg^{-1} (parts per thousand), and the resulting estimate of K_p^* in Figure 2.4.5 could vary between 2.0 and 4.0 m^3 μg^{-1}.

Non-representative house venting occurred between the occupied and vacant periods; four associated measurements were excluded from analysis. One single-point particle concentration determined from the Grimm 11-A particle counter on 21 Dec 2017 was similarly excluded. The point corresponded to the beginning of an emission event and may not have been fully representative of the house because of incomplete mixing.

2.7.3 Supporting Figures

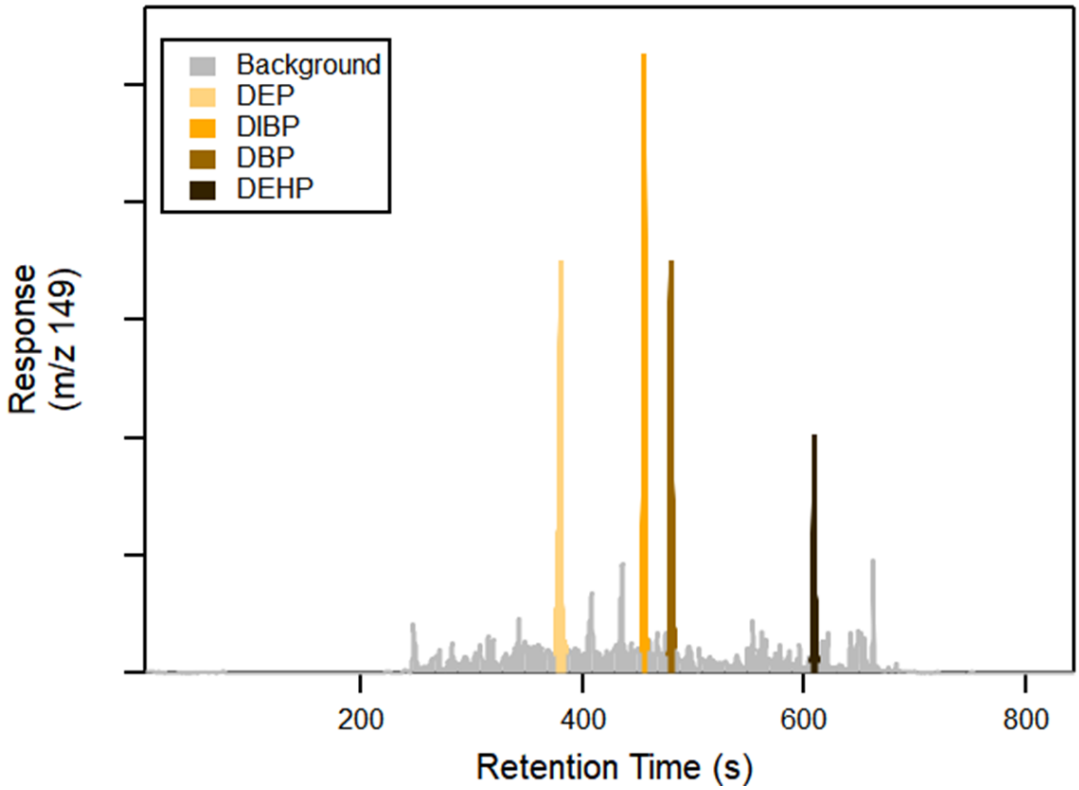

Figure 2.7.1: The response of ion m/z = 149 is plotted against the chromatograph retention time on 16 Dec 2017, a period of high particle loading when phthalate levels are expected to be elevated. Phthalate diesters (other than dimethyl phthalate) have a prominent characteristic ion at m/z = 149. In the above spectrum, DEP, DIBP, DBP, and DEHP were clearly identified in comparison to a mass spectral database and the known retention times of authentic external standards (EPA 525 phthalate esters update mix: DMP, DEP, DBP, DEHP, butyl benzyl phthalate). No other species above chromatographic background levels were identifiable as phthalates in reference to the NIST/EPA/NIH Mass Spectral Library over the selected analysis periods.

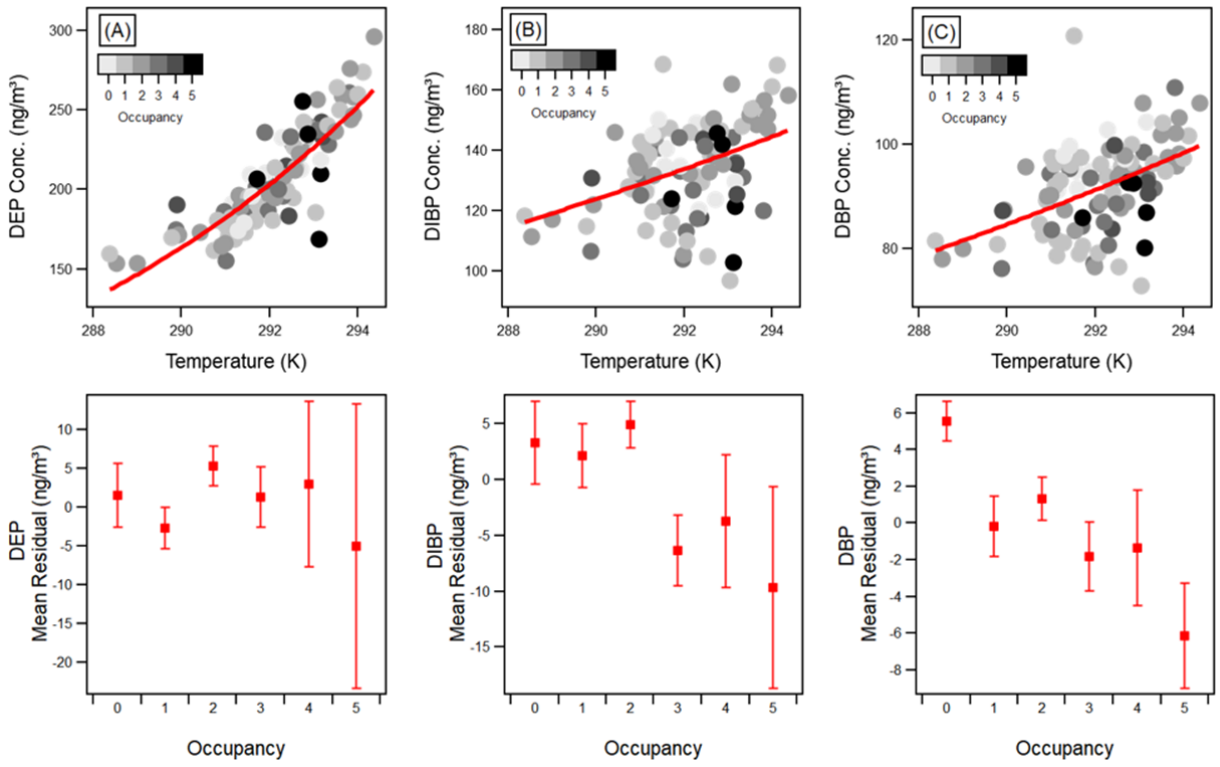

Figure 2.7.2: Upper: Total (gas-plus-particle) indoor phthalate concentrations are plotted against temperature during waking hours of the occupied period. Lower: The residuals of respective exponential fits are compared against residential occupancy, where uncertainties correspond to the standard error of the mean. Parameters of the exponential fits ($y = A \times e^{kx}$) are: $A = 3.5 \times 10^{-12}$, $k = 0.109$, $R^2 = 0.73$ (panel A), $A = 1.8 \times 10^{-3}$, $k = 0.038$, $R^2 = 0.15$ (panel B), $A = 1.6 \times 10^{-3}$, $k = 0.038$, $R^2 = 0.23$ (panel C). Units of measure on the fit parameters are inverse temperature for k (K^{-1}) and concentration for A (ng m^{-3}).

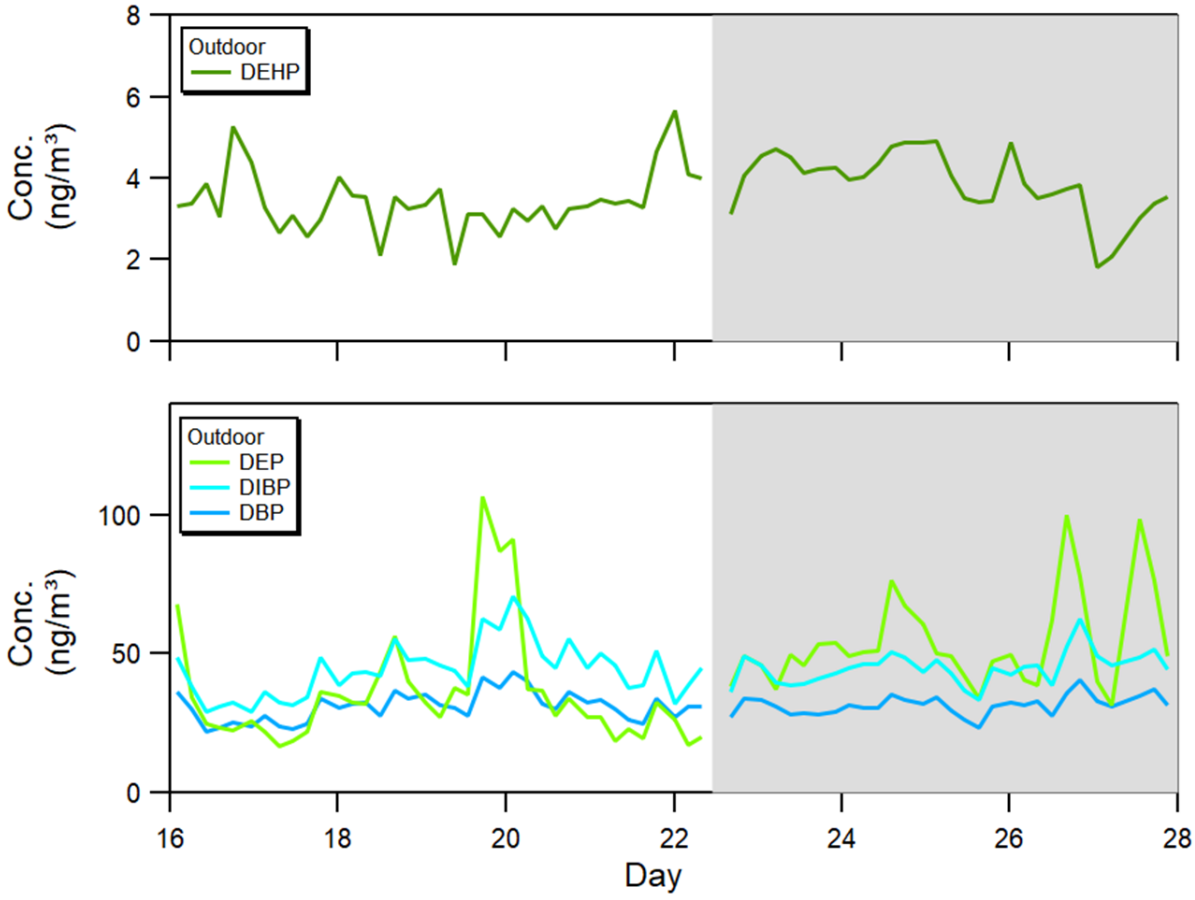

Figure 2.7.3: The gas-plus-particle outdoor concentrations of DEP, DIBP, DBP, and DEHP are displayed, where the shaded region corresponds to the vacant period.

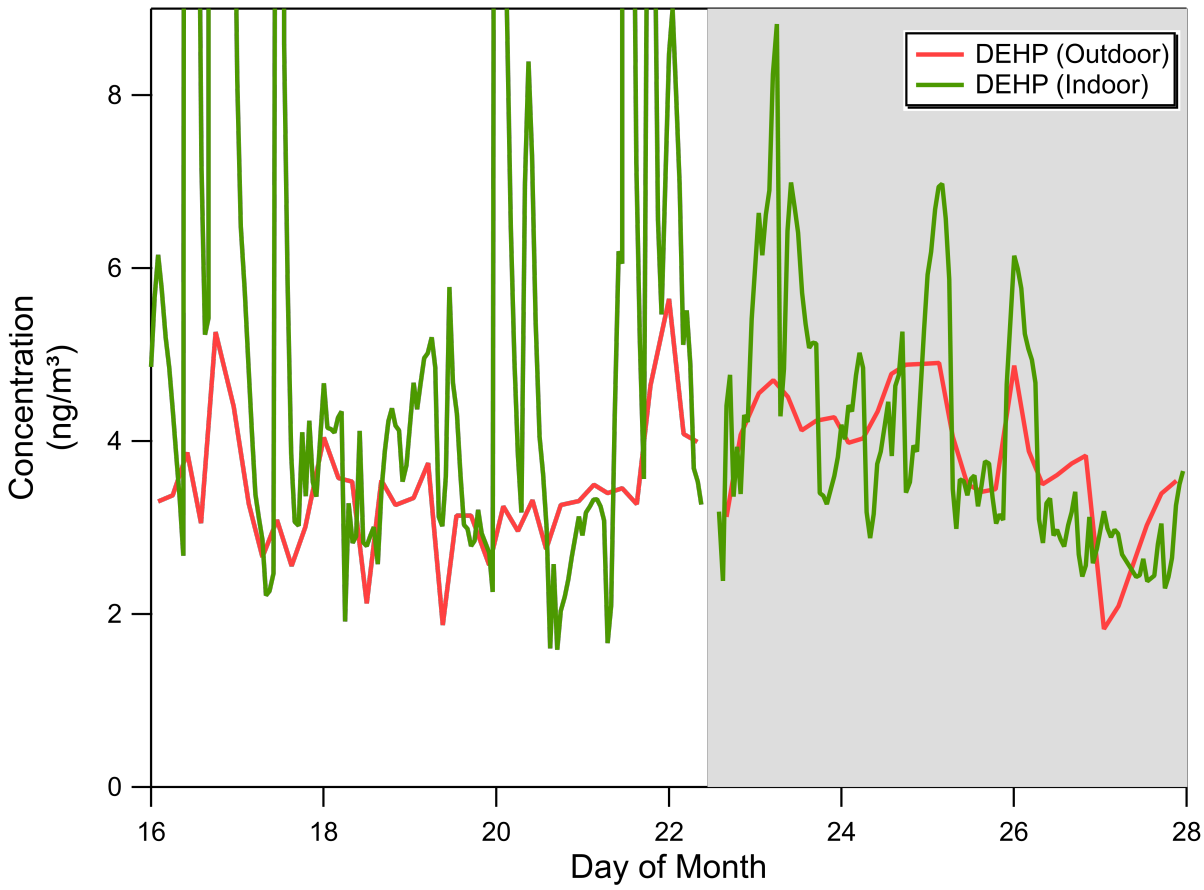

Figure 2.7.4: The total (gas-plus-particle) indoor and outdoor concentrations of DEHP are displayed, where the scaling emphasizes baseline concentrations and excludes episodic concentrations above 9 ng m^{-3}. The shaded region corresponds to the vacant period.

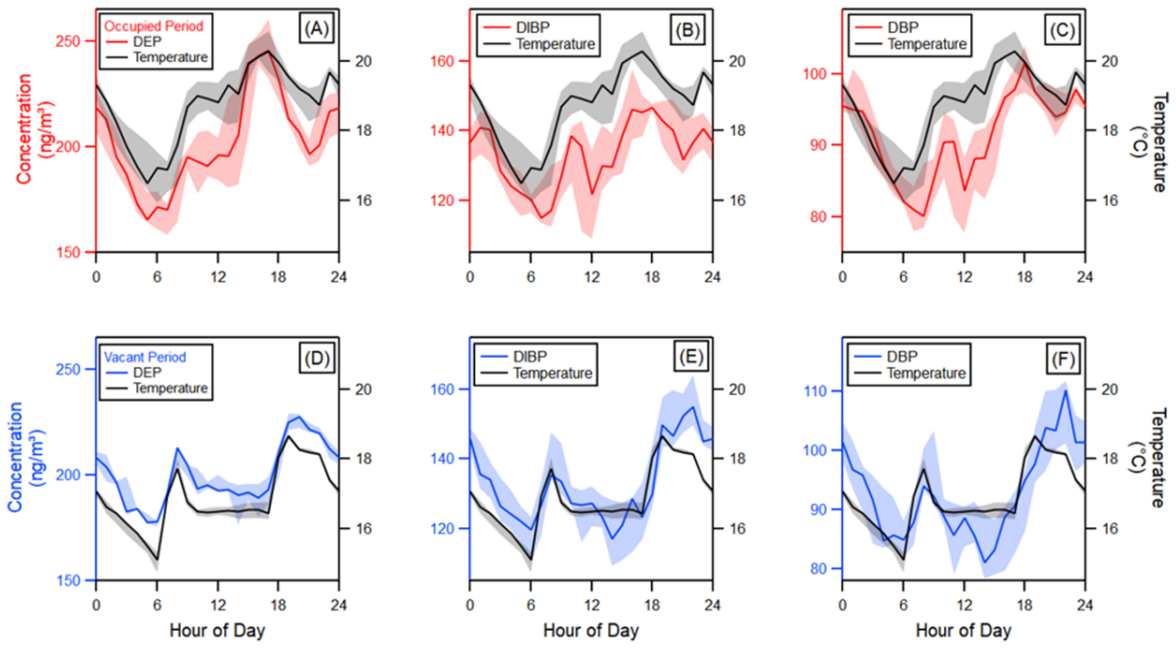

Figure 2.7.5: Diel plots (median, interquartile range by hour of day) are shown for gas-plus-particle DEP, DIBP, and DBP concentrations and indoor air temperature over the occupied (upper frames) and vacant (lower frames) periods.

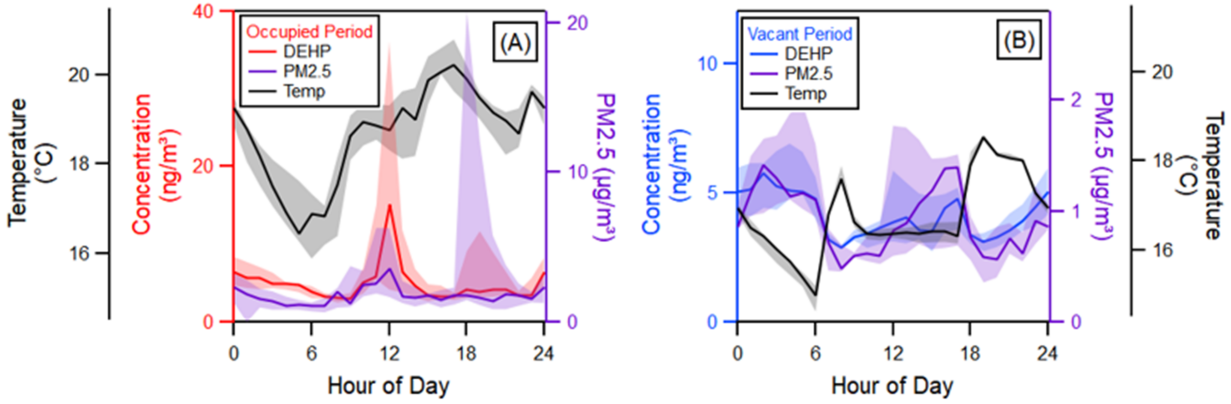

Figure 2.7.6: Diel plots (median, interquartile range by hour of day) are shown for gas-plus-particle DEHP concentrations and PM2.5 particle loading over the occupied (left frame) and vacant (right frame) periods.

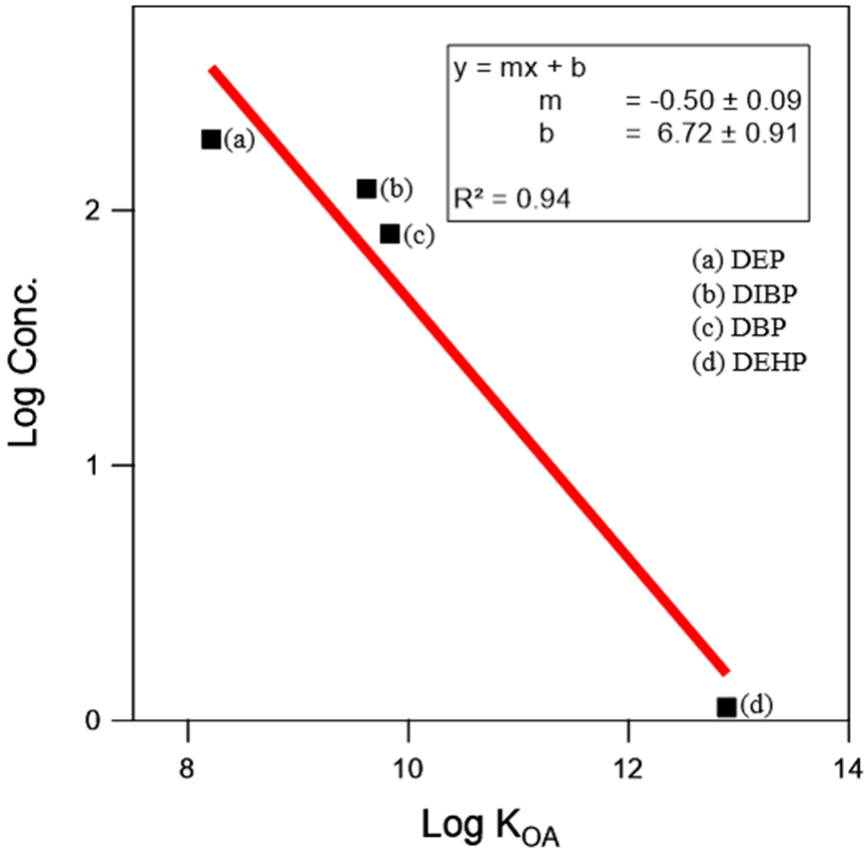

Figure 2.7.7: The median gas-phase concentration in ng m^{-3} of each phthalate species over the vacant period is compared against the octanol-air partition coefficient at T = 298 K (as reported by Salthammer et al.[10]) on a log-log scale. A linear least-squares fit of the transformed data is presented.

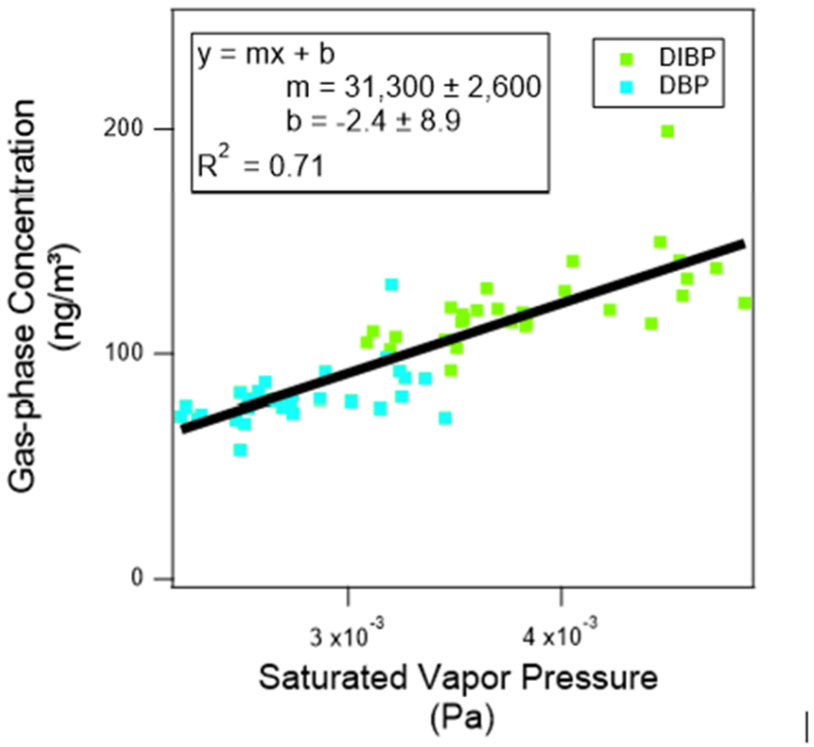

Figure 2.7.8: The measured gas-phase concentrations of DIBP and DBP are displayed against the calculated saturation vapor pressure at the measured indoor air temperature. Vapor pressures for DIBP and DBP as a function of temperature were calculated according to Wu et al.[11] Units of measure for the fit parameters are ng m^{-3} Pa^{-1} for the slope, m, and ng m^{-3} for the intercept, b.

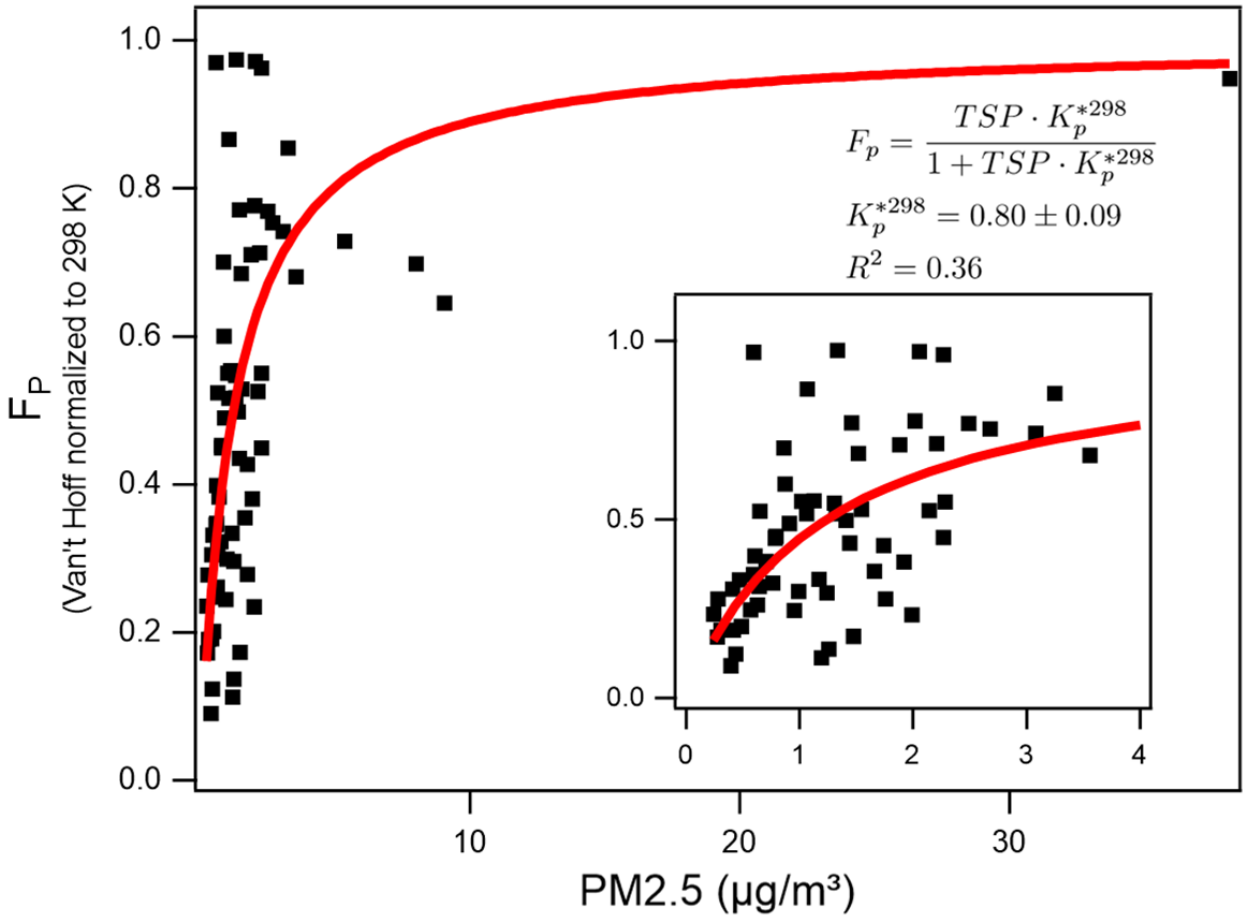

Figure 2.7.9: Each particle fraction value of DEHP is normalized from ambient air temperature to 298 K using the van't Hoff equation and assuming -116,700 J mol^{-1} as the phase-change enthalpy.[12] Normalized particle fractions are compared against PM2.5 mass concentrations as measured throughout the campaign. The inset panel highlights the dynamic region with PM2.5 concentrations between 0 and 4 µg m^{-3}. Three datapoints with experimentally determined F_p greater than one were defined to have maximum particle:gas fractions of 100:1 (i.e., $F_p = 0.99$) to facilitate the normalization process.

2.7.4 Supporting Information References

[1] Dhawan, S; Biswas, P. Sampling artifacts in denuders during phase partitioning measurements of semi-volatile organic compounds. *Aerosol Sci. Technol.* **2019**, *53*, 73–85.

[2] Zhao, Y.; Kresiberg, N. M.; Worton, D. R.; Teng, A. P.; Hering, S. V.; Goldstein, A. H. Development of an in situ thermal desorption gas chromatography instrument for quantifying atmospheric semi-volatile organic compounds, *Aerosol Sci. Technol.* **2013**, *47*, 258–266.

[3] Isaacman-VanWertz, G.; Yee, L. D.; Kreisberg, N. M.; Wernis, R.; Moss, J. A.; Hering, S. V.; de Sá, S. S.; Martin, S. T.; Alexander, M. L.; Palm, B. B.; Hu, W.; Campuzano-Jost, P.; Day, D. A.; Jimenez, J. L.; Riva, M.; Surratt, J. D.; Viegas, J.; Manzi, A.; Edgerton, E.; Baumann, K.; Souza, R.; Artaxo, P.; Goldstein, A. H. Ambient gas-particle partitioning of tracers for biogenic oxidation, *Environ. Sci. Technol.* **2016**, *50*, 9952–9962.

[4] Isaacman-VanWertz, G.; Sueper, D. T.; Aikin, K. C.; Lerner, B. M.; Gilman, J. B.; de Gouw, J. A.; Worsnop, D. R.; Goldstein A. H. Automated single-ion peak fitting as an efficient approach for analyzing complex chromatographic data. *J. Chromatogr. A* **2017**, *1529*, 81–92.

[5] Isaacman, G.; Kreisberg, N. M.; Yee, L. D.; Worton, D. R.; Chan, A. W. H.; Moss, J. A.; Hering, S. V.; Goldstein, A. H. Online derivatization for hourly measurements of gas- and particle-phase semi-volatile oxygenated organic compounds by thermal desorption aerosol gas chromatography (SV-TAG). *Atmos. Meas. Tech.* **2014**, *7*, 4417–4429.

[6] Yee, L. D.; Isaacman-VanWertz, G.; Wernis, R. A.; Meng, M.; Rivera, V.; Kreisberg, N. M.; Hering, S. V.; Bering, M. S.; Glasius, M.; Upshur, M. A.; Gray Bé, A.; Thomson, R. J.; Geiger, F. M.; Offenberg, J. H.; Lewandowski, M.; Kourtchev, I.; Kalberer, M.; de Sá, S.; Martin, S. T.; Alexander, M. L.; Palm, B. B.; Hu, W.; Campuzano-Jost, P.; Day, D. A.; Jimenez, J. L.; Liu, Y.; McKinney, K. A.; Artaxo, P.; Viegas, J.; Manzi, A.; Oliveira, M. B.; de Souza, R.; Machado, L. A. T.; Longo, K.; and Goldstein, A. H. Observations of sesquiterpenes and their oxidation products in central Amazonia during the wet and dry seasons. *Atmos. Chem. Phys.* **2018**, *18*, 10433–10457.

[7] Stein, S. E.; Mirokhin, Y.; Tchekhovskoi, D.; Mallard, W. National Institute of Standards and Technology (NIST) Mass Spectral Search Program for the NIST/EPA/NIH Mass Spectral Library, National Institute of Standards and Technology Standard Reference Data Program, Gaithersburg, 2014.

[8] Hu, M.; Peng, J.; Sun, K.; Yue, D.; Guo, S.; Wiedensohler, A.; Wu, Z. Estimation of size-resolved ambient particle density based on the measurement of aerosol number,

mass, and chemical size distributions in the winter in Beijing. *Environ. Sci. Technol.* **2012**, *46*, 9941-9947.

[9] Zhou, J.; Chen, A.; Cao, Q.; Yang, B.; Chang, V.W.C.; Nazaroff, W.W. Particle exposure during the 2013 haze in Singapore: Importance of the built environment, *Build. Environ.* **2015**, *93*, 14-23.

[10] Salthammer, T.; Zhang, Y.; Mo, J.; Koch, H. M.; Weschler, C. J. Assessing human exposure to organic pollutants in the indoor environment. *Angew. Chem., Int. Ed.* **2018**, *57*, 12228–12263.

[11] Wu, Y.; Eichler, C. M. A.; Chen, S.; Little, J. C. Simple method to measure the vapor pressure of phthalates and their alternatives. *Environ. Sci. Technol.* **2016**, *50*, 10082–10088.

[12] Salthammer, T.; Goss, K.-U. Predicting the gas/particle distribution of SVOCs in the indoor environment using poly parameter linear free energy relationships. *Environ. Sci. Technol.* **2019**, *53*, 2491–2499.

Chapter 3

Surface emissions modulate indoor SVOC concentrations through volatility-dependent partitioning

This chapter is adapted from:

Lunderberg, D.M.; Kristensen, K.; Tian, Y.; Arata, C.; Misztal, P.K.; Liu, Y.; Kreisberg, N.; Katz, E.F.; DeCarlo, P.F.; Patel, S.; Vance, M.E.; Nazaroff, W.W.; Goldstein, A.H. Surface emissions modulate indoor SVOC concentrations through volatility-dependent partitioning. *Environ. Sci. Technol.* **2020**, *54*, 6751–6760.

3.1 Abstract

Measurements by semivolatile thermal desorption aerosol gas chromatography (SV-TAG) were used to investigate how semivolatile organic compounds (SVOCs) partition among indoor reservoirs in (1) a manufactured test house under controlled conditions (HOMEChem campaign) and (2) a single-family residence when vacant (H2 campaign). Data for phthalate diesters and siloxanes suggest that volatility-dependent partitioning processes modulate airborne SVOC concentrations through interactions with surface-laden condensed-phase reservoirs. Airborne concentrations of SVOCs with vapor pressures in the range of C13 to C23 alkanes correlated with indoor air temperature. Observed temperature dependencies were quantitatively similar to theoretical predictions that assumed a surface-air boundary layer with equilibrium partitioning maintained at the air-surface interface. Airborne concentrations of SVOCs with vapor pressures corresponding to C25 to C31 alkanes correlated with airborne particle mass concentration. For SVOCs with higher vapor pressures, which are expected to be predominantly gaseous, correlations with particle mass concentration were weak or nonexistent. During primary particle emission events, enhanced gas-phase emissions from condensed-phase reservoirs partition to airborne particles, contributing substantially to

organic particulate matter. An emission event related to oven-usage was inferred to deposit siloxanes in condensed-phase reservoirs throughout the house, leading to the possibility of reemission during subsequent periods with high particle loading.

3.2 Introduction

In indoor environments, semivolatile organic compounds (SVOC) dynamically partition between the gas phase and various condensed-phase reservoirs, such as airborne particles, surface films, settled dust, and building materials.[1] Many specific indoor SVOCs are of concern for human health, such as endocrine-disrupting phthalate diesters and halogenated flame retardants.[2] Airborne particles are often partly composed of SVOCs. Exposure to particulate matter is among the leading global mortality risk factors,[3] although the specific roles of SVOCs and the relative importance of indoor particle exposure contributing to this risk are unknown. Understanding the dynamics and physical behavior of indoor airborne SVOC concentrations is important for risk assessment and exposure mitigation.

Emerging evidence indicates that interactions between indoor air and condensed-phase reservoirs influence airborne SVOC concentrations. Surface reservoirs are defined as "condensed-phase materials containing chemical constituents that undergo exchange with the gas phase."[4] Recent field measurements of volatile organic compounds (VOCs) and SVOCs in real indoor settings suggest that organics readily desorb from condensed-phase reservoirs into bulk air. The high rate of desorption suggests that, for many compounds, the condensed-phase reservoirs are either interior surface films or thin layers of building materials closely in contact with indoor air.[4–8] Weschler and Nazaroff described a model for the growth of SVOC-laden organic surface films indoors and suggested that surface films may provide functional and chemical homogeneity among the diverse surfaces interacting with bulk indoor air.[9]

Models describing indoor surface emissions have assumed the existence of a boundary layer immediately adjacent to surfaces, with equilibrium partitioning maintained at the surface-air interface.[10–14] Emissions from surfaces are then regulated by the concentration difference across the boundary layer combined with a convective mass transfer coefficient that limits mass transfer between the boundary layer and bulk air. In a chamber study of vinyl flooring, Clausen et al. noted that temperature was a primary factor controlling diethyl hexyl phthalate (DEHP) emissions.[14] Temperature changes affect equilibrium partitioning between the gas-phase and condensed-phase surface reservoirs, including surface films. Such processes have been characterized using thermodynamic models.[15–18]

Airborne particles may significantly influence SVOC emission rates from surfaces by transporting SVOC mass out of the boundary layer and/or by providing an airborne condensed-phase sink.[19] Chamber studies of organophosphate flame retardants and plasticizers have demonstrated similar partitioning phenomena whereby the presence of airborne particles enhances the rate of SVOC emissions from source materials.[20–22] Moreover, the affinity of SVOCs for airborne particles is affected by both SVOC and particle composition for phthalate diesters[22, 23] and for third-hand smoke (THS) species.[24] These findings have

been supported by measurements in real indoor environments for specific compounds. For example, in a study of a university classroom, DeCarlo et al. reported that increases in particle mass concentration led to increases in the concentrations of airborne THS species; they inferred that surface-sorbed THS species were transported through the gas phase onto aqueous airborne particles, with particle capacity influenced by acid-base processes.[25] Similarly, increases in DEHP concentrations were found to be associated with increased airborne particle concentrations in a normally occupied residence.[8]

Indoor environments are subject to dynamic changes in temperature and particle concentration as influenced by occupants, their activities, and building interactions with the outdoor environment. Indoor airborne SVOC concentrations may be modulated by both direct primary emissions and by indirect interactions with surfaces. Few studies have examined how airborne SVOC concentrations evolve in real indoor settings. In this paper, we report hourly SVOC concentrations from two field campaigns, H2 and HOMEChem, and we use these data to characterize SVOC volatility-dependent dynamics and partitioning. We focus on three specific species groupings: (a) total SVOC concentrations binned by volatility, (b) phthalate diesters, and (c) cyclic siloxanes. These emphases are intended to explore SVOC behavior as a bounded class and as discrete compounds with varying vapor pressures. The specific objectives of the study are: (a) to quantitatively describe indoor SVOC dynamics as functions of volatility, temperature, and particle loading; (b) to connect observations with predictions from theory and laboratory experiments; and (c) to evaluate the impact of surface emissions on airborne SVOC concentrations.

3.3 Experimental Methods

Data analysis from the H2 observational field campaign focuses on a period of vacancy in an otherwise normally occupied residence. At H2, SVOC concentrations are binned by volatility and compared against temperature and particle mass concentrations. The HOMEChem campaign was structured around controlled occupant activities in a research house. At HOMEChem, the physical behavior of two classes of compounds, phthalate diesters and cyclic siloxanes, is investigated in relation to their volatility.

3.3.1 Study Sites.

The H2 field campaign was conducted a single-family dwelling in Contra Costa County, California, from 7 December 2017 to 4 February 2018. In this residence, air temperature was regulated by a forced-air gas-fired furnace incorporating a MERV 13 filter that influenced indoor particle levels. The furnace operated under control of a programmable thermostat, with “on” periods occurring twice daily (06:45–07:15 and 17:45–22:00). The H2 site and field monitoring campaign are detailed elsewhere.[7, 8] The analysis here focuses on a five-day period (22–27 December) during which the house was unoccupied (the H2 ‘vacant period’).

The HOMEChem field campaign was conducted during June 2018 at the UTest House, a manufactured house located at the JJ Pickle Research Campus of the University of Texas at Austin. The three-bedroom, 111-m^2 facility was operated with an air-conditioning system set to maintain a constant indoor air temperature of ∼25 °C (298 K). A series of controlled experiments was conducted over the one-month campaign. Experiments were designed to explore the influence of cooking, cleaning, and occupancy on indoor air chemical composition. Two categories of experiments were undertaken. During 'sequential' experimental days, repeated 'stir fry cooking' or 'cleaning' experiments were conducted with intermittent venting periods to reset indoor conditions. 'Layered' experimental days simulated 'day-in-the-life' conditions for a residence, with meal preparation and cleaning occurring in a sequential manner without venting. Two high-emission 'layered' days were conducted to simulate 'Thanksgiving,' with more intensive cooking and occupancy of the type typical of the holiday meal in an American household. A full description of the HOMEChem campaign experimental design and an overview of all instrumental data acquisition is reported elsewhere.[26]

3.3.2 Instrumentation and Measurement Methods

The research reported here focuses on data acquired using semivolatile thermal desorption aerosol gas chromatography (SV-TAG), a dual-channel gas chromatograph mass spectrometer (GC-MS) that quantifies, with hourly time resolution, gas-phase and gas-plus-particle-phase concentrations of SVOCs with vapor pressures corresponding to alkanes between ∼C14 and ∼C35.[27–29] SV-TAG collected the PM2.5 particle fraction, excluding larger particles by means of a cyclone (BGI by Mesa Labs, SCC 2.654). After each sampling period (15 minutes at H2, 20 minutes at HOMEChem), the captured analytes are thermally desorbed from the collection cells, separated based on volatility using a gas chromatograph (Agilent 7890A) and analyzed using a 70-eV electron ionization (EI) mass spectrometer (Agilent 5975C). Measurements are repeated automatically at hourly intervals. SV-TAG was deployed during the H2 and HOMEChem campaigns. Operating and sampling parameters during the H2 campaign are described in the SI (Table 3.7.1) and in prior publications.[7, 8] Operating parameters during the HOMEChem campaign were unchanged from the H2 campaign. Sampling parameters during HOMEChem are described in Table 3.7.2 and in Farmer et al.[26] Characteristic ions of most species were integrated using the TERN software, normalized to relevant internal standards, and calibrated against authentic external standards.[30] Quantification of low-volatility siloxanes (Figure 3.7.1), for which authentic external standards were not available, is described in the SI.

At HOMEChem, particle number concentrations were quantified by two separate scanning mobility particle sizers, with one implementing a nano differential mobility analyzer (4-105 nm: TSI 3080 EC + 3085 nano-DMA + 3788 water CPC) and one implementing a long differential mobility analyzer (105-532 nm: TSI 3080 EC + 3081 long-DMA + 3787 water CPC). Size-resolved concentrations of larger particles (diameter > 542 nm) were determined by an aerodynamic particle sizer (TSI 3321). At H2, particle number concentrations were quantified by a Grimm 11-A optical particle counter reporting time-resolved measure-

ments in 31 size-segregated bins with particle diameters ranging from 0.25 to 32 μm. For the HOMEChem study, an assumed particle density of 1 g cm^{-3} (similar to the density of cooking-related aerosol) was used for consistency with other work.[31, 32] The present work similarly assumed a particle density of 1 g cm^{-3} at the H2 site for internal consistency. (A density of 1.67 g cm^{-3} was assumed in prior published work at the H2 site.[8, 33, 34]) The presence of particle-bound siloxanes was confirmed with supporting measurements from a high-resolution time-of-flight aerosol mass spectrometer (HR-ToF-AMS), with experimental details available in the SI (Figure 3.7.2).

3.3.3 SVOC Integration

The chromatographic signal from SV-TAG was converted into total SVOC concentrations following the approach of Kristensen et al.[7] In the present work, the chromatogram was subdivided into bins where bin borders were defined by the midpoints of the retention times of adjacent alkanes. Then, each bin was normalized to the closest alkane internal standard in retention time and quantified using calibration curves prepared for the closest alkane in retention time (Figure 3.3.1). Normalization by internal standards is needed to account for a general decline in ion-source response (restorable by source-cleaning) and for matrix loading effects. Alkane-internal standards are used as the closest surrogate for each SVOC-bin in volatility space but may not be fully representative for highly polar compounds contained within each bin. The retention time is closely related to compound volatility, although other parameters, such as polar interactions with the column, can influence retention. Summing all bins and subtracting blank 'internal-standard only' measurements yielded the 'total SVOC' concentration. SV-TAG incorporates in-situ derivatization in its analytical procedure, which may affect the retention time of derivatized compounds. The derivatization agent, N-methyl-N-(trimethylsilyl)trifluoroacetamide (MSTFA), reacts with hydroxy groups such as carboxylic acids, alcohols, sugars, and similar analytes, and replaces active hydrogen atoms with trimethylsilyl groups. Silylation occurs for only a small subset of captured analytes and generally shifts the retention time by no more than 1-2 alkane-equivalent volatility bins. Most of the volatility bins are expected to be captured by the collection and thermal desorption (CTD) cell with negligible loss through the collection and transfer processes. Collection efficiencies of gas-phase organics on the CTD cell are expected to be high (80-100% for most measured compounds). Transfer efficiencies off the CTD cell and focusing trap were >95% for the C15 – C26 alkanes and decreased to 50% by the C32 alkane, while the transfer efficiency of the C14 alkane was 40%. The uncharacterized C13 alkane transfer efficiency is expected to be lower.[27] Quantitative corrections for transfer losses were made using deuterated alkane internal standards deposited on the CTD cell and analyzed with every sample.

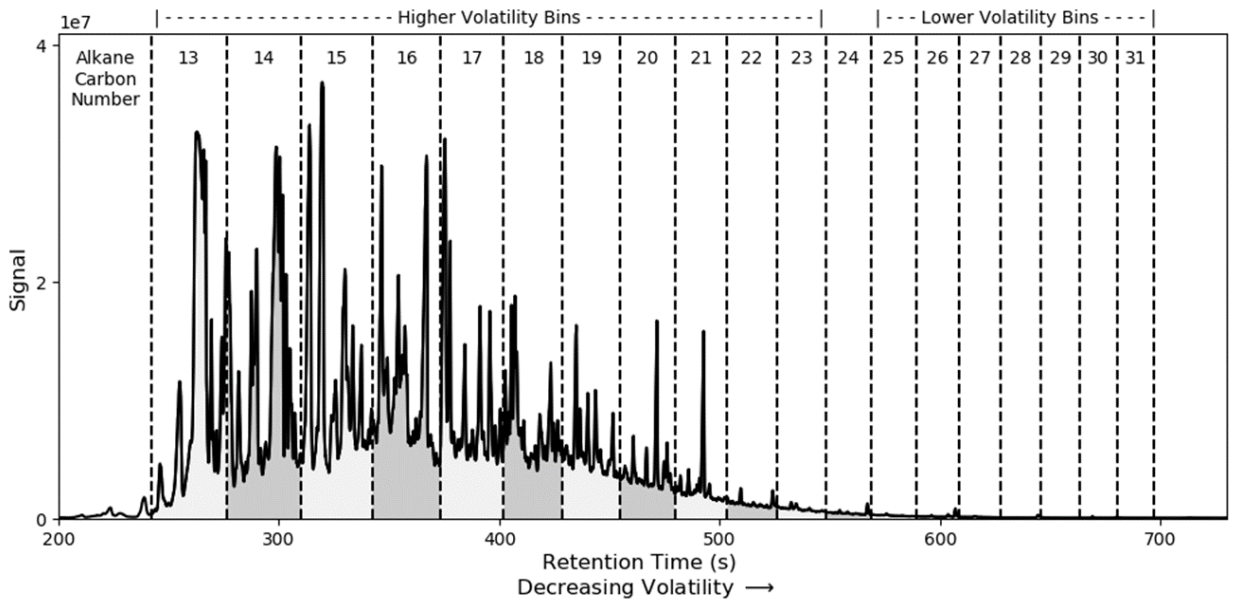

Figure 3.3.1: Quantified bins of the SV-TAG chromatogram are displayed for a typical chromatogram. Bins were subdivided and quantified based on the closest alkane in retention time.

3.3.4 Modeling Temperature Dependence of Gaseous SVOCs

Past models have been developed to estimate gas-phase SVOC concentrations in two separate cases.[35] In one case, SVOCs are emitted from surfaces when additive SVOCs are released from a parent material, such as in the case of plasticizers. Then, Equation 3.1 describes the gas-phase concentration y, where h is the convective mass-transfer coefficient over the emission surface, y_0 is the gaseous SVOC concentration immediately adjacent to the surface, A is the source surface area, and Q^* is the "equivalent ventilation rate," a parameter related to the ventilation rate that accounts for particle-associated removal and is described more thoroughly in the SI.

$$y = \frac{h \times y_0 \times A}{h \times A + Q^*} \tag{3.1}$$

In another case, SVOCs can be emitted from surfaces when a previously sorbed or otherwise deposited SVOC is released from that surface, such as in the case of pesticide or water-repellant treatments. This process occurs over two phases. For each phase, Equation 3.2 describes the gas-phase SVOC concentration, where A_s refers to the sorbing interior surface area and h_s is the convective mass-transfer coefficient over interior surfaces.

$$y = \frac{h \times y_0 \times A}{h \times A + h_s \times A_s + Q^*} \tag{3.2}$$

Under variable temperature, changes in y across the observed temperature range (288 – 292 K) are assumed to be governed by changes in the equilibrium constant controlling y_0, as described in Equation 3.3 where $[SVOC_{\text{surf}}]$ is the condensed-phase SVOC concentration at the surficial interface.

$$K_{\text{eq}}(T) = \frac{y_0}{[SVOC_{\text{surf}}]} \tag{3.3}$$

Such changes in equilibrium partitioning are anticipated to be similar to those described by the van't Hoff equation as shown in equation 3.4, where T is temperature, ΔS is the entropy of vaporization, R is the gas constant, and k is a constant described by $-\Delta H R^{-1}$, where $-\Delta H$ is the heat of vaporization.[18]

$$K_{\text{eq}}(T) = \exp\left[\frac{\Delta S}{R} + k\left(\frac{1}{T}\right)\right] \tag{3.4}$$

We present a model describing gas-phase SVOC concentrations based on the framework developed in Equations 3.1–3.4. Then, y as a function of temperature is described by Equation 3.5, where a is a variable containing terms that are generally independent of temperature. A full derivation of Equation 3.5 is available in the SI. Because the van't Hoff equation applies to equilibrium partitioning of a pure material and the studied indoor physical system consists of a complex mixture, we refer to experimentally derived k values as k^*.

$$y(T) = a \times \exp\left[k^*\left(\frac{1}{T}\right)\right] \tag{3.5}$$

3.4 Results and Discussion

At H2, SVOC concentrations were determined for chromatographic bins corresponding to the volatility of the nearest alkane in retention time ('alkane-equivalent volatility bin'). Estimated vapor pressures and saturation concentrations (C^*) for each bin are reported in Table 3.7.3. Concentrations are reported for the vacant period when no occupant activities, such as cooking or cleaning, occurred. Departures from steady-state conditions during the vacant period are likely to occur with (1) controlled indoor temperature changes related to the home heating system and (2) changes in indoor air PM2.5 concentrations. During the period of vacancy, indoor primary particles are expected to originate only from infiltration of outdoor particles and not from any indoor source.[8] Observed dynamic behavior of SVOCs was separated into two categories based on volatility: the C13-C23 bins, which are predominantly gaseous and display dependence on temperature, and the C25-C31 bins, which partition appreciably into airborne particles and display dependence on particle concentration.

3.4.1 Abundance of Higher Volatility SVOCs is Associated with Temperature

During the vacant period at H2, observed total (gas-plus-particle) SVOC concentrations of the C13-C23 bins generally decreased with decreasing volatility. Average concentrations and associated summary statistics of each alkane-equivalent volatility bin are reported in Table 3.7.3. Concentrations in the C23 bin were roughly fifty times lower than concentrations in the C13 bin. In Figure 3.4.1, SVOC concentrations are compared binwise against indoor air temperature, with ordinary least squares regression lines superimposed. For the C13-C23 bins (C13-C22 shown), SVOC concentrations showed statistically significant positive variation with temperature. Furthermore, the magnitude of the fitted slopes tended to decrease with decreasing bin volatility. Significant positive variation with temperature was not observed beyond the C23 bin. Time series and comparisons against temperature for each bin are shown in the SI (Figures 3.7.3, 3.7.4).

Observed temperature dependencies can be connected to the model described in equation (5). Predicted k^* values were calculated from literature values for alkane heats of vaporization, which correlate with vapor pressure.[37, 38] Experimental k^* values are within 50% of predicted k^* values, a remarkably close correspondence (Figure 3.7.5). Discrepancies between the two values may arise because the vapor pressures of the measured organics differ from alkane vapor pressures and because the studied system involves vaporization from a complex mixture rather than from a pure condensed phase. Furthermore, the application of equation (5) requires that emissions from surfaces are the dominant source process. Larger differences between the experimental and predicted values of k^* are observed for the C21 and C22 alkane-equivalent volatility bins. Other factors, such as appreciable interactions with airborne particles, are expected to partially account for this observation.

3.4.2 Abundance of Lower Volatility SVOCs is Associated with Particle Concentration

During the vacant period at H2, consistent associations between total airborne SVOC concentrations and particle mass concentration were observed for the C25-C31 bins (Figure 3.4.2). We stress that SV-TAG samples only the PM2.5 particle fraction; coarse-mode particles (as observed during resuspension events) likely have a different chemical composition than PM2.5, which may alter equilibrium partition behavior. Furthermore, equilibration time scales are slower for larger particles and faster for smaller particles. As such, equilibration is less likely to be achieved during the time of indoor suspension for coarse particles as compared to fine particles.[36] Time series and comparisons against particle mass concentrations for each bin are shown in the SI (Figures 3.4.2, 3.4.5). These bins had substantial fractions ($\sim$0.4 to $\sim$1.0) of airborne mass in the particle-phase (Table 3.7.3). Conversely, positive associations between SVOC concentrations and particle mass concentration were not observed for the C13-C23 bins. SVOCs contained in these higher volatility bins were predominantly in the gas-phase and are not expected to strongly partition to particles. The

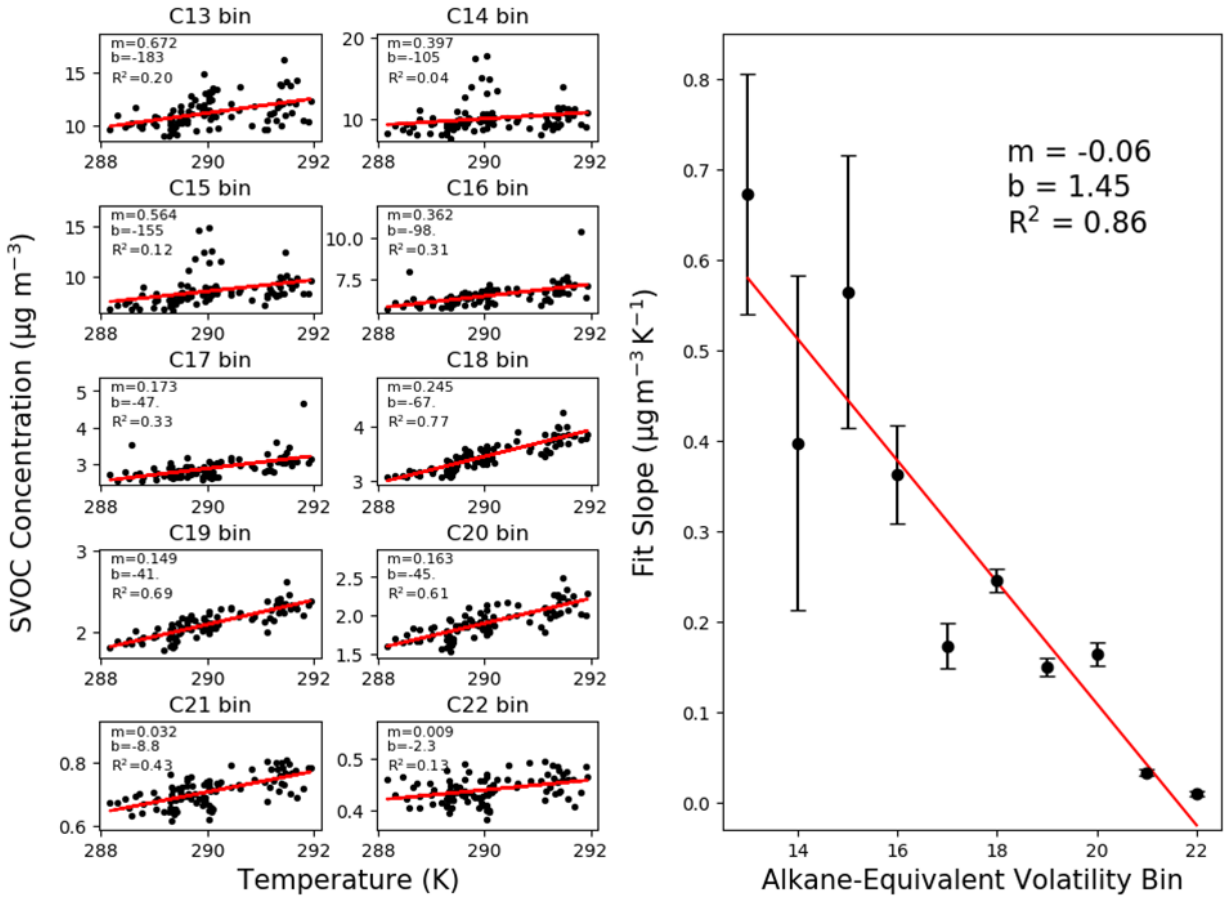

Figure 3.4.1: In the left panel, total (gas-plus-particle) SVOC concentrations (μg m^{-3}) are compared against temperature. Each measured point represents a 15-minute sample collection period with hourly replication during the observational period. Units of measure for the linear fit slope and intercept are μg K^{-1} m^{-3} and μg m^{-3}, respectively. In the right panel, the magnitude of the linear fit slope is compared against the corresponding alkane-equivalent volatility bin.

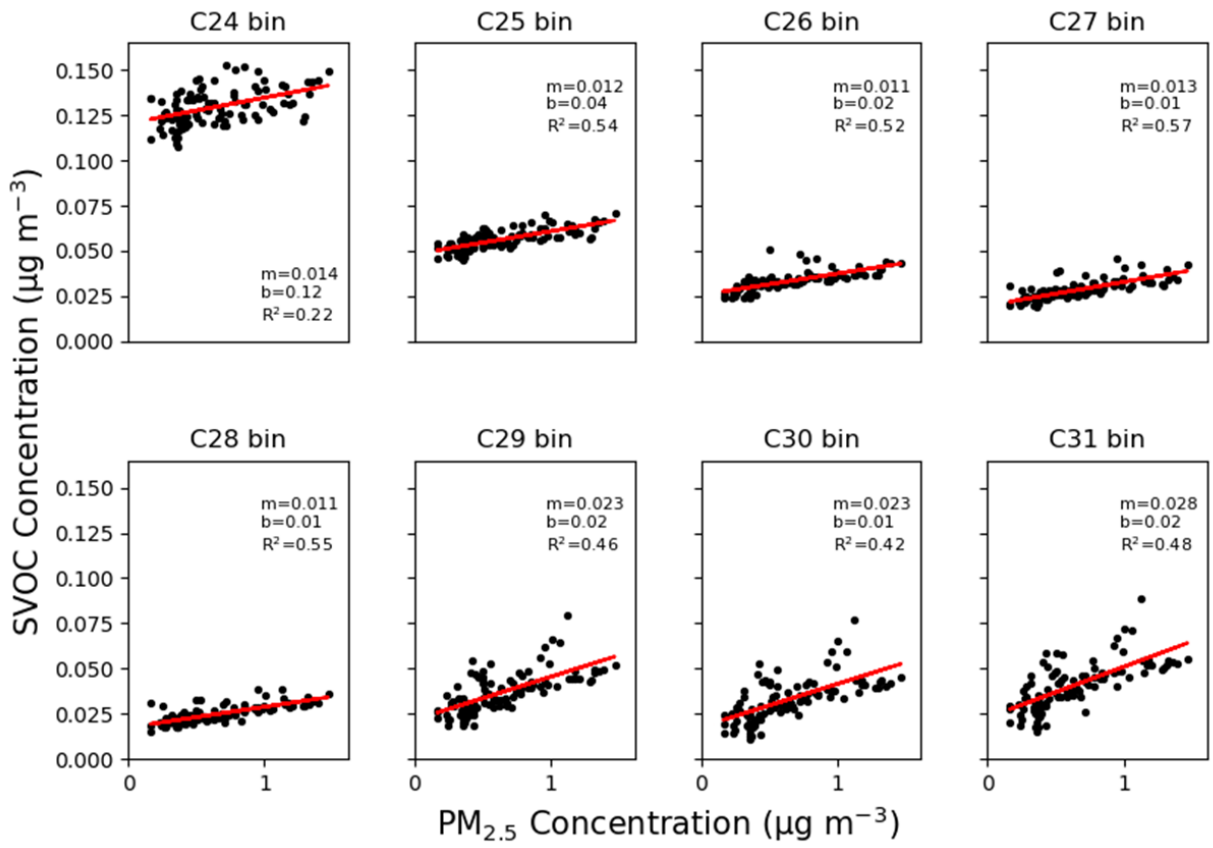

Figure 3.4.2: Binned total (gas-plus-particle) SVOC concentrations (µg m^{-3}) are compared against PM2.5 mass concentrations (µg m^{-3}) at H2 during the vacant period. The linear fit slope (m) is dimensionless; the intercept (b) has units of µg m^{-3}. Each measured point represents a 15-minute sample collection period with hourly replication during the observational period.

intercepts of the ordinary least-squares fits displayed in Figure 3.4.2 are related to the airborne gas-phase concentration in the absence of particles. As SVOC volatility decreases, the background gas-phase SVOC concentration generally decreases. Gas-particle partitioning by bin is displayed in Figure 3.7.7. As expected, the observed particle fraction, F_p, generally increases with increased particle mass concentration and with decreased vapor pressure.

The strong correlation ($R^2 > 0.4$) between PM2.5 and the airborne SVOC concentrations in the C25-C31 bins suggests a net outcome of surface-particle partitioning as SVOCs are transported from condensed-phase reservoirs. We infer that the gas-phase acts as a transport medium between condensed-phase SVOC surface reservoirs and airborne particles. Gas-phase SVOC concentrations were relatively constant under variable particle concentrations considering experimental uncertainty (Figure 3.7.8). Correlations between PM2.5 and SVOC

concentrations for bins below C25, which are predominantly in the gas-phase, were weaker ($R^2 < \sim 0.3$) or not observed (Figure 3.7.6).

Infiltration of outdoor gas- and particle-phase SVOCs as well as changes in source emission rates may also influence observed concentrations in indoor air. Indoor-outdoor concentration ratios of the alkane-equivalent volatility bins were slightly below unity with moderate variability (Figure 3.7.9). However, because outdoor particle mass concentrations were greater than indoor particle mass concentrations, SVOC concentrations per particle mass were greater indoors than outdoors. As indoor particles during the H2 vacant period are expected to be primarily of outdoor origin,[8] this evidence suggests the occurrence of net partitioning of indoor SVOCs to outdoor particles upon transport to the indoors. Particle-normalized indoor/outdoor ratios of alkane-equivalent volatility bins display substantial variability, whereas indoor SVOC concentrations were highly regular. The regular correspondence between SVOC concentrations and PM2.5, coupled with high normalized indoor/outdoor ratios, suggests that partitioning processes may be modulating observed indoor SVOC concentrations at time scales comparable to or faster than the air-exchange rate. Under classical partitioning theory, it is assumed that SVOCs partition by absorption into the organic PM2.5 fraction rather than by adsorption to bulk particle surfaces.[15]

3.4.3 Indirect Surface Emissions Contribute to Indoor Particle Mass

During the first HOMEChem 'Thanksgiving' experiment, substantial proportions of airborne PM2.5 mass originated from primary cooking emissions. Among primary species emitted are palmitic acid, stearic acid, and other carboxylic acids with varying degrees of unsaturation. Such species have been reported to be directly emitted from cooking in laboratory studies.[40–42] We also found that squalene emissions were strongly associated with oven usage on Thanksgiving; the expected source is volatilization of oils from the skin of the roasting turkey. An additional source could be from human skin oils present on heated surfaces or cookware. Squalene was observed during other cooking events at roughly one-to-two orders of magnitude smaller abundance.

Surprisingly, we also observed on this day elevated indoor particle-phase concentrations of specific SVOCs that should not originate from the food itself, in particular phthalates, adipates, and siloxanes (Figure 3.4.3, Figures 3.7.1, 3.7.2). Phthalates and adipates are plasticizers commonly used in vinyl flooring.[43] Low-volatility siloxanes are used as thermally stable lubricating greases and sealants. Remarkably, plasticizer and siloxane concentrations accounted for approximately 10% of airborne particle mass at certain times on this experimental day, suggesting that partitioning processes between particles and condensed-phase reservoirs significantly influenced the observed airborne concentrations. Moreover, these observations highlight difficulties in determining exact SVOC emission profiles of events in a real-world setting: surface emissions that were indirectly stimulated by primary event-driven particle emissions contributed sizeable fractions of indoor PM2.5 mass.

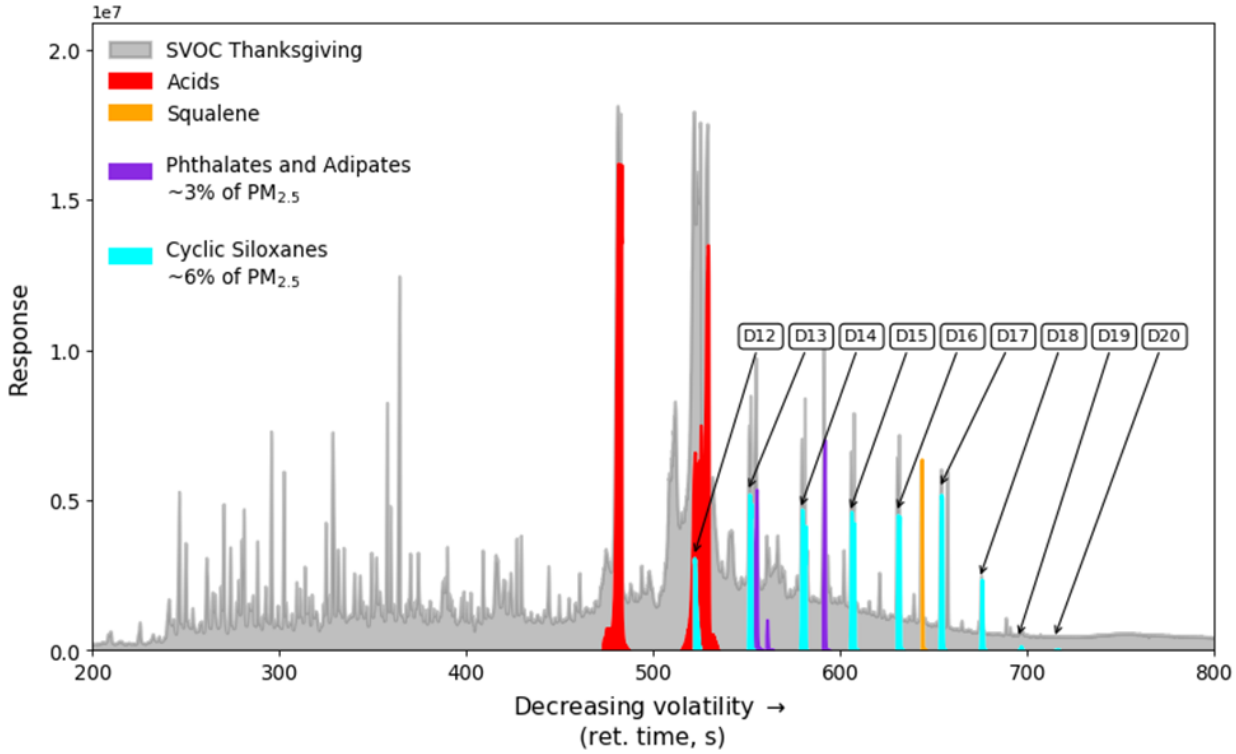

Figure 3.4.3: A particle-phase chromatogram from the first 'Thanksgiving' experiment day (PM2.5 concentration = 245 μg m^{-3}) on June 18 at 3:05 PM is displayed. Direct emissions attributable to cooking (carboxylic acids and squalene) are highlighted in red and orange, respectively. Indirect emissions likely attributable to the building composition are highlighted in purple (plasticizers) and teal (siloxane lubricants and heat-transfer materials).

In previous analyses of data from the H2 field campaign, correlations between particle mass concentration and airborne DEHP concentration suggested that particulate matter rapidly acquired surface-laden DEHP from reservoirs such as organic surface films and dust.[8] Prior analysis of airborne DEHP concentrations at the UTest House characterized the role of temperature over a 9 K range.[44] In that case, on a long-term basis, a 9 K increase in temperature approximately doubled airborne DEHP and butyl benzyl phthalate (BBzP) concentrations. However, there was no systematic examination in that study of particle-dependent variations in phthalate concentrations. In the current work at the UTest House, with temperature approximately constant at 298 K, strong associations between particle concentration and total airborne SVOC concentrations were observed for both DEHP and BBzP (Figure 3.4.4).

Substantial portions of the UTest House vinyl flooring are known to contain phthalates.[44] Because both DEHP and BBzP are expected to originate from the composition of the flooring material, and because airborne phthalate concentrations are strongly asso-

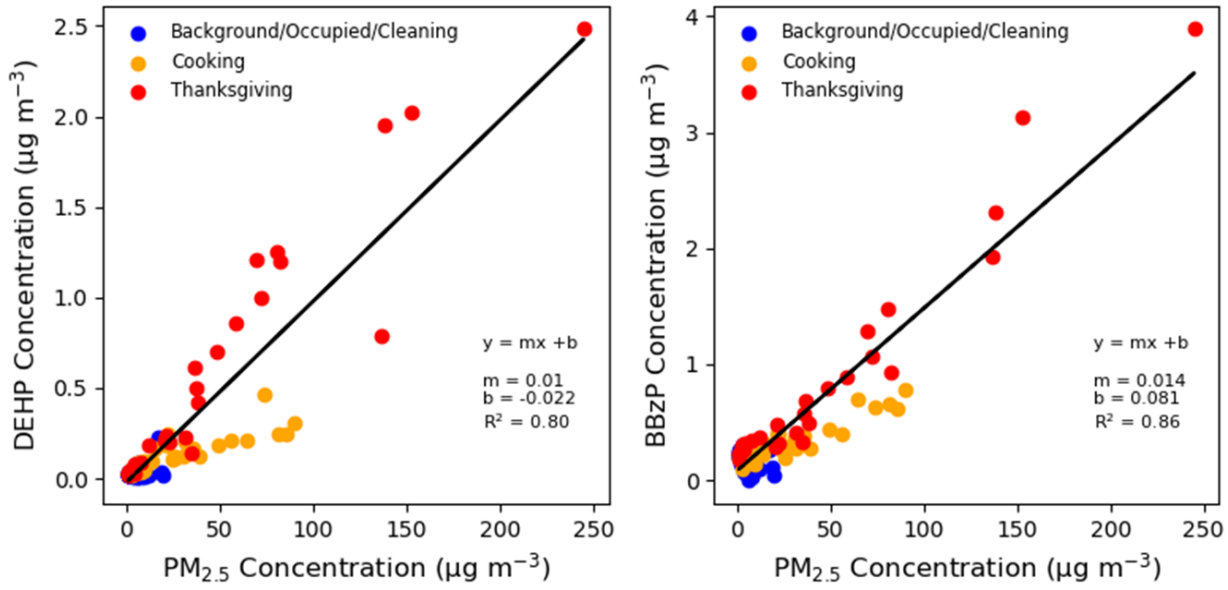

Figure 3.4.4: Total (gas-plus-particle) concentrations (µg m^{-3}) of two phthalates, DEHP and BBzP, are compared against particle mass concentration (µg m^{-3}) for measurements from the HOMEChem campaign. Units of measure for the fit slope (m) and intercept (b) are unitless and µg m^{-3}, respectively.

ciated with particle concentration for many different source events, it is similarly inferred that transport through the gas phase from condensed-phase stationary reservoirs to airborne particles is the principal source of observed particulate phthalate concentrations during the HOMEChem campaign. DEHP resides in the C25 alkane-equivalent volatility bin and BBzP resides in the C24 alkane-equivalent volatility bin based on chromatographic retention time.

3.4.4 Lower Volatility Siloxanes Exhibit Ongoing Emissions after a High Emission Event

Surprisingly high concentrations of low-volatility siloxanes (D13-D20 cyclic and L13-L19 linear siloxanes) were observed during a particle loading event associated with the HOMEChem 'Thanksgiving' experiment day on June 18 in association with cooking and oven use. We hypothesize that the low-volatility siloxane source is the oven, an appliance that likely contains heat-transfer compounds and thermally stable lubricants. Commercially available products containing siloxanes have been recommended for such uses in ovens.[45] In principle, high temperatures attained throughout the oven during cooking could have driven appreciable amounts of low-volatility siloxanes into the gas-phase, which subsequently condensed onto airborne particles as air exited the oven and cooled. Although the oven was approximately

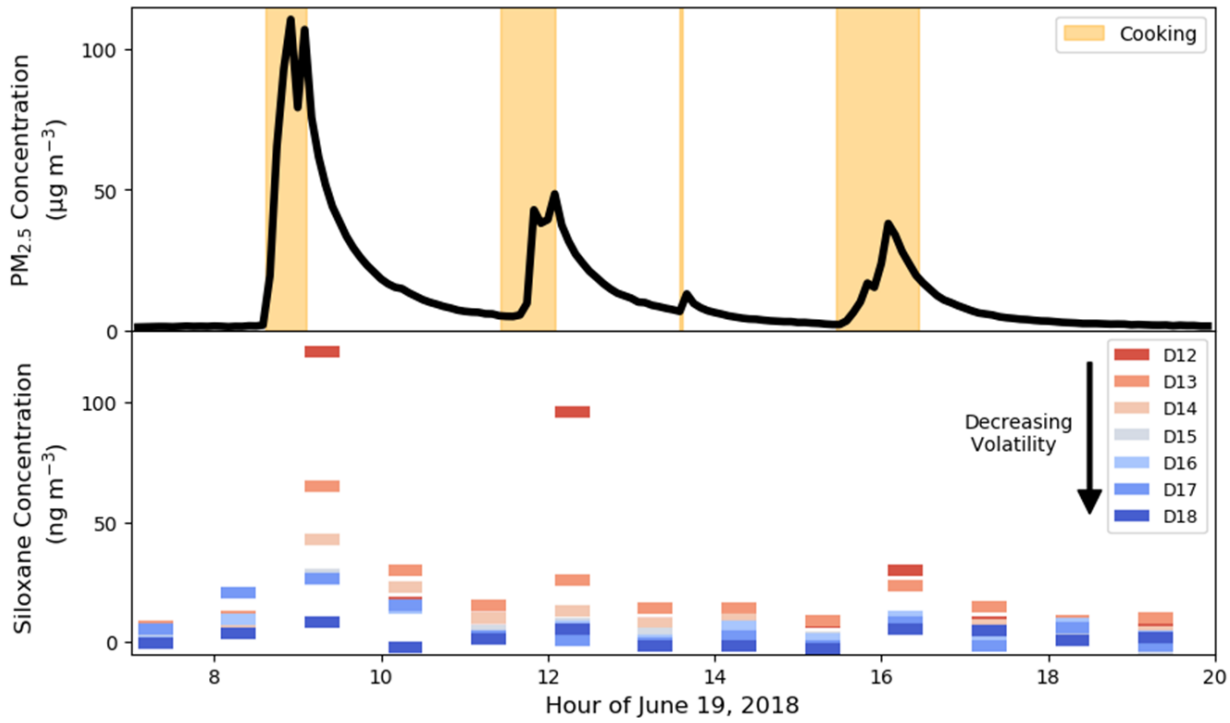

Figure 3.4.5: Total (gas-plus-particle) airborne concentrations (μg m^{-3}) of a siloxane homologous series superimposed on PM2.5 concentrations (μg m^{-3}) for a 'layered' experiment day on June 19 following the June 18 'Thanksgiving' experiment day.

thirteen years old, it had been operated only three times prior to the June 18 Thanksgiving event. Peak concentrations of low-volatility siloxanes during the 'Thanksgiving' experiment day are reported in Table 3.7.4. Minor siloxane enhancements were observed in the morning (stovetop breakfast preparation) and evening (oven cooking) of the June 8 layered day, but not during the lunch-time stir-fry event.

Small enhancements of D18 were observed during cooking events on the June 17 sequential stir-fry day; enhancements of other siloxanes were not observed. In contrast, D12-D14 siloxanes were strongly enhanced during cooking events on the June 19 'layered' experiment day. A plausible explanation for these observations is that siloxanes emitted during the June 18 'Thanksgiving' experiment day were deposited on surfaces throughout the residence and were subsequently reemitted during high particle emission events (Figure 3.4.5). Reemission of the semivolatile siloxanes occurred more readily for smaller homologues, which have correspondingly higher vapor pressures. Lower-volatility siloxanes are expected to preferentially partition to airborne particles; however, airborne concentration enhancements may not be observed for species with especially low volatility, for which equilibration time scales are significantly longer than the particle residence time indoors.

The D12-D19 siloxanes reside in the C22-C31 alkane-equivalent volatility bins, suggesting that their physicochemical properties may be well suited for reemission from surfaces. Vapor pressures and octanol-air partition coefficient (K_{oa}) values for D12-D19 were calculated using SPARC and are reported in Table 3.7.5. Using the method of Weschler and Nazaroff1 and assuming a condensing-particle diameter of 100 nm and a gas-phase diffusivity of 0.03 cm^2 s^{-1}, gas-particle equilibration time scales for D12 are expected to be on the order of 8 days while equilibration time scales for D19 are expected to be effectively infinite (∼109 y). A mechanical ventilation system was operated to maintain an air-exchange rate of ∼0.5 per hour during the HOMEChem campaign.[26] The calculated vapor pressure of D12 ($10^{-12.1}$ atm) is similar in magnitude to that of DEHP ($10^{-11.85}$ atm), a compound that displayed prominent gas-particle interactions in a normally occupied residence.[8] The calculated vapor pressure of D19 is eight orders of magnitude lower. In summary, airborne concentration enhancements may occur for D12 in association with increased PM2.5 loading but are not expected to occur for D19 without an additional stimulus, such as the inference that the high-temperature event associated with oven-use drove D19 into the gas-phase. Linear siloxanes, which were emitted at far lower concentrations during the June 18 Thanksgiving emission event, were not observed significantly above background during the June 19 layered day. Small siloxane enhancements were observed for D12-D16 siloxanes on the June 12 sequential stir-fry day. These observations may be related to deposition events from oven use on June 5 and June 8.

3.4.5 Implications

In the absence of episodic emission sources, key driving factors influencing variability of indoor airborne SVOC concentrations are volatility and partitioning phenomena. Airborne concentrations of the higher volatility (C13-C23 bins; predominantly gaseous) SVOCs are mainly sensitive to surface temperatures. Concentrations of lower volatility (C25-C31 bins; substantially particle-phase) SVOCs are sensitive to airborne particle concentrations. This work suggests that, at the H2 residence, the dynamic behavior of specific SVOCs can be predicted if their volatility is known. Ultimately, if demonstrated to be generalizable, such understanding would contribute to improving exposure assessment and mitigation strategies.

Emissions of low-volatility siloxanes and phthalates from surfaces are inferred to have been indirectly stimulated by event-driven emissions of particles. Analysis of low-volatility siloxane concentrations suggests that SVOCs can be deposited throughout a residence and then reemitted during subsequent particle loading events. This effect was most important for siloxanes with significant particle-bound fractions and appreciable gas-phase fractions. Despite similar total (gas-plus-particle) airborne concentrations during the initial source event, smaller concentrations of lower volatility siloxanes were observed during reemission events compared to higher volatility siloxanes. Because indoor air is the transporting medium between condensed-phase surface reservoirs and airborne particles, the lowest-volatility siloxanes are expected to remain in condensed-phase reservoirs when considering kinetic transport

limitations. These lowest-volatility siloxanes were observed during primary emission events involving oven use but not appreciably during reemission episodes.

These observations of airborne SVOC concentrations are consistent with, but not fully demonstrative of prior modeling and laboratory results. More work is needed to strengthen confidence in current models by connecting speciated measurements of surface-sorbed organics to airborne SVOC concentrations over longer time scales and in other indoor spaces. Future analysis would benefit from chemically differentiating primary event emissions and indirect event emissions where surface-sorbed species are enhanced in indoor air by primary particles. The same primary emission event could produce significantly different airborne SVOC concentrations, and ultimately occupant exposures, in indoor environments with different condensed-phase reservoirs.

3.5 Acknowledgements

This work was supported by the Alfred P. Sloan Foundation Program on Chemistry of Indoor Environments via Grants G-2016-7050, G-2017-9944, and G-2019-11412. The authors thank the HOMEChem science team for a successful field campaign, Atila Novoselac and Steve Bourne for their operation of the UTest house, and Robin Weber for technical assistance. D.L. acknowledges support from the National Science Foundation (grant no. DGE 1752814). K.K. acknowledges support from the Carlsberg Foundation (grant no. CF16-0624). The authors thank the occupants of the H2 residence for participating in the study. The occupants of the H2 site gave informed consent for the study, which was conducted under a protocol approved in advance by the Committee for Protection of Human Subjects for the University of California, Berkeley (Protocol #2016 04 8656).

3.6 References

[1] Weschler, C. J.; Nazaroff, W. W. Semivolatile organic compounds in indoor environments. *Atmos. Environ.* **2008**, *42*, 9018–9040.

[2] Rudel, R. A.; Perovich, L. J. Endocrine disrupting chemicals in indoor and outdoor air. *Atmos. Environ.* **2009**, *43*, 170–181.

[3] Cohen, A. J.; Brauer, M.; Burnett, R.; Anderson, H. R.; Frostad, J.; Estep, K.; Balakrishnan, K.; Brunekreef, B.; Dandona, L.; Dandona, R.; Feigin, V.; Freedman, G.; Hubbell, B.; Jobling, A.; Kan, H.; Knibbs, L.; Liu, Y.; Martin, R.; Morawska, L.; Pope III, C. A.; Shin, H.; Straif, K.; Shaddick, G.; Thomas, M.; van Dingenen, R.; van Donkelaar, A.; Vos, T.; Murray, C. J. L.; Forouzanfar, M. H. Estimates and 25-year trends of the global burden of disease attributable to ambient air pollution: an analysis of data from the Global Burden of Diseases Study 2015. *Lancet* **2017**, *389*, 1907–1918.

[4] Wang, C.; Collins, D. B.; Arata, C.; Goldstein, A. H.; Mattila, J. M.; Farmer, D. K.; Ampollini, L.; DeCarlo, P. F.; Novoselac, A.; Vance, M. E.; Nazaroff, W. W.; Abbatt, J. P. D. Surface reservoirs dominate dynamic gas-surface partitioning of many indoor air constituents. *Sci. Adv.* **2020**, *6*, eaay8973.

[5] Ampollini, L.; Katz, E. F.; Bourne, S.; Tian, Y.; Novoselac, A.; Goldstein, A. H.; Lucic, G.; Waring, M. S.; DeCarlo, P. F. Observations and contributions of real-time indoor ammonia concentrations during HOMEChem. *Environ. Sci. Technol.* **2019**, *53*, 8591–8598.

[6] Collins, D. B.; Hems, R. F.; Zhou, S.; Wang, C.; Grignon, E.; Alavy, M.; Siegel, J. A.; Abbatt, J. P. D. Evidence for gas-surface equilibrium control of indoor nitrous acid. *Environ. Sci. Technol.* **2018**, *52*, 12419–12427.

[7] Kristensen, K.; Lunderberg, D. M.; Liu, Y; Misztal, P. K.; Tian, Y.; Arata, C.; Nazaroff, W. W.; Goldstein, A. H. Sources and dynamics of semivolatile organic compounds in a single-family residence in northern California. *Indoor Air* **2019**, *29*, 645–655.

[8] Lunderberg, D. M.; Kristensen, K.; Liu, Y.; Misztal, P. K.; Tian, Y.; Arata, C.; Wernis, R.; Kreisberg, N.; Nazaroff, W. W.; Goldstein, A. H. Characterizing airborne phthalate concentrations and dynamics in a normally occupied residence. *Environ. Sci. Technol.* **2019**, *53*, 7337–7346.

[9] Weschler, C. J.; Nazaroff, W. W. Growth of organic films on indoor surfaces. *Indoor Air* **2017**, *27*, 1101–1112.

[10] Cox, S. S.; Little, J. C.; Hodgson, A. T. Predicting the emission rate of volatile organic compounds from vinyl flooring. *Environ. Sci. Technol.* **2002**, *36*, 709–714.

[11] Xu, Y.; Zhang, Y. An improved mass transfer based model for analyzing VOC emissions from building materials. *Atmos. Environ.* **2003**, *37*, 2497–2505.

[12] Xu, Y.; Little, J. C. Predicting emissions of SVOCs from polymeric materials and their interaction with airborne particles. *Environ. Sci. Technol.* **2006**, *40*, 456–461.

[13] Xu, Y.; Cohen Hubal, E. A.; Clausen, P. A.; Little, J. C. Predicting Residential Exposure to Phthalate Plasticizer Emitted from Vinyl Flooring: A Mechanistic Analysis. *Environ. Sci. Technol.* **2009**, *43*, 2374–2380.

[14] Clausen, P. A.; Liu, Z.; Kofoed-Sørensen, V.; Little, J.; Wolkoff, P. Influence of temperature on the emission of di-(2-ethylhexyl)phthalate (DEHP) from PVC flooring in the emission cell FLEC. *Environ. Sci. Technol.* **2012**, *46*, 909–915.

[15] Pankow, J. F. An absorption model of gas/particle partitioning of organic compounds in the atmosphere. *Atmos. Environ.* **1994**, *28*, 185–188.

[16] Goss, K.-U.; Schwarzenbach, R. P. Gas/solid and gas/liquid partitioning of organic compounds: critical evaluation of the interpretation of equilibrium constants. *Environ. Sci. Technol.* **1998**, *32*, 2025–2032.

[17] Lyng, N. L.; Clausen, P. A.; Lundsgaard, C.; Andersen, H. V. Modelling the impact of room temperature on concentrations of polychlorinated biphenyls (PCBs) in indoor air. *Chemosphere* **2016**, *144*, 2127–2133.

[18] Salthammer, T.; Goss, K.-U. Predicting the gas/particle distribution of SVOCs in the indoor environment using poly parameter linear free energy relationships. *Environ. Sci. Technol.* **2019**, *53*, 2491–2499.

[19] Liu, C.; Morrison, G. C.; Zhang, Y. Role of aerosols in enhancing SVOC flux between air and indoor surfaces and its influence on exposure. *Atmos. Environ.* **2012**, *55*, 347–356.

[20] Benning, J. L.; Liu, Z.; Tiwari, A.; Little, J. C.; Marr, L. C. Characterizing gas-particle interactions of phthalate plasticizer emitted from vinyl flooring. *Environ. Sci. Technol.* **2013**, *47*, 2696–2703.

[21] Lazarov, B.; Swinnen, R.; Poelmans, D.; Spruyt, M.; Goelen, E.; Covaci, A.; Stranger, M. Influence of suspended particles on the emission of organophosphate flame retardant from insulation boards. *Environ. Sci. Pollut. Res.* **2016**, *23*, 17183–17190.

[22] Wu, Y.; Eichler, C. M. A.; Cao, J.; Benning, J.; Olson, A.; Chen, S.; Liu, C.; Vejerano, E. P.; Marr, L. C.; Little, J. C. Particle/gas partitioning of phthalates to organic and inorganic airborne particles in the indoor environment. *Environ. Sci. Technol.* **2018**, *52*, 3583–3590.

[23] Eriksson, A. C.; Andersen, C.; Krais, A. M.; Nøjgaard, J. K.; Clausen, P.-A.; Gudmundsson, A.; Wierzbicka, A.; Pagels, J. Influence of airborne particles' chemical composition on SVOC uptake from PVC flooring — Time-resolved analysis with aerosol mass spectrometry. *Environ. Sci. Technol.* **2019**, *54*, 85–91.

[24] Collins, D. B.; Wang, C.; Abbatt, J. P. D. Selective uptake of third-hand tobacco smoke components to inorganic and organic aerosol particles. *Environ. Sci. Technol.* **2018**, *52*, 13195–13201.

[25] DeCarlo, P. F.; Avery, A. M.; Waring, M. S. Thirdhand smoke uptake to aerosol particles in the indoor environment. *Sci. Adv.* **2018**, *4*, eaap8368.

[26] Farmer, D. K.; Vance, M. E.; Abbatt, J. P. D.; Abeleira, A.; Alves, M. R.; Arata, C.; Boedicker, E.; Bourne, S.; Cardoso-Saldaña, F.; Corsi, R.; DeCarlo, P. F.; Goldstein, A. H.; Grassian, V. H.; Hildebrandt Ruiz, L.; Jimenez, J. L.; Kahan, T. F.; Katz, E. F.; Mattila, J. M.; Nazaroff, W. W.; Novoselac, A.; O'Brien, R. E.; Or, V. W.;

Patel, S.; Sankhyan, S.; Stevens, P. S.; Tian, Y.; Wade, M.; Wang, C.; Zhou, S.; Zhou, Y. Overview of HOMEChem: House Observations of Microbial and Environmental Chemistry. *Environ. Sci.: Processes Impacts* **2019**, *21*, 1280–1300.

[27] Zhao, Y.; Kreisberg, N. M.; Worton, D. R.; Teng, A. P.; Hering, S. V.; Goldstein, A. H. Development of an in situ thermal desorption gas chromatography instrument for quantifying atmospheric semi-volatile organic compounds. *Aerosol Sci. Technol.* **2013**, *47*, 258–266.

[28] Kreisberg, N. M.; Worton, D. R.; Zhao, Y.; Isaacman, G.; Goldstein, A. H.; Hering, S. V. Development of an automated high-temperature valveless injection system for online gas chromatography. *Atmos. Meas. Tech.* **2014**, *7*, 4431–4444.

[29] Isaacman, G.; Kreisberg, N. M.; Yee, L. D.; Worton, D. R.; Chan, A. W. H.; Moss, J. A.; Hering, S. V.; Goldstein, A. H. Online derivatization for hourly measurements of gas- and particle-phase semi-volatile oxygenated organic compounds by thermal desorption aerosol gas chromatography (SV-TAG). *Atmos. Meas. Tech.* **2014**, *7*, 4417–4429.

[30] Isaacman-VanWertz, G.; Sueper, D. T.; Aikin, K. C.; Lerner, B. M.; Gilman, J. B.; de Gouw, J. A.; Worsnop, D. R.; Goldstein A. H. Automated single-ion peak fitting as an efficient approach for analyzing complex chromatographic data. *J. Chromatogr. A* **2017**, *1529*, 81–92.

[31] Patel, S.; Sankhyan. S.; Boedicker, E.; DeCarlo, P. F.; Farmer, D. K.; Goldstein, A. H.; Katz, E. F.; Nazaroff, W. W.; Tian, Y.; Vanhanen, J.; Vance, M. E. Indoor particulate matter during HOMEChem: Concentrations, size distributions, and exposures. *Environ. Sci. Technol.* **2020**, *54*,7107–7116.

[32] Tian, Y.; Arata, C.; Boedicker, E.; Lunderberg, D. M.; Patel, S.; Sankhyan, S.; Kristensen, K.; Misztal, P. K.; Farmer, D. K.; Vance, M.; Novoselac, A.; Nazaroff, W. W; Goldstein, A. H. Indoor emissions of total and fluorescent supermicron particles during HOMEChem. *Indoor Air* **2021**, *31*, 88–98.

[33] Hu, M.; Peng, J.; Sun, K.; Yue, D.; Guo, S.; Wiedensohler, A.; Wu, Z. Estimation of size-resolved ambient particle density based on the measurement of aerosol number, mass, and chemical size distributions in the winter in Beijing. *Environ. Sci. Technol.* **2012**, *46*, 9941–9947.

[34] Zhou, J.; Chen, A.; Cao, Q.; Yang, B.; Chang, V. W.-C.; Nazaroff, W. W. Particle exposure during the 2013 haze in Singapore: Importance of the built environment. *Build. Environ.* **2015**, *93*, 14–23.

[35] Little, J. C.; Weschler, C. J.; Nazaroff, W. W.; Liu, Z.; Cohen Hubal, E. A.; Rapid methods to estimate potential exposure to semivolatile organic compounds in the indoor environment. *Environ. Sci. Technol.* **2012**, *46*, 11171–11178.

[36] Liu, C.; Shi, S.; Weschler, C.; Zhao, B.; Zhang, Y. Analysis of the dynamic interaction between SVOCs and airborne particles. *Aerosol Sci. Technol.* **2013**, *47*, 125-136.

[37] Chickos, J. S.; Hanshaw, W. Vapor pressures and vaporization enthalpies of the n-alkanes from C21 to C30 at T = 298.15 K by correlation gas chromatography. *J. Chem. Eng. Data* **2004**, *49*, 77–85.

[38] Ruzicka, K.; Majer, V. Simultaneous treatment of vapor pressures and related thermal data between the triple and normal boiling temperatures for n-alkanes C5–C20. *J. Phys. Chem. Ref. Data* **1994**, *23*, 1–39.

[39] Jimenez, J. L.; Canagaratna, M. R.; Donahue, N. M.; Prevot, A. S. H.; Zhang, Q.; Kroll, J. H.; DeCarlo, P. F.; Allan, J. D.; Coe, H.; Ng, N. L.; Aiken, A. C.; Docherty, K. S.; Ulbrich, I. M.; Grieshop, A. P.; Robinson, A. L.; Duplissy, J.; Smith, J. D.; Wilson, K. R.; Lanz, V. A.; Hueglin, C.; Sun, Y. L.; Tian, J.; Laaksonen, A.; Raatikainen, T.; Rautiainen, J.; Vaattovaara, P.; Ehn, M.; Kulmala, M.; Tomlinson, J. M.; Collins, D. R.; Cubison, M. J.; Dunlea, E. J.; Huffman, J. A.; Onasch, T. B.; Alfarra, M. R.; Williams, P. I.; Bower, K.; Kondo, Y.; Schneider, J.; Drewnick, F.; Borrmann, S.; Weimer, S.; Demerjian, K.; Salcedo, D.; Cottrell, L.; Griffin, R.; Takami, A.; Miyoshi, T.; Hatakeyama, S.; Shimono, A.; Sun, J. Y.; Zhang, Y. M.; Dzepina, K.; Kimmel, J. R.; Sueper, D.; Jayne, J. T.; Herndon, S. C.; Trimborn, A. M.; Williams, L. R.; Wood, E. C.; Middlebrook, A. M.; Kolb, C. E.; Baltensperger, U.; Worsnop, D. R. Evolution of organic aerosols in the atmosphere. *Science* **2009**, *326*, 1525–1529.

[40] Schauer, J. J.; Kleeman, M. J.; Cass, G. R.; Simoneit, B. R. T. Measurement of emissions from air pollution sources. 1. C1 through C29 organic compounds from meat charbroiling. *Environ. Sci. Technol.* **1999**, *33*, 1566–1577.

[41] McDonald, J. D.; Zielinska, B.; Fujita, E. M.; Sagebiel, J. C.; Chow, J. C.; Watson, J. G. Emissions from charbroiling and grilling of chicken and beef. *J. Air Waste Manage. Assoc.* **2003**, *53*, 185–194.

[42] Robinson, A. L.; Subramanian, R.; Donahue, N. M.; Bernardo-Bricker, A.; Rogge, W. F. Source apportionment of molecular markers and organic aerosol. 3. Food cooking emissions. *Environ. Sci. Technol.* **2006**, *40*, 7820–7827.

[43] Liu, Z.; Little, J. C. Semivolatile organic compounds (SVOCs): Phthalates and flame retardants. In Toxicity of Building Materials; Pacheco-Torgal, F., Jalali, S., Fucic, A.; Eds.; Woodhead Publishing: Oxford, 2012; pp 122–137.

[44] Bi, C.; Liang, Y.; Xu, Y. Fate and transport of phthalates in indoor environments and the influence of temperature: a case study in a test house. *Environ. Sci. Technol.* **2015**, *49*, 9674–9681.

[45] Dow Corning. Home Appliances: Ovens. https://web.archive.org/web/20170705093112/http://www.dowcorning.com/content/appliance/appliancehome/Ovens.asp (retrieved on Oct. 25, 2019)

3.7 Supporting Information

3.7.1 Instrument Operation

SV-TAG Data Analysis. Higher volatility siloxanes (D6-D9 and L6-L9) were identified by comparing observed mass spectra to a NIST mass spectral database.1 D6 was conclusively identified using its known retention time and mass spectrum as determined by an authentic external standard. Siloxanes in the homologous series with chain lengths greater than D9 and L9 are not available in the NIST mass spectral database. Their identifications were made on the basis of identified siloxane characteristic mass fragments (m/z 73, 147, 207, 221, and 281) and spacing patterns in retention time. (See Figure 3.7.1.) The characteristic mass fragments and the consistent retention time spacing of homologous series were used to identify linear and cyclic siloxanes up to 20 chain units in length. Because external standards were not available for siloxanes with chain lengths greater than D6, estimated calibration curves were applied. First, the siloxane characteristic ion was normalized to the closest alkane internal standard in retention time. Second, the normalized siloxane response was converted to a concentration using the closest alkane calibration curve in retention time after normalizing for molecular mass and fragmentation ratios of the characteristic ions.

Table 3.7.1: Sampling cycle of SV-TAG during the H2 campaign.[a]

Start Time (hh:mm)	End Time (hh:mm)	Cell 1	Cell 2
00:00	00:15	Indoor G+P	Indoor G+P
01:00	01:15	Indoor G+P	Indoor P
02:00	02:15	Indoor G+P	Outdoor G+P
03:00	03:15	Indoor G+P	Outdoor P

[a] 'G+P' refers to collection of the gas and particle phases and 'P' refers to collection of the particle-phase only. The SV-TAG sampling cycle was repeated approximately six times per day followed by analysis of an external standard mixture.

Table 3.7.2: Sampling cycle of SV-TAG during the HOMEChem campaign.[a]

Start Time (hh:mm)	End Time (hh:mm)	Cell 1	Cell 2
00:05	00:25	Indoor G+P	Outdoor G+P
01:05	01:25	Indoor G+P	Outdoor P
02:05	02:25	Indoor G+P	Indoor P
03:05	03:25	Blank	Blank
04:05	04:25	Standard	Standard
05:05	05:25	Indoor G+P	Indoor G+P
06:05	06:25	Indoor G+P	Indoor P
07:05	07:25	Indoor G+P	Indoor P
08:05	08:25	Indoor G+P	Indoor P
09:05	09:25	Indoor G+P	Indoor P
10:05	10:25	Indoor G+P	Indoor P
11:05	11:25	Indoor G+P	Indoor P
12:05	12:25	Indoor G+P	Indoor P
13:05	13:25	Indoor G+P	Indoor G+P
14:05	14:25	Indoor G+P	Indoor P
15:05	15:25	Indoor G+P	Indoor P
16:05	16:25	Indoor G+P	Indoor P
17:05	17:25	Indoor G+P	Indoor P
18:05	18:25	Indoor G+P	Indoor P
19:05	19:25	Indoor G+P	Indoor P
20:05	20:25	Indoor G+P	Indoor P
21:05	21:25	Indoor G+P	Indoor G+P
22:05	22:25	Indoor G+P	Indoor P
23:05	23:25	Indoor G+P	Indoor P

[a] 'G+P' refers to collection of the gas and particle phases and 'P' refers to collection of the particle-phase only. Full calibration curves were acquired from analysis of external standards in the middle and at the end of the HOMEChem campaign. Sampling flow rates onto the collection cell were 2.5 L min^{-1} (10 L min^{-1} through the sampling line with a 7.5 L min^{-1} bypass immediately upstream of the collection cell).

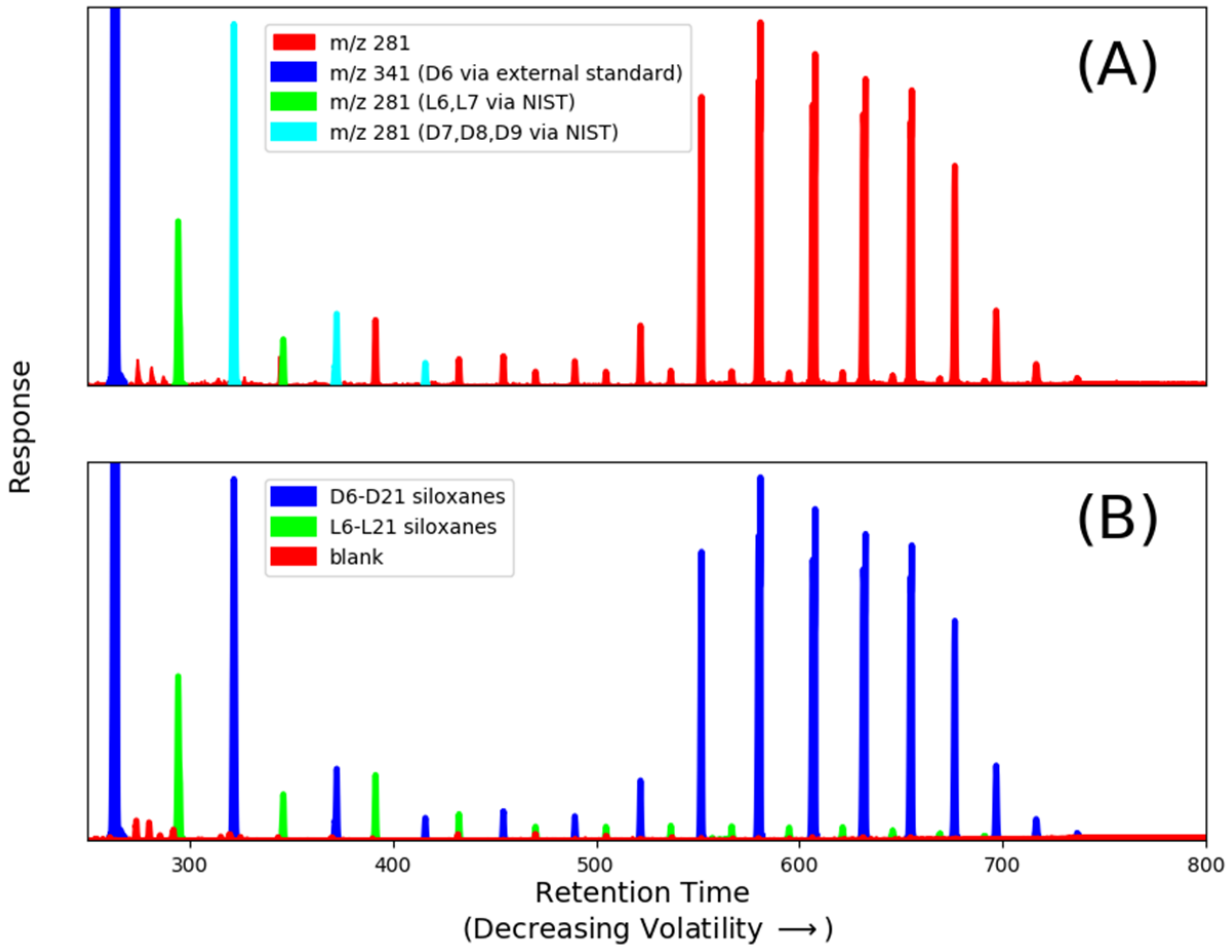

Figure 3.7.1: Single-ion chromatogram of siloxanes during the June 18 Thanksgiving event. The same single-ion chromatogram of a characteristic siloxane fragment (m/z 281) from the first simulated Thanksgiving-day event is displayed in panels (A) and (B). Panel (A) highlights confirmed siloxane identifications for which there is an external standard or match in the NIST database. Panel (B) displays proposed identifications on the basis of retention times and mass spectral patterns for a homologous series of cyclic and linear siloxanes. A method blank measurement is overlaid on the bottom of panel (B), demonstrating that the background is very small relative to observed siloxane concentrations.

HR-ToF-AMS. The high-resolution time-of-flight aerosol mass spectrometer (HR-ToF-AMS or AMS, Aerodyne Inc.) analyzes submicron particulate matter with 1-minute time resolution.[2] AMS sampling conditions at HOMEChem are presented elsewhere.[3] Sampled particles are focused by an aerodynamic lens system before impacting a tungsten plate heated to 600 °C to promote analyte vaporization. Vaporized analytes are then ionized by 70 eV electron ionization (EI) and detected by a time-of-flight (ToF) mass spectrometer. Siloxanes were identified in AMS mass spectra using high-resolution peak fitting of the same characteristic siloxane ions observed by SV-TAG. Analytes are generally quantified using an ammonium nitrate primary calibrant and an ionization efficiency scaling factor (RIE) relating the calibrant to the compound of interest. Because the siloxane relative ionization efficiency scaling factor is currently under investigation, raw ion counts of the siloxane family are used in comparisons with SV-TAG measurements.

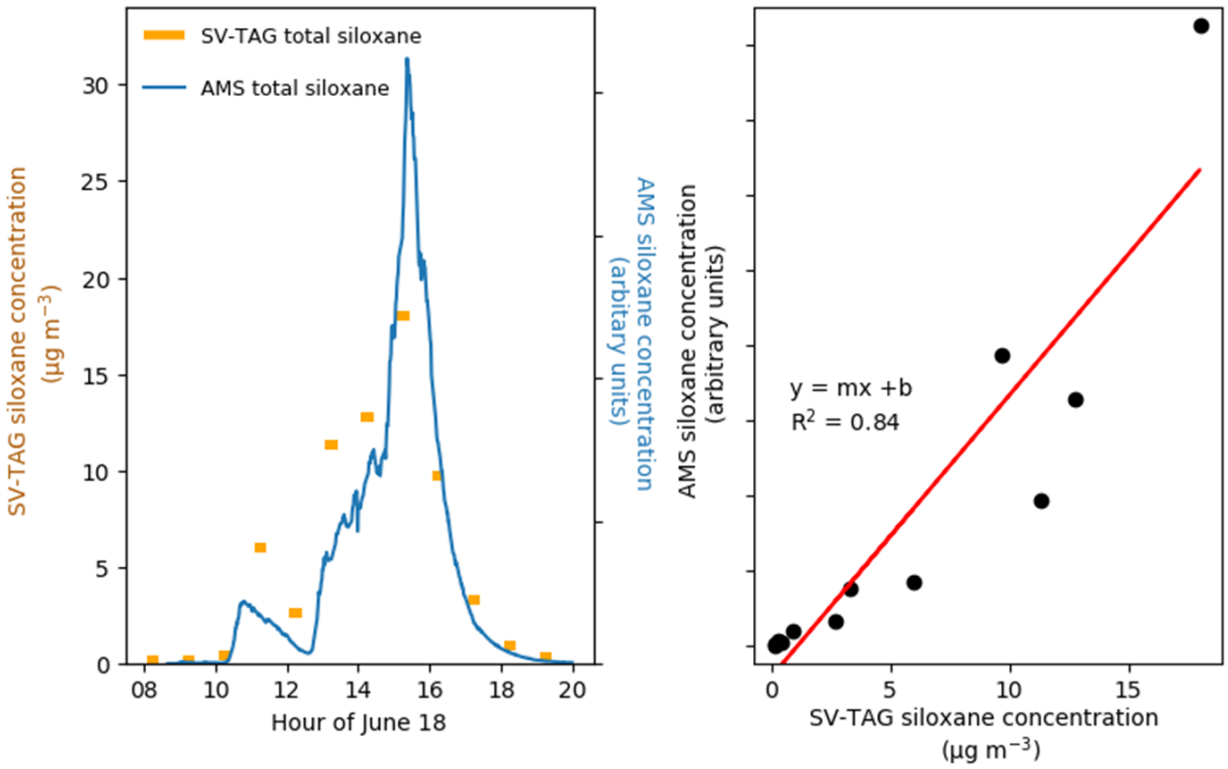

Figure 3.7.2: Intercomparison of SV-TAG and AMS siloxane measurements during the June 18 Thanksgiving event. In the left panel, total (gas-plus-particle) concentrations (µg m^{-3}) for D12-D19 sum siloxanes as measured by SV-TAG and siloxane family concentrations (arbitrary units) as measured by the AMS are plotted against time. In the right panel, corresponding AMS siloxane family concentrations (arbitrary units) are plotted against total (gas-plus-particle) concentrations (µg m^{-3}) for D12-D19 sum siloxanes as measured by SV-TAG.

3.7.2 Modeling Temperature Dependence of Airborne SVOCs

We describe a material mass balance in Equation 3.6, where y refers to observed airborne SVOC concentration, F_{in} refers to transport into the house, P refers to chemical production, E refers to emissions, F_{out} refers to transport out of the house, L refers to chemical losses, D refers to deposition, and V refers to the volume of the house.

$$\frac{dy}{dt} = \text{Sources} - \text{Losses} = \frac{F_{\text{in}} + P + E - F_{\text{out}} - L - D}{V} \tag{3.6}$$

We assume that net surface emissions, referred to as E_{surf}, are the dominant source process and that indoor-to-outdoor transport is the dominant loss process. F_{out} is assumed to be well-described by $y \times Q^* \times V$, where Q^* refers to the "equivalent ventilation rate"

accounting for SVOCs associated with airborne particles, yielding Equation 3.7. It is noted that $Q^* = (1 + K_p TSP) \times Q$, where TSP is the mass concentration of suspended particles, K_p is the gas-particle partition coefficient, and Q is the ventilation rate.

$$\frac{dy}{dt} = \frac{E_{surf}}{V} - y \times Q^* \tag{3.7}$$

Assume that, on a time-averaged basis, the net SVOC loss or accumulation is much smaller than the time-averaged source and sink terms. Solve for y.

$$y = \frac{E_{surf}}{Q^* \times V} \tag{3.8}$$

Emissions from surfaces are well characterized by Equation 3.9, where h_m is the convective mass-transfer coefficient and A is surface area.[4–8] In a previous study of the H2 site, Kristensen et al. demonstrated that surface deposition was comparable to indoor-to-outdoor exchange.[9] We assume that net surface emissions, that is total surface emissions minus surface deposition, remain adequately represented by Equation 3.9.

$$E_{surf} = A \times h_m \times (y_0 - y) \tag{3.9}$$

Substitute Equation 3.9 into Equation 3.8 and solve for y.

$$y = \frac{A \times h_m \times y_0}{Q^* \times V} \times \left(1 + \frac{A \times h_m}{Q^* \times V}\right)^{-1} \tag{3.10}$$

The equilibrium gaseous SVOC concentration at the surface-air interface, y_0, can be estimated from van't Hoff theory as shown in Equation 3.11, where T refers to temperature, $[SVOC_{surf}]$ refers to the condensed-phase concentration at the surficial interface, ΔS refers to the entropy of vaporization, and k refers to a constant described by -$\Delta H R^{-1}$, where ΔH is the heat of vaporization and R is the gas constant.[10]

$$K_{eq}(T) = \frac{y_0}{SVOC_{surf}} = \exp\left[\frac{\Delta S}{R} + k\left(\frac{1}{T}\right)\right] \tag{3.11}$$

Solve Equation 3.11 for y_0 and substitute into Equation 3.10.

$$y(T) = \frac{A \times h_m \times [SVOC_{surf}] \times \exp\left[\frac{\Delta S}{R}\right] \times \exp\left[k\frac{1}{T}\right]}{Q^* \times V} \times \left(1 + \frac{A \times h_m}{Q^* \times V}\right)^{-1} \tag{3.12}$$

It is noted that h_m does not strongly change within the observed temperature range (288–292 K). It is also noted that Q^* is not expected to strongly change over the observed temperature range, assuming that Q is independent of T. It is further assumed that the thermodynamic terms can be treated as constant for the observed temperature range and that $[SVOC_{surf}]$ is sufficiently large relative to emissions as to be treated as constant. Using

Equation 3.12, terms independent of indoor temperature are amalgamated into the parameter a as shown in Equation 3.13. Because the van't Hoff equation applies to equilibrium partitioning of a pure material and the studied indoor physical system consists of a complex mixture, we refer to experimentally derived k values as k^*.

$$y(T) = a \times \exp\left[k^* \left(\frac{1}{T}\right)\right] \tag{3.13}$$

3.7.3 H2 Supplementary Analysis

Table 3.7.3: Estimated physical parameters and summary statistics of reported alkane-equivalent volatility bin concentrations and gas-particle partitioning.[a]

Alkane-Equivalent Volatility Bin	Estimated Log Vapor Pressure (Pa)	Estimated Log C* ($\mu g\ m^{-3}$)	Concentration ($\mu g\ m^{-3}$)	Concentration Mean-to-Median ratio	Particle-Phase Fraction, F_p
C13	0.75	5.6	10.7 ± 1.4	1.02	0.04 ± 0.01
C14	0.26	5.2	9.5 ± 1.8	1.05	0.04 ± 0.01
C15	-0.24	4.7	8.0 ± 1.5	1.04	0.05 ± 0.01
C16	-0.72	4.2	6.0 ± 0.6	1.01	0.06 ± 0.01
C17	-1.21	3.8	2.7 ± 0.3	1.03	0.08 ± 0.02
C18	-1.70	3.3	3.1 ± 0.3	1.01	0.07 ± 0.01
C19	-2.18	2.9	1.9 ± 0.2	1.02	0.07 ± 0.01
C20	-2.68	2.4	1.8 ± 0.2	1.02	0.06 ± 0.01
C21	-3.17	1.9	0.62 ± 0.05	1.00	0.12 ± 0.01
C22	-3.67	1.4	0.34 ± 0.02	1.01	0.14 ± 0.01
C23	-4.15	1.0	0.19 ± 0.01	1.00	0.12 ± 0.02
C24	-4.63	0.5	0.13 ± 0.01	1.01	0.14 ± 0.04
C25	-5.09	0.1	0.06 ± 0.01	1.00	0.37 ± 0.06
C26	-5.55	-0.4	0.03 ± 0.01	1.02	0.56 ± 0.14
C27	-5.95	-0.8	0.03 ± 0.01	1.02	0.63 ± 0.25
C28	-6.50	-1.3	0.02 ± 0.01	1.05	0.66 ± 0.38
C29	-6.99	-1.8	0.04 ± 0.01	1.03	0.95 ± 0.28
C30	-7.48	-2.2	0.03 ± 0.01	1.02	1.04 ± 0.31
C31	-8.02	-2.8	0.04 ± 0.01	1.00	0.91 ± 0.23

[a] Vapor pressures of the alkane-equivalent volatility bins were estimated using literature values for the corresponding alkane.[11–13] The saturation concentration (C^*) was estimated from the saturation vapor pressure while assuming ideality. Concentrations refer to the total (gas-plus-particle) observed signal. Reported values refer to averages of the population plus-or-minus the population standard deviation.

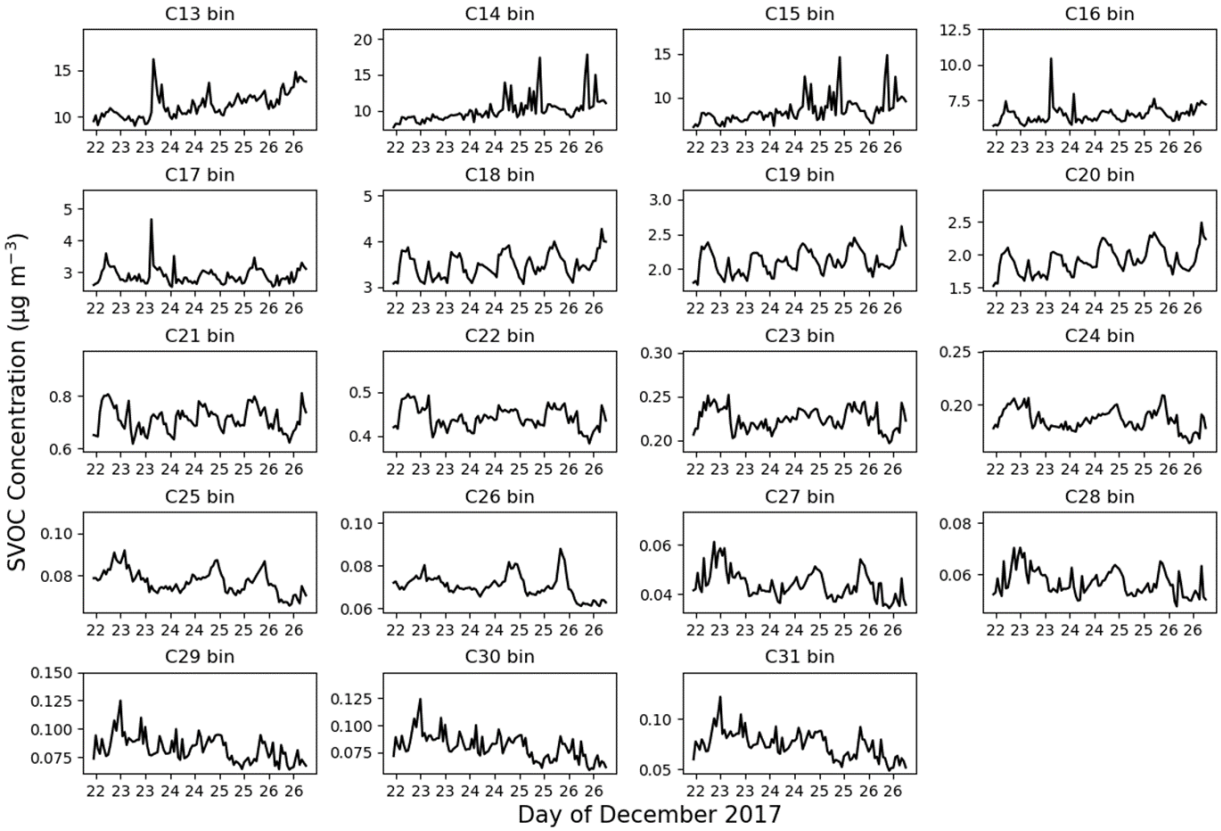

Figure 3.7.3: Time series of total (gas-plus-particle) alkane-equivalent volatility bin concentrations during the H2 vacant period.

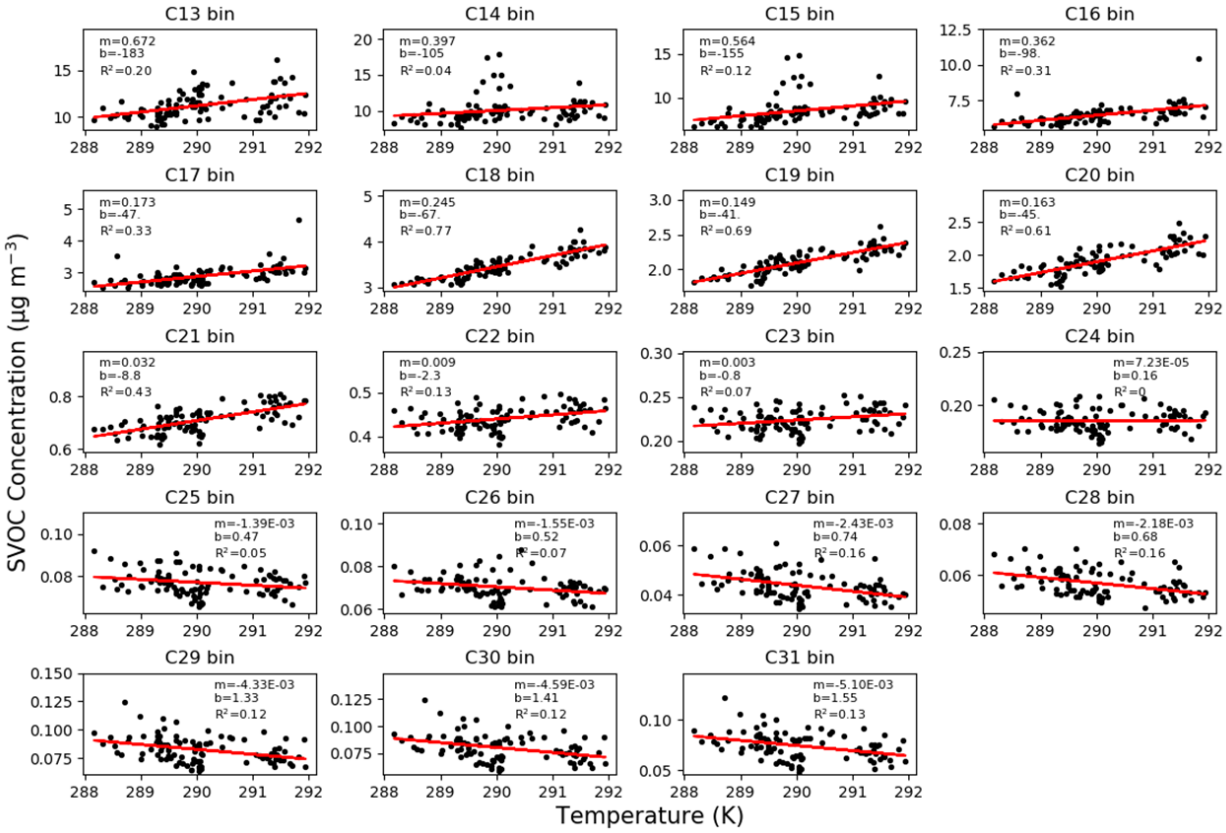

Figure 3.7.4: Total (gas-plus-particle) concentrations for each alkane-equivalent volatility bin compared against air temperature during the H2 vacant period. Units of measure for the linear fits are m = µg m^{-3} K^{-1} and b = µg m^{-3}. (Note: In the C25–C32 bins, there is an anti-correlation between temperature and particle-loading because particles were removed by the MERV 13 filter when the heating system was operating. Temperature increases from the heating system cause enhanced SVOCs emissions from surfaces; however, species in the C25-C32 bins are primarily found in the particle-phase. It seems that they weakly anti-correlate with temperature because of particle removal by the filter.)

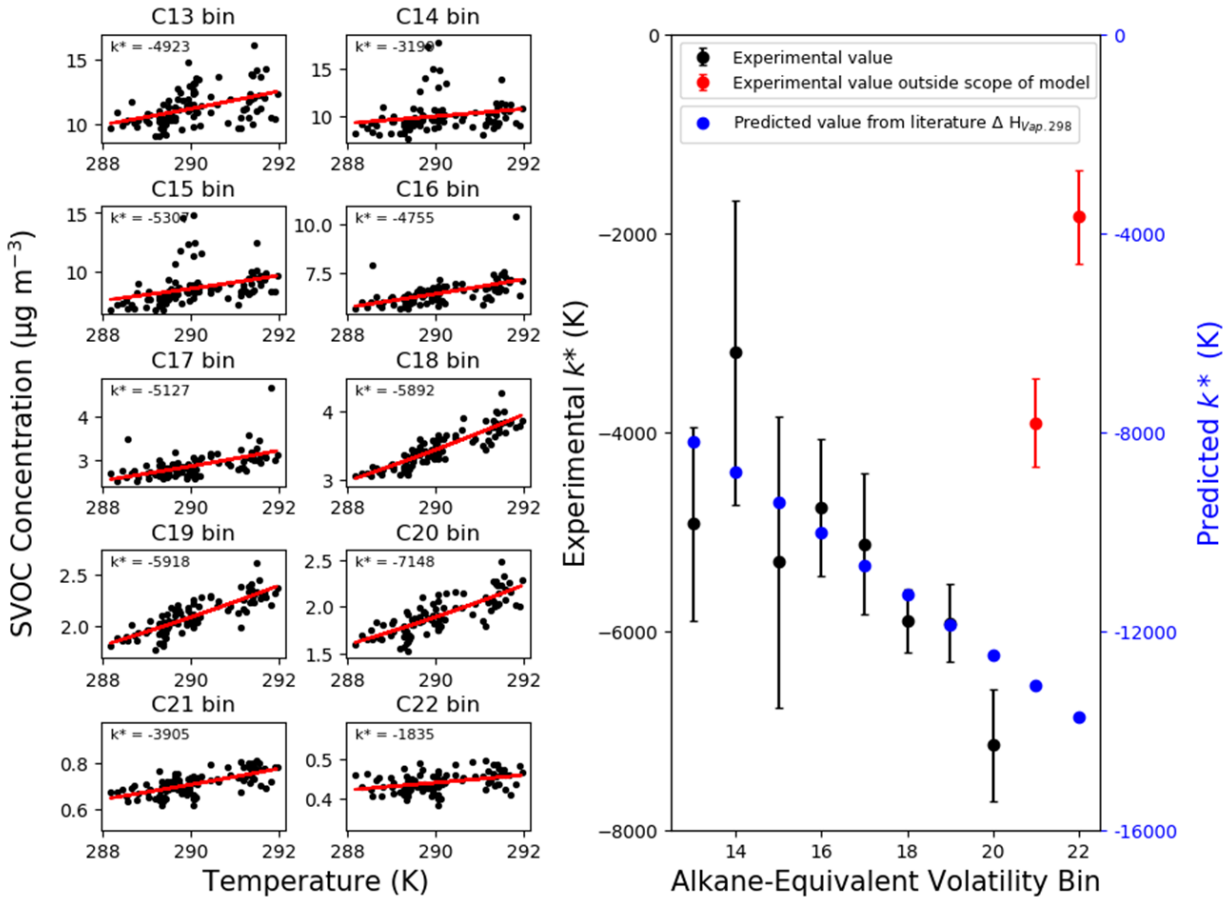

Figure 3.7.5: Alkane-equivalent volatility bins total (gas-plus-particle) concentration versus temperature and fit comparison with heats of vaporization during the H2 vacant period. In the left panel, total (gas-plus-particle) SVOC concentrations are compared against temperature for the H2 vacant period and fitted according to Equation (4) of the main text. Units of measure for k^* are kelvin. In the right panel, experimentally determined k^* values are compared against the corresponding alkane equivalent volatility bin. Predicted k^* values determined from the closest alkane heat of vaporization are displayed in blue. While displaying temperature dependence, bins C21 and C22 show deviations from the expected trend, probably owing to their increased particle-phase fractions.

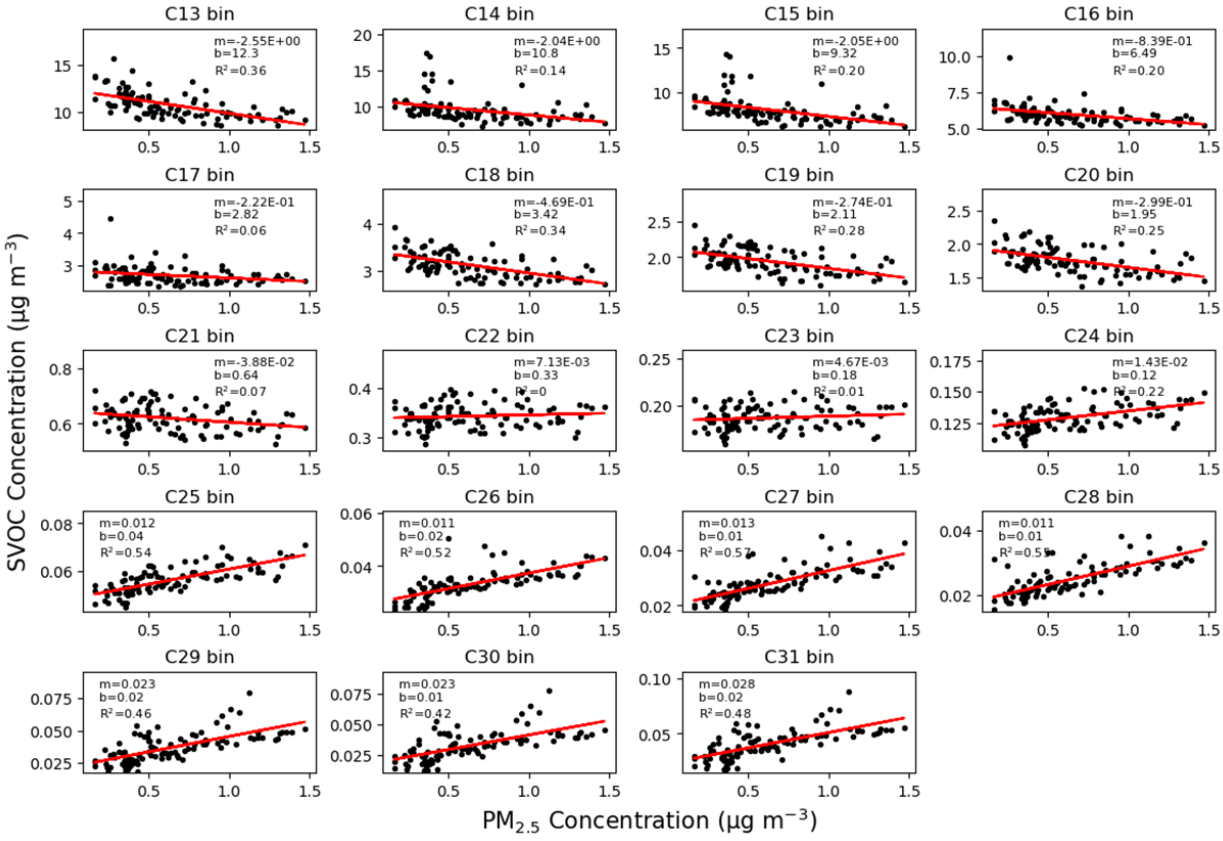

Figure 3.7.6: Alkane-equivalent volatility bins total (gas-plus-particle) concentration versus particle mass loading during the H2 vacant period. Units of measure for the linear fits are m = unitless and b = µg m^{-3}. (Note: The C13-C21 alkane-equivalent volatility bins weakly anticorrelate with particle mass concentrations. This observation is expected to originate from a weak anti-correlation between temperature and particle mass loading. Airborne particles were efficiently removed by a MERV 13 filter during the operation of the home heating system causing this weak anti-correlation. Because the C13-C21 bins increase in concentration with increasing temperature and because temperature and particle-loading are anti-correlated, weak anti-correlations between C13-C21 concentrations and particle loading are observed.)

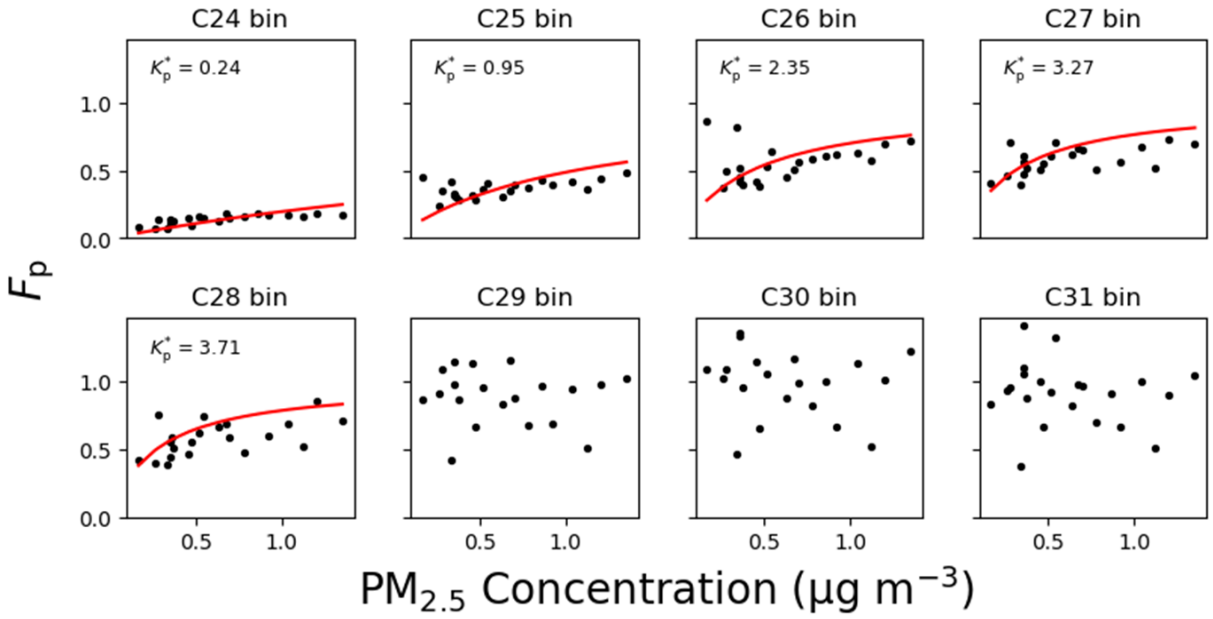

Figure 3.7.7: Alkane-equivalent volatility bin gas-particle partitioning versus particle mass loading during the H2 vacant period. The fraction of the airborne SVOC in the particle phase for each alkane-equivalent volatility bin is compared against particle mass loading during the H2 vacant period and fit according to classical equilibrium partitioning theory.[a] Alkane-equivalent volatility bins smaller than the C24 bin were predominantly in the gas-phase. The reported gas-particle partitioning of alkane-equivalent volatility bins greater than the C31 bin is highly variable owing to measurement uncertainties related to low instrumental response in this volatility range. SVOCs in bins greater than C31 are expected to be predominantly in the particle phase.

[a] Classical equilibrium partitioning is described by $F_{\mathrm{p}} = \frac{TSP \times K_{\mathrm{p}}}{1+TSP \times K_{\mathrm{p}}}$, where F_{p} refers to the particle fraction of the airborne SVOC, TSP refers to the particle mass concentration and K_{p} refers to the partition coefficient. Because the studied systems involve a complex mixture of different components and may not be at equilibrium, we report calculated K_{p} values as the apparent partition coefficient K_{p}^*. Units of measure for K_{p}^* are m^3 µg^{-1} and for TSP are µg m^{-3}. TSP is estimated as the measured PM2.5

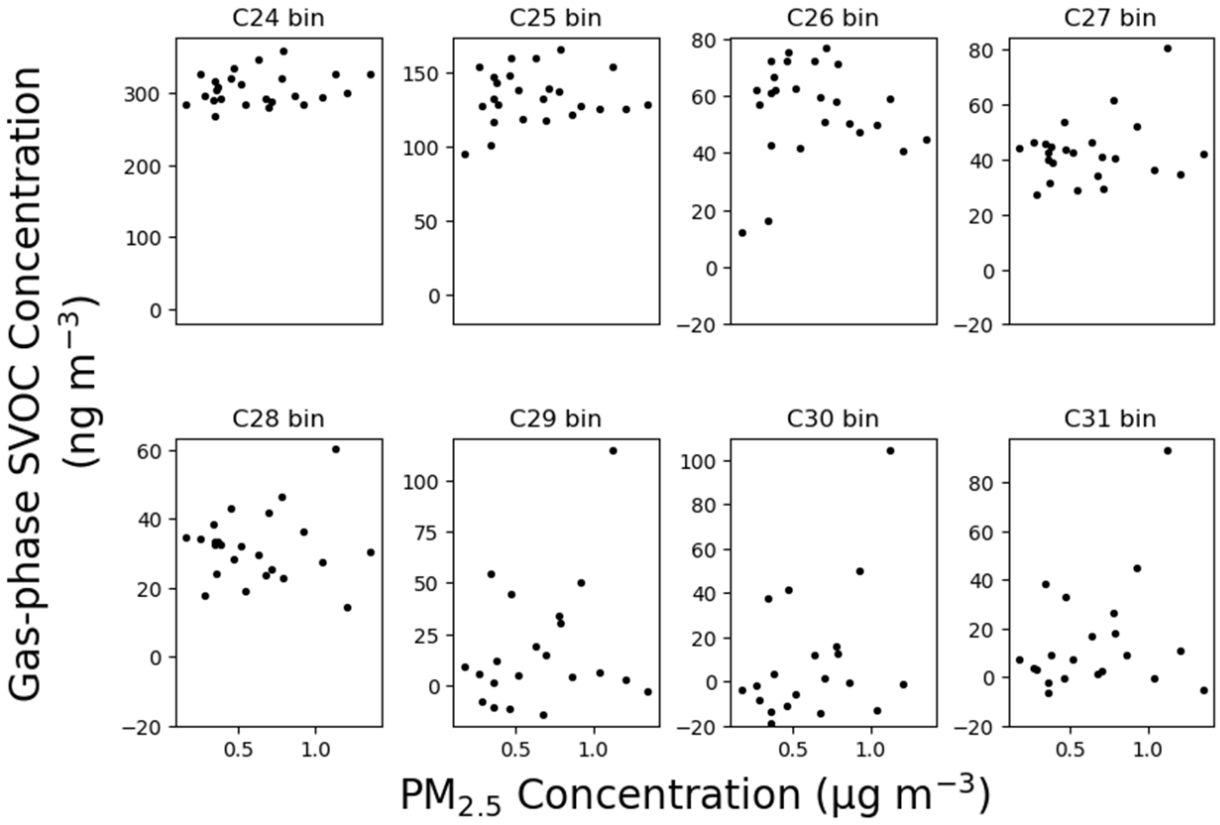

Figure 3.7.8: Alkane-equivalent volatility bin gas-phase concentration versus particle mass loading during the H2 vacant period. Alkane-equivalent volatility bins smaller than the C24 bin were predominantly in the gas phase. The reported gas-particle partitioning of alkane-equivalent volatility bins greater than the C31 bin was highly variable because of measurement uncertainties related to low instrumental response in this range.

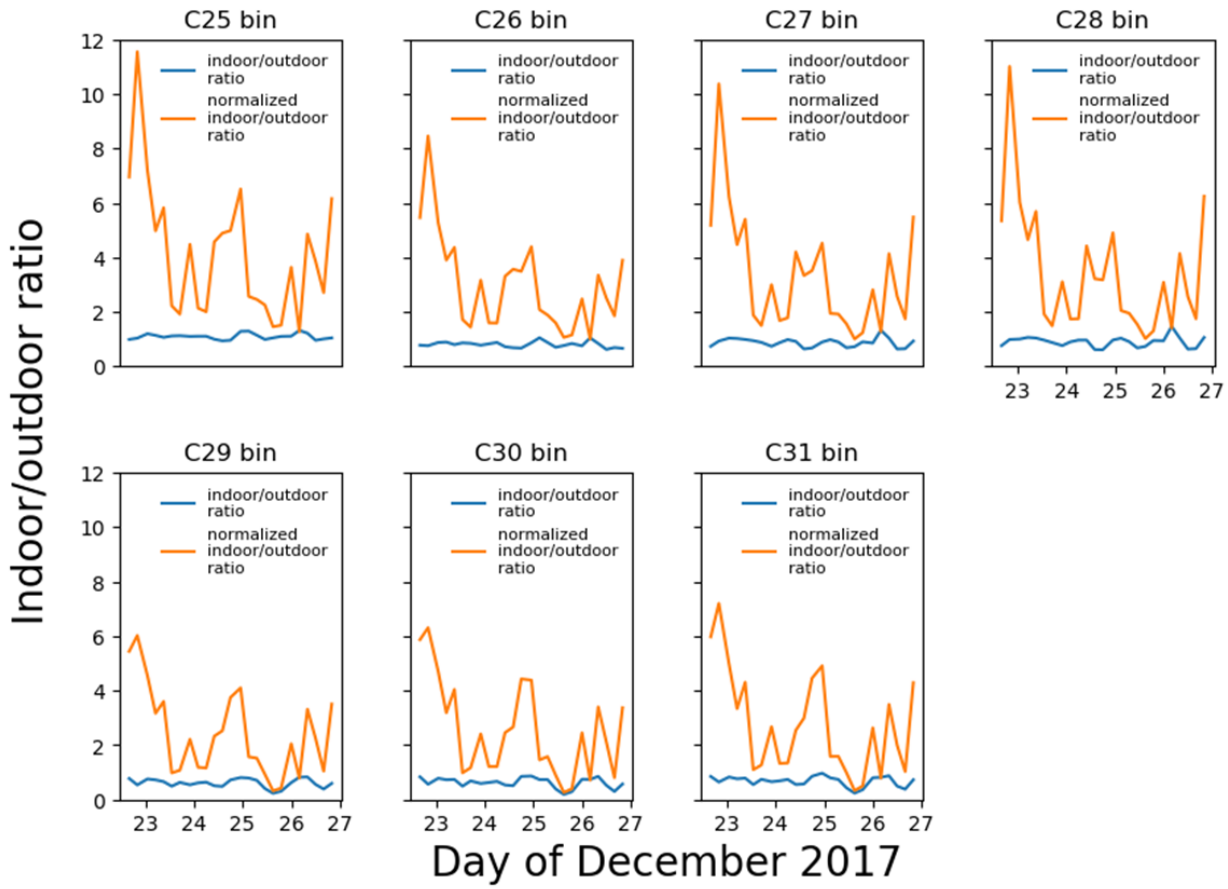

Figure 3.7.9: Time series of alkane-equivalent volatility bin indoor/outdoor concentration ratios during the H2 vacant period. The indoor/outdoor ratio is calculated from the quotient of the total (gas-plus-particle) indoor and outdoor bin concentrations. The normalized indoor/outdoor ratio is the quotient of (1) the indoor bin concentration divided by the indoor PM2.5 mass concentration and (2) the outdoor bin concentration divided by outdoor PM2.5 mass concentration.

3.7.4 HOMEChem Supplementary Analysis

Table 3.7.4: Peak total (gas-plus-particle) siloxane concentrations during the simulated Thanksgiving-day event on June 18.[a]

Compound	Maximum Concentration ($\mu g\ m^{-3}$)
D10	0.2
D11	0.2
D12	0.7
D13	1.3
D14	1.3
D15	1.5
D16	3.4
D17	3.7
D18	3.0
D19	3.2

[a] Concentrations are reported by SV-TAG during the twenty-minute sampling period between **:05 to **:25.

Table 3.7.5: Peak total (gas-plus-particle) siloxane concentrations during the simulated Thanksgiving-day event on June 18.[a]

Name	**log** P_s	**log** K_H	**log** K_{ow}	**log** K_{oa}
D5	-3.87	-3.06	8.5	6.83
D6	-5.23	-2.19	9.39	8.59
D7	-6.08	-3.4	11.58	9.57
D8	-7.26	-4.39	13.95	10.95
D9	-8.45	-5.57	16.49	12.31
D10	-9.66	-6.89	19.17	13.67
D11	-10.87	-8.39	22.01	15.01
D12	-12.09	-9.14	24.18	16.43
D13	-13.32	-9.82	26.29	17.86
D14	-14.56	-10.49	28.4	19.3
D15	-15.81	-11.15	30.51	20.75
D16	-17.07	-11.79	32.62	22.22
D17	-18.34	-12.43	34.74	23.7
D18	-19.62	-13.05	36.85	25.19
D19	-20.91	-13.67	38.96	26.68
D20	-22.2	-14.27	41.07	28.19
D21	-23.51	-14.86	43.19	29.72
L6	-4.46	-6.55	12.07	6.91
L7	-5.27	-7.48	13.88	7.79
L8	-6.08	-8.5	15.78	8.67
L9	-6.89	-9.63	17.77	9.53
L10	-7.7	-10.85	19.86	10.4
L11	-8.52	-12.18	22.03	11.24
L12	-9.33	-13.62	24.3	12.07
L13	-10.14	-15.15	26.66	12.9
L14	-10.95	-16.79	29.11	13.71
L15	-11.77	-18.53	31.65	14.51
L16	-12.58	-19.71	33.68	15.36
L17	-13.39	-20.75	35.57	16.21

[a] Values as predicted by the SPARC online chemical property calculator (calculations performed on 8 October 2019).[14, 15] Values were computed at 298 K. The vapor pressure P_s is reported in atm and K_H is reported in M atm^{-1}. Octanol-water (K_{ow}) and octanol-air (K_{oa}) values are dimensionless. Note that K_{oa} is related to K_H and K_{ow}, where $\log K_{oa} = \log K_{ow} + \log K_H + 1.39$

3.7.5 Supporting Information References

[1] Stein, S. E.; Mirokhin, Y.; Tchekhovskoi, D.; Mallard, W. National Institute of Standards and Technology (NIST) Mass Spectral Search Program for the NIST/EPA/NIH Mass Spectral Library, National Institute of Standards and Technology Standard Reference Data Program, Gaithersburg, 2014.

[2] DeCarlo, P. F.; Kimmel, J. R.; Trimborn, A.; Northway, M. J.; Jayne, J. T.; Aiken, A. C.; Gonin, M.; Fuhrer, K.; Horvath, T.; Docherty, K. S.; Worsnop, D. R. Field-deployable, high-resolution, time-of-flight aerosol mass spectrometer. *Anal. Chem.* **2006**, *78*, 8281–8289.

[3] Farmer, D. K.; Vance, M. E.; Abbatt, J. P. D.; Abeleira, A.; Alves, M. R.; Arata, C.; Boedicker, E.; Bourne, S.; Cardoso-Saldaña, F.; Corsi, R.; DeCarlo, P. F.; Goldstein, A. H.; Grassian, V. H.; Hildebrandt Ruiz, L.; Jimenez, J. L.; Kahan, T. F.; Katz, E. F.; Mattila, J. M.; Nazaroff, W. W.; Novoselac, A.; O'Brien, R. E.; Or, V. W.; Patel, S.; Sankhyan, S.; Stevens, P. S.; Tian, Y.; Wade, M.; Wang, C.; Zhou, S.; Zhou, Y. Overview of HOMEChem: House Observations of Microbial and Environmental Chemistry. *Environ. Sci.: Processes Impacts* **2019**, *21*, 1280–1300.

[4] Cox, S. S.; Little, J. C.; Hodgson, A. T. Predicting the emission rate of volatile organic compounds from vinyl flooring. *Environ. Sci. Technol.* **2002**, *36*, 709–714.

[5] Xu, Y.; Zhang, Y. An improved mass transfer based model for analyzing VOC emissions from building materials. *Atmos. Environ.* **2003**, *37*, 2497–2505.

[6] Xu, Y.; Little, J. C. Predicting emissions of SVOCs from polymeric materials and their interaction with airborne particles. *Environ. Sci. Technol.* **2006**, *40*, 456–461.

[7] Xu, Y.; Cohen Hubal, E. A.; Clausen, P. A.; Little, J. C. Predicting residential exposure to phthalate plasticizer emitted from vinyl flooring: A mechanistic analysis. *Environ. Sci. Technol.* **2009**, *43*, 2374–2380.

[8] Clausen, P. A.; Liu, Z.; Kofoed-Sørensen, V.; Little, J.; Wolkoff, P. Influence of temperature on the emission of di-(2-ethylhexyl)phthalate (DEHP) from PVC flooring in the emission cell FLEC. *Environ. Sci. Technol.* **2012**, *46*, 909–915.

[9] Kristensen, K; Lunderberg, D. M.; Liu, Y; Misztal, P. K.; Tian, Y; Arata, C; Nazaroff, W. W.; Goldstein, A. H. Sources and dynamics of semivolatile organic compounds in a single-family residence in northern California. *Indoor Air* **2019**, *29*, 645–655.

[10] Salthammer, T.; Goss, K.-U. Predicting the gas/particle distribution of SVOCs in the indoor environment using poly parameter linear free energy relationships. *Environ. Sci. Technol.* **2019**, *53*, 2491–2499.

[11] Růžička, K.; Majer, V. Simultaneous treatment of vapor pressures and related thermal data between the triple and normal boiling temperatures for n-alkanes C5–C20. *J. Phys. Chem. Ref. Data* **1994**, *23*, 1–39.

[12] Chickos, J. S.; Hanshaw, W. Vapor pressures and vaporization enthalpies of the n-alkanes from C21 to C30 at T = 298.15 K by correlation gas chromatography. *J. Chem. Eng. Data* **2004**, *49*, 77–85.

[13] Chickos, J. S.; Hanshaw, W. Vapor pressures and vaporization enthalpies of the n-alkanes from C31 to C38 at T = 298.15 K by correlation gas chromatography. *J. Chem. Eng. Data* **2004**, *49*, 620–630.

[14] Hilal, S. H.; Carreira, L. A.; Karickhoff, S. W. Prediction of the vapor pressure, boiling point, heat of vaporization and diffusion coefficient of organic compounds. *QSAR Comb. Sci.* **2003**, *22*, 565–574.

[15] Hilal, S. H.; Carreira, L. A.; Karickhoff, S. W. Prediction of the solubility, activity coefficient, gas/liquid and liquid/liquid distribution coefficients of organic compounds. *QSAR Comb. Sci.* **2004**, *23*, 709–720.

Chapter 4

High-resolution exposure assessment for volatile organic compounds in two California residences

This chapter is adapted from:

Lunderberg, D.M.; Misztal, P.K.; Liu, Y.; Tian, Y.; Arata, C.; Nazaroff, Kristensen, K.; Weber, R.J.; W.W.; Goldstein, A.H. High-resolution exposure assessment for volatile organic compounds in two California residences. *Environ. Sci. Technol.* **2021**, *55*, 6740–6751.

4.1 Abstract

Time spent in residences substantially contributes to human exposure to volatile organic compounds (VOC). Such exposures have been difficult to study deeply, in part because VOC concentrations and indoor occupancy vary rapidly. Using a fast-response online mass spectrometer, we report time-resolved exposures from multi-season sampling of more than 200 VOC species in two California residences. Chemical-specific source apportionment revealed that time-averaged exposures for most VOCs were mainly attributable to continuous indoor emissions from buildings and their static contents. Also contributing to exposures are occupant-related activities, such as cooking, and outdoor-to-indoor transport. Health-risk assessments are possible for a subset of observed VOCs. Acrolein, acetaldehyde, and acrylic acid concentrations were above chronic advisory health guidelines, whereas exposures for other assessable species were typically well below guideline levels. Studied residences were built in the mid-20th century, indicating that VOC emissions even from older buildings and their contents can substantially contribute to occupant exposures.

4.2 Introduction

Exposures to volatile organic compounds (VOCs) can be associated with adverse health outcomes.[1–5] Considering that modern populations spend most of their time in residences and that most VOC concentrations and associated exposures are substantially higher indoors than outdoors,[6–8] evaluating the residential component is critical for understanding total VOC exposures. Certain VOCs and very volatile organic compounds (henceforth bundled as VOCs for brevity), such as formaldehyde, some halogenated solvents, and BTEX (benzene, toluene, ethyl benzene, xylene), among others, have been the subject of substantial attention.[9–11] However, for many VOCs, the levels of exposure, the controlling physical processes, and the consequent health risks remain understudied.[12, 13]

Residential VOC abundances are attributable to multiple sources, which vary among compounds. Potential sources include building materials,[14] outdoor-to-indoor transport,[8] indoor chemistry,[15] consumer products,[16] activities such as cooking,[17, 18] and the human occupants themselves.[19, 20] For most VOCs and in most buildings, the relative contributions from each source to indoor concentrations are not known. In addition, indoor VOC abundances are modulated by physicochemical parameters, such as the ventilation rate,[21] temperature (through sorptive interactions with interior surfaces[22] and temperature-dependent material emissions,[18] humidity[23] and both seasonal and diel variations in outdoor VOC concentrations[18]. Some studies have suggested that VOC emissions from building materials are most important immediately after construction or renovation and can decline by orders of magnitude within a few years.[24–26]

Time-resolved measurements of VOCs in residences and associated exposures are scarce. Time-averaged VOC measurements, either actively collected on sorbent tubes or passively collected on diffusive samplers over fixed intervals, have been used to characterize VOC exposures in cross-sectional studies.[7, 8, 27, 28] Samples are sometimes collected in multiple locations specific to each research participant, including direct monitoring of air immediately proximate to study subjects using personal samplers. In many cases, studies implement a targeted screening approach where analysis is restricted to a subset of chemicals of relevant health interest.

Typically, source apportionment has not been conducted via intensive study of individual residences. Studies focusing on source apportionment of indoor VOCs may collect time-averaged samples and conduct source apportionment via multivariate receptor models. These analyses typically use data reduction techniques such as principal component analysis (PCA) or positive matrix factorization (PMF) on population-level data acquired in survey studies.[8, 29–31] In one such study of Canadian residences, Bari et al. reported that a majority of indoor VOCs were attributable to indoor sources with household products being the largest contributor and off-gassing of building materials the smallest.[31]

Personal exposures measured by portable samplers are often greater than those predicted by stationary monitoring of outdoor, home, and occupational environments.[7, 32] Predictions based on stationary monitoring often assume a well-mixed single-zone space, an assumption which may not be fully justified for strongly localized source events that create

spatial heterogeneities.[33, 34] Proximity of occupants to source events has been used to explain the discrepancy between personal monitoring and stationary monitoring for particles.[35–37] This effect may partially explain the discrepancy between microenvironmental monitoring and personal monitoring when assessing exposures to VOCs released by occupant activities, such as cooking, cleaning or application of personal care products. Another important point is that stationary exposure estimates using time-integrated sampling rest on the assumption that average measured VOC concentrations are representative of average VOC concentrations during occupancy. For VOCs with significant contributions from occupant-related episodic sources, such as cooking or use of personal care products, concentrations may be elevated during occupancy and so occupant exposures would be underestimated if based on time-average concentration measurements that include periods of vacancy. Sporadic, high-concentration events might produce significant temporal variability in VOC abundances and, if so, would necessitate the acquisition of time-resolved VOC measurements and occupant activity data for estimating VOC exposures and apportioning exposure sources. Owing to advances in analytical capabilities, such measurements have begun to be acquired in recent years in several field monitoring campaigns.[17–20, 22]

In this work, we discuss the first broad-scale application of time-resolved VOC measurements coupled with a) occupant time budgets to assess residential exposures to VOCs and b) occupant time-activity budgets to attribute exposures to source categories. The 250 monitored analytes in this work span a broad range of volatilities, chemical functionalities, and toxicities (Tables 4.7.1–4.7.3). Among the characterized analytes are aromatics (including benzene, toluene, xylene), carbonyls (including acetaldehyde and acrolein), furanoids, halogenates, organosulfur compounds, carboxylic acids, alcohols and alkenes, siloxanes, and other compounds of potential health interest (acetonitrile, acrylic acid, acrylonitrile).

In total, we assess residential VOC exposures for more than 200 VOCs sampled with high time resolution over three multiweek monitoring campaigns conducted in two California households. We implement a source apportionment model for VOCs to attribute exposures to four broad source categories: continuous indoor sources, outdoor origin, cooking, and other. We contextualize our observations by utilizing information that relates exposure to health risk, as reported by two U.S. governmental agencies and one California state agency. Lastly, we assess the performance of stationary time-averaged exposure estimates relative to time-resolved best estimates of exposure.

4.3 Experimental Methods

4.3.1 Site Information

This work utilizes measurements from three field campaigns conducted at two normally occupied California residences in the East Bay region of the San Francisco Bay Area in summer and winter seasons (H1 summer, H1 winter, H2 winter). The monitoring campaigns in these residences have been described elsewhere in detail.[18, 38, 39, 40] This paper represents

a continuation of prior analyses describing indoor ventilation patterns[38] and VOC emissions[18] at the H1 residence. It also represents the first reporting of VOC data acquired at the H2 residence. Briefly, the H1 site is a single-family, split-level wood-frame residence, constructed in the 1930s, with two adult occupants designated here as "H1M1" and "H1F1." Measurements were made for 8 weeks in 2016 from mid-August to early October (H1 summer) and for 5 weeks in 2017 from late January to early March (H1 winter). The house did not have air conditioning. During (mild) winter, the residence was sometimes heated by a gas furnace. The H2 site consisted of a single-family, single-story wood-frame residence, constructed in the 1950s, with two adult occupants designated "H2M1" and "H2F1", a teenager, and a dog. A third adult occupant designated "H2M2" was present for approximately half of the measurement period. Measurements were made for an 8-week campaign in 2017-18, from early December to early February. The H2 site was heated by a forced-air gas-fired furnace operating twice a day, in morning and evening.

At each residence, occupants maintained daily logs describing their temporal presence and activity. Occupant presence data was recorded with approximately 5-min resolution and coded as "indoors," "indoors sleeping," and "away." Time-resolved activities, including cooking, cleaning, candle combustion, and some use of personal care products, were also recorded by the occupants. A network of >50 wireless sensors collected metadata during each measurement period, including temperature, humidity, motion, appliance use, and door/window status.

4.3.2 Chemical Measurements

A proton-transfer-reaction time-of-flight mass spectrometer (PTR-ToF-MS, Ionicon Analytik GmbH, Austria, PTRTOF 8000) was used to measure VOCs during each campaign. The PTR-ToF-MS was located in an external garage (H1 summer, H1 winter) or an external shed (H2 winter). The PTR-ToF-MS uses soft ionization with H_3O^+ as the primary reagent ion, yielding parent masses (1.000 amu – 500.00 amu) of gaseous species whose proton affinities are greater than the proton affinity of water. Most unsaturated hydrocarbons and compounds with heteroatoms are quantifiable with detection limits on the order of 0.005 ppb and time-resolution on the order of minutes. PTR-ToF-MS operating parameters and quantification during the H1 summer and winter campaigns have been described elsewhere[18, 38] and are summarized in the supporting information (SI, Section 1).

4.3.3 Exposure Analysis

Time-integrated exposures (hereafter "exposures") were calculated as the integral of time-instantaneous exposures over the time period of exposure. Daily occupant exposures in units of ppb-hours per day (ppb-h d^{-1}) were calculated by integrating ion formula concentrations for each day during periods when each occupant was present. Measurement periods with major interferences from researcher activities were excluded from all analyses. The kitchen concentration was used at H1 as the best-estimate for calculating occupant exposures and

the living room concentration was used at H2. VOC concentrations throughout the living spaces and kitchen in both residences were well-coupled. During sleeping hours at H2, the concentration in the kitchen may not be fully representative of occupant exposures as each closed bedroom is partially decoupled from the main living space. In this condition, occupant exposures to bioeffluents emitted during sleeping periods may be underestimated. At H1, the bedroom doors were left open throughout the sampling campaign and so the sleeping environment is expected to be well-coupled to the kitchen, although biogenic emissions may still be higher within the bedroom. Simulated distributions of time-averaged exposures were constructed by random sampling. These distributions may be biased by 1-2 data gaps (<2 days) in concentration time series related to instrumental down time or intentional manipulation experiments conducted by researchers. Data gaps encountered during random selection were treated by using the next available measurement in the "time-averaged" sample.

4.3.4 Source Apportionment

VOC time series were typically characterized by a persistent background modulated by regular changes in temperature in association with the diurnal temperature cycle (H1 summer) or house heating cycle (H2 winter) and punctuated by rapid concentration spikes related to specific events. The temperature-dependent background was clearly identified during periods of vacancy when occupant-related events did not occur. Concentration spikes and associated peak boundaries were manually identified for each ion formula and assigned to specific source categories based on coincident events during the growth phase of the peak. The peak baseline was determined by a linear regression between the concentrations observed at peak boundaries. Net peak areas were defined as the total integrated area above the peak baseline. Event peaks were excluded if at least 50% of the event by peak-height was attributable to outdoor infiltration. More detailed information about the peak selection process is available in the SI. Outdoor VOC concentrations were assumed to enter the indoors without attenuation, allowing for outdoor VOC concentrations to be used as a proxy for the indoor VOC concentrations of outdoor origin. On the rare circumstance that outdoor concentrations were greater than indoor concentrations, the indoor concentration was assumed to be derived wholly from outdoor-to-indoor transport. The integrated areal remainder after subtracting contributions from events and from outdoor transport was defined as "continuous indoor sources." In total, more than 12,000 peaks were identified from among the 594 chemical concentration time series acquired during the three campaigns.

4.3.5 Risk-Based Prioritization

Advisory health guidelines for acute and chronic exposures to VOCs were acquired from three organizations: the U.S. Environmental Protection Agency (USEPA) Integrated Risk Information System (IRIS, chronic only),[41] the California Environmental Protection Agency Office of Environmental Health Hazard Assessment (OEHHA),[42] and the Agency for Toxic Substances and Disease Registry (ATSDR).[43] Each organization has independently de-

veloped concentration guidelines for chronic VOC exposures. The IRIS database reports reference concentrations (RfCs), "an estimate (with uncertainty spanning perhaps an order of magnitude) of a continuous inhalation exposure to the human population (including sensitive subgroups) that is likely to be without an appreciable risk of deleterious effects during a lifetime." OEHHA reports reference exposure levels (RELs), an estimate of concentrations for inhalation exposure "at or below which no adverse health effects are anticipated following long-term exposure." ATSDR reports minimal risk levels (MRLs), "an estimate of the amount of a chemical a person can eat, drink, or breathe each day without a detectable risk to health." These health guidelines were selected as three major guidelines from state and federal agencies in the United States that are relevant to the location of the studied residences. Other international guidelines have also been developed.[44–48]

4.4 Results and Discussion

4.4.1 Time-Resolved Exposures

Indoor VOC concentrations and occupant time-activity budgets were acquired at two normally occupied California residences in the summer and winter seasons over three monitoring periods: the H1 summer campaign (8 weeks), the H1 winter campaign (5 weeks), and the H2 winter campaign (8 weeks). In total, 250 ion masses corresponding to molecular formulas of VOCs were identified (H1 summer: 217 ions; H1 winter: 170 ions; H2 winter: 205 ions), with substantial overlap among campaigns. Of these ions, 115 were assigned to specific chemical structures based on site-specific knowledge, fragmentation patterns, and supporting measurements using thermal desorption two-dimensional gas chromatography time-of-flight mass spectrometry (TD-GC×GC-ToF-MS). Paired indoor/outdoor VOC concentrations were acquired every 30 minutes. Figure 4.4.1 displays occupant time-budgets and activities for the H2 winter campaign. During each campaign, VOC concentrations generally increased with increasing temperature or specific occupant activities and decreased with increasing ventilation. Concentrations were higher indoors when compared to outdoors ($> 2\times$) for most VOCs ($\sim$95%) at the H1[18] and H2 sites, consistent with past field studies. Moreover, for about half of the observed VOCs, concentrations were substantially higher ($> 10\times$) indoors than outdoors.

Source apportionment in this study attributed the residential VOC exposures to four source categories: "continuous indoor sources," "outdoor origin," "cooking," and "other." Time-resolved exposures and associated source apportionments are displayed in Figure 4.4.1 for site H2 and subject H2M1 for the case of acrolein, an illustrative compound of health interest with prior evidence of both continuous indoor sources (lumber) and episodic sources (combustion, cooking).[48–52] We note that acrolein has been previously measured in outdoor ambient air and retail stores near the H1 and H2 residences.[53, 54] In the present study, daily occupant exposures to acrolein were mainly attributable to continuous indoor sources, with a median exposure of $\sim$ 4.6 ppb-hours per day (ppb-h d^{-1}). Substantial variation was observed

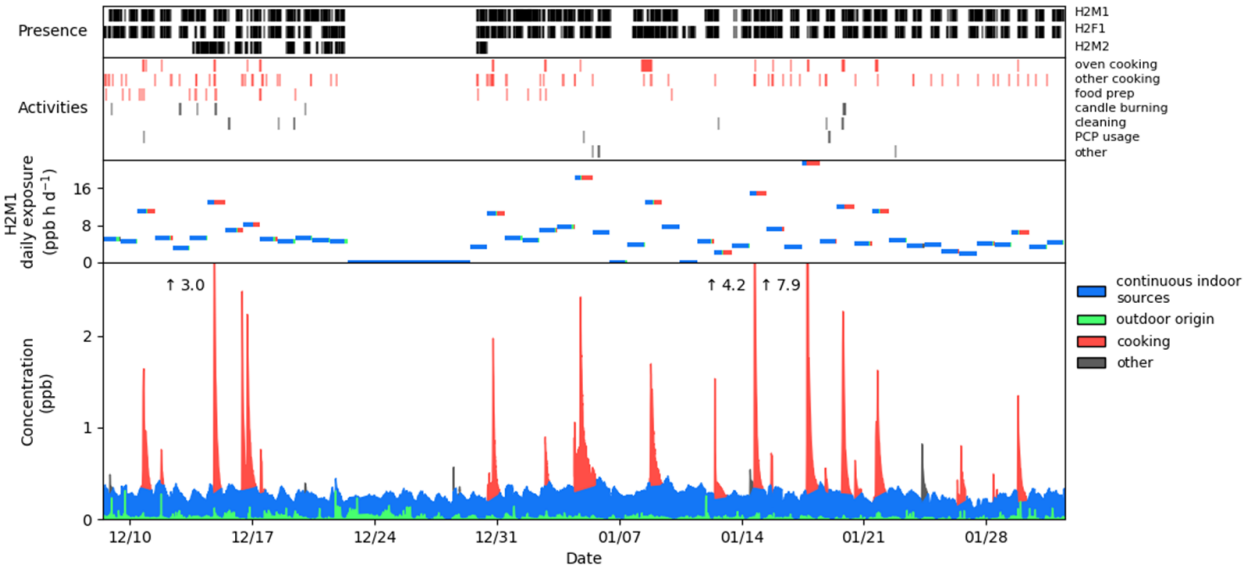

Figure 4.4.1: Acrolein exposure data at H2. In the two uppermost panels, occupant presence and activity data are displayed during the H2 campaign. In the bottommost panel, the time series and associated source apportionment of indoor acrolein ($C_3H_5O^+$) is displayed, with colors corresponding to the relative contribution from each source category. Integrated daily exposures are shown in the second panel from the bottom for occupant H2M1. The shading of the horizontal bar is colored according to the proportion of exposure attributable to each source category.

in daily exposures, principally due to variations in the fraction of time that occupants spent indoors combined with the effects of event-specific sources. Certain days with cooking events doubled the daily occupant acrolein exposures. Due to the infrequency of cooking events that emitted acrolein at H2, exposures attributable to continuous indoor sources accounted for ∼65% of cumulative occupant acrolein exposures, with cooking contributing 25-30% and outdoor-to-indoor transport the small remainder. Most episodic enhancements in acrolein concentrations were specifically attributed to cooking. Only two episodic enhancements remained unassociated with any reported events. (These enhancements did not significantly influence cumulative occupant acrolein exposures, indicating that episodic contributors to acrolein exposures are well understood at this site and are principally derived from cooking.) At H2, oven cooking produced the largest enhancements in acrolein concentrations. At H1, stovetop cooking produced the largest acrolein enhancements. Both the H2 oven and the H1 stovetop were electric, suggesting that heated food (rather than natural gas combustion) was the largest episodic contributor to acrolein emissions in agreement with past studies observing no differences between types of cooking appliances.[48] While enhancements in acrolein concentrations at H2 were also observed in association with use of a natural gas

stove-top, these enhancements were much smaller in abundance than those from the electric oven. Most acrolein enhancements at H2 were observed in association with the use of cooking oil. This finding aligns with previous reports that heated cooking oil is a primary source of acrolein during cooking.[50–52]

4.4.2 Source Apportionment

Source apportionment of occupant VOC exposures was performed for all VOCs observed in the H1 winter, H1 summer, and H2 winter campaigns following the method shown in Figure 4.4.1. At each site, exposures are assessed separately for each of the primary adult occupants. The relative contributions to the total exposure from each source category were identified for each VOC and are reported on a percentage basis. Source apportionment of residential exposures to 205 VOCs for occupant H2M1 is shown in Figure 4.4.2. Approximately 90% of observed VOCs produced time-averaged exposures that were primarily attributable to continuous indoor sources during all three monitoring campaigns at these two residences. Compounds with predominantly indoor continuous sources spanned diverse ranges of volatilities and chemical functionalities, including carboxylic acids (octanoic acid – 95% of exposure from indoor continuous emissions), siloxanes (caprylyl methicone – 95%), aromatics (phenol – 93%), carbonyls (C9 carbonyl – 92%), among others, and were not easily generalizable to specific categories. Caprylyl methicone is a trisiloxane commonly used in cosmetics; surprisingly, its presence was dominated by continuous emissions with the exception of two short-term concentration spikes in the evening. Cooking was the most important episodic source of indoor VOC exposures[18]; however, only eight specific VOCs had exposures that were principally attributable to cooking during any of the campaigns for any occupant: ethanol, methanethiol, pyrrole, dimethyl sulfide, $C_6H_9O_4^+$, D4 siloxane, L5 siloxane, and dimethoxysilane. The latter three compounds were emitted synchronously with cooking events, but it is not certain that they originated directly from the food, cookware or cooking appliances. Apart from cooking, exposures of only three volatile compounds—acetone, an unidentified siloxane ($C_7H_{21}O_3Si_3^+$), and the inorganic gas dichloramine—were otherwise largely attributable to episodic indoor emission events for any occupant. Acetone was identified as originating from the indoor use of nail polish remover during the H2 winter campaign. Dichloramine was identified as originating from episodic cleaning events. Cyclic siloxanes are known additives to consumer personal care products. Noting that three of five concentration spikes of the unidentified siloxane over the H2 winter campaign occurred immediately following sleeping periods when a personal care product might have been applied as part of a morning routine, it is suspected that the unidentified siloxane is a component of a personal care product. Only ten specific VOCs had exposures that were primarily attributable to outdoor-to-indoor transport for any occupant. Four of these compounds were observed in all campaigns (chloroform, acetonitrile, parachlorobenzotrifluoride, $C_4H_3O_3^+$), four compounds were unique to the H1 summer campaign ($C_10H_9O_3^+$, $C_2H_5O_3^+$, $C_5H_5O_3^+$, CCl_2F^+), and two compounds were unique to the H2 winter campaign (ethane thiol + DMS and C10H15O+). We also highlight $C_8H_9O_2^+$ (anisaldehyde, a floral fragrance) and $C_{10}H_{17}^+$ (monoterpenes,

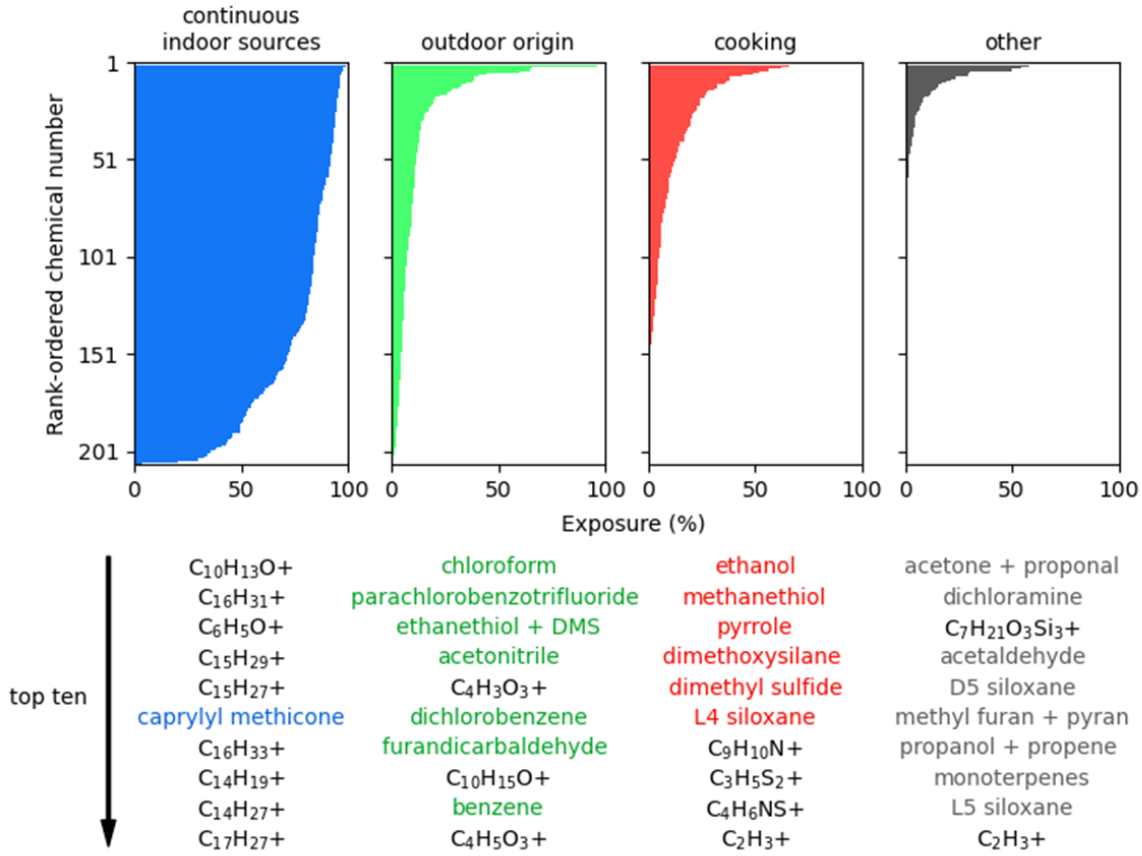

Figure 4.4.2: Rank-ordered VOC exposures by source category for occupant H2M1 during the winter campaign at H2. Residential VOC exposures to 205 VOCs were calculated for occupant H2M1. The contributions from each source category to the total exposure of each VOC were identified and are reported on a percentage basis. The relative contributions from each VOC were then rank-ordered from greatest-to-least for each source category. Source categories include continuous indoor sources (blue), outdoor-origin (green), cooking (red), and other (gray). The unique rank-orderings for each source category are displayed in the upper panel and the top ten VOCs in each rank-ordered source category are identified in the lower section of the figure.

emitted during citrus consumption) as compounds of interest. In addition to cooking, we observed large contributions from episodic events unrelated to cooking (31% and 36%, respectively during the H1 winter campaign), expected to partially originate from personal care product use and citrus consumption.

Relative contributions for each source category were calculated for all observed VOCs and

for each occupant during each campaign (Figure 4.4.3). Absolute daily exposures and relative source apportionments can be found in the SI (Figure 4.7.1, Tables 4.7.1–4.7.3). Time-activity budgets exhibit some differences (Figure 4.7.2); however, source apportionments for each occupant were qualitatively and quantitatively similar. For the H1 campaigns, relative contributions from source categories for occupant exposures were within 15 absolute percentage points of relative source apportionments derived from concentration time series for all but $C_6H_9O_4^+$. (Source apportionments from concentration time series are equivalent to relative source apportionments of exposures for an occupant who is always present.)

In contrast, deviations were observed between source apportionments for a substantial subset of VOCs that were dominantly event-driven during the H2 winter campaign (19 of 205 ions). These mainly occurred for the H2M2 occupant, who was present for only part of the measurement campaign. If the H2M2 occupant is excluded, only two exceptions are observed, the inorganic gas dichloramine (related to cleaning) and the $C_3H_6^+$ ion. Generally, if an occupant was absent for a large emission event, as in the case of H2M2 for much of the measurement campaign, discrepancies were observed.

Absolute exposures were comparable between the H1 summer and winter seasons for most VOCs. Of 166 ions concurrent to both seasons, absolute mean concentrations for 66% (97%) of VOCs differed by no more than 50% (factor of 2) between seasons (Figure 4.7.3). Large exceptions ($> 2\times$ difference) were observed for D5 siloxane, monoterpenes, $C_2H_3^+$, and methane sulfonic acid (greater during the H1 winter season) and for cinnamaldehyde (greater during the H1 summer season). During the H1 summer season, 47 more compounds were observed above the detection threshold than during the H1 winter season. These compounds are chemically diverse, including halogens, aromatics, oxygenates, and organosulfurs. We are unable to assign most of these ions to specific chemical structures. While only four VOCs were principally attributable to outdoor-to-indoor transport during the H1 winter season, the same four plus four additional VOCs were attributable to outdoor-to-indoor transport during the H1 summer season, of which three were highly oxygenated species ($C_2H_5O_3^+$, $C_5H_5O_3^+$, $C_10H_9O_3^+$). The highly oxygenated species had cyclical outdoor fluctuations with afternoon peaks, suggesting that these compounds may be arising as secondary VOCs produced through summertime enhanced outdoor photochemistry or as biogenic emissions. In general, outdoor-to-indoor transport was more important during the summer season as opposed to the winter season. Indoor concentrations attributable to outdoor-to-indoor transport were greater on an absolute basis for 147 compounds concurrent to both the H1 summer and H1 winter campaigns (88%). However, contributions for these compounds remained low, accounting, on average, for 16% and 11% of total indoor concentrations in summer and winter, respectively.

A recent review of longitudinal studies measuring total volatile organic compound (TVOC) levels asserts that emissions from buildings and their contents are a "new building" phenomenon that is most important only soon after construction, renovation, or refurbishing as new materials off-gas. After an initial 1-2 year off-gassing period, TVOC emissions from building materials decline such that they are assumed to be unimportant relative to VOC emissions related to occupants and their activities.[26] However, measurements of TVOC levels are not generalizable to specific VOCs that may be of interest to public health. One

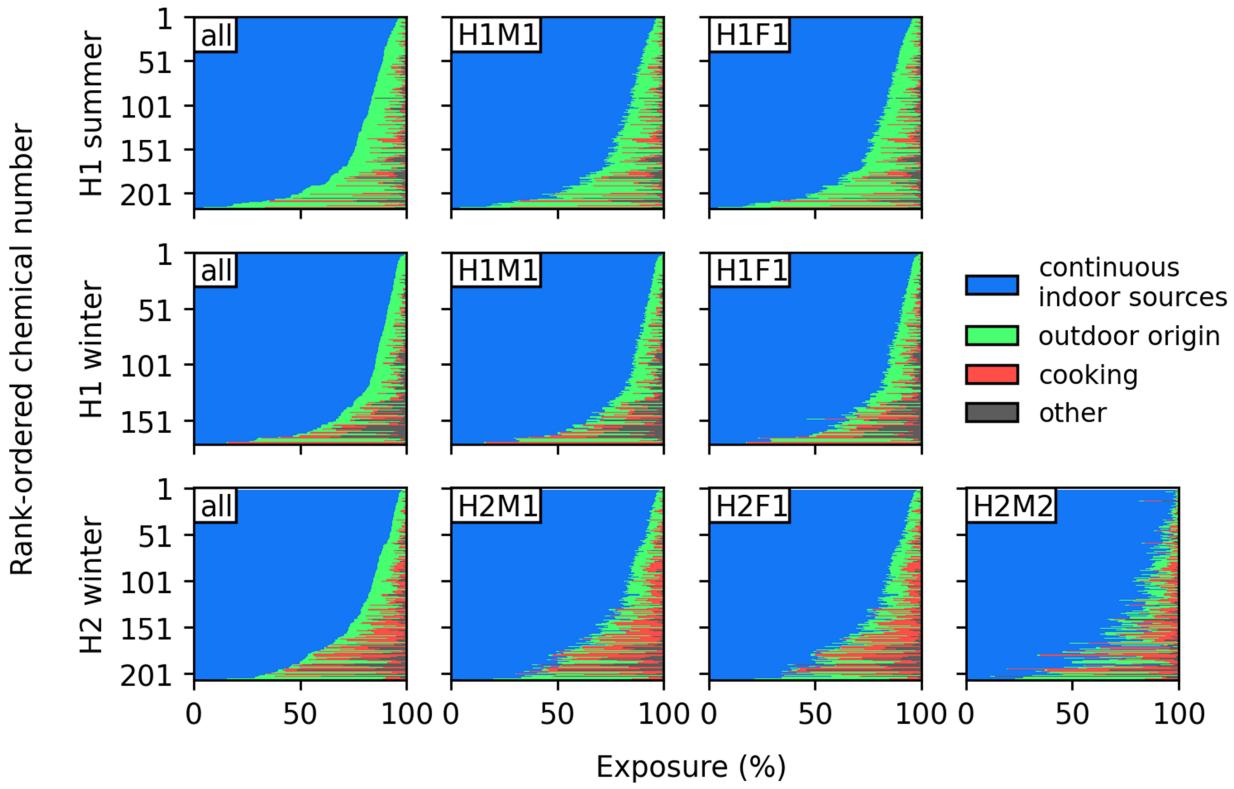

Figure 4.4.3: Relative source apportionment of VOC exposures. Residential exposures to (217, 170, 205) detected VOC ions were calculated for each occupant during the (H1 summer, H1 winter, H2 winter) monitoring campaigns and were apportioned into specific source categories. Subpanels display relative VOC exposures for individual occupants; the heading 'all' refers to a hypothetical occupant who is present for all of the measurement period. In subpanels, each horizontal bar corresponds to a single VOC and is colored according to the relative contribution from each source category (continuous indoor sources [blue], outdoor-origin [green], cooking [red], and other [gray]). Each row of panels uses the same rank-ordering defined by the first 'all' subpanel, which has VOCs rank-ordered from greatest-to-least by the relative contribution from "continuous indoor sources." The top, middle, and bottom rows correspond to the H1 summer, H1 winter, and H2 winter campaigns, respectively.

longitudinal study of 25 speciated VOCs including alkanes, aromatics, and aldehydes in 251 Japanese residences similarly found that VOC concentrations in wood-framed housing will generally decrease over a 1-2 year off-gassing period before stabilizing at levels consistent with much older residences.[24] In contrast, homes with ferroconcrete or light-steel frames, regardless of age, produced VOC profiles consistent with aged-wood frames. The present study focused on measurements acquired at two houses of wood-frame construction, as is common in the US housing stock. We caution that certain features of wood-framed houses, such as temperature-dependent emissions originating from wood and substantial buffering of indoor humidity,[55] may not be fully generalizable to other construction types.

While it may be true for some chemicals that VOC emissions from buildings are less important in older residences, observations at the H1 and H2 sites indicate that continuous indoor sources were the largest contributors to VOC exposures for more than 90% of observed species, even though the residences were many decades old and had not been recently remodeled or refurnished. Plausible sources might include continued material off-gassing as deeply bound VOCs migrate to surfaces; oxidative, thermal or microbial decomposition of building materials yielding decomposition products; or sorptive interactions as VOCs related to occupant events deposit on surfaces and then slowly off-gas. The last mechanism has been traditionally understood to apply to semivolatile organic compounds (SVOCs), but recent studies suggest that sorption in surface reservoirs is also important for VOCs.[22] That phenomenon may cause primary emissions from episodic sources to be interpreted as originating from building materials.

Source control efforts prioritize building materials and furnishings with the specific goal of encouraging use of materials with low short-term VOC emissions. Unified regulatory limits are generally not available, but some countries have implemented product certification and voluntary emissions testing programs. The H1 and H2 sites suggest that ongoing VOC emissions can be expected to occur from building materials long after any short-term VOC reservoirs are depleted. While we expect that these sites are ordinary for their age and location, further study is warranted to see if these findings generalize to other sites, especially those with higher concentrations of airborne VOCs. If exposures associated with long-term VOC emissions from building materials prove to be significant for occupant health and well-being, current control strategies may need augmentation. Some compounds associated with wood degradation, such as carboxylic acids, furanoids and acetaldehyde, may prove particularly challenging to address via source-control strategies of the type currently employed.

Past source apportionment studies using multivariate receptor models of population-level data have diverged on the relative importance of off-gassing from building materials.[29–31] For instance, Bari et al. noted that off-gassing from building materials contributed only 6% of measured total VOCs ($n = 119$ analytes; alkanes, alkenes, aromatics, halogens, carbonyls, alcohols, terpenes, others) in Canadian residences.[31] Conversely, Guo reported that 77% of measured VOCs in Hong Kong residences were attributable to emissions from building materials ($n = 16$ representative analytes; alkanes, aromatics, carbonyls, terpenes, acids, others).[30] Such differences between studies may reflect the choice of studied ana-

lytes rather than differences in building age and composition. Furthermore, dimensionality reduction techniques, such as positive matrix factorization (PMF) and principal component analysis (PCA), reduce complex datasets to specific factors or components unique to each dataset that must be interpreted and assigned to specific source categories. While such source apportionment studies yield qualitatively similar results reflecting commonalities in residential VOC sources, it is difficult, and often unjustifiable, to generalize quantitatively between different source apportionment analyses. Contrasting findings between the present study, indicating substantial contributions from continuous indoor sources, and past studies, indicating that off-gassing from aged building materials is less important, may be related to subjective choices for source assignment in multivariate receptor models. This observation emphasizes that detailed characterizations of single-residences are needed to complement and justify inferences from population-level surveys.

4.4.3 Risk-Based Prioritization

Chronic advisory health guidelines from at least one agency were acquired for 31 VOCs consistent with chemical formulas identified at the H1 and H2 field sites. Of these 31 VOCs, 18 were specifically identified at the H1 and H2 field sites with high degrees of confidence (Table 4.4.1, Table 4.4.2). Considering residential exposures at these two study sites, three compounds exceeded a health-risk guideline given by IRIS, OEHHA, or ATSDR. Acrolein concentrations were 1–2 orders of magnitude higher than the health-risk guidelines of IRIS and ATSDR, and ∼3–4 times higher than the OEHHA guideline, for each occupant during all three campaigns. Acetaldehyde concentrations were above the USEPA IRIS health guideline and within an order of magnitude of the OEHHA health guideline for all occupants during all three campaigns. Acrylic acid concentrations were comparable to the USEPA IRIS health guideline for all occupants during all three campaigns. Health guidelines for acrylic acid were not available from OEHHA and ATSDR. Acrolein and acetaldehyde have already been identified as two of nine "priority hazards based on the robustness of measured concentration data and the fraction of residences that appear to be impacted."[3]

We also consider acute advisory health guidelines from OEHHA and ATSDR for 15 VOCs consistent with chemical formulas identified at the H1 and H2 fields sites, all of which were identified with high confidence (Table 4.7.4). Acrolein concentrations exceeded acute concentration guidelines 1–2 times each week during the H1 summer and H2 winter campaigns, often in association with cooking. Exceedances were less common during the H1 winter campaign, occurring only twice over the five-week monitoring period. Three events during the H2 winter campaign produced acetaldehyde concentrations that exceeded OEHHA acute concentration guidelines. Benzene concentration spikes reached concentrations roughly one third that of the acute guideline value. A short-term spike in acetone concentration associated with the use of nail polish remover reached 20% of the acute guideline value during the H2 winter campaign. All other compounds with available acute concentration guidelines were typically 2–3 orders lower than the guideline value.

Table 4.4.1: Indoor concentrations are presented as time averages of measured living space concentrations for the periods that individual occupants are indoors at home.

	Mean abundance (ppb)									
	H1 summer			H1 winter			H2 winter			
Ion Formula	all	H1M1	H1F1	all	H1M1	H1F1	all	H2M1	H2F1	H2M2
$C_3H_5O^+$	0.57	0.56	0.57	0.44	0.44	0.45	0.36	0.39	0.39	0.38
$C_2H_5O^+$	9.3	9.7	9.5	8.3	8.2	9.1	24	28	26	14
$C_3H_5O_2^+$	0.37	0.37	0.37	0.29	0.29	0.31	0.27	0.29	0.29	0.27
$C_6H_7^+$	0.24	0.24	0.24	0.46	0.46	0.46	0.31	0.33	0.33	0.27
$C_8H_{11}^+$	0.25	0.24	0.25	0.25	0.24	0.24	0.33	0.34	0.34	0.31
CH_5O^+	28	27	27	28	28	28	45	50	50	42
$C_3H_7O^+$	11	11	11	9.9	10	10	30	39	39	19
$C_7H_9^+$	0.36	0.34	0.35	0.75	0.76	0.75	1.3	1.3	1.3	1
$C_6H_7O^+$	0.52	0.52	0.52	0.48	0.48	0.48	0.34	0.36	0.36	0.31
CCl_3^+	0.17	0.17	0.17	0.13	0.13	0.13	0.14	0.13	0.13	0.14
$C_2H_4N^+$	0.16	0.16	0.16	0.11	0.11	0.11	0.14	0.14	0.14	0.14
$C_6H_{15}O_2^+$	<LOD	<LOD	<LOD	<LOD	<LOD	<LOD	0.05	0.053	0.053	0.043
$C_6H_5Cl_2^+$	0.018	0.018	0.018	0.019	0.019	0.019	0.01	0.011	0.01	0.01
$C_7H_9O^+$	0.18	0.17	0.17	0.15	0.14	0.14	0.1	0.11	0.11	0.1
$C_4H_9O^+$	0.76	0.76	0.76	0.75	0.74	0.78	1.3	1.5	1.5	1.2
$C_8H_9^+$	0.14	0.14	0.14	0.15	0.14	0.15	0.16	0.17	0.17	0.15
$C_4H_3O_3^+$	0.014	0.015	0.014	0.019	0.019	0.019	0.015	0.016	0.016	0.014
$C_4H_7O_2^+$	0.69	0.68	0.69	0.59	0.58	0.6	0.59	0.62	0.62	0.56
$C_3H_4N^+$	0.022	0.021	0.021	0.022	0.022	0.022	0.034	0.035	0.035	0.033
$C_6H_{13}O^+$	0.23	0.22	0.23	0.16	0.16	0.16	0.21	0.21	0.21	0.19
$C_9H_{13}^+$	0.13	0.12	0.12	0.14	0.14	0.13	0.16	0.18	0.18	0.14
$C_5H_9O_2^+$	0.54	0.53	0.54	0.31	0.31	0.31	0.31	0.32	0.32	0.28

Public health guidelines often incorporate large uncertainty factors to account for limitations in the available toxicological data. In some cases, this may lead to uncertainties "spanning perhaps an order of magnitude" as explicitly stated by USEPA IRIS. In the event that USEPA guidelines are an order-of-magnitude overestimate, several of the flagged VOCs would no longer be expected to be of health interest at observed levels. If guidelines are an-order-of-magnitude underestimate, additional compounds may be of health interest at observed levels.

Source apportionment reveals that acrolein, acetaldehyde and acrylic acid at these study sites are principally attributable to continuous indoor sources with important contributions from cooking and smaller contributions from outdoor-to-indoor transport. During the H1 summer and H1 winter campaigns, acetaldehyde exposures were principally attributed to continuous indoor sources (∼60-70%) with contributions from cooking (∼20-30%) and outdoor-to-indoor transport (∼5-10%). In contrast, during the H2 winter campaign, continuous indoor sources accounted for half of occupant exposures, with significant contributions from both cooking (∼20%) and unidentified indoor source events (∼30%). Acrylic acid exposures were principally attributed to continuous indoor sources (∼60-80%) with contributions from cooking (∼5-20%) and outdoor-to-indoor transport (∼15-25%) across the three campaigns. Acrolein exposures were principally attributed to continuous indoor sources (∼70-90%) with contributions from cooking (∼5-10%) and outdoor-to-indoor transport (∼5-20%) across the three campaigns.

Table 4.4.2: Chronic hazard assessment of select VOCs. [a]

	Name	Concentration Guideline Ratio	OEHHA REL (ppb)	USEPA IRIS RfC (ppb)	ATSDR MRL (ppb)
$C_3H_5O^+$	acrolein	66	0.15	0.0087	0.04 (int.)
$C_2H_5O^+$	acetaldehyde	5.6	78	5	
$C_3H_5O_2^+$	acrylic acid	1.1		0.34	
$C_6H_7^+$	benzene	0.15	94	9.4	3
$C_8H_{11}^+$	xylene	0.15#	160	2.3	50 (int)
	ethyl benzene	0.0057	460		60
CH_5O^+	methanol	0.033	3100	1500	
$C_3H_7O^+$	acetone	0.03			1300
	propionaldehyde*	11		3.4	
$C_7H_9^+$	toluene	0.016	80	1300	1000
$C_6H_7O^+$	phenol	0.001	52		
CCl_3^+	chloroform	0.0085			20
$C_2H_4N^+$	acetonitrile	0.0044		36	
$C_6H_{15}O_2^+$	2-butoxyethanol	0.0031	17		
	butoxyethanol	0.00027			200
$C_6H_5Cl_2^+$	dichlorobenzene	0.0019	130	130	10
$C_7H_9O^+$	cresols	0.0011	140		
$C_4H_9O^+$	ethyl methyl ketone	0.00088		1700	
	tetrahydrofuran*	0.0022		680	
$C_8H_9^+$	styrene	0.00085	210	240	200
$C_4H_3O_3^+$	maleic anhydride*	0.11#	0.17		
$C_4H_7O_2^+$	vinyl acetate*	0.012	57	57	10 (int)
$C_3H_4N^+$	acrylonitrile*	0.038	2.3	0.92	
$C_6H_{13}O^+$	2-hexanone*	0.032		7.3	
	methyl isobutyl ketone*	0.00032		730	
$C_9H_{13}^+$	ethylmethylbenzene*	NA	NA	NA	NA
	cumene*	0.0023		80	
	trimethylbenzene*	0.015		12	
$C_5H_9O_2^+$	acetylpropionyl	NA	NA	NA	NA
	glutaraldehyde*	27#	0.02		0.03 (int)
	methyl methacrylate*	0.0032		170	

[a] Reference concentrations (USEPA IRIS), reference exposure levels (OEHHA), and minimal risk levels (ATSDR) are presented for chronic and intermediate (int.) VOC exposures. Ion formulas with uncertain confidence in compound assignment are designated with an asterisk. All other compounds are possible assignments. OEHHA and IRIS values were converted from mass per volume concentrations to mixing ratios by applying the ideal gas law and assuming standard conditions (298 K, 1 atm). The "Concentration-to-Guideline Ratio" is defined as the ratio between the greatest mean occupant exposure concentration (see Table 4.4.1) among the campaigns and the smallest health guideline concentration. All concentrations are reported in ppb. Values marked with "#" are uncertain ion formula assignments that, if assigned correctly, may be exceeding health advisory guidelines or warrant additional interest.

We highlight other VOCs with concentrations within an order magnitude of health guidelines as meriting further consideration. Concentrations of benzene were well below the OEHHA health advisory limit but are within an order of magnitude of the USEPA IRIS and ATSDR guidelines. Residential benzene exposures at these study sites were principally attributed to continuous indoor emissions (∼50-60%) and outdoor-to-indoor transport (∼40-50%), highlighting the importance of both indoor sources and outdoor emissions (which are likely traffic-related). Similar results are observed for other BTEX (benzene, toluene, ethylbenzene, xylene) compounds that have been the subject of significant interest and have been attributed to both indoor sources and outdoor fossil-fuel related sources.[11]

There were no health guidelines available for ∼90% of the 250 VOC ions observed. Furthermore, both VOC concentrations and associated toxicities can vary by orders of magnitude, indicating that it may not be sufficient to assume that there are minimal impacts on human health when compounds are present at relatively low concentrations. The possibility of additive or synergistic interactions arising from exposure to complex VOC mixtures may similarly influence health risks from air pollutant exposures in residences.

We were unable to conclusively assign some molecular ions to specific VOCs; these may represent an isomeric mixture of compounds with the same molecular formula but (potentially) different toxicities. We note that concentrations of the $C_8H_{11}^+$, $C_4H_3O_3^+$, and the $C_5H_9O_2^+$ ions, if attributed solely to xylene, maleic anhydride, and glutaraldehyde, respectively, would be of potential health-risk concern. Static measurements acquired by offline TD-GC×GC-ToF-MS at during the H2 winter campaign suggest that xylene isomers accounted for 80% of observed mass of $C_8H_{11}^+$ with ethylbenzene accounting for the remainder. There was no evidence of any analyte with structural formulas consistent with $C_4H_3O_3^+$ or $C_5H_9O_2^+$ that might correspond to maleic anhydride or glutaraldehyde in the TD-GC×GC-ToF-MS measurements. However, given instrumental parameters, the presence or absence of maleic anhydride and glutaraldehyde was not assessable.

4.4.4 Methodological Considerations for Future Exposure Studies

Occupant exposures in their homes were determined using time-resolved data and compared against simulated time-averaged methods using the H1 summer, H1 winter and H2 winter datasets. Time-averaged samples collected on sorbent tubes for later offline analysis commonly use sampling durations in the range of hours to weeks. We constructed simulated distributions of time-averaged samples using three hypothetical sampling durations (1-hour, 1-day, 1-week). Then, we normalized each value by the time-resolved best estimate of exposure. A value of "1" indicates that the time-averaged exposure estimate equals the time-resolved exposure estimate. Summary statistics of these distributions are compared against the relative standard deviation (RSD) of observed VOC concentrations for each compound during the three measurement campaigns (Figure 4.4.4). As a measure of variability, the RSD will increase with contributions from emission patterns that are both

periodic (typically related to the temperature-based diurnal cycle) and episodic (typically related to emission events). Because the mean-to-median ratio (18), a measure of episodic variability, strongly correlates with the RSD ($R^2 = 0.86$), it is qualitatively assumed that episodic variability is more important than periodic variability at this site. For VOCs with small RSDs (RSD < 0.4) indicating low periodic fluctuations and low episodic emissions, all three sampling durations tend to produce exposures that are consistent (within $\pm$ 50%) with best-estimate exposures. However, as the RSD of the VOC concentration time series increases, so too would the variability in occupant exposures derived from time-averaged samples. These effects can be particularly important when a sampling period directly coincides with an infrequently occurring episodic emission, which would produce exposures estimates potentially much higher than the best estimate based on time-resolved information. In the illustrative case of pyrrole during the H2 winter campaign, estimated exposures were up to 100 times higher for occupant H2M1 than the best-estimate when an hourly time-averaged sample coincided with an episodic cooking event that released pyrrole. The effects of this bias decreased with increasing sampling duration. Pyrrole exposures estimated from daily time-averaged samples were up to 13 times higher than the time-resolved best estimate of exposure and pyrrole exposures from weekly time-averaged samples were up to 3.3 times higher than the time-resolved best estimate of exposure.

Hourly time-averaged samples produce unsatisfactory estimates of exposures ($> \pm$50% of best-estimate) for most VOCs with moderate-to-high RSDs (RSD > 0.4). The performance of the time-averaged method slightly improved when sampling durations increased to daily but was similarly unsatisfactory for compounds with moderate-to-high RSDs (RSD > 0.4). Only when the time-averaged method increased to weekly sampling intervals did performance appear satisfactory for most VOCs ($\sim$90% of VOCs during H1 summer and H1 winter, $\sim$75% during H2 winter), yielding exposure estimates that were within 50% of the best-estimate. However, even with this longer sampling duration, the time-averaged and best-estimate time-resolved methods were less comparable for VOCs with high RSDs, mostly due to the large influence of episodic events.

Population-level environmental risk assessments require the ability to estimate exposures with both adequate precision and ease of implementation. Often, samples are collected on sorbent tubes for offline analysis giving time-averaged VOC concentrations and then coupled with occupant time budgets to estimate pollutant exposures. A comparison of time-averaged methods with time-resolved methods has not been previously reported to substantiate this approach. In this study, time-averaged sampling methods appeared to yield adequate measures of occupant exposure, provided that the studied compound of interest has proportionately small contributions from episodic sources. As expected, longer sampling times produce more precise estimates of occupant exposures. Hourly and daily time-averaged samples would be ineffective at estimating exposures to VOCs with substantial contributions from episodic sources. Weekly time-averaged samples can yield more precise ($\pm$ 50%) estimates of exposures for VOCs with moderate contributions from episodic sources and order of magnitude precision for compounds with substantial contributions from episodic sources. Conversely, sampling duration matters little for compounds with small contributions from

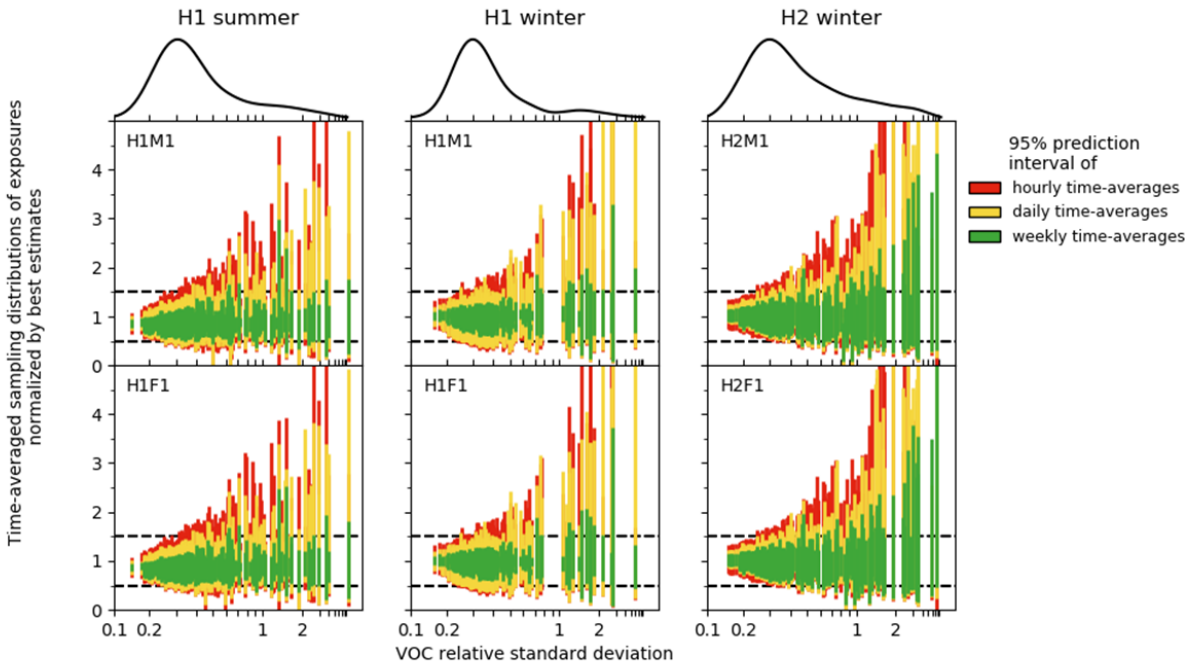

Figure 4.4.4: Comparison of traditional and time-resolved exposure estimates against compound time-series variability. Occupant exposures during the H1 summer, H1 winter, and H2 winter campaigns were calculated from a) simulated time-averaged concentrations (1-h, 1-day, 1-week time-averages) coupled with occupant time budgets and b) time-resolved methods ('best-estimate'). Distributions of randomly sampled time-averaged exposure estimates (n = 1000) normalized by the time-resolved best-estimate are compared against a VOC's relative standard deviation. Vertical bars correspond to the 95% observation window for individual VOC distributions (with one outlier excluded in each campaign). Red, orange, and green colors indicate distributions of hourly, daily, and weekly time-averages, respectively. Columns correspond to the H1 summer, H1 winter, and H2 winter campaigns. Subpanels in each column correspond to exposures for individual occupants during a campaign. The kernel density estimate of the relative standard deviation is shown above each scatterplot. Horizontal dashed lines designate the ± 50% boundary of the best-estimate exposure. Note that the horizontal axis has non-linear scaling.

episodic sources, indicating that many VOCs can be measured rapidly for exposure estimates, provided that source mechanisms are well understood.

VOCs were sampled in two or three locations in the occupied portion of each studied residence to provide some evidence about spatial variability. On the whole, concentrations were well-coupled between open living spaces. It has been noted that the assumption of a well-mixed room may not be sufficient when estimating exposures to strongly localized sources due to spatial heterogeneities.[33, 34] For this reason, contributions from episodic sources to occupant exposures within these residences may have been higher if an occupant was in close proximity to an episodic source, regardless of whether time-averaged or time-resolved methods were used to estimate exposures. Personal sampling overcomes this spatial limitation; however, no methods are presently available for conducting personal sampling for VOC exposures with both high chemical specificity and time-resolved concentrations.

This study incorporated health-risk data from three governmental organizations yielding advisory guidelines for chronic exposures to 31 separate VOCs (22 VOC ions). We compared the guideline values against VOC concentrations for summer (one residence) and winter seasons (two residences). Residential VOC concentrations were above guideline values for two compounds already well-known to the public health community (acrolein, acetaldehyde) and for one compound for which there is less evident awareness (acrylic acid). We also note that available advisory health guidelines address fewer than 10% of the 250 VOC ions observed. Larger VOC ions likely correspond to many distinct chemical isomers, further reducing the estimate of observed VOCs with associated health data. Because it is not feasible to acquire detailed toxicology or exposure data for the thousands of chemicals to which populations may be exposed, recent efforts have developed tools for high-throughput screening of chemical toxicities (ToxCast) and exposures (ExpoCast).[56] High-throughput models like ExpoCast may benefit from improved understanding that can be gained in high-resolution studies. This study was limited to two residences and five occupants. While we expect that these residences are ordinary for their age and location, it remains to be seen how well our findings generalize to other residences. Further research is warranted to study the health effects of the substantial chemical diversity found at levels much higher than outdoors in residential air.

4.5 Acknowledgements

This work was supported by the Alfred P. Sloan Foundation Program on Chemistry of Indoor Environments via Grants 2016-7050 and 2019-11412. D.L. acknowledges support from the National Science Foundation (grant no. DGE 1752814). K.K. acknowledges support from the Carlsberg Foundation (grant no. CF16-0624). We thank the house residents for allowing their homes to be studied, for their patience, and for their geniality. The authors thank Betty Molinier for siloxane identification and Michael Kado for helpful conversations. The H1 and H2 occupants gave informed consent for this study, which was conducted under a protocol approved in advance by the Committee for Protection of Human Subjects for the

University of California, Berkeley (Protocol #2016 04 8656).

4.6 References

[1] Wieslander, G.; Norbäck, D.; Björnsson, E.; Janson, C.; Boman, G. Asthma and the indoor environment: the significance of emission of formaldehyde and volatile organic compounds from newly painted indoor surfaces. *Int. Arch. Occup. Environ. Health* **1997**, *69*, 115–124.

[2] Guo, H.; Lee, S. C.; Chan, L. Y.; Li, W. M. Risk assessment of exposure to volatile organic compounds in different indoor environments. *Environ. Res.* **2004**, *94*, 57–66.

[3] Logue, J. M.; McKone, T. E.; Sherman, M. H.; Singer, B. C. Hazard assessment of chemical air contaminants measured in residences. *Indoor Air* **2011**, *21*, 92–109.

[4] Logue, J. M.; Price, P. N.; Sherman, M. H.; Singer, B. C. A Method to Estimate the Chronic Health Impact of Air Pollutants in U.S. *Residences. Environ. Health Perspect.* **2012**, *120*, 216–222.

[5] Allen, J. G.; MacNaughton, P.; Satish, U.; Santanam, S.; Vallarino, J.; Spengler, J. D. Associations of Cognitive Function Scores with Carbon Dioxide, Ventilation, and Volatile Organic Compound Exposures in Office Workers: A Controlled Exposure Study of Green and Conventional Office Environments. *Environ. Health Perspect.* **2016**, *124*, 805–812.

[6] Klepeis, N. E.; Nelson, W. C.; Ott, W. R.; Robinson, J. P.; Tsang, A. M.; Switzer, P.; Behar, J. V.; Hern, S. C.; Engelmann, W. H. The National Human Activity Pattern Survey (NHAPS): a resource for assessing exposure to environmental pollutants. *J. Expo. Anal. Environ. Epidemiol.* **2001**, *11*, 231–252.

[7] Adgate, J. L.; Church, T. R.; Ryan, A. D.; Ramachandran, G.; Fredrickson, A. L.; Stock, T. H.; Morandi, M. T.; Sexton, K. Outdoor, Indoor, and Personal Exposure to VOCs in Children. *Environ. Health Perspect.* **2004**, *112*, 1386–1392.

[8] Edwards, R. D.; Jurvelin, J.; Koistinen, K.; Saarela, K.; Jantunen, M. VOC source identification from personal and residential indoor, outdoor and workplace microenvironment samples in EXPOLIS-Helsinki, Finland. *Atmos. Environ.* **2001**, *35*, 4829–4841.

[9] Wallace, L. A. Human Exposure to Volatile Organic Pollutants: Implications for Indoor Air Studies. *Annu. Rev. Energy Environ.* **2001**, *26*, 269–301.

[10] Salthammer, T.; Mentese, S.; Marutzky, R. Formaldehyde in the Indoor Environment. *Chem. Rev.* **2010**, *110*, 2536–2572.

[11] Bolden, A. L.; Kwiatkowski, C. F.; Colborn, T. New Look at BTEX: Are Ambient Levels a Problem? *Environ. Sci. Technol.* **2015**, *49*, 5261–5276.

[12] Salthammer, T. Very volatile organic compounds: an understudied class of indoor air pollutants. *Indoor Air* **2016**, *26*, 25–38.

[13] Salthammer, T.; Zhang, Y.; Mo, J.; Koch, H. M.; Weschler, C. J. Assessing Human Exposure to Organic Pollutants in the Indoor Environment. *Angew. Chem. Int. Ed.* **2018**, *57*, 12228–12263.

[14] Wolkoff, P. How to measure and evaluate volatile organic compound emissions from building products. A perspective. *Sci. Total Environ.* **1999**, *227*, 197–213.

[15] Weschler, C. J.; Carslaw, N. Indoor Chemistry. *Environ. Sci. Technol.* **2018**, *52*, 2419–2428.

[16] Steinemann, A. Volatile emissions from common consumer products. *Air Qual. Atmos. Health* **2015**, *8*, 273–281.

[17] Farmer, D. K.; Vance, M. E.; Abbatt, J. P. D.; Abeleira, A.; Alves, M. R.; Arata, C.; Boedicker, E.; Bourne, S.; Cardoso-Saldaña, F.; Corsi, R.; DeCarlo, P. F.; Goldstein, A. H.; Grassian, V. H.; Hildebrandt Ruiz, L.; Jimenez, J. L.; Kahan, T. F.; Katz, E. F.; Mattila, J. M.; Nazaroff, W. W.; Novoselac, A.; O'Brien, R. E.; Or, V. W.; Patel, S.; Sankhyan, S.; Stevens, P. S.; Tian, Y.; Wade, M.; Wang, C.; Zhou, S.; Zhou, Y. Overview of HOMEChem: House Observations of Microbial and Environmental Chemistry. *Environ. Sci.: Processes Impacts* **2019**, *21*, 1280–1300.

[18] Liu, Y.; Misztal, P. K.; Xiong, J.; Tian, Y.; Arata, C.; Weber, R. J.; Nazaroff, W. W.; Goldstein, A. H. Characterizing sources and emissions of volatile organic compounds in a northern California residence using space- and time-resolved measurements. *Indoor Air* **2019**, *29*, 630–644.

[19] Liu, S.; Li, R.; Wild, R. J.; Warneke, C.; de Gouw, J. A.; Brown, S. S.; Miller, S. L.; Luongo, J. C.; Jimenez, J. L.; Ziemann, P. J. Contribution of human-related sources to indoor volatile organic compounds in a university classroom. *Indoor Air* **2016**, *26*, 925–938.

[20] Tang, X.; Misztal, P. K.; Nazaroff, W. W.; Goldstein, A. H. Volatile Organic Compound Emissions from Humans Indoors. *Environ. Sci. Technol.* **2016**, *50*, 12686–12694.

[21] Rackes, A.; Waring, M. S. Do time-averaged, whole-building, effective volatile organic compound (VOC) emissions depend on the air exchange rate? A statistical analysis of trends for 46 VOCs in U.S. offices. *Indoor Air* **2016**, *26*, 642–659.

[22] Wang, C.; Collins, D. B.; Arata, C.; Goldstein, A. H.; Mattila, J. M.; Farmer, D. K.; Ampollini, L.; DeCarlo, P. F.; Novoselac, A.; Vance, M. E.; Nazaroff, W. W.; Abbatt, J. P. D. Surface reservoirs dominate dynamic gas-surface partitioning of many indoor air constituents. *Sci. Adv.* **2020**, *6*, eaay8973.

[23] Xiong, J.; Zhang, P.; Huang, S.; Zhang, Y.; Comprehensive influence of environmental factors on the emission rate of formaldehyde and VOCs in building materials: Correlation development and exposure assessment. *Environ. Res.* **2016**, *151*, 734–741.

[24] Park, J. S.; Ikeda, K. Variations of formaldehyde and VOC levels during 3 years in new and older homes. *Indoor Air* **2006**, *16*, 129–135.

[25] Shin, S.-H.; Jo, W.-K. Longitudinal variations in indoor VOC concentrations after moving into new apartments and indoor source characterization. *Environ. Sci. Pollut. Res.* **2013**, *20*, 3696–3707.

[26] Holøs, S. B.; Yang, A.; Lind, M.; Thunshelle, K.; Schild, P.; Mysen, M. VOC emission rates in newly built and renovated buildings, and the influence of ventilation – A review and meta-analysis. *Int. J. Vent.* **2019**, *18*, 153–166.

[27] Son, B.; Breysse, P.; Yang, W. Volatile organic compounds concentrations in residential indoor and outdoor and its personal exposure in Korea. *Environ. Int.* **2003**, *29*, 79–85.

[28] Su, F.-C.; Mukherjee, B.; Batterman, S. Determinants of personal, indoor and outdoor VOC concentrations: An analysis of the RIOPA data. *Environ. Res.* **2013**, *126*, 192–203.

[29] Jia, C.; Batterman, S.; Godwin, C. VOCs in industrial, urban and suburban neighborhoods—Part 2: Factors affecting indoor and outdoor concentrations. *Atmos. Environ.* **2008**, *42*, 2101–2116.

[30] Guo, H. Source apportionment of volatile organic compounds in Hong Kong homes. *Build. Environ.* **2011**, *46*, 2280–2286.

[31] Bari, M. A.; Kindzierski, W. B.; Wheeler, A. J.; Héroux, M.-È.; Wallace, L. A. Source apportionment of indoor and outdoor volatile organic compounds at homes in Edmonton, Canada. *Build. Environ.* **2015**, *90*, 114–124.

[32] Wallace, L. A.; Pellizzari, E. D.; Hartwell, T. D.; Sparacino, C. M.; Sheldon, L. S.; Zelon, H. Personal Exposures, Indoor-Outdoor Relationships, and Breath Levels of Toxic Air Pollutants Measured for 355 Persons in New Jersey. *Atmos. Environ.* **1985**, *19*, 1651–1661.

[33] Earnest, C.M.; Corsi, R.L.; Inhalation Exposure to Cleaning Products: Application of a Two-Zone Model. *J. Occup. Environ. Hyg.* **2013**, *10*, 328–335.

[34] Huang, L.; Ernstoff, A.; Fantke, P.; Csiszar, S.A.; Jolliet, O. A review of models for near-field exposure pathways of chemicals in consumer products. *Sci. Total Environ.* **2017**, *574*, 1182–1208.

[35] Acevedo-Bolton, V.; Cheng, K.-C.; Jiang, R.-T.; Ott, W. R.; Klepeis, N. E.; Hildemann, L. M. Measurement of the proximity effect for indoor air pollutant sources in two homes. *J. Environ. Monit.* **2012**, *14*, 94–104.

[36] Acevedo-Bolton, V.; Ott, W. R.; Cheng, K.-C.; Jiang, R.-T.; Klepeis, N. E.; Hildemann, L. M. Controlled experiments measuring personal exposure to PM2.5 in close proximity to cigarette smoking. *Indoor Air* **2014**, *24*, 199–212.

[37] Licina, D.; Tian, Y.; Nazaroff, W. W. Inhalation intake fraction of particulate matter from localized indoor emissions. *Build. Environ.* **2017**, *123*, 14–22.

[38] Liu, Y.; Misztal, P. K.; Xiong, J.; Tian, Y.; Arata, C.; Nazaroff, W. W.; Goldstein, A. H. Detailed investigation of ventilation rates and airflow patterns in a northern California residence. *Indoor Air* **2018**, *28*, 572–584.

[39] Kristensen, K.; Lunderberg, D. M.; Liu, Y.; Misztal, P. K.; Tian, Y.; Arata, C.; Nazaroff, W. W.; Goldstein, A. H. Sources and dynamics of semivolatile organic compounds in a single-family residence in northern California. *Indoor Air* **2019**, *29*, 645–655.

[40] Lunderberg, D. M.; Kristensen, K.; Liu, Y.; Misztal, P. K.; Tian, Y.; Arata, C.; Wernis, R.; Kreisberg, N.; Nazaroff, W. W.; Goldstein, A. H. Characterizing Airborne Phthalate Concentrations and Dynamics in a Normally Occupied Residence. *Environ. Sci. Technol.* **2019**, *53*, 7337–7346.

[41] USEPA. Integrated Risk Information System (IRIS). USEPA, 2010. https://cfpub.epa.gov/ncea/iris/search/index.cfm (accessed 2020-06)

[42] CalEPA, Office of Environmental Health Hazard Assessment (OEHHA). OEHHA Acute, 8-hour and Chronic Reference Exposure Level (REL) Summary. OEHHA, 2019. https://oehha.ca.gov/air/general-info/oehha-acute-8-hour-and-chronic-reference-exposure-level-rel-summary (accessed 2020-06).

[43] Agency for Toxic Substances and Disease Registry (ATSDR). MINIMAL RISK LEVELS (MRLS). ATSDR, 2020. https://www.atsdr.cdc.gov/mrls/pdfs/ATSDR%20MRLs%20-%20May%202020%20-%20H.pdf (accessed 2020-06).

[44] Agence nationale de sécurité sanitaire de l'alimentation, de l'environnement et du travail (ANSES). Indoor Air Reference Levels. Paris, France, March 2018. https://www.anses.fr/en/content/indoor-air-quality-guidelines-iaqgs (accessed 2021-04).

[45] Fromme, H.; Debiak, M.; Sagunski, H.; Röhl, C.; Kraft, M.; Kolossa-Gehring, M. The German approach to regulate indoor air contaminants. *Int. J. Hyg. Environ. Health* **2019**, *222*, 347–354.

[46] Kunkel, S.; Kontonasiou, E.; Arcipowska, A.; Mariottini, F.; Atanasiu, B. Indoor air quality, thermal comfort and daylight; Report for the Buildings Performance Institute Europe (BPIE), March 2015. https://www.bpie.eu/wp-content/uploads/2015/10/BPIE__IndoorAirQuality2015.pdf (accessed 2021-04)

[47] Government of Canada. Indoor Air Reference Levels. Ottawa, Canada, February 2018. https://www.canada.ca/en/health-canada/services/air-quality/residential-indoor-air-quality-guidelines.html (accessed 2021-04).

[48] WHO. WHO Guidelines for Indoor Air Quality: Selected Pollutants. Geneva, Switzerland, 2010. https://www.euro.who.int/__data/assets/pdf_file/0009/128169/e94535.pdf (accessed 2021-04).

[49] Seaman, V. Y.; Bennett, D. H.; Cahill, T. M. Origin, Occurrence, and Source Emission Rate of Acrolein in Residential Indoor Air. *Environ. Sci. Technol.* **2007**, *41*, 6940–6946.

[50] Seaman, V. Y.; Bennett, D. H.; Cahill, T. M. Indoor acrolein emission and decay rates resulting from domestic cooking events. *Atmos. Environ.* **2009**, *43*, 6199–6204.

[51] Katragadda, H. R.; Fullana, A.; Sidhu, S.; Carbonell-Barrachina, Á. A. Emissions of volatile aldehydes from heated cooking oils. *Food Chem.* **2010**, *120*, 59–65.

[52] Stevens, J. F.; Maier, C. S. Acrolein: Sources, metabolism, and biomolecular interactions relevant to human health and disease. *Mol. Nutr. Food Res.* **2008**, *52*, 7–25.

[53] Destaillats, H.; Spaulding, R. S.; Charles, M. J. Ambient Air Measurement of Acrolein and Other Carbonyls at the Oakland-San Francisco Bay Bridge Toll Plaza. *Environ. Sci. Technol.* **2002**, *36*, 2227–2235.

[54] Chan, W. R.; Sidheswaran, M.; Sullivan, D. P.; Cohn, S.; Fisk, W. J. Cooking-related PM2.5 and acrolein measured in grocery stores and comparison with other retail types. *Indoor Air* **2015**, *26*, 489–500.

[55] Alapieti, T.; Mikkola, R.; Pasanen, P.; Salonen, H. The influence of wooden interior materials on indoor environment: a review. *Eur. J. Wood Wood Prod.* **2020**, *78*, 617–634.

[56] National Research Council. Exposure Science in the 21st Century: A Vision and a Strategy. The National Academies Press: Washington, DC, 2012.

4.7 Supporting Information

4.7.1 Chemical Measurements

The PTR-ToF-MS was located in a detached garage with other gas-phase instruments during the H1 campaigns. Air was continuously drawn to the garage from six locations (outdoors, kitchen, bedroom hallway, basement, crawlspace, attic) through separate 30-m PFA sampling tubes (6.4 mm OD). Particles were removed by a PTFE filter with 2.0-μm pores. The gas-phase instruments switched between sampling locations using a 6-way manifold (NResearch, 648T091; PTFE inner contact surfaces). Air was drawn through all sampling lines continuously at flow rates of ∼2 L min^{-1}, which rose to ∼3.4 L min^{-1} during sequential sampling. Instruments typically switched sampling lines every 5 minutes yielding a 30-minute rotating sampling cycle. An altered cycle (5 minutes outdoors, 20 minutes kitchen, 5 minutes bedroom area) was used for two weeks during the H1 summer campaign and for one week in H1 winter. A house floorplan with sampling locations is provided in Liu et al. (2018).[1] The first two minutes of sampling at each location were discarded to allow chemicals to equilibrate through the valve and inlet system. Similar operating conditions were used during the H2 campaign, with the exception that the instrument was housed in a purpose-built shed situated adjacent to the residence. Air was continuously drawn to the instrument from six locations (outdoors, kitchen, bedroom hallway, living room, crawlspace, attic). A floorplan and sampling locations at the H2 site are provided as Figure 4.7.4.

VOC quantification during the H2 winter campaign followed the same approach as at H1.2 Data processing included combining isotopic and fragmentation masses into singular components, subtracting instrumental background signal, normalizing for ion-transmission and reagent ion signal, and calibrating via daily measurements of multicomponent gas standards. When authentic external standards were not available, a default sensitivity factor was used with estimated uncertainties ranging from -40% to +60%. After applying a 0.005 ppb abundance threshold and removing a small subset ($n = 11$) of ion masses that evidently interacted with sampling lines, ion formulas were determined for 218 masses in the H1 summer campaign, 171 masses in the H1 winter campaign, and 206 masses in the H2 winter campaign and then quantified. In this work, we excluded measurements of CH_3O^+ (formaldehyde) from analysis. Ion formulas represent contributions from all structural isomers; many can be assigned to specific structures with high confidence based on supporting chromatographic measurements and site-specific knowledge. Sorbent tubes were collected for offline thermal desorption two-dimensional gas chromatography time-of-flight mass spectrometry (TD-GC×GC-ToF-MS) with electron ionization (EI) to aid compound identification. Liu et al.[2] reported $C_3H_5O^+$ as "acrolein + propionic acid." In this paper, contributions to $C_3H_5O^+$ from propionic acid were removed via the laboratory determined fragmentation rate of propionic acid. $C_3H_5O^+$ was then quantified using acrolein's specific reaction rate coefficient.[3]

4.7.2 Peak Selection

Candidates were identified by selecting peaks with a prominence of 0.03 that were spaced at least 2.5 h apart. Peak candidates were narrowed by removing all peaks whose height was below a threshold defined as 20% greater than an 8-hour rolling average. Peak candidate boundaries were defined semi-empirically as when the derivative changed sign and was sustained for at least three successive measurement periods. Peak candidates and associated peak boundaries were confirmed, modified and/or supplemented by visual analysis and manual selection. For some compounds with lower abundances and higher uncertainties, the automated method was poorly suited, and peaks were assessed solely by manual identification. Example integrations for representative time series are shown in the Figure 4.7.5. In total, more than 12,000 peaks were identified for the 594 chemical concentration time series acquired during the three campaigns. Peaks were assigned to specific source categories based on coincident events recorded in occupant event logs. Peaks were categorized as "cooking" or "other" based on coincident events during the growth phase of the peak. If events from multiple categories occurred simultaneously, preference was given in the order of the stated source categories with "cooking" taking highest priority unless unambiguous indicators suggested otherwise, as in the case of an acetone-based nail polish remover being used during a cooking event. "Cooking" is a broad category that includes stovetop use, oven use, microwave use, and any other food or drink preparation. "Other" is also a broad category that includes all other activities, such as cleaning, candle combustion, use of personal care products, and unidentified events. This form of source apportionment is unable to resolve specific sources of chemical emissions. For example, occupants may emit bioeffluents at higher rates as their activity increases during cooking events. Peaks generated under such conditions would be attributed to the broad activity labeled "cooking."

4.7.3 Figures

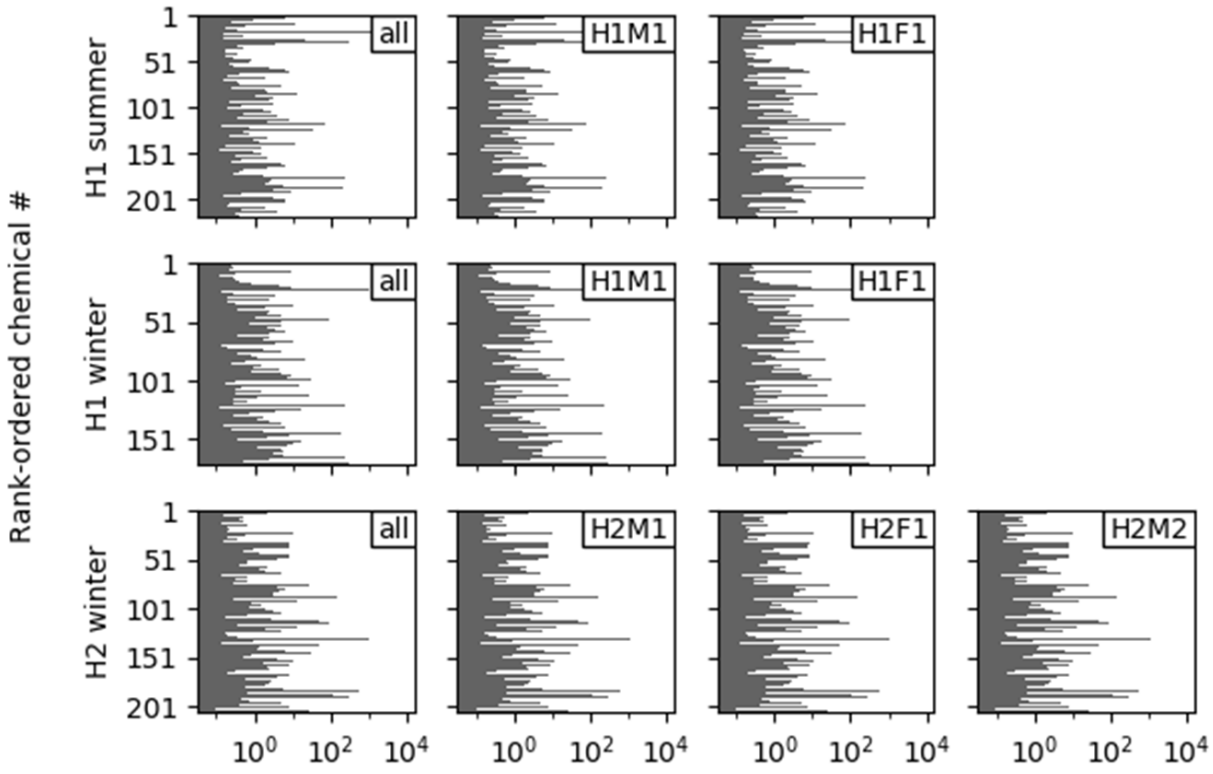

Figure 4.7.1: Absolute daily exposures. Each subpanel displays absolute VOC exposures for occupants during each campaign. The subpanel 'all' corresponds to exposure source apportionment over the entirety of the measurement period. Horizontal bars in each subpanel correspond to the absolute contribution for discrete VOCs. The top, middle, and bottom rows correspond to the H1 summer, H1 winter, and H2 winter campaigns, respectively. Each row uses the same rank-ordering as defined in Figure 4.4.3 in the main article.

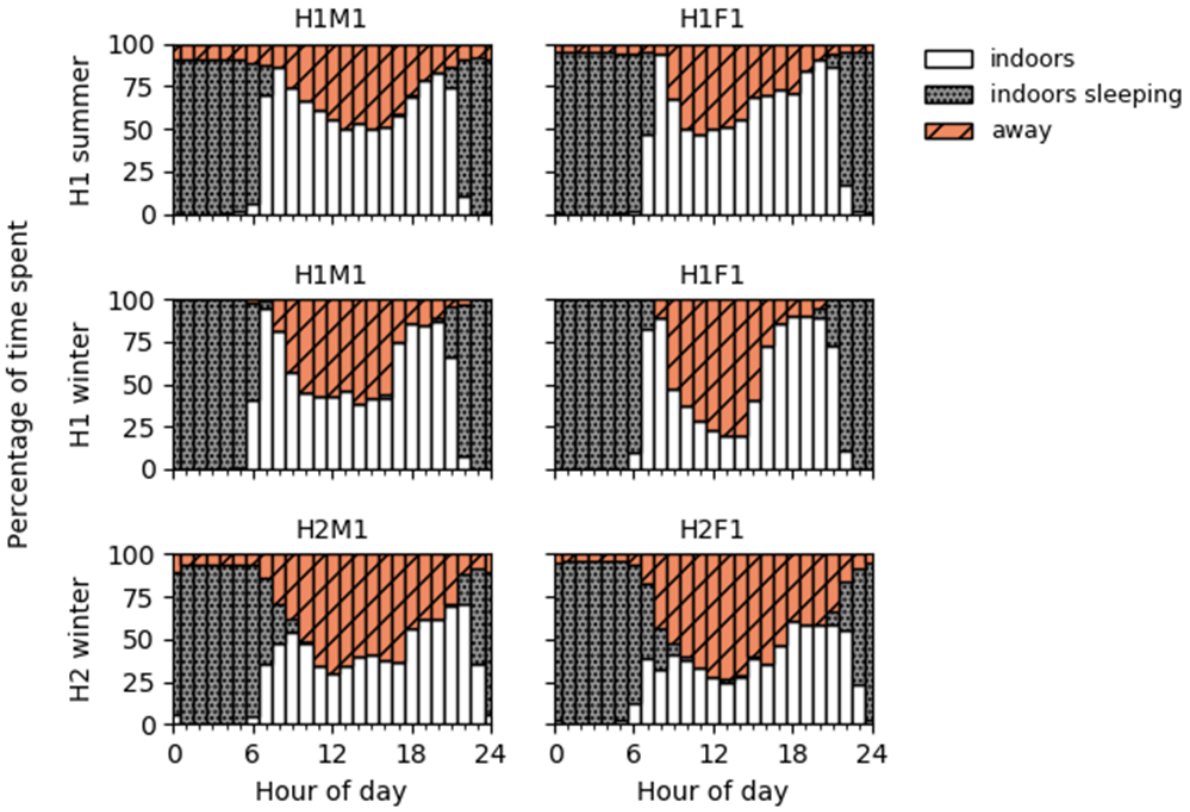

Figure 4.7.2: Occupant time-activity budgets. Average daily occupant time budgets are displayed during periods of occupancy (extended vacant periods of more than one day are excluded).

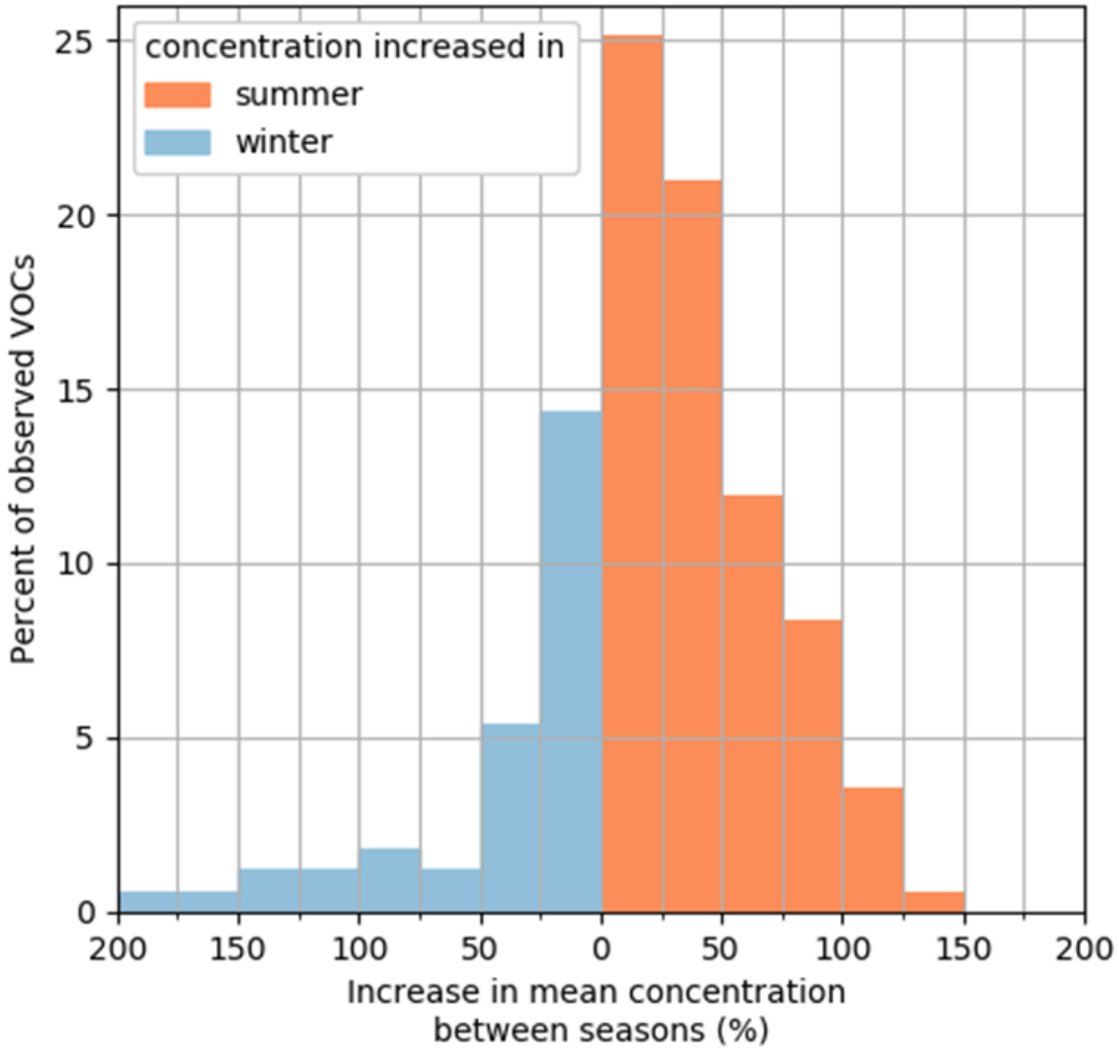

Figure 4.7.3: Seasonal concentration differences. Differences in mean abundance between the H1 summer and H1 winter seasons (vacant + occupied) are displayed for the 167 VOCs observed in both seasons. VOCs with higher mean concentrations in summer are aggregated in orange bins, while VOCs with higher mean concentrations in winter are aggregated in blue bins. One outlier with much greater concentration in summer (cinnamaldehyde: 370%) and three outliers with much greater concentrations in winter (D5 siloxane: 1490%; monoterpenes: 610%; $C_2H_3^+$: 420%) are not shown.

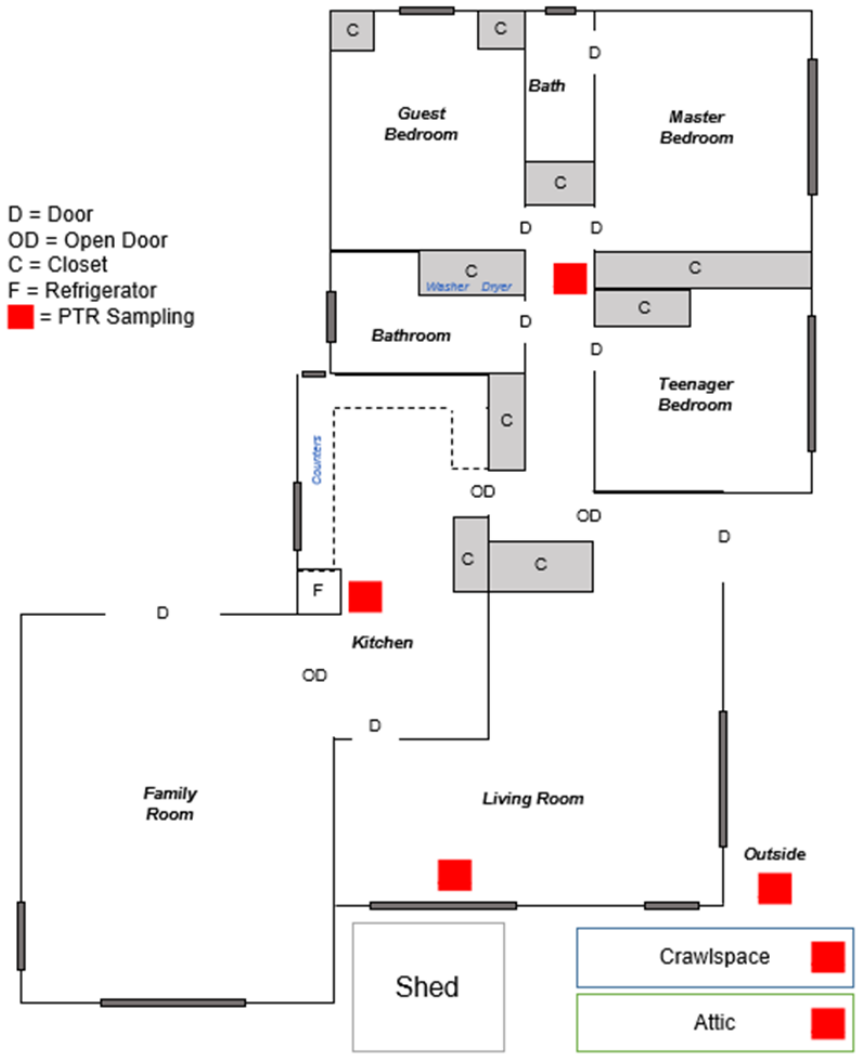

Figure 4.7.4: Floor plan of the H2 residence. Sampling locations in the 180 m^2 (1970 ft^2) residence are shown in red. The outdoor sampling line was situated near the outermost corner of the living room. Living space and outdoor sampling line inlets were positioned at approximately 2 m above floor or ground level. Crawlspace and attic inlets were approximately at mid-height of respective zones, minimizing the risk of sample interference from nearby surfaces.

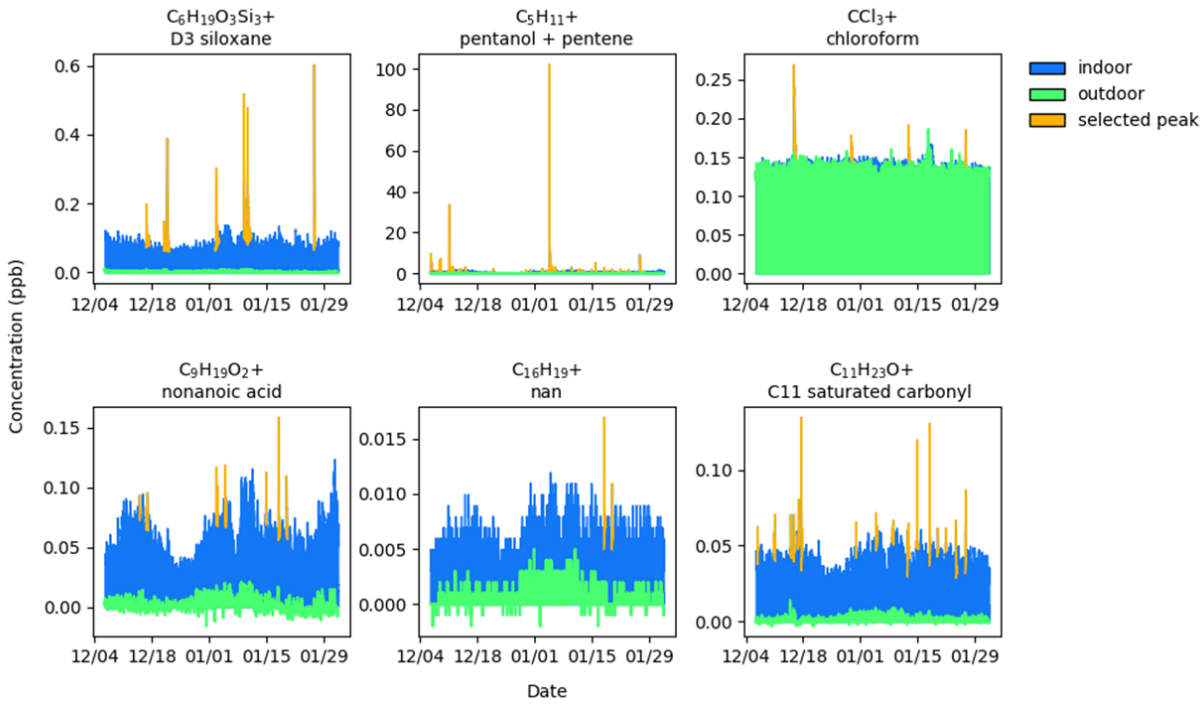

Figure 4.7.5: Representative time series of peak assignments. Sample of representative VOCs from the H2 campaign. Selected episodic peaks are highlighted in tan following the process described in the SI." Outdoor VOC concentrations were used as a proxy for indoor VOCs of outdoor origin and are highlighted in green. The remainder is defined as the indoor background and is highlighted in blue.

4.7.4 Data Tables

Table 4.7.1: Summary table of exposures during the H1 summer campaign. The mean concentration during occupancy (MC) is in units of ppb, the campaign average daily exposure (ADE) is in units of ppb-hour day^{-1}, and the relative contributions from continuous indoor sources (CIS), outdoor origin (OO), cooking (C), and other (O) are unitless (%). In rare cases, statistical noise generates a slight negative relative fraction for the background of outdoor origin. The relative standard deviation (RSD) indicates the variability in the indoor concentration time series. The heading 'all' refers to source apportionments and exposures for a hypothetical occupant who is present for the entirety of the measurement period.

				all						H1M1		H1F1	
Class	**Ion**	**Name**	**RSD**	**CIS** %	**OO** %	**C** %	**O** %	**MC** ppb	**ADE** ppb h d-1	**MC** ppb	**ADE** ppb h d-1	**MC** ppb	**ADE** ppb h d-1
alcohol + alkene	CH_5O^+	methanol	0.3	87	8	4	2	28	620	27	480	27	500
alcohol + alkene	$C_2H_7O^+$	ethanol	2.9	32	3	41	23	120	2600	130	2300	130	2300
alcohol + alkene	$C_3H_7^+$	propanol fragment (-H_2O) + propene	2.1	82	8	3	6	3.5	79	3.5	62	3.5	62
alcohol + alkene	$C_4H_9^+$	butanol fragment (-H_2O) + butene	0.34	83	9	3	5	2.1	48	2.1	37	2.1	37
alcohol + alkene	$C_5H_{11}^+$	pentanol fragment (-H_2O) + pentene	0.41	82	8	5	5	0.81	18	0.81	14	0.81	15
alcohol + alkene	$C_6H_{13}^+$	hexanol fragment (-H_2O) + hexene	0.56	73	13	8	6	0.23	5.3	0.23	4.1	0.23	4.2
alcohol + alkene	$C_8H_{17}^+$	octanol fragment (-H_2O) + octene	NA	NA	NA	NA	NA	NA	NA	NA	NA	NA	NA
aromatic	$C_6H_7^+$	benzene	0.32	64	34	1	2	0.24	5.5	0.24	4.2	0.24	4.3
aromatic	$C_7H_9^+$	toluene	0.37	60	38	1	2	0.36	8.1	0.34	6	0.35	6.4
aromatic	$C_8H_9^+$	styrene	0.26	84	11	3	2	0.14	3.1	0.14	2.4	0.14	2.5
aromatic	$C_8H_{11}^+$	xylene + ethyl benzene	0.33	51	49	0	0	0.25	5.7	0.24	4.3	0.25	4.4
aromatic	$C_6H_7O^+$	phenol	0.18	94	2	1	3	0.52	12	0.52	9.1	0.52	9.4
aromatic	$C_6H_7O_2^+$	benzene diol	0.9	73	8	6	14	0.1	2.3	0.1	1.8	0.1	1.8
aromatic	$C_7H_9O^+$	cresols	0.24	89	7	1	3	0.18	4	0.17	3.1	0.17	3.1
aromatic	$C_7H_7O^+$	benzaldehyde	0.22	91	8	1	0	0.37	8.3	0.36	6.3	0.36	6.5
aromatic	$C_4H_6N^+$	pyrrole	3.7	34	1	36	28	0.09	2	0.1	1.8	0.091	1.6
aromatic	$C_9H_{13}^+$	benzene (+3 sat. carbons) + isomers	0.32	51	47	0	2	0.13	2.8	0.12	2.2	0.12	2.2

aromatic	$C_{10}H_{15}^+$	benzene (+4 sat. carbons) + isomers	0.58	65	27	3	5	0.1	2.4	0.1	1.8	0.1	1.9
aromatic	$C_{11}H_{17}^+$	benzene (+5 sat. carbons) + isomers	0.44	77	16	2	5	0.034	0.76	0.033	0.59	0.034	0.61
aromatic	$C_{13}H_{21}^+$	benzene (+7 sat. carbons) + isomers	0.36	86	10	3	2	0.016	0.36	0.016	0.28	0.016	0.29
aromatic	$C_{14}H_{23}^+$	benzene (+8 sat. carbons) + isomers	0.2	86	14	1	0	0.016	0.37	0.016	0.29	0.016	0.29
aromatic	$C_{16}H_{27}^+$	benzene (+10 sat. carbons) + isomers	0.2	94	6	0	0	0.025	0.57	0.025	0.44	0.025	0.46
aromatic	$C_{17}H_{29}^+$	benzene (+11 sat. carbons) + isomers	0.18	95	5	0	0	0.022	0.5	0.022	0.39	0.022	0.4
aromatic	$C_{18}H_{31}^+$	benzene (+12 sat. carbons) + isomers	0.2	93	7	0	0	0.02	0.45	0.02	0.35	0.02	0.36
aromatic	$C_7H_6NS^+$	benzothiazole	0.2	85	14	0	1	0.049	1.1	0.049	0.85	0.049	0.88
carbonyl (sat.)	$C_2H_5O^+$	acetaldehyde (C2)	0.96	63	9	22	6	9.3	210	9.7	170	9.5	170
carbonyl (sat.)	$C_3H_7O^+$	acetone + propanal (C3)	0.41	68	16	8	8	11	250	11	200	11	200
carbonyl (sat.)	$C_4H_9O^+$	C4 sat. carbonyl (methylethylketone + others)	0.63	66	20	8	6	0.76	17	0.76	13	0.76	14
carbonyl (sat.)	$C_5H_{11}O^+$	C5 sat. carbonyl (pentanone + others)	0.64	73	11	6	10	0.29	6.6	0.3	5.2	0.29	5.3
carbonyl (sat.)	$C_6H_{13}O^+$	C6 sat. carbonyl (hexanone + others)	0.24	86	12	2	0	0.23	5.2	0.22	3.9	0.23	4.1
carbonyl (sat.)	$C_7H_{15}O^+$	C7 sat. carbonyl	0.24	87	11	1	0	0.14	3.2	0.14	2.4	0.14	2.5
carbonyl (sat.)	$C_8H_{17}O^+$	C8 sat. carbonyl + 1-octen-3-ol	0.26	91	5	2	1	0.16	3.6	0.15	2.7	0.16	2.8
carbonyl (sat.)	$C_9H_{19}O^+$	C9 sat. carbonyl	0.27	96	3	1	0	0.49	11	0.48	8.4	0.49	8.9

carbonyl (sat.)	$C_{10}H_{21}O^+$	C10 sat. carbonyl	0.28	96	4	0	0	0.27	6.1	0.27	4.7	0.27	4.9
carbonyl (sat.)	$C_{11}H_{23}O^+$	C11 sat. carbonyl	0.27	91	8	1	0	0.061	1.4	0.061	1.1	0.061	1.1
carbonyl (sat.)	$C_{12}H_{25}O^+$	C12 sat. carbonyl	0.3	89	10	1	0	0.037	0.84	0.037	0.64	0.037	0.67
carbonyl (sat.)	$C_{14}H_{29}O^+$	C14 sat. carbonyl	0.49	76	24	0	0	0.0068	0.15	0.0064	0.11	0.0067	0.12
carbonyl (unsat.)	$C_3H_5O^+$	acrolein (C3 unsat. carbonyl)	0.55	85	11	4	1	0.57	13	0.56	9.9	0.57	10
carbonyl (unsat.)	$C_4H_7O^+$	unsat. carbonyl (C4)	0.38	73	24	2	1	0.56	13	0.53	9.4	0.56	10
carbonyl (unsat.)	$C_5H_9O^+$	unsat. carbonyl (C5) + cyclopentanone	0.27	83	13	2	2	0.23	5.3	0.23	4	0.23	4.2
carbonyl (unsat.)	$C_6H_{11}O^+$	unsat. carbonyl (C6) + cis-3-hexenal + isomers	0.43	81	8	7	4	0.36	8.1	0.36	6.3	0.36	6.5
carbonyl (unsat.)	$C_7H_{13}O^+$	unsat. carbonyl (C7) + isomers	0.35	81	14	5	0	0.097	2.2	0.096	1.7	0.097	1.7
carbonyl (unsat.)	$C_8H_{15}O^+$	unsat. carbonyl (C8) + oct-1-en-3-one + isomers	0.33	93	5	2	0	0.24	5.4	0.24	4.2	0.24	4.3
carbonyl (unsat.)	$C_9H_{17}O^+$	unsat. carbonyl (C9) + isomers	0.3	91	8	1	0	0.11	2.5	0.11	1.9	0.11	2
carboxylic acid	$CH_3O_2^+$	formic acid (C1) + isomers	0.14	91	8	1	0	14	310	14	240	14	250
carboxylic acid	$C_2H_5O_2^+$	acetic acid (C2) + isomers	0.43	93	3	3	1	52	1200	51	910	51	930
carboxylic acid	$C_3H_7O_2^+$	propionic acid (C3) + isomers	1.4	80	10	7	3	3.2	73	3.3	58	3.3	59
carboxylic acid	$C_4H_9O_2^+$	butryic acid (C4) + isomers	0.46	79	7	9	5	1.4	32	1.5	26	1.5	26
carboxylic acid	$C_5H_{11}O_2^+$	valeric acid (C5) + isomers	0.71	77	5	15	4	0.54	12	0.56	9.8	0.54	9.8
carboxylic acid	$C_6H_{13}O_2^+$	caproic acid (C6) + isomers	0.26	94	4	1	1	0.61	14	0.6	11	0.61	11
carboxylic acid	$C_7H_{15}O_2^+$	enanthic acid (C7) + isomers	0.33	93	6	1	1	0.14	3.2	0.14	2.4	0.14	2.5
carboxylic acid	$C_8H_{17}O_2^+$	caprylic acid (C8) + isomers	0.34	94	5	0	1	0.28	6.4	0.27	4.8	0.28	5.1

carboxylic acid	$C_9H_{19}O_2^+$	pelargonic acid (C9) + isomers	0.43	89	9	1	1	0.1	2.4	0.1	1.8	0.1	1.9
carboxylic acid	$C_{10}H_{21}O_2^+$	decanoic acid (C10) + isomers	0.47	89	10	1	0	0.038	0.86	0.036	0.63	0.038	0.69
carboxylic acid	$C_{11}H_{23}O_2^+$	undecylic acid (C11) + isomers	0.57	87	4	6	3	0.019	0.43	0.019	0.33	0.02	0.35
furanoid	$C_6H_9O^+$	dimethyl furan	0.36	89	6	2	3	0.2	4.5	0.2	3.5	0.2	3.5
furanoid	$C_5H_7O_2^+$	fufuranol	0.83	66	20	8	6	0.12	2.7	0.12	2	0.12	2.1
furanoid	$C_4H_5O^+$	furan	0.67	75	8	5	12	0.1	2.2	0.1	1.8	0.1	1.8
furanoid	$C_4H_5O_2^+$	furanone	0.69	83	8	5	3	0.13	3	0.13	2.3	0.13	2.4
furanoid	$C_5H_7O^+$	methyl furan + pyran	0.86	64	9	3	24	0.16	3.7	0.16	2.9	0.16	2.9
furanoid	$C_5H_5O_2^+$	furfural	0.39	91	4	3	2	0.92	21	0.92	16	0.92	17
furanoid	$C_7H_9O_3^+$	methoxymethylfurfurol	0.55	52	38	1	10	0.012	0.27	0.012	0.21	0.012	0.21
furanoid	$C_6H_5O_3^+$	furandicarbaldehyde	2.9	38	39	14	9	0.018	0.4	0.018	0.32	0.018	0.32
halogen	CCl_3^+	chloroform	0.088	5	95	0	0	0.17	3.9	0.17	3	0.17	3.1
halogen	$H_2NCl_2^+$	dichloramine	NA	NA	NA	NA	NA	NA	NA	NA	NA	NA	NA
halogen	$C_6H_5Cl_2^+$	dichlorobenzene	0.33	75	25	0	0	0.018	0.41	0.018	0.31	0.018	0.32
halogen	$C_7H_4ClF_2^+$	parachlorobenzotrifluoride	0.77	15	85	0	0	0.033	0.74	0.031	0.55	0.031	0.56
halogen	CCl_2F^+		0.18	23	77	0	0	0.036	0.82	0.036	0.64	0.036	0.65
halogen	$CHCl_2^+$		0.53	82	7	3	8	0.11	2.5	0.1	1.8	0.1	1.9
halogen	CHF_2^+		NA	NA	NA	NA	NA	NA	NA	NA	NA	NA	NA
halogen	$C_2H_3Cl_2^+$		0.39	73	17	2	9	0.16	3.6	0.16	2.8	0.16	2.8
halogen	$C_2H_3ClF^+$		0.37	62	25	2	11	0.13	2.8	0.12	2.2	0.12	2.2
halogen	$C_2H_4OCl^+$		0.24	80	19	0	0	0.013	0.3	0.013	0.23	0.013	0.23
halogen	$C_2H_5NCl^+$		NA	NA	NA	NA	NA	NA	NA	NA	NA	NA	NA
halogen	$C_3H_6OCl^+$		0.4	79	19	2	0	0.031	0.7	0.03	0.53	0.03	0.54
nitrile	$C_2H_4N^+$	acetonitrile	0.3	19	78	2	1	0.16	3.5	0.16	2.8	0.16	2.9
nitrile	$C_3H_4N^+$	acrylonitrile	0.29	90	10	1	0	0.022	0.49	0.021	0.38	0.021	0.39
organosulfurs	CH_5S^+	methanethiol	0.98	65	13	18	4	0.074	1.7	0.077	1.3	0.077	1.4
organosulfurs	$C_2H_7S^+$	ethanethiol + DMS	0.54	55	37	7	1	0.33	7.4	0.34	6	0.34	6.1
organosulfurs	$C_2H_5OS^+$	mercaptoacetaldehyde	0.23	90	9	1	0	0.019	0.44	0.019	0.34	0.019	0.34
organosulfurs	$CH_5O_3S^+$	methane sulfonic acid	0.64	89	9	1	2	0.031	0.7	0.031	0.54	0.03	0.53
organosulfurs	$C_2H_7S_2^+$	dimethyl sulfide	0.36	85	9	3	4	0.031	0.7	0.031	0.54	0.031	0.56
organosulfurs	C2H7O2S+	dimethyl sulfone	0.24	89	7	1	2	0.14	3.3	0.14	2.5	0.14	2.6
organosulfurs	$C_3H_5S_2^+$		NA	NA	NA	NA	NA	NA	NA	NA	NA	NA	NA
organosulfurs	$C_4H_6NS^+$		NA	NA	NA	NA	NA	NA	NA	NA	NA	NA	NA
organosulfurs	$C_5H_{11}S^+$		NA	NA	NA	NA	NA	NA	NA	NA	NA	NA	NA
organosulfurs	$C_7H_5OS^+$		0.28	85	13	2	0	0.01	0.23	0.01	0.18	0.01	0.19
organosulfurs	$C_9H_9S^+$		NA	NA	NA	NA	NA	NA	NA	NA	NA	NA	NA

outdoor importance	**im-**	$C_2H_3O_2^+$	glyoxal	0.61	68	15	4	13	0.075	1.7	0.077	1.4	0.075	1.3
outdoor importance	**im-**	$C_5H_9^+$	isoprene	0.33	79	12	6	3	1.4	31	1.4	24	1.4	25
outdoor importance	**im-**	$C_{10}H_{19}O^+$	monoterpene alcohols	0.44	86	8	2	3	0.082	1.9	0.081	1.4	0.082	1.5
outdoor importance	**im-**	$C_{10}H_{17}^+$	monoterpenes	1.2	68	10	17	6	1.5	34	1.6	28	1.6	28
outdoor importance	**im-**	$C_{10}H_{17}O_2^+$	pinonaldehyde + isomers	0.35	72	27	1	0	0.018	0.41	0.018	0.31	0.018	0.33
outdoor importance	**im-**	$C_{15}H_{25}^+$	sesquiterpenes + isomers	0.36	88	5	4	4	0.11	2.5	0.11	1.9	0.11	2
possible ment	**frag-**	$C_2H_3^+$	alkyl fragment or acetylene	1.8	76	7	9	8	0.058	1.3	0.059	1	0.058	1
possible ment	**frag-**	$C_2H_4^+$	alkyl fragment	0.43	90	10	0	0	0.073	1.6	0.074	1.3	0.073	1.3
possible ment	**frag-**	$C_3H_5^+$	alkyl fragment	1.4	84	8	4	3	0.74	17	0.75	13	0.74	13
possible ment	**frag-**	$C_4H_5^+$	alkyl fragment	0.36	78	18	3	2	0.0096	0.22	0.0096	0.17	0.0096	0.17
possible ment	**frag-**	$C_4H_7^+$	alkyl fragment	0.24	74	22	3	1	0.95	22	0.94	17	0.95	17
possible ment	**frag-**	$C_5H_7^+$	alkyl fragment	0.4	81	9	8	2	0.051	1.1	0.051	0.9	0.051	0.93
possible ment	**frag-**	$C_5H_5O^+$	fragment of furanoid compound	1.2	64	7	6	23	0.22	5	0.24	4.1	0.23	4.1
possible ment	**frag-**	$C_6H_5^+$	aromatic fragment	NA	NA	NA	NA	NA	NA	NA	NA	NA	NA	NA
possible ment	**frag-**	$C_6H_5O^+$	aromatic fragment	0.25	95	3	0	2	0.46	10	0.45	7.9	0.45	8.1
possible ment	**frag-**	$C_3H_6^+$	alkyl fragment	NA	NA	NA	NA	NA	NA	NA	NA	NA	NA	NA
siloxane		C2H7O2Si+	dimethoxysilane	NA	NA	NA	NA	NA	NA	NA	NA	NA	NA	NA
siloxane		C6H19O3Si3+	D3 siloxane	0.47	86	13	0	0	0.1	2.3	0.099	1.7	0.097	1.7
siloxane		C8H25O4Si4+	D4 siloxane	0.65	76	23	0	0	0.11	2.4	0.11	1.9	0.1	1.9
siloxane		C10H31O5Si5+	D5 siloxane	2.6	43	4	4	49	0.89	20	0.73	13	0.72	13
siloxane		C12H37O6Si6+	D6 siloxane	1.5	84	1	0	15	0.11	2.6	0.11	1.9	0.1	1.8
siloxane		C10H31O3Si4+	L4 siloxane	NA	NA	NA	NA	NA	NA	NA	NA	NA	NA	NA
siloxane		C12H37O4Si5+	L5 siloxane	NA	NA	NA	NA	NA	NA	NA	NA	NA	NA	NA
siloxane		C15H39O2Si3+	caprylyl trisiloxane	NA	NA	NA	NA	NA	NA	NA	NA	NA	NA	NA
siloxane		C7H21O3Si3+		NA	NA	NA	NA	NA	NA	NA	NA	NA	NA	NA
uncategorized		$C_6H_{15}O_2^+$	2-butoxyethanol + isomers	NA	NA	NA	NA	NA	NA	NA	NA	NA	NA	NA

uncategorized	$C_2H_5O_3^+$	glycolic acid + isomers	0.34	46	53	1	0	0.034	0.77	0.032	0.57	0.034	0.61
uncategorized	$C_3H_5O_2^+$	acrylic acid + isomers	0.61	77	17	6	1	0.37	8.5	0.37	6.6	0.37	6.7
uncategorized	$C_6H_{11}^+$	cis-3-hexen-1-ol + isomers	0.26	88	5	5	1	1.3	29	1.3	23	1.3	23
uncategorized	$C_4H_7O_2^+$	diacetyl + isomers	0.38	78	13	6	4	0.69	16	0.68	12	0.69	13
uncategorized	$C_9H_{17}^+$	hydrindane + isomers	0.24	91	5	3	0	0.2	4.5	0.2	3.4	0.2	3.6
uncategorized	$C_5H_9O_2^+$	acetylpropionyl + glutaraldehyde + isomers	0.25	85	12	1	1	0.54	12	0.53	9.4	0.54	9.8
uncategorized	$C_4H_7O_3^+$	acetate anhydrate**	0.62	88	10	1	1	0.28	6.3	0.28	4.9	0.27	4.9
uncategorized	$C_8H_{15}^+$	1-octen-3-ol fragment (-H_2O) + isomers	0.25	87	10	3	0	0.3	6.9	0.3	5.2	0.3	5.4
uncategorized	$C_{10}H_{17}O^+$	citral + others	0.29	76	18	5	1	0.073	1.7	0.073	1.3	0.073	1.3
uncategorized	$C_6H_9O_4^+$	3-deoxyglucosone**	11	5	29	61	6	0.018	0.4	0.021	0.36	0.02	0.36
uncategorized	$C_4H_5O_3^+$		NA	NA	NA	NA	NA	NA	NA	NA	NA	NA	NA
uncategorized	$C_{15}H_{27}N_2^+$	sparteine**	0.32	92	6	1	1	0.022	0.49	0.022	0.38	0.022	0.39
uncategorized	$C_4H_3O_3^+$		1.9	18	71	10	1	0.014	0.32	0.015	0.26	0.014	0.25
uncategorized	$C_8H_9O^+$		0.4	87	7	3	2	0.13	3	0.13	2.3	0.13	2.4
uncategorized	$C_{14}H_{21}O_2^+$	chromanol + isomers	0.21	96	4	0	0	0.038	0.85	0.037	0.65	0.037	0.67
uncategorized	$C_8H_9O_2^+$	4-anisaldehyde + isomers	0.24	85	13	1	1	0.082	1.9	0.08	1.4	0.082	1.5
uncategorized	$C_7H_7^+$	1,3,5-norcaratriene or aromatic fragment	1	82	10	0	7	0.15	3.4	0.13	2.3	0.14	2.5
uncategorized	$C_9H_9O^+$	cinnamaldehyde + isomers	2.3	49	6	38	7	0.29	6.6	0.31	5.4	0.31	5.6
unknown	$C_8H_{19}O_3^+$		0.33	82	15	3	0	0.022	0.5	0.022	0.38	0.022	0.4
unknown	$C_{12}H_{25}O_2^+$		NA	NA	NA	NA	NA	NA	NA	NA	NA	NA	NA
unknown	$C_5H_{11}O_5^+$		NA	NA	NA	NA	NA	NA	NA	NA	NA	NA	NA
unknown	$C_7H_{15}O_5^+$		0.34	69	31	0	0	0.0094	0.21	0.009	0.16	0.0092	0.17
unknown	$C_{14}H_{29}^+$		0.32	79	21	0	0	0.0072	0.16	0.007	0.12	0.0071	0.13
unknown	$C_{15}H_{31}^+$		0.32	86	14	0	0	0.0065	0.15	0.0063	0.11	0.0064	0.12
unknown	$C_3H_7O_3^+$		1.2	77	10	13	1	0.1	2.3	0.098	1.7	0.1	1.8
unknown	$C_{16}H_{33}^+$		0.27	90	10	0	0	0.0072	0.16	0.007	0.12	0.0071	0.13
unknown	$C_{17}H_{35}^+$		0.27	91	8	0	0	0.0063	0.14	0.0061	0.11	0.0062	0.11
unknown	$C_{12}H_{23}^+$		NA	NA	NA	NA	NA	NA	NA	NA	NA	NA	NA

unknown	$C_{13}H_{25}^+$	NA	NA	NA	NA	NA	NA	NA	NA	NA	NA	NA
unknown	$C_{14}H_{27}^+$	NA	NA	NA	NA	NA	NA	NA	NA	NA	NA	NA
unknown	$C_{10}H_{19}O_2^+$	NA	NA	NA	NA	NA	NA	NA	NA	NA	NA	NA
unknown	C3H8N3O2+	NA	NA	NA	NA	NA	NA	NA	NA	NA	NA	NA
unknown	$C_2H_3O_4^+$	4	18	45	37	1	0.014	0.31	0.014	0.25	0.015	0.27
unknown	$C_4H_7O_4^+$	0.43	53	46	0	1	0.0075	0.17	0.0071	0.12	0.0073	0.13
unknown	$C_{12}H_{23}O^+$	0.37	75	24	0	0	0.012	0.28	0.012	0.21	0.012	0.22
unknown	$C_7H_{13}O_2^+$	0.23	75	23	1	0	0.074	1.7	0.073	1.3	0.074	1.3
unknown	$C_6H_{11}O_3^+$	0.43	74	20	3	3	0.02	0.46	0.02	0.35	0.02	0.37
unknown	$C_{11}H_{21}O^+$	0.6	77	18	4	0	0.02	0.46	0.02	0.35	0.02	0.37
unknown	$C_5H_9O_3^+$	0.57	73	17	4	6	0.044	0.99	0.043	0.76	0.044	0.79
unknown	$C_6H_{11}O_2^+$	0.22	82	16	1	0	0.17	3.8	0.17	2.9	0.17	3
unknown	$C_{12}H_{23}O_2^+$	0.41	79	21	0	0	0.034	0.77	0.032	0.57	0.034	0.61
unknown	$C_{18}H_{35}^+$	0.31	86	14	0	0	0.007	0.16	0.0067	0.12	0.0069	0.12
unknown	$C_9H_{17}O_2^+$	0.31	84	14	2	1	0.046	1	0.045	0.79	0.046	0.83
unknown	$C_3H_5O_3^+$	0.43	77	18	4	1	0.041	0.92	0.041	0.72	0.041	0.73
unknown	$C_{10}H_{19}^+$	0.28	84	12	1	2	0.059	1.3	0.058	1	0.059	1.1
unknown	$C_{15}H_{29}^+$	0.25	89	11	0	0	0.0073	0.17	0.0072	0.13	0.0073	0.13
unknown	$C_8H_{15}O_2^+$	0.24	88	10	2	0	0.12	2.7	0.12	2.1	0.12	2.1
unknown	$C_{10}H_{19}O_3^+$	0.33	89	10	0	0	0.0075	0.17	0.0073	0.13	0.0075	0.14
unknown	$C_7H_{13}^+$	0.28	87	8	4	1	0.36	8.2	0.36	6.3	0.36	6.5
unknown	$C_{16}H_{31}^+$	0.23	92	8	0	0	0.007	0.16	0.0068	0.12	0.0069	0.13
unknown	$C_{17}H_{33}^+$	0.23	94	6	0	0	0.0073	0.16	0.0071	0.13	0.0072	0.13
unknown	$C_2H_3O_3^+$	0.36	95	2	2	0	0.041	0.92	0.039	0.69	0.04	0.72
unknown	$C_{12}H_{21}O_2^+$	NA	NA	NA	NA	NA	NA	NA	NA	NA	NA	NA
unknown	$C_{10}H_{18}N^+$	NA	NA	NA	NA	NA	NA	NA	NA	NA	NA	NA
unknown	$C_6H_9O_3^+$	0.65	61	33	3	3	0.033	0.74	0.032	0.56	0.033	0.59
unknown	$C_8H_{13}O_4^+$	0.36	72	27	0	0	0.0068	0.15	0.0065	0.11	0.0068	0.12
unknown	$C_7H_{11}O_3^+$	0.32	73	25	1	1	0.024	0.55	0.024	0.41	0.024	0.44
unknown	$C_{13}H_{23}^+$	0.26	79	18	3	0	0.015	0.33	0.014	0.25	0.015	0.26
unknown	$C_7H_{11}O_2^+$	0.49	77	18	2	3	0.056	1.3	0.056	0.98	0.056	1
unknown	$C_9H_{15}O^+$	0.32	77	19	2	2	0.077	1.7	0.075	1.3	0.076	1.4
unknown	$C_{12}H_{21}^+$	0.78	72	16	12	0	0.022	0.51	0.022	0.39	0.022	0.4
unknown	$C_8H_{13}O_3^+$	0.27	82	17	1	1	0.02	0.44	0.019	0.33	0.019	0.35
unknown	$C_{13}H_{23}O^+$	0.4	83	15	1	1	0.0089	0.2	0.009	0.16	0.009	0.16
unknown	$C_6H_9O_2^+$	0.41	77	16	4	2	0.096	2.2	0.095	1.7	0.096	1.7
unknown	$C_8H_{13}O_2^+$	0.27	84	15	1	1	0.04	0.89	0.039	0.68	0.039	0.71
unknown	$C_9H_{15}O_3^+$	0.27	83	15	1	0	0.016	0.35	0.015	0.27	0.016	0.28
unknown	$C_{11}H_{19}^+$	0.87	76	13	11	0	0.042	0.94	0.042	0.74	0.041	0.75
unknown	$C_{19}H_{35}^+$	0.26	87	13	0	0	0.0091	0.2	0.0089	0.16	0.009	0.16
unknown	$C_{14}H_{25}^+$	0.22	88	12	0	0	0.012	0.28	0.012	0.22	0.012	0.22
unknown	$C_9H_{15}O_2^+$	0.33	86	12	2	0	0.043	0.98	0.042	0.75	0.043	0.78
unknown	$C_7H_{11}O^+$	0.28	85	10	2	3	0.087	2	0.086	1.5	0.087	1.6
unknown	$C_9H_{15}^+$	0.27	85	9	4	2	0.093	2.1	0.093	1.6	0.094	1.7
unknown	$C_{15}H_{27}^+$	0.21	92	8	0	0	0.015	0.33	0.015	0.26	0.015	0.26
unknown	$C_8H_{13}O^+$	0.25	89	7	2	2	0.081	1.8	0.081	1.4	0.081	1.5

unknown	$C_2HO_3^+$	2.4	55	12	28	5	0.0075	0.17	0.0074	0.13	0.0074	0.13
unknown	$C_{16}H_{29}^+$	0.19	94	6	0	0	0.019	0.43	0.019	0.33	0.019	0.34
unknown	$C_8H_{13}^+$	0.29	88	5	5	2	0.21	4.8	0.21	3.8	0.21	3.9
unknown	$C_{18}H_{33}^+$	0.21	95	5	0	0	0.011	0.26	0.011	0.2	0.011	0.21
unknown	C_3HO^+	NA	NA	NA	NA	NA	NA	NA	NA	NA	NA	NA
unknown	$C_8H_{11}O^+$	NA	NA	NA	NA	NA	NA	NA	NA	NA	NA	NA
unknown	$C_{11}H_{18}N^+$	NA	NA	NA	NA	NA	NA	NA	NA	NA	NA	NA
unknown	$C_5H_5O_3^+$	1.2	26	61	10	3	0.019	0.42	0.019	0.33	0.019	0.34
unknown	$C_4H_3O_2^+$	0.36	69	23	3	5	0.011	0.26	0.011	0.2	0.011	0.2
unknown	$C_{11}H_{17}O_2^+$	0.37	76	22	1	0	0.0056	0.13	0.0054	0.096	0.0056	0.1
unknown	$C_9H_{13}O_3^+$	0.32	77	23	0	0	0.0076	0.17	0.0075	0.13	0.0075	0.14
unknown	$C_{10}H_{15}O_2^+$	0.28	79	20	1	0	0.022	0.49	0.021	0.38	0.022	0.39
unknown	$C_7H_9O_2^+$	0.5	73	17	2	7	0.037	0.84	0.037	0.66	0.037	0.67
unknown	$C_8H_{11}O_3^+$	0.35	79	19	1	1	0.012	0.27	0.011	0.2	0.012	0.21
unknown	$C_{20}H_{35}^+$	0.29	83	17	0	0	0.0094	0.21	0.0091	0.16	0.0093	0.17
unknown	$C_{14}H_{23}O^+$	0.44	83	15	1	1	0.0069	0.16	0.0068	0.12	0.0069	0.12
unknown	$C_{10}H_{15}O^+$	0.91	77	12	9	2	0.074	1.7	0.076	1.3	0.075	1.3
unknown	$C_{19}H_{33}^+$	0.21	90	10	0	0	0.016	0.36	0.016	0.28	0.016	0.29
unknown	$C_{13}H_{21}O^+$	0.39	89	9	1	1	0.0056	0.13	0.0056	0.099	0.0056	0.1
unknown	$C_9H_{11}O_3^+$	NA	NA	NA	NA	NA	NA	NA	NA	NA	NA	NA
unknown	$C_6H_5O_2^+$	1.6	46	51	2	1	0.033	0.75	0.033	0.59	0.033	0.6
unknown	$C_{15}H_{23}O_3^+$	1.3	64	36	0	0	0.014	0.31	0.011	0.2	0.014	0.25
unknown	$C_{11}H_{15}^+$	0.28	77	22	0	0	0.0088	0.2	0.0086	0.15	0.0087	0.16
unknown	$C_{12}H_{17}O^+$	0.3	81	19	0	0	0.0093	0.21	0.009	0.16	0.0092	0.17
unknown	$C_9H_{11}O_2^+$	0.58	74	18	6	2	0.011	0.26	0.011	0.2	0.011	0.21
unknown	$C_9H_{11}^+$	0.26	83	14	2	1	0.076	1.7	0.075	1.3	0.075	1.4
unknown	$C_{20}H_{33}^+$	0.27	84	16	0	0	0.01	0.23	0.0099	0.17	0.01	0.18
unknown	$C_{16}H_{25}^+$	0.55	83	15	2	0	0.019	0.42	0.018	0.31	0.019	0.34
unknown	$C_9H_{11}O^+$	0.19	86	13	1	0	0.11	2.5	0.11	1.9	0.11	2
unknown	$C_{10}H_{13}O_2^+$	1	80	14	6	1	0.018	0.4	0.018	0.31	0.018	0.32
unknown	$C_{10}H_{13}^+$	1.4	64	11	20	4	0.088	2	0.091	1.6	0.091	1.7
unknown	$C_{10}H_{13}O^+$	0.95	77	12	9	2	0.04	0.9	0.039	0.69	0.04	0.72
unknown	$C_{14}H_{21}^+$	0.24	89	10	1	0	0.012	0.28	0.012	0.21	0.012	0.22
unknown	$C_{19}H_{31}^+$	0.23	89	11	0	0	0.015	0.34	0.015	0.26	0.015	0.27
unknown	$C_{18}H_{29}^+$	0.19	93	7	0	0	0.015	0.35	0.015	0.27	0.015	0.28
unknown	$C_{15}H_{23}^+$	0.39	91	6	3	0	0.018	0.42	0.018	0.32	0.019	0.34
unknown	$C_{17}H_{27}^+$	0.19	96	4	0	0	0.015	0.35	0.015	0.27	0.015	0.28
unknown	$C_{14}H_{19}^+$	NA	NA	NA	NA	NA	NA	NA	NA	NA	NA	NA
unknown	$C_9H_{10}N^+$	NA	NA	NA	NA	NA	NA	NA	NA	NA	NA	NA
unknown	$C_{10}H_{11}O_2^+$	0.34	51	49	0	0	0.01	0.24	0.01	0.18	0.01	0.19
unknown	$C_8H_7O_3^+$	0.42	52	43	5	0	0.0065	0.15	0.0064	0.11	0.0064	0.12
unknown	$C_7H_5O_2^+$	0.47	54	41	3	2	0.021	0.48	0.02	0.35	0.021	0.38
unknown	$C_8H_7O_2^+$	0.27	68	30	2	1	0.013	0.29	0.013	0.22	0.013	0.23
unknown	$C_{11}H_{13}O^+$	0.4	70	29	1	0	0.0077	0.17	0.0074	0.13	0.0076	0.14
unknown	$C_{16}H_{23}^+$	0.29	75	24	0	0	0.013	0.3	0.013	0.23	0.013	0.24
unknown	$C_{10}H_{11}O^+$	0.35	79	18	2	1	0.01	0.23	0.0098	0.17	0.01	0.18

unknown	$C_{20}H_{31}^+$	0.43	80	20	0	0	0.0059	0.13	0.0056	0.098	0.0058	0.11
unknown	$C_{15}H_{21}^+$	0.4	87	12	1	1	0.017	0.38	0.016	0.28	0.017	0.31
unknown	$C_{18}H_{27}^+$	0.3	88	10	0	1	0.0092	0.21	0.0089	0.16	0.0091	0.16
unknown	$C_{19}H_{29}^+$	0.29	90	10	0	0	0.007	0.16	0.0068	0.12	0.0069	0.12
unknown	$C_{17}H_{25}^+$	0.27	92	8	0	0	0.01	0.23	0.0097	0.17	0.0099	0.18
unknown	$C_{10}H_9O_3^+$	0.51	38	62	0	0	0.0091	0.21	0.0087	0.15	0.0089	0.16
unknown	$C_8H_5O_3^+$	0.32	63	35	1	0	0.022	0.5	0.022	0.39	0.022	0.4
unknown	$C_8H_5O_2^+$	1.6	49	30	17	4	0.0075	0.17	0.0074	0.13	0.0076	0.14
unknown	$C_9H_7O_2^+$	1.6	46	29	23	2	0.01	0.23	0.0098	0.17	0.01	0.18
unknown	$C_{14}H_{17}^+$	0.3	82	18	0	0	0.016	0.35	0.015	0.26	0.015	0.28
unknown	$C_{13}H_{15}^+$	0.31	83	16	1	0	0.019	0.42	0.018	0.32	0.019	0.34
unknown	$C_{16}H_{21}^+$	0.3	86	14	0	0	0.0061	0.14	0.0059	0.1	0.006	0.11
unknown	$C_{16}H_{19}^+$	0.36	82	18	0	0	0.0073	0.17	0.0071	0.13	0.0073	0.13
unknown	$C_{15}H_{17}^+$	0.31	84	16	0	0	0.006	0.13	0.0058	0.1	0.0059	0.11
unknown	$C_{16}H_{17}^+$	NA	NA	NA	NA	NA	NA	NA	NA	NA	NA	NA
unknown	$C_{13}H_{11}O^+$	0.4	80	20	0	0	0.054	1.2	0.051	0.9	0.054	0.97

Table 4.7.2: Summary table of exposures during the H1 summer campaign. The mean concentration during occupancy (MC) is in units of ppb, the campaign average daily exposure (ADE) is in units of ppb-hour day^{-1}, and the relative contributions from continuous indoor sources (CIS), outdoor origin (OO), cooking (C), and other (O) are unitless (%). In rare cases, statistical noise generates a slight negative relative fraction for the background of outdoor origin. The relative standard deviation (RSD) indicates the variability in the indoor concentration time series. The heading 'all' refers to source apportionments and exposures for a hypothetical occupant who is present for the entirety of the measurement period.

				all						H1M1		H1F1	
Class	**Ion**	**Name**	**RSD**	**CIS**	**OO**	**C**	**O**	**MC**	**ADE**	**MC**	**ADE**	**MC**	**ADE**
				%	%	%	%	ppb	ppb h d-1	ppb	ppb h d-1	ppb	ppb h d-1
alcohol + alkene	CH_5O^+	methanol	0.25	88	4	7	2	28	620	28	480	28	500
alcohol + alkene	$C_2H_7O^+$	ethanol	2.7	30	1	60	8	160	3500	160	2700	200	3600
alcohol + alkene	$C_3H_7^+$	propanol fragment (-H_2O) + propene	1.6	60	6	33	1	4.3	97	4.5	78	4.4	77
alcohol + alkene	$C_4H_9^+$	butanol fragment (-H_2O) + butene	0.34	85	9	1	5	1.9	42	1.9	32	1.9	33
alcohol + alkene	$C_5H_{11}^+$	pentanol fragment (-H_2O) + pentene	0.32	85	7	4	3	0.64	14	0.64	11	0.64	11
alcohol + alkene	$C_6H_{13}^+$	hexanol fragment (-H_2O) + hexene	0.36	81	13	0	5	0.15	3.4	0.15	2.6	0.15	2.7
alcohol + alkene	$C_8H_{17}^+$	octanol fragment (-H_2O) + octene	0.31	91	6	1	2	0.022	0.5	0.022	0.38	0.022	0.39
aromatic	$C_6H_7^+$	benzene	0.37	63	29	4	4	0.46	10	0.46	7.9	0.46	8
aromatic	$C_7H_9^+$	toluene	0.52	80	16	2	3	0.75	17	0.76	13	0.75	13
aromatic	$C_8H_9^+$	styrene	0.25	91	9	0	0	0.15	3.3	0.14	2.5	0.15	2.6
aromatic	$C_8H_{11}^+$	xylene + ethyl benzene	0.32	54	39	2	4	0.25	5.4	0.24	4.1	0.24	4.2
aromatic	$C_6H_7O^+$	phenol	0.25	93	3	2	3	0.48	11	0.48	8.2	0.48	8.4
aromatic	$C_6H_7O_2^+$	benzene diol	0.62	75	7	4	15	0.11	2.5	0.11	1.9	0.11	2
aromatic	$C_7H_9O^+$	cresols	0.26	86	9	1	4	0.15	3.2	0.14	2.5	0.14	2.5
aromatic	$C_7H_7O^+$	benzaldehyde	0.21	93	7	0	0	0.34	7.5	0.33	5.7	0.34	5.9
aromatic	$C_4H_6N^+$	pyrrole	1.8	58	3	6	33	0.06	1.3	0.064	1.1	0.057	0.99
aromatic	$C_9H_{13}^+$	benzene (+3 sat. carbons) + isomers	0.4	49	37	5	9	0.14	3	0.14	2.3	0.13	2.3

aromatic	$C_{10}H_{15}^+$	benzene (+4 sat. carbons) + isomers	NA	NA	NA	NA	NA	NA	NA	NA	NA	NA	NA
aromatic	$C_{11}H_{17}^+$	benzene (+5 sat. carbons) + isomers	0.28	83	14	3	1	0.029	0.65	0.029	0.5	0.029	0.52
aromatic	$C_{13}H_{21}^+$	benzene (+7 sat. carbons) + isomers	0.34	93	6	0	1	0.013	0.29	0.013	0.22	0.013	0.23
aromatic	$C_{14}H_{23}^+$	benzene (+8 sat. carbons) + isomers	0.32	93	6	0	2	0.015	0.34	0.015	0.26	0.015	0.27
aromatic	$C_{16}H_{27}^+$	benzene (+10 sat. carbons) + isomers	0.24	96	4	0	0	0.019	0.43	0.019	0.33	0.019	0.34
aromatic	$C_{17}H_{29}^+$	benzene (+11 sat. carbons) + isomers	0.22	95	4	0	0	0.015	0.34	0.015	0.26	0.015	0.26
aromatic	$C_{18}H_{31}^+$	benzene (+12 sat. carbons) + isomers	0.24	97	3	0	0	0.012	0.27	0.012	0.21	0.012	0.21
aromatic	$C_7H_6NS^+$	benzothiazole	0.3	88	12	0	0	0.037	0.81	0.036	0.62	0.036	0.63
carbonyl (sat.)	$C_2H_5O^+$	acetaldehyde (C2)	1.1	69	7	19	4	8.3	180	8.2	140	9.1	160
carbonyl (sat.)	$C_3H_7O^+$	acetone + propanal (C3)	0.25	82	10	3	5	9.9	220	10	170	10	180
carbonyl (sat.)	$C_4H_9O^+$	C4 sat. carbonyl (methylethylketone + others)	0.58	63	19	8	10	0.75	17	0.74	13	0.78	14
carbonyl (sat.)	$C_5H_{11}O^+$	C5 sat. carbonyl (pentanone + others)	0.52	71	9	7	13	0.3	6.6	0.29	5.1	0.3	5.3
carbonyl (sat.)	$C_6H_{13}O^+$	C6 sat. carbonyl (hexanone + others)	0.26	89	9	2	1	0.16	3.6	0.16	2.8	0.16	2.9
carbonyl (sat.)	$C_7H_{15}O^+$	C7 sat. carbonyl	0.25	90	8	1	0	0.11	2.4	0.11	1.9	0.11	1.9
carbonyl (sat.)	$C_8H_{17}O^+$	C8 sat. carbonyl + 1-octen-3-ol	0.24	94	5	1	0	0.11	2.4	0.11	1.8	0.11	1.9
carbonyl (sat.)	$C_9H_{19}O^+$	C9 sat. carbonyl	0.18	97	2	1	0	0.25	5.5	0.25	4.2	0.25	4.3

carbonyl (sat.)	$C_{10}H_{21}O^+$	C10 sat. carbonyl	0.23	97	2	0	0	0.14	3.2	0.14	2.4	0.14	2.5
carbonyl (sat.)	$C_{11}H_{23}O^+$	C11 sat. carbonyl	0.27	96	4	0	0	0.035	0.77	0.034	0.59	0.035	0.61
carbonyl (sat.)	$C_{12}H_{25}O^+$	C12 sat. carbonyl	0.35	95	5	0	0	0.018	0.39	0.017	0.29	0.017	0.31
carbonyl (sat.)	$C_{14}H_{29}O^+$	C14 sat. carbonyl	NA	NA	NA	NA	NA	NA	NA	NA	NA	NA	NA
carbonyl (unsat.)	$C_3H_5O^+$	acrolein (C3 unsat. carbonyl)	0.33	87	7	5	1	0.44	9.7	0.44	7.5	0.45	7.9
carbonyl (unsat.)	$C_4H_7O^+$	unsat. carbonyl (C4)	0.25	86	9	3	2	0.4	9	0.4	6.8	0.41	7.1
carbonyl (unsat.)	$C_5H_9O^+$	unsat. carbonyl (C5) + cyclopentanone	0.26	84	9	4	4	0.21	4.6	0.21	3.5	0.21	3.7
carbonyl (unsat.)	$C_6H_{11}O^+$	unsat. carbonyl (C6) + cis-3-hexenal + isomers	0.26	88	7	2	2	0.21	4.7	0.21	3.6	0.21	3.7
carbonyl (unsat.)	$C_7H_{13}O^+$	unsat. carbonyl (C7) + isomers	0.34	87	10	3	0	0.066	1.5	0.065	1.1	0.066	1.2
carbonyl (unsat.)	$C_8H_{15}O^+$	unsat. carbonyl (C8) + oct-1-en-3-one + isomers	0.27	93	5	1	1	0.13	2.8	0.13	2.2	0.13	2.2
carbonyl (unsat.)	$C_9H_{17}O^+$	unsat. carbonyl (C9) + isomers	0.27	92	7	0	0	0.052	1.2	0.052	0.88	0.052	0.91
carboxylic acid	$CH_3O_2^+$	formic acid (C1) + isomers	0.18	92	6	2	0	11	250	11	190	11	200
carboxylic acid	$C_2H_5O_2^+$	acetic acid (C2) + isomers	0.22	94	3	1	2	44	980	44	750	44	780
carboxylic acid	$C_3H_7O_2^+$	propionic acid (C3) + isomers	0.29	87	8	3	3	2.6	57	2.5	44	2.6	46
carboxylic acid	$C_4H_9O_2^+$	butryic acid (C4) + isomers	0.38	83	5	9	3	1.1	25	1.1	19	1.1	20
carboxylic acid	$C_5H_{11}O_2^+$	valeric acid (C5) + isomers	0.71	89	4	0	6	0.46	10	0.46	7.8	0.45	7.9
carboxylic acid	$C_6H_{13}O_2^+$	caproic acid (C6) + isomers	0.33	95	5	0	0	0.4	9	0.4	6.8	0.4	7
carboxylic acid	$C_7H_{15}O_2^+$	enanthic acid (C7) + isomers	0.37	94	6	0	0	0.07	1.5	0.068	1.2	0.069	1.2
carboxylic acid	$C_8H_{17}O_2^+$	caprylic acid (C8) + isomers	0.37	94	6	0	0	0.15	3.4	0.15	2.5	0.15	2.6

carboxylic acid	$C_9H_{19}O_2^+$	pelargonic acid (C9) + isomers	0.36	91	9	0	0	0.055	1.2	0.054	0.93	0.055	0.96
carboxylic acid	$C_{10}H_{21}O_2^+$	decanoic acid (C10) + isomers	0.34	92	8	0	0	0.017	0.37	0.016	0.28	0.017	0.29
carboxylic acid	$C_{11}H_{23}O_2^+$	undecylic acid (C11) + isomers	0.29	95	4	0	0	0.0083	0.19	0.0082	0.14	0.0083	0.15
furanoid	$C_6H_9O^+$	dimethyl furan	0.34	86	6	3	5	0.2	4.4	0.2	3.4	0.2	3.5
furanoid	$C_5H_7O_2^+$	fufuranol	0.67	68	15	6	10	0.096	2.1	0.095	1.6	0.1	1.7
furanoid	$C_4H_5O^+$	furan	0.45	79	7	4	10	0.15	3.3	0.15	2.5	0.15	2.6
furanoid	$C_4H_5O_2^+$	furanone	0.45	84	10	2	3	0.14	3	0.14	2.3	0.14	2.4
furanoid	$C_5H_7O^+$	methyl furan + pyran	0.51	75	6	3	16	0.21	4.7	0.21	3.6	0.21	3.7
furanoid	$C_5H_5O_2^+$	furfural	0.43	87	4	4	5	0.94	21	0.94	16	0.96	17
furanoid	$C_7H_9O_3^+$	methoxymethylfurfural	0.46	70	14	2	14	0.01	0.23	0.01	0.18	0.01	0.18
furanoid	$C_6H_5O_3^+$	furandicarbaldehyde	0.63	66	31	2	2	0.018	0.4	0.017	0.3	0.018	0.32
halogen	CCl_3^+	chloroform	0.061	5	95	0	0	0.13	3	0.13	2.3	0.13	2.4
halogen	$H_2NCl_2^+$	dichloramine	NA	NA	NA	NA	NA	NA	NA	NA	NA	NA	NA
halogen	$C_6H_5Cl_2^+$	dichlorobenzene	0.25	80	19	0	0	0.019	0.43	0.019	0.32	0.019	0.33
halogen	$C_7H_4ClF_2^+$	parachlorobenzotrifluoride	0.75	26	74	0	0	0.021	0.48	0.02	0.35	0.021	0.37
halogen	CCl_2F^+		NA	NA	NA	NA	NA	NA	NA	NA	NA	NA	NA
halogen	$CHCl_2^+$		NA	NA	NA	NA	NA	NA	NA	NA	NA	NA	NA
halogen	CHF_2^+		NA	NA	NA	NA	NA	NA	NA	NA	NA	NA	NA
halogen	$C_2H_3Cl_2^+$		0.37	69	14	2	15	0.14	3.1	0.14	2.3	0.14	2.4
halogen	$C_2H_3ClF^+$		0.77	56	11	12	21	0.23	5.1	0.24	4	0.23	4
halogen	$C_2H_4OCl^+$		NA	NA	NA	NA	NA	NA	NA	NA	NA	NA	NA
halogen	$C_2H_5NCl^+$		NA	NA	NA	NA	NA	NA	NA	NA	NA	NA	NA
halogen	$C_3H_6OCl^+$		NA	NA	NA	NA	NA	NA	NA	NA	NA	NA	NA
nitrile	$C_2H_4N^+$	acetonitrile	0.23	30	68	2	1	0.11	2.5	0.11	1.9	0.11	2
nitrile	$C_3H_4N^+$	acrylonitrile	0.23	89	11	1	0	0.022	0.49	0.022	0.37	0.022	0.39
organosulfurs	CH_5S^+	methanethiol	0.63	72	6	15	7	0.072	1.6	0.072	1.2	0.076	1.3
organosulfurs	$C_2H_7S^+$	ethanethiol + DMS	2.1	68	6	25	1	0.36	8.1	0.39	6.6	0.39	6.9
organosulfurs	$C_2H_5OS^+$	mercaptoacetaldehyde	0.25	95	5	0	0	0.035	0.78	0.035	0.59	0.035	0.61
organosulfurs	$CH_5O_3S^+$	methane sulfonic acid	0.44	90	4	2	3	0.11	2.5	0.11	1.9	0.11	2
organosulfurs	$C_2H_7S_2^+$	dimethyl sulfide	0.32	90	4	3	2	0.062	1.4	0.063	1.1	0.062	1.1
organosulfurs	C2H7O2S+	dimethyl sulfone	0.27	95	3	1	1	0.19	4.2	0.19	3.3	0.19	3.3
organosulfurs	$C_3H_5S_2^+$		NA	NA	NA	NA	NA	NA	NA	NA	NA	NA	NA
organosulfurs	$C_4H_6NS^+$		NA	NA	NA	NA	NA	NA	NA	NA	NA	NA	NA
organosulfurs	$C_5H_{11}S^+$		NA	NA	NA	NA	NA	NA	NA	NA	NA	NA	NA
organosulfurs	$C_7H_5OS^+$		NA	NA	NA	NA	NA	NA	NA	NA	NA	NA	NA
organosulfurs	$C_9H_9S^+$		NA	NA	NA	NA	NA	NA	NA	NA	NA	NA	NA

outdoor	impor-tance	$C_2H_3O_2^+$	glyoxal	NA	NA	NA	NA	NA	NA	NA	NA	NA	NA	NA
outdoor	impor-tance	$C_5H_9^+$	isoprene	0.3	85	4	5	6	1.3	29	1.3	23	1.3	23
outdoor	impor-tance	$C_{10}H_{19}O^+$	monoterpene alcohols	0.49	91	4	4	1	0.094	2.1	0.093	1.6	0.095	1.7
outdoor	impor-tance	$C_{10}H_{17}^+$	monoterpenes	1.7	40	1	23	36	12	260	13	220	11	200
outdoor	impor-tance	$C_{10}H_{17}O_2^+$	pinonaldehyde + isomers	0.37	84	15	1	0	0.019	0.42	0.018	0.31	0.019	0.33
outdoor	impor-tance	$C_{15}H_{25}^+$	sesquiterpenes + isomers	0.38	90	4	5	1	0.078	1.7	0.077	1.3	0.078	1.4
possible	frag-ment	$C_2H_3^+$	alkyl fragment or acetylene	1.2	60	5	11	24	0.33	7.4	0.35	5.9	0.36	6.2
possible	frag-ment	$C_2H_4^+$	alkyl fragment	0.32	92	7	1	0	0.2	4.5	0.2	3.5	0.21	3.7
possible	frag-ment	$C_3H_5^+$	alkyl fragment	1.2	67	7	2	24	1.2	27	1.3	22	1.2	22
possible	frag-ment	$C_4H_5^+$	alkyl fragment	0.65	59	10	12	19	0.023	0.51	0.024	0.41	0.023	0.4
possible	frag-ment	$C_4H_7^+$	alkyl fragment	0.23	83	13	2	2	1.1	25	1.1	19	1.1	20
possible	frag-ment	$C_5H_7^+$	alkyl fragment	NA	NA	NA	NA	NA	NA	NA	NA	NA	NA	NA
possible	frag-ment	$C_5H_5O^+$	fragment of furanoid compound	1.2	53	1	18	28	0.54	12	0.58	9.9	0.54	9.4
possible	frag-ment	$C_6H_5^+$	aromatic fragment	0.27	79	18	1	2	0.033	0.73	0.033	0.57	0.033	0.58
possible	frag-ment	$C_6H_5O^+$	aromatic fragment	0.29	96	4	0	0	0.41	9	0.4	6.9	0.4	7
possible	frag-ment	$C_3H_6^+$	alkyl fragment	NA	NA	NA	NA	NA	NA	NA	NA	NA	NA	NA
siloxane		C2H7O2Si+	dimethoxysilane	1.4	70	4	24	2	0.074	1.6	0.078	1.3	0.078	1.4
siloxane		C6H19O3Si3+	D3 siloxane	0.31	92	5	1	1	0.094	2.1	0.093	1.6	0.093	1.6
siloxane		C8H25O4Si4+	D4 siloxane	0.5	86	4	1	10	0.22	4.8	0.22	3.7	0.21	3.7
siloxane		C10H31O5Si5+	D5 siloxane	2.8	16	0	83	1	14	320	14	240	12	220
siloxane		C12H37O6Si6+	D6 siloxane	1.7	58	7	0	35	0.055	1.2	0.05	0.85	0.051	0.89
siloxane		C10H31O3Si4+	L4 siloxane	NA	NA	NA	NA	NA	NA	NA	NA	NA	NA	NA
siloxane		C12H37O4Si5+	L5 siloxane	NA	NA	NA	NA	NA	NA	NA	NA	NA	NA	NA
siloxane		C15H39O2Si3+	caprylyl trisiloxane	NA	NA	NA	NA	NA	NA	NA	NA	NA	NA	NA
siloxane		C7H21O3Si3+		NA	NA	NA	NA	NA	NA	NA	NA	NA	NA	NA
uncategorized		$C_6H_{15}O_2^+$	2-butoxyethanol + isomers	NA	NA	NA	NA	NA	NA	NA	NA	NA	NA	NA

uncategorized	$C_2H_5O_3^+$	glycolic acid + isomers	0.22	90	10	0	0	0.035	0.78	0.035	0.59	0.035	0.61
uncategorized	$C_3H_5O_2^+$	acrylic acid + isomers	0.62	79	16	4	1	0.29	6.5	0.29	5	0.31	5.4
uncategorized	$C_6H_{11}^+$	cis-3-hexen-1-ol + isomers	0.24	93	4	3	1	1.1	24	1.1	18	1.1	19
uncategorized	$C_4H_7O_2^+$	diacetyl + isomers	0.35	82	7	4	7	0.59	13	0.58	10	0.6	10
uncategorized	$C_9H_{17}^+$	hydrindane + isomers	0.16	93	5	1	1	0.13	2.8	0.13	2.2	0.13	2.2
uncategorized	$C_5H_9O_2^+$	acetylpropionyl + glutaraldehyde + isomers	0.25	86	9	2	4	0.31	7	0.31	5.4	0.31	5.5
uncategorized	$C_4H_7O_3^+$	acetate anhydrate**	0.27	89	9	1	1	0.16	3.5	0.15	2.6	0.16	2.7
uncategorized	$C_8H_{15}^+$	1-octen-3-ol fragment (-H_2O) + isomers	0.2	91	6	2	1	0.22	4.8	0.22	3.7	0.22	3.8
uncategorized	$C_{10}H_{17}O^+$	citral + others	0.39	76	16	6	2	0.074	1.6	0.075	1.3	0.074	1.3
uncategorized	$C_6H_9O_4^+$	3-deoxyglucosone**	5.9	67	11	20	2	0.013	0.28	0.012	0.2	0.018	0.32
uncategorized	$C_4H_5O_3^+$		NA	NA	NA	NA	NA	NA	NA	NA	NA	NA	NA
uncategorized	$C_{15}H_{27}N_2^+$	sparteine**	0.29	95	4	0	0	0.013	0.3	0.013	0.22	0.013	0.23
uncategorized	$C_4H_3O_3^+$		0.59	28	61	6	5	0.019	0.42	0.019	0.32	0.019	0.34
uncategorized	$C_8H_9O^+$		0.3	91	6	2	1	0.11	2.4	0.11	1.8	0.11	1.9
uncategorized	$C_{14}H_{21}O_2^+$	chromanol + isomers	0.34	94	6	0	0	0.024	0.53	0.023	0.4	0.024	0.41
uncategorized	$C_8H_9O_2^+$	4-anisaldehyde + isomers	1.4	47	3	19	31	0.25	5.6	0.27	4.6	0.24	4.3
uncategorized	$C_7H_7^+$	1,3,5-norcaratriene or aromatic fragment	0.28	91	7	1	1	0.21	4.7	0.21	3.6	0.21	3.7
uncategorized	$C_9H_9O^+$	cinnamaldehyde + isomers	0.42	86	6	4	4	0.061	1.4	0.06	1	0.061	1.1
unknown	$C_8H_{19}O_3^+$		0.26	88	12	0	0	0.016	0.37	0.016	0.28	0.016	0.29
unknown	$C_{12}H_{25}O_2^+$		NA	NA	NA	NA	NA	NA	NA	NA	NA	NA	NA
unknown	$C_5H_{11}O_5^+$		NA	NA	NA	NA	NA	NA	NA	NA	NA	NA	NA
unknown	$C_7H_{15}O_5^+$		0.36	74	26	0	0	0.0071	0.16	0.0069	0.12	0.007	0.12
unknown	$C_{14}H_{29}^+$		NA	NA	NA	NA	NA	NA	NA	NA	NA	NA	NA
unknown	$C_{15}H_{31}^+$		NA	NA	NA	NA	NA	NA	NA	NA	NA	NA	NA
unknown	$C_3H_7O_3^+$		NA	NA	NA	NA	NA	NA	NA	NA	NA	NA	NA
unknown	$C_{16}H_{33}^+$		NA	NA	NA	NA	NA	NA	NA	NA	NA	NA	NA
unknown	$C_{17}H_{35}^+$		NA	NA	NA	NA	NA	NA	NA	NA	NA	NA	NA
unknown	$C_{12}H_{23}^+$		NA	NA	NA	NA	NA	NA	NA	NA	NA	NA	NA

unknown	$C_{13}H_{25}^+$	NA	NA	NA	NA	NA	NA	NA	NA	NA	NA	NA
unknown	$C_{14}H_{27}^+$	NA	NA	NA	NA	NA	NA	NA	NA	NA	NA	NA
unknown	$C_{10}H_{19}O_2^+$	NA	NA	NA	NA	NA	NA	NA	NA	NA	NA	NA
unknown	C3H8N3O2+	NA	NA	NA	NA	NA	NA	NA	NA	NA	NA	NA
unknown	$C_2H_3O_4^+$	NA	NA	NA	NA	NA	NA	NA	NA	NA	NA	NA
unknown	$C_4H_7O_4^+$	NA	NA	NA	NA	NA	NA	NA	NA	NA	NA	NA
unknown	$C_{12}H_{23}O^+$	NA	NA	NA	NA	NA	NA	NA	NA	NA	NA	NA
unknown	$C_7H_{13}O_2^+$	0.28	83	16	1	1	0.051	1.1	0.051	0.87	0.051	0.9
unknown	$C_6H_{11}O_3^+$	0.4	85	12	1	2	0.016	0.36	0.016	0.27	0.016	0.28
unknown	$C_{11}H_{21}O^+$	NA	NA	NA	NA	NA	NA	NA	NA	NA	NA	NA
unknown	$C_5H_9O_3^+$	NA	NA	NA	NA	NA	NA	NA	NA	NA	NA	NA
unknown	$C_6H_{11}O_2^+$	0.29	87	12	0	1	0.12	2.7	0.12	2.1	0.12	2.2
unknown	$C_{12}H_{23}O_2^+$	0.39	90	10	0	0	0.016	0.36	0.016	0.27	0.016	0.28
unknown	$C_{18}H_{35}^+$	NA	NA	NA	NA	NA	NA	NA	NA	NA	NA	NA
unknown	$C_9H_{17}O_2^+$	0.28	92	8	0	0	0.044	0.98	0.043	0.74	0.044	0.77
unknown	$C_3H_5O_3^+$	NA	NA	NA	NA	NA	NA	NA	NA	NA	NA	NA
unknown	$C_{10}H_{19}^+$	0.35	91	6	2	2	0.069	1.5	0.069	1.2	0.069	1.2
unknown	$C_{15}H_{29}^+$	NA	NA	NA	NA	NA	NA	NA	NA	NA	NA	NA
unknown	$C_8H_{15}O_2^+$	0.25	92	8	0	0	0.11	2.5	0.11	1.9	0.11	2
unknown	$C_{10}H_{19}O_3^+$	NA	NA	NA	NA	NA	NA	NA	NA	NA	NA	NA
unknown	$C_7H_{13}^+$	0.19	91	7	2	0	0.28	6.3	0.28	4.8	0.28	5
unknown	$C_{16}H_{31}^+$	NA	NA	NA	NA	NA	NA	NA	NA	NA	NA	NA
unknown	$C_{17}H_{33}^+$	NA	NA	NA	NA	NA	NA	NA	NA	NA	NA	NA
unknown	$C_2H_3O_3^+$	NA	NA	NA	NA	NA	NA	NA	NA	NA	NA	NA
unknown	$C_{12}H_{21}O_2^+$	NA	NA	NA	NA	NA	NA	NA	NA	NA	NA	NA
unknown	$C_{10}H_{18}N^+$	NA	NA	NA	NA	NA	NA	NA	NA	NA	NA	NA
unknown	$C_6H_9O_3^+$	0.31	71	26	2	1	0.03	0.66	0.029	0.5	0.03	0.52
unknown	$C_8H_{13}O_4^+$	NA	NA	NA	NA	NA	NA	NA	NA	NA	NA	NA
unknown	$C_7H_{11}O_3^+$	NA	NA	NA	NA	NA	NA	NA	NA	NA	NA	NA
unknown	$C_{13}H_{23}^+$	0.53	83	10	0	7	0.012	0.26	0.012	0.2	0.012	0.21
unknown	$C_7H_{11}O_2^+$	0.34	86	11	1	2	0.046	1	0.046	0.78	0.046	0.8
unknown	$C_9H_{15}O^+$	0.33	89	6	3	2	0.075	1.7	0.074	1.3	0.075	1.3
unknown	$C_{12}H_{21}^+$	0.29	84	13	0	3	0.014	0.3	0.013	0.23	0.014	0.24
unknown	$C_8H_{13}O_3^+$	NA	NA	NA	NA	NA	NA	NA	NA	NA	NA	NA
unknown	$C_{13}H_{23}O^+$	0.38	94	5	0	1	0.0057	0.13	0.0057	0.097	0.0058	0.1
unknown	$C_6H_9O_2^+$	0.3	84	12	2	3	0.068	1.5	0.068	1.2	0.068	1.2
unknown	$C_8H_{13}O_2^+$	0.33	87	11	0	1	0.025	0.56	0.025	0.42	0.025	0.44
unknown	$C_9H_{15}O_3^+$	NA	NA	NA	NA	NA	NA	NA	NA	NA	NA	NA
unknown	$C_{11}H_{19}^+$	NA	NA	NA	NA	NA	NA	NA	NA	NA	NA	NA
unknown	$C_{19}H_{35}^+$	NA	NA	NA	NA	NA	NA	NA	NA	NA	NA	NA
unknown	$C_{14}H_{25}^+$	0.49	85	7	0	8	0.014	0.31	0.014	0.24	0.014	0.25
unknown	$C_9H_{15}O_2^+$	0.39	91	8	1	0	0.034	0.76	0.034	0.58	0.034	0.6
unknown	$C_7H_{11}O^+$	0.41	83	8	4	5	0.087	1.9	0.087	1.5	0.087	1.5
unknown	$C_9H_{15}^+$	0.24	87	10	1	2	0.053	1.2	0.053	0.91	0.053	0.93
unknown	$C_{15}H_{27}^+$	0.32	94	3	0	3	0.013	0.28	0.013	0.21	0.013	0.22
unknown	$C_8H_{13}O^+$	0.27	93	5	0	2	0.084	1.9	0.083	1.4	0.083	1.5

unknown	$C_2HO_3^+$	NA	NA	NA	NA	NA	NA	NA	NA	NA	NA	NA
unknown	$C_{16}H_{29}^+$	0.26	96	4	0	0	0.014	0.31	0.014	0.24	0.014	0.25
unknown	$C_8H_{13}^+$	0.25	89	6	3	2	0.15	3.4	0.15	2.6	0.15	2.7
unknown	$C_{18}H_{33}^+$	0.25	99	1	0	0	0.0065	0.14	0.0064	0.11	0.0065	0.11
unknown	C_3HO^+	NA	NA	NA	NA	NA	NA	NA	NA	NA	NA	NA
unknown	$C_8H_{11}O^+$	0.3	86	10	1	3	0.035	0.79	0.035	0.6	0.035	0.62
unknown	$C_{11}H_{18}N^+$	NA	NA	NA	NA	NA	NA	NA	NA	NA	NA	NA
unknown	$C_5H_5O_3^+$	0.47	48	44	4	4	0.021	0.47	0.021	0.36	0.021	0.37
unknown	$C_4H_3O_2^+$	NA	NA	NA	NA	NA	NA	NA	NA	NA	NA	NA
unknown	$C_{11}H_{17}O_2^+$	NA	NA	NA	NA	NA	NA	NA	NA	NA	NA	NA
unknown	$C_9H_{13}O_3^+$	NA	NA	NA	NA	NA	NA	NA	NA	NA	NA	NA
unknown	$C_{10}H_{15}O_2^+$	0.36	84	15	0	1	0.013	0.29	0.013	0.22	0.013	0.23
unknown	$C_7H_9O_2^+$	0.37	75	16	2	6	0.039	0.87	0.039	0.66	0.039	0.68
unknown	$C_8H_{11}O_3^+$	NA	NA	NA	NA	NA	NA	NA	NA	NA	NA	NA
unknown	$C_{20}H_{35}^+$	NA	NA	NA	NA	NA	NA	NA	NA	NA	NA	NA
unknown	$C_{14}H_{23}O^+$	0.37	94	5	0	0	0.0063	0.14	0.0061	0.1	0.0062	0.11
unknown	$C_{10}H_{15}O^+$	1.1	76	12	2	10	0.054	1.2	0.055	0.94	0.055	0.97
unknown	$C_{19}H_{33}^+$	0.27	93	7	0	0	0.0088	0.2	0.0086	0.15	0.0087	0.15
unknown	$C_{13}H_{21}O^+$	NA	NA	NA	NA	NA	NA	NA	NA	NA	NA	NA
unknown	$C_9H_{11}O_3^+$	NA	NA	NA	NA	NA	NA	NA	NA	NA	NA	NA
unknown	$C_6H_5O_2^+$	NA	NA	NA	NA	NA	NA	NA	NA	NA	NA	NA
unknown	$C_{15}H_{23}O_3^+$	NA	NA	NA	NA	NA	NA	NA	NA	NA	NA	NA
unknown	$C_{11}H_{15}^+$	0.35	82	16	0	1	0.013	0.29	0.013	0.21	0.013	0.22
unknown	$C_{12}H_{17}O^+$	0.36	89	11	0	0	0.0061	0.14	0.006	0.1	0.0061	0.11
unknown	$C_9H_{11}O_2^+$	0.65	77	16	4	4	0.012	0.28	0.012	0.21	0.013	0.22
unknown	$C_9H_{11}^+$	0.28	83	15	1	1	0.053	1.2	0.052	0.9	0.053	0.93
unknown	$C_{20}H_{33}^+$	0.32	91	9	0	0	0.0056	0.13	0.0055	0.095	0.0055	0.097
unknown	$C_{16}H_{25}^+$	0.26	95	5	0	0	0.012	0.27	0.012	0.2	0.012	0.21
unknown	$C_9H_{11}O^+$	0.26	85	15	0	0	0.1	2.3	0.1	1.8	0.1	1.8
unknown	$C_{10}H_{13}O_2^+$	0.35	87	11	1	0	0.011	0.25	0.011	0.19	0.011	0.19
unknown	$C_{10}H_{13}^+$	0.26	86	13	1	0	0.042	0.93	0.041	0.71	0.042	0.73
unknown	$C_{10}H_{13}O^+$	0.42	88	6	4	2	0.05	1.1	0.049	0.84	0.05	0.88
unknown	$C_{14}H_{21}^+$	0.27	94	5	0	1	0.0099	0.22	0.0098	0.17	0.0099	0.17
unknown	$C_{19}H_{31}^+$	0.29	94	6	0	0	0.0086	0.19	0.0084	0.14	0.0085	0.15
unknown	$C_{18}H_{29}^+$	0.23	97	3	0	0	0.0097	0.22	0.0096	0.16	0.0096	0.17
unknown	$C_{15}H_{23}^+$	0.28	95	4	1	0	0.015	0.33	0.015	0.25	0.015	0.26
unknown	$C_{17}H_{27}^+$	0.23	98	2	0	0	0.011	0.24	0.011	0.18	0.011	0.19
unknown	$C_{14}H_{19}^+$	NA	NA	NA	NA	NA	NA	NA	NA	NA	NA	NA
unknown	$C_9H_{10}N^+$	NA	NA	NA	NA	NA	NA	NA	NA	NA	NA	NA
unknown	$C_{10}H_{11}O_2^+$	0.33	81	19	0	0	0.0055	0.12	0.0054	0.093	0.0055	0.096
unknown	$C_8H_7O_3^+$	0.49	78	19	1	2	0.0069	0.15	0.0069	0.12	0.0069	0.12
unknown	$C_7H_5O_2^+$	0.35	86	12	1	1	0.032	0.72	0.032	0.55	0.032	0.56
unknown	$C_8H_7O_2^+$	NA	NA	NA	NA	NA	NA	NA	NA	NA	NA	NA
unknown	$C_{11}H_{13}O^+$	NA	NA	NA	NA	NA	NA	NA	NA	NA	NA	NA
unknown	$C_{16}H_{23}^+$	0.32	89	11	0	0	0.0086	0.19	0.0085	0.14	0.0085	0.15
unknown	$C_{10}H_{11}O^+$	0.35	85	15	0	0	0.0075	0.17	0.0074	0.13	0.0075	0.13

unknown	$C_{20}H_{31}^+$	NA	NA	NA	NA	NA	NA	NA	NA	NA	NA	NA
unknown	$C_{15}H_{21}^+$	0.31	95	5	0	0	0.0096	0.21	0.0094	0.16	0.0095	0.17
unknown	$C_{18}H_{27}^+$	NA	NA	NA	NA	NA	NA	NA	NA	NA	NA	NA
unknown	$C_{19}H_{29}^+$	NA	NA	NA	NA	NA	NA	NA	NA	NA	NA	NA
unknown	$C_{17}H_{25}^+$	0.34	96	4	0	0	0.0053	0.12	0.0051	0.088	0.0052	0.091
unknown	$C_{10}H_9O_3^+$	NA	NA	NA	NA	NA	NA	NA	NA	NA	NA	NA
unknown	$C_8H_5O_3^+$	0.32	69	30	1	0	0.02	0.44	0.02	0.34	0.02	0.34
unknown	$C_8H_5O_2^+$	NA	NA	NA	NA	NA	NA	NA	NA	NA	NA	NA
unknown	$C_9H_7O_2^+$	0.5	76	16	7	1	0.006	0.13	0.0059	0.1	0.006	0.1
unknown	$C_{14}H_{17}^+$	0.33	88	12	0	0	0.011	0.23	0.01	0.18	0.01	0.18
unknown	$C_{13}H_{15}^+$	0.28	89	11	0	0	0.022	0.5	0.022	0.38	0.022	0.39
unknown	$C_{16}H_{21}^+$	NA	NA	NA	NA	NA	NA	NA	NA	NA	NA	NA
unknown	$C_{16}H_{19}^+$	NA	NA	NA	NA	NA	NA	NA	NA	NA	NA	NA
unknown	$C_{15}H_{17}^+$	NA	NA	NA	NA	NA	NA	NA	NA	NA	NA	NA
unknown	$C_{16}H_{17}^+$	NA	NA	NA	NA	NA	NA	NA	NA	NA	NA	NA
unknown	$C_{13}H_{11}O^+$	0.45	75	25	0	0	0.024	0.54	0.023	0.4	0.024	0.41

Table 4.7.3: Summary table of exposures during the H1 summer campaign. The mean concentration during occupancy (MC) is in units of ppb, the campaign average daily exposure (ADE) is in units of ppb-hour day^{-1}, and the relative contributions from continuous indoor sources (CIS), outdoor origin (OO), cooking (C), and other (O) are unitless (%). In rare cases, statistical noise generates a slight negative relative fraction for the background of outdoor origin. The relative standard deviation (RSD) indicates the variability in the indoor concentration time series. The heading 'all' refers to source apportionments and exposures for a hypothetical occupant who is present for the entirety of the measurement period.

				all						H2M1		H2F1	
Class	**Ion**	**Name**	**RSD**	**CIS %**	**OO %**	**C %**	**O %**	**MC ppb**	**ADE ppb h d-1**	**MC ppb**	**ADE ppb h d-1**	**MC ppb**	**ADE ppb h d-1**
alcohol + alkene	CH_5O^+	methanol	0.7	79	3	18	0	45	1100	50	780	50	750
alcohol + alkene	$C_2H_7O^+$	ethanol	3.4	34	0	61	4	630	15000	730	11000	640	9700
alcohol + alkene	$C_3H_7^+$	propanol fragment (-H_2O) + propene	1.6	50	6	20	25	4.7	110	4.6	73	4.5	68
alcohol + alkene	$C_4H_9^+$	butanol fragment (-H_2O) + butene	0.75	82	7	7	4	2.8	66	2.8	44	2.8	41
alcohol + alkene	$C_5H_{11}^+$	pentanol fragment (-H_2O) + pentene	1.5	74	5	19	3	1.3	30	1.4	21	1.3	19
alcohol + alkene	$C_6H_{13}^+$	hexanol fragment (-H_2O) + hexene	0.51	80	12	3	5	0.22	5.3	0.22	3.5	0.22	3.3
alcohol + alkene	$C_8H_{17}^+$	octanol fragment (-H_2O) + octene	0.59	84	6	6	3	0.031	0.74	0.032	0.5	0.032	0.48
aromatic	$C_6H_7^+$	benzene	0.36	50	41	7	2	0.31	7.4	0.33	5.2	0.33	5
aromatic	$C_7H_9^+$	toluene	0.38	83	10	4	2	1.3	30	1.3	21	1.3	20
aromatic	$C_8H_9^+$	styrene	0.3	87	11	2	0	0.16	3.8	0.17	2.6	0.17	2.5
aromatic	$C_8H_{11}^+$	xylene + ethyl benzene	0.28	65	29	4	2	0.33	7.8	0.34	5.3	0.34	5.1
aromatic	$C_6H_7O^+$	phenol	0.26	93	4	2	1	0.34	8.1	0.36	5.6	0.36	5.4
aromatic	$C_6H_7O_2^+$	benzene diol	0.87	69	12	14	5	0.091	2.1	0.1	1.6	0.1	1.5
aromatic	$C_7H_9O^+$	cresols	0.29	68	23	7	2	0.1	2.4	0.11	1.7	0.11	1.6
aromatic	$C_7H_7O^+$	benzaldehyde	0.2	93	6	1	0	0.32	7.7	0.33	5.2	0.33	5
aromatic	$C_4H_6N^+$	pyrrole	3.3	45	5	49	1	0.079	1.9	0.1	1.6	0.1	1.5
aromatic	$C_9H_{13}^+$	benzene (+3 sat. carbons) + isomers	0.49	51	31	14	5	0.16	3.9	0.18	2.8	0.18	2.7

aromatic	$C_{10}H_{15}^+$	benzene (+4 sat. carbons) + isomers	0.68	63	16	16	6	0.17	3.9	0.18	2.8	0.18	2.6
aromatic	$C_{11}H_{17}^+$	benzene (+5 sat. carbons) + isomers	NA	NA	NA	NA	NA	NA	NA	NA	NA	NA	NA
aromatic	$C_{13}H_{21}^+$	benzene (+7 sat. carbons) + isomers	0.26	93	6	0	1	0.021	0.48	0.021	0.33	0.021	0.32
aromatic	$C_{14}H_{23}^+$	benzene (+8 sat. carbons) + isomers	0.2	94	5	0	1	0.021	0.5	0.022	0.34	0.022	0.33
aromatic	$C_{16}H_{27}^+$	benzene (+10 sat. carbons) + isomers	0.16	96	4	0	0	0.027	0.64	0.028	0.43	0.028	0.41
aromatic	$C_{17}H_{29}^+$	benzene (+11 sat. carbons) + isomers	0.16	96	4	0	0	0.022	0.51	0.022	0.34	0.022	0.33
aromatic	$C_{18}H_{31}^+$	benzene (+12 sat. carbons) + isomers	0.17	94	6	0	0	0.018	0.43	0.018	0.29	0.018	0.28
aromatic	$C_7H_6NS^+$	benzothiazole	0.24	87	12	0	0	0.027	0.63	0.028	0.43	0.028	0.42
carbonyl (sat.)	$C_2H_5O^+$	acetaldehyde (C2)	3.4	51	3	19	27	24	560	28	440	26	390
carbonyl (sat.)	$C_3H_7O^+$	acetone + propanal (C3)	5.8	46	4	1	49	30	710	39	600	39	590
carbonyl (sat.)	$C_4H_9O^+$	C4 sat. carbonyl (methylethylketone + others)	0.97	73	12	15	1	1.3	31	1.5	23	1.5	22
carbonyl (sat.)	$C_5H_{11}O^+$	C5 sat. carbonyl (pentanone + others)	1	71	8	20	1	0.39	9.2	0.45	7	0.44	6.7
carbonyl (sat.)	$C_6H_{13}O^+$	C6 sat. carbonyl (hexanone + others)	0.31	89	8	3	0	0.21	4.9	0.21	3.3	0.21	3.2
carbonyl (sat.)	$C_7H_{15}O^+$	C7 sat. carbonyl	0.41	86	6	7	0	0.14	3.2	0.14	2.2	0.14	2.1
carbonyl (sat.)	$C_8H_{17}O^+$	C8 sat. carbonyl + 1-octen-3-ol	0.46	86	6	8	0	0.12	2.8	0.13	2	0.13	1.9
carbonyl (sat.)	$C_9H_{19}O^+$	C9 sat. carbonyl	0.32	93	2	4	0	0.33	7.9	0.35	5.4	0.35	5.2

carbonyl (sat.)	$C_{10}H_{21}O^+$	C10 sat. carbonyl	0.22	96	2	1	0	0.15	3.5	0.15	2.4	0.15	2.3
carbonyl (sat.)	$C_{11}H_{23}O^+$	C11 sat. carbonyl	0.22	93	5	2	1	0.04	0.94	0.041	0.64	0.041	0.62
carbonyl (sat.)	$C_{12}H_{25}O^+$	C12 sat. carbonyl	0.26	92	6	1	1	0.026	0.63	0.027	0.43	0.027	0.41
carbonyl (sat.)	$C_{14}H_{29}O^+$	C14 sat. carbonyl	NA	NA	NA	NA	NA	NA	NA	NA	NA	NA	NA
carbonyl (unsat.)	$C_3H_5O^+$	acrolein (C3 unsat. carbonyl)	0.9	71	7	22	1	0.36	8.4	0.39	6.1	0.39	5.8
carbonyl (unsat.)	$C_4H_7O^+$	unsat. carbonyl (C4)	0.5	82	9	10	0	0.55	13	0.58	9.1	0.58	8.7
carbonyl (unsat.)	$C_5H_9O^+$	unsat. carbonyl (C5) + cyclopentanone	0.39	84	9	7	0	0.22	5.1	0.23	3.6	0.23	3.4
carbonyl (unsat.)	$C_6H_{11}O^+$	unsat. carbonyl (C6) + cis-3-hexenal + isomers	0.27	93	5	2	0	0.34	8.1	0.35	5.5	0.35	5.3
carbonyl (unsat.)	$C_7H_{13}O^+$	unsat. carbonyl (C7) + isomers	0.65	81	9	9	0	0.083	2	0.09	1.4	0.089	1.3
carbonyl (unsat.)	$C_8H_{15}O^+$	unsat. carbonyl (C8) + oct-1-en-3-one + isomers	0.3	92	5	2	1	0.17	4	0.18	2.7	0.18	2.6
carbonyl (unsat.)	$C_9H_{17}O^+$	unsat. carbonyl (C9) + isomers	0.41	86	7	7	0	0.068	1.6	0.071	1.1	0.071	1.1
carboxylic acid	$CH_3O_2^+$	formic acid (C1) + isomers	0.25	89	7	4	0	12	280	12	190	12	180
carboxylic acid	$C_2H_5O_2^+$	acetic acid (C2) + isomers	0.23	95	3	3	0	52	1200	54	840	54	810
carboxylic acid	$C_3H_7O_2^+$	propionic acid (C3) + isomers	1.3	82	6	3	9	3.9	92	3.7	59	3.8	56
carboxylic acid	$C_4H_9O_2^+$	butryic acid (C4) + isomers	0.87	77	3	18	1	2.1	49	2.4	37	2.3	35
carboxylic acid	$C_5H_{11}O_2^+$	valeric acid (C5) + isomers	0.48	92	7	1	0	0.33	7.9	0.35	5.4	0.35	5.2
carboxylic acid	$C_6H_{13}O_2^+$	caproic acid (C6) + isomers	0.28	95	4	2	0	0.43	10	0.45	7.1	0.46	6.8
carboxylic acid	$C_7H_{15}O_2^+$	enanthic acid (C7) + isomers	0.33	92	4	2	2	0.084	2	0.087	1.4	0.087	1.3
carboxylic acid	$C_8H_{17}O_2^+$	caprylic acid (C8) + isomers	0.31	94	4	1	0	0.13	3.2	0.14	2.2	0.14	2.1

carboxylic acid	$C_9H_{19}O_2^+$	pelargonic acid (C9) + isomers	0.31	93	6	1	0	0.058	1.4	0.06	0.94	0.06	0.91
carboxylic acid	$C_{10}H_{21}O_2^+$	decanoic acid (C10) + isomers	0.47	95	4	1	0	0.04	0.94	0.042	0.66	0.043	0.65
carboxylic acid	$C_{11}H_{23}O_2^+$	undecylic acid (C11) + isomers	NA	NA	NA	NA	NA	NA	NA	NA	NA	NA	NA
furanoid	$C_6H_9O^+$	dimethyl furan	NA	NA	NA	NA	NA	NA	NA	NA	NA	NA	NA
furanoid	$C_5H_7O_2^+$	fufuranol	0.66	73	16	11	0	0.085	2	0.091	1.4	0.092	1.4
furanoid	$C_4H_5O^+$	furan	0.51	62	14	12	12	0.15	3.5	0.17	2.6	0.16	2.5
furanoid	$C_4H_5O_2^+$	furanone	0.35	81	13	6	0	0.13	3.1	0.14	2.1	0.14	2.1
furanoid	$C_5H_7O^+$	methyl furan + pyran	0.62	53	10	11	26	0.24	5.7	0.26	4.1	0.26	3.9
furanoid	$C_5H_5O_2^+$	furfural	0.41	87	9	4	0	1.2	28	1.2	19	1.2	19
furanoid	$C_7H_9O_3^+$	methoxymethylfurfural	0.33	78	16	3	3	0.0099	0.23	0.01	0.16	0.01	0.16
furanoid	$C_6H_5O_3^+$	furandicarbaldehyde	1.4	36	49	14	0	0.016	0.39	0.018	0.28	0.018	0.27
halogen	CCl_3^+	chloroform	0.071	4	95	0	1	0.14	3.2	0.13	2.1	0.13	2
halogen	$H_2NCl_2^+$	dichloramine	7.7	30	8	22	40	0.004	0.094	0.0034	0.053	0.0022	0.034
halogen	$C_6H_5Cl_2^+$	dichlorobenzene	0.22	59	39	2	0	0.01	0.25	0.011	0.16	0.01	0.16
halogen	$C_7H_4ClF_2^+$	parachlorobenzotrifluoride	0.76	31	69	0	0	0.032	0.76	0.032	0.51	0.032	0.48
halogen	CCl_2F^+		NA	NA	NA	NA	NA	NA	NA	NA	NA	NA	NA
halogen	$CHCl_2^+$		0.62	55	11	23	11	0.095	2.2	0.1	1.6	0.1	1.5
halogen	CHF_2^+		0.39	88	7	5	1	0.11	2.5	0.11	1.7	0.11	1.6
halogen	$C_2H_3Cl_2^+$		NA	NA	NA	NA	NA	NA	NA	NA	NA	NA	NA
halogen	$C_2H_3ClF^+$		NA	NA	NA	NA	NA	NA	NA	NA	NA	NA	NA
halogen	$C_2H_4OCl^+$		NA	NA	NA	NA	NA	NA	NA	NA	NA	NA	NA
halogen	$C_2H_5NCl^+$		1.4	76	6	2	16	0.0078	0.18	0.0074	0.12	0.0073	0.11
halogen	$C_3H_6OCl^+$		NA	NA	NA	NA	NA	NA	NA	NA	NA	NA	NA
nitrile	$C_2H_4N^+$	acetonitrile	0.36	29	62	7	3	0.14	3.2	0.14	2.2	0.14	2.1
nitrile	$C_3H_4N^+$	acrylonitrile	0.25	85	12	3	0	0.034	0.81	0.035	0.55	0.035	0.53
organosulfurs	CH_5S^+	methanethiol	2.4	39	4	56	1	0.21	4.9	0.26	4	0.25	3.8
organosulfurs	$C_2H_7S^+$	ethanethiol + DMS	0.93	16	73	11	0	1.1	26	1.1	17	1	15
organosulfurs	$C_2H_5OS^+$	mercaptoacetaldehyde	NA	NA	NA	NA	NA	NA	NA	NA	NA	NA	NA
organosulfurs	$CH_5O_3S^+$	methane sulfonic acid	0.5	85	8	7	0	0.065	1.5	0.069	1.1	0.069	1
organosulfurs	$C_2H_7S_2^+$	dimethyl sulfide	2.3	57	2	41	0	0.099	2.3	0.12	1.9	0.12	1.8
organosulfurs	C2H7O2S+	dimethyl sulfone	0.4	93	2	5	0	0.19	4.5	0.2	3.2	0.21	3.1
organosulfurs	$C_3H_5S_2^+$		1.4	67	1	31	0	0.011	0.26	0.013	0.2	0.013	0.19
organosulfurs	$C_4H_6NS^+$		1.9	53	4	38	5	0.025	0.6	0.027	0.42	0.028	0.43
organosulfurs	$C_5H_{11}S^+$		0.52	79	19	0	2	0.18	4.2	0.17	2.7	0.17	2.5
organosulfurs	$C_7H_5OS^+$		NA	NA	NA	NA	NA	NA	NA	NA	NA	NA	NA
organosulfurs	$C_9H_9S^+$		0.65	79	13	4	5	0.015	0.36	0.016	0.24	0.016	0.23

outdoor tance	impor-	$C_2H_3O_2^+$	glyoxal	NA	NA	NA	NA	NA	NA	NA	NA	NA	NA	NA
outdoor tance	impor-	$C_5H_9^+$	isoprene	0.54	75	5	17	4	1.7	40	1.9	30	1.9	28
outdoor tance	impor-	$C_{10}H_{19}O^+$	monoterpene alcohols	0.5	84	4	8	4	0.14	3.4	0.16	2.5	0.16	2.4
outdoor tance	impor-	$C_{10}H_{17}^+$	monoterpenes	1.2	54	2	23	21	17	390	19	300	20	310
outdoor tance	impor-	$C_{10}H_{17}O_2^+$	pinonaldehyde + isomers	0.37	79	17	4	0	0.018	0.42	0.019	0.29	0.019	0.28
outdoor tance	impor-	$C_{15}H_{25}^+$	sesquiterpenes + isomers	0.3	91	5	3	1	0.15	3.6	0.16	2.5	0.16	2.4
possible ment	frag-	$C_2H_3^+$	alkyl fragment or acetylene	1.6	45	4	33	18	0.36	8.6	0.39	6	0.36	5.5
possible ment	frag-	$C_2H_4^+$	alkyl fragment	0.73	73	13	14	0	0.17	4.1	0.18	2.7	0.17	2.6
possible ment	frag-	$C_3H_5^+$	alkyl fragment	1.3	52	5	30	13	1.7	40	1.8	28	1.7	25
possible ment	frag-	$C_4H_5^+$	alkyl fragment	0.58	66	15	15	4	0.024	0.58	0.027	0.43	0.028	0.42
possible ment	frag-	$C_4H_7^+$	alkyl fragment	0.39	82	11	4	2	2.1	49	2.1	33	2.1	31
possible ment	frag-	$C_5H_7^+$	alkyl fragment	NA	NA	NA	NA	NA	NA	NA	NA	NA	NA	NA
possible ment	frag-	$C_5H_5O^+$	fragment of furanoid compound	0.74	53	26	14	7	0.58	14	0.63	9.8	0.64	9.5
possible ment	frag-	$C_6H_5^+$	aromatic fragment	0.57	77	12	10	1	0.037	0.88	0.039	0.61	0.039	0.59
possible ment	frag-	$C_6H_5O^+$	aromatic fragment	0.27	98	2	0	0	0.58	14	0.6	9.4	0.61	9.1
possible ment	frag-	$C_3H_6^+$	alkyl fragment	1.5	33	10	33	24	0.32	7.6	0.23	3.5	0.23	3.4
siloxane		C2H7O2Si+	dimethoxysilane	2.8	54	3	44	0	0.077	1.8	0.093	1.5	0.09	1.3
siloxane		C6H19O3Si3+	D3 siloxane	0.41	91	2	3	4	0.086	2	0.086	1.3	0.087	1.3
siloxane		C8H25O4Si4+	D4 siloxane	2.4	72	4	20	4	0.45	11	0.39	6.1	0.39	5.8
siloxane		C10H31O5Si5+	D5 siloxane	1.4	46	1	24	30	12	290	11	180	9.8	150
siloxane		C12H37O6Si6+	D6 siloxane	0.64	80	3	11	7	0.052	1.2	0.053	0.83	0.051	0.77
siloxane		C10H31O3Si4+	L4 siloxane	2.6	42	1	42	14	0.031	0.73	0.029	0.46	0.03	0.46
siloxane		C12H37O4Si5+	L5 siloxane	1.1	62	0	20	18	0.024	0.56	0.025	0.39	0.025	0.37
siloxane		C15H39O2Si3+	caprylyl trisiloxane	0.45	96	1	1	1	0.0057	0.14	0.0056	0.088	0.0057	0.086
siloxane		C7H21O3Si3+		3.5	40	3	6	51	0.021	0.5	0.02	0.31	0.022	0.32
uncategorized		$C_6H_{15}O_2^+$	2-butoxyethanol + isomers	0.74	76	8	9	7	0.05	1.2	0.053	0.83	0.053	0.8

uncategorized	$C_2H_5O_3^+$	glycolic acid + isomers	0.25	89	8	2	1	0.057	1.3	0.059	0.91	0.059	0.88
uncategorized	$C_3H_5O_2^+$	acrylic acid + isomers	0.58	75	15	10	0	0.27	6.4	0.29	4.5	0.29	4.4
uncategorized	$C_6H_{11}^+$	cis-3-hexen-1-ol + isomers	0.26	93	4	3	1	1.5	35	1.6	24	1.6	23
uncategorized	$C_4H_7O_2^+$	diacetyl + isomers	0.4	85	8	6	0	0.59	14	0.62	9.7	0.62	9.4
uncategorized	$C_9H_{17}^+$	hydrindane + isomers	0.27	92	5	3	1	0.17	4	0.17	2.7	0.17	2.6
uncategorized	$C_5H_9O_2^+$	acetylpropionyl + glutaraldehyde + isomers	0.36	86	9	4	0	0.31	7.3	0.32	5	0.32	4.8
uncategorized	$C_4H_7O_3^+$	acetate anhydrate**	0.25	88	10	1	1	0.2	4.7	0.2	3.1	0.2	3
uncategorized	$C_8H_{15}^+$	1-octen-3-ol fragment (-H_2O) + isomers	0.37	87	7	5	1	0.27	6.3	0.28	4.4	0.28	4.2
uncategorized	$C_{10}H_{17}O^+$	citral + others	0.53	75	11	10	3	0.23	5.4	0.24	3.8	0.24	3.6
uncategorized	$C_6H_9O_4^+$	3-deoxyglucosone**	2.4	66	11	23	0	0.011	0.27	0.013	0.21	0.014	0.2
uncategorized	$C_4H_5O_3^+$		0.63	50	43	7	0	0.026	0.61	0.027	0.42	0.026	0.39
uncategorized	$C_{15}H_{27}N_2^+$	sparteine**	0.32	92	5	1	2	0.028	0.67	0.029	0.46	0.03	0.44
uncategorized	$C_4H_3O_3^+$		0.8	38	55	7	0	0.015	0.36	0.016	0.25	0.016	0.24
uncategorized	$C_8H_9O^+$		0.39	86	8	5	0	0.14	3.2	0.14	2.2	0.14	2.2
uncategorized	$C_{14}H_{21}O_2^+$	chromanol + isomers	0.4	90	4	1	5	0.03	0.72	0.031	0.48	0.031	0.47
uncategorized	$C_8H_9O_2^+$	4-anisaldehyde + isomers	NA	NA	NA	NA	NA	NA	NA	NA	NA	NA	NA
uncategorized	$C_7H_7^+$	1,3,5-norcaratriene or aromatic fragment	0.25	93	4	2	1	0.32	7.6	0.33	5.2	0.33	5
uncategorized	$C_9H_9O^+$	cinnamaldehyde + isomers	1	60	9	16	15	0.11	2.7	0.13	2	0.13	2
unknown	$C_8H_{19}O_3^+$		0.27	93	5	0	1	0.018	0.42	0.018	0.29	0.018	0.28
unknown	$C_{12}H_{25}O_2^+$		0.35	95	5	0	0	0.02	0.47	0.021	0.32	0.021	0.32
unknown	$C_5H_{11}O_5^+$		0.67	72	12	14	1	0.018	0.43	0.019	0.3	0.019	0.29
unknown	$C_7H_{15}O_5^+$		0.26	66	33	1	0	0.0079	0.19	0.0081	0.13	0.0081	0.12
unknown	$C_{14}H_{29}^+$		0.26	94	5	0	1	0.0084	0.2	0.0087	0.14	0.0087	0.13
unknown	$C_{15}H_{31}^+$		0.29	95	4	0	1	0.0082	0.19	0.0083	0.13	0.0083	0.13
unknown	$C_3H_7O_3^+$		NA	NA	NA	NA	NA	NA	NA	NA	NA	NA	NA
unknown	$C_{16}H_{33}^+$		0.19	96	3	0	0	0.0083	0.2	0.0085	0.13	0.0086	0.13
unknown	$C_{17}H_{35}^+$		0.21	93	7	0	0	0.0062	0.15	0.0063	0.098	0.0063	0.094
unknown	$C_{12}H_{23}^+$		0.48	86	9	3	3	0.011	0.25	0.011	0.17	0.011	0.17

unknown	$C_{13}H_{25}^+$	0.67	88	6	2	4	0.0058	0.14	0.0061	0.095	0.0061	0.091
unknown	$C_{14}H_{27}^+$	0.24	97	3	0	0	0.0067	0.16	0.0069	0.11	0.0069	0.1
unknown	$C_{10}H_{19}O_2^+$	0.27	85	13	1	1	0.019	0.45	0.02	0.31	0.02	0.3
unknown	C3H8N3O2+	0.44	80	11	8	1	0.007	0.16	0.0074	0.12	0.0074	0.11
unknown	$C_2H_3O_4^+$	NA	NA	NA	NA	NA	NA	NA	NA	NA	NA	NA
unknown	$C_4H_7O_4^+$	NA	NA	NA	NA	NA	NA	NA	NA	NA	NA	NA
unknown	$C_{12}H_{23}O^+$	0.25	95	5	0	0	0.023	0.54	0.022	0.35	0.023	0.34
unknown	$C_7H_{13}O_2^+$	0.31	77	20	3	0	0.058	1.4	0.06	0.93	0.06	0.9
unknown	$C_6H_{11}O_3^+$	0.33	83	13	3	1	0.023	0.54	0.024	0.38	0.024	0.36
unknown	$C_{11}H_{21}O^+$	1.1	73	10	17	0	0.023	0.54	0.025	0.4	0.025	0.37
unknown	$C_5H_9O_3^+$	NA	NA	NA	NA	NA	NA	NA	NA	NA	NA	NA
unknown	$C_6H_{11}O_2^+$	0.31	84	12	4	0	0.13	3	0.13	2.1	0.13	2
unknown	$C_{12}H_{23}O_2^+$	0.32	88	12	0	0	0.028	0.65	0.028	0.44	0.029	0.43
unknown	$C_{18}H_{35}^+$	NA	NA	NA	NA	NA	NA	NA	NA	NA	NA	NA
unknown	$C_9H_{17}O_2^+$	0.28	87	10	3	1	0.045	1.1	0.047	0.73	0.047	0.7
unknown	$C_3H_5O_3^+$	NA	NA	NA	NA	NA	NA	NA	NA	NA	NA	NA
unknown	$C_{10}H_{19}^+$	0.33	86	5	5	4	0.12	2.8	0.12	1.9	0.13	1.9
unknown	$C_{15}H_{29}^+$	0.2	97	3	0	0	0.0086	0.2	0.0088	0.14	0.0088	0.13
unknown	$C_8H_{15}O_2^+$	0.27	87	9	3	0	0.1	2.4	0.11	1.7	0.11	1.6
unknown	$C_{10}H_{19}O_3^+$	NA	NA	NA	NA	NA	NA	NA	NA	NA	NA	NA
unknown	$C_7H_{13}^+$	0.36	87	7	5	1	0.36	8.6	0.38	6	0.38	5.7
unknown	$C_{16}H_{31}^+$	0.19	98	2	0	0	0.008	0.19	0.0082	0.13	0.0082	0.12
unknown	$C_{17}H_{33}^+$	0.2	96	4	0	0	0.0071	0.17	0.0073	0.11	0.0073	0.11
unknown	$C_2H_3O_3^+$	NA	NA	NA	NA	NA	NA	NA	NA	NA	NA	NA
unknown	$C_{12}H_{21}O_2^+$	0.3	89	10	0	0	0.0065	0.15	0.0066	0.1	0.0067	0.1
unknown	$C_{10}H_{18}N^+$	0.65	73	9	10	8	0.022	0.52	0.024	0.37	0.023	0.35
unknown	$C_6H_9O_3^+$	0.4	73	22	5	0	0.037	0.86	0.038	0.59	0.038	0.57
unknown	$C_8H_{13}O_4^+$	NA	NA	NA	NA	NA	NA	NA	NA	NA	NA	NA
unknown	$C_7H_{11}O_3^+$	NA	NA	NA	NA	NA	NA	NA	NA	NA	NA	NA
unknown	$C_{13}H_{23}^+$	0.58	87	10	0	3	0.022	0.53	0.023	0.36	0.023	0.35
unknown	$C_7H_{11}O_2^+$	0.35	83	12	4	0	0.047	1.1	0.049	0.76	0.049	0.73
unknown	$C_9H_{15}O^+$	0.33	83	11	4	2	0.12	2.8	0.12	1.9	0.12	1.8
unknown	$C_{12}H_{21}^+$	0.91	84	10	0	6	0.026	0.61	0.027	0.43	0.027	0.4
unknown	$C_8H_{13}O_3^+$	NA	NA	NA	NA	NA	NA	NA	NA	NA	NA	NA
unknown	$C_{13}H_{23}O^+$	0.31	95	4	1	0	0.0057	0.13	0.006	0.093	0.006	0.09
unknown	$C_6H_9O_2^+$	0.35	81	14	5	0	0.063	1.5	0.067	1	0.067	1
unknown	$C_8H_{13}O_2^+$	0.3	85	12	3	0	0.026	0.6	0.027	0.42	0.027	0.4
unknown	$C_9H_{15}O_3^+$	0.42	85	11	0	4	0.015	0.36	0.015	0.24	0.015	0.23
unknown	$C_{11}H_{19}^+$	NA	NA	NA	NA	NA	NA	NA	NA	NA	NA	NA
unknown	$C_{19}H_{35}^+$	0.24	88	12	0	0	0.0063	0.15	0.0064	0.1	0.0065	0.097
unknown	$C_{14}H_{25}^+$	0.23	94	5	0	1	0.025	0.58	0.025	0.4	0.025	0.38
unknown	$C_9H_{15}O_2^+$	0.31	84	12	4	0	0.035	0.83	0.037	0.58	0.037	0.56
unknown	$C_7H_{11}O^+$	0.47	78	9	10	2	0.11	2.6	0.11	1.8	0.11	1.7
unknown	$C_9H_{15}^+$	0.32	84	11	4	1	0.078	1.8	0.082	1.3	0.082	1.2
unknown	$C_{15}H_{27}^+$	0.19	97	3	0	1	0.022	0.52	0.023	0.35	0.023	0.34
unknown	$C_8H_{13}O^+$	0.27	89	8	3	0	0.084	2	0.088	1.4	0.088	1.3

unknown	$C_2HO_3^+$	NA	NA	NA	NA	NA	NA	NA	NA	NA	NA	NA
unknown	$C_{16}H_{29}^+$	0.2	96	3	0	1	0.022	0.52	0.022	0.35	0.023	0.34
unknown	$C_8H_{13}^+$	0.31	86	8	4	2	0.2	4.7	0.2	3.2	0.2	3.1
unknown	$C_{18}H_{33}^+$	0.18	95	5	0	0	0.0095	0.22	0.0097	0.15	0.0098	0.15
unknown	C_3HO^+	1.1	67	5	23	5	0.013	0.32	0.014	0.23	0.015	0.22
unknown	$C_8H_{11}O^+$	0.29	82	13	3	1	0.025	0.59	0.026	0.41	0.026	0.39
unknown	$C_{11}H_{18}N^+$	3	64	1	7	28	0.0087	0.2	0.0081	0.13	0.008	0.12
unknown	$C_5H_5O_3^+$	0.89	45	44	11	0	0.019	0.46	0.021	0.32	0.021	0.31
unknown	$C_4H_3O_2^+$	NA	NA	NA	NA	NA	NA	NA	NA	NA	NA	NA
unknown	$C_{11}H_{17}O_2^+$	NA	NA	NA	NA	NA	NA	NA	NA	NA	NA	NA
unknown	$C_9H_{13}O_3^+$	NA	NA	NA	NA	NA	NA	NA	NA	NA	NA	NA
unknown	$C_{10}H_{15}O_2^+$	0.34	79	17	3	1	0.014	0.33	0.015	0.23	0.015	0.22
unknown	$C_7H_9O_2^+$	0.36	70	25	4	1	0.034	0.8	0.035	0.55	0.035	0.53
unknown	$C_8H_{11}O_3^+$	NA	NA	NA	NA	NA	NA	NA	NA	NA	NA	NA
unknown	$C_{20}H_{35}^+$	0.29	82	18	0	0	0.0057	0.13	0.0058	0.09	0.0058	0.087
unknown	$C_{14}H_{23}O^+$	0.34	93	4	1	2	0.016	0.38	0.017	0.26	0.017	0.25
unknown	$C_{10}H_{15}O^+$	0.31	56	37	5	1	0.14	3.4	0.15	2.4	0.15	2.3
unknown	$C_{19}H_{33}^+$	0.19	88	12	0	0	0.012	0.29	0.013	0.2	0.013	0.19
unknown	$C_{13}H_{21}O^+$	NA	NA	NA	NA	NA	NA	NA	NA	NA	NA	NA
unknown	$C_9H_{11}O_3^+$	0.54	80	17	0	4	0.0083	0.2	0.0082	0.13	0.0081	0.12
unknown	$C_6H_5O_2^+$	0.39	78	18	3	0	0.039	0.91	0.041	0.64	0.041	0.61
unknown	$C_{15}H_{23}O_3^+$	NA	NA	NA	NA	NA	NA	NA	NA	NA	NA	NA
unknown	$C_{11}H_{15}^+$	0.26	82	14	2	1	0.015	0.35	0.015	0.23	0.015	0.23
unknown	$C_{12}H_{17}O^+$	NA	NA	NA	NA	NA	NA	NA	NA	NA	NA	NA
unknown	$C_9H_{11}O_2^+$	NA	NA	NA	NA	NA	NA	NA	NA	NA	NA	NA
unknown	$C_9H_{11}^+$	1.3	72	11	16	1	0.072	1.7	0.075	1.2	0.071	1.1
unknown	$C_{20}H_{33}^+$	0.25	83	17	0	0	0.0072	0.17	0.0073	0.11	0.0074	0.11
unknown	$C_{16}H_{25}^+$	0.21	94	6	0	0	0.016	0.38	0.017	0.26	0.017	0.25
unknown	$C_9H_{11}O^+$	0.26	84	13	3	1	0.068	1.6	0.07	1.1	0.071	1.1
unknown	$C_{10}H_{13}O_2^+$	0.36	91	4	2	2	0.017	0.4	0.018	0.28	0.018	0.27
unknown	$C_{10}H_{13}^+$	0.44	79	9	7	5	0.081	1.9	0.086	1.3	0.087	1.3
unknown	$C_{10}H_{13}O^+$	0.84	97	3	-3	2	0.095	2.2	0.097	1.5	0.098	1.5
unknown	$C_{14}H_{21}^+$	0.21	93	6	0	1	0.013	0.31	0.014	0.21	0.014	0.21
unknown	$C_{19}H_{31}^+$	0.22	87	13	0	0	0.012	0.29	0.012	0.19	0.013	0.19
unknown	$C_{18}H_{29}^+$	0.17	94	6	0	0	0.015	0.35	0.015	0.24	0.015	0.23
unknown	$C_{15}H_{23}^+$	0.19	93	6	1	0	0.021	0.49	0.021	0.33	0.021	0.32
unknown	$C_{17}H_{27}^+$	0.16	96	4	0	0	0.016	0.38	0.017	0.26	0.017	0.25
unknown	$C_{14}H_{19}^+$	0.2	97	3	0	0	0.011	0.26	0.011	0.18	0.011	0.17
unknown	$C_9H_{10}N^+$	3.4	63	6	31	0	0.0079	0.19	0.0092	0.14	0.0097	0.14
unknown	$C_{10}H_{11}O_2^+$	NA	NA	NA	NA	NA	NA	NA	NA	NA	NA	NA
unknown	$C_8H_7O_3^+$	NA	NA	NA	NA	NA	NA	NA	NA	NA	NA	NA
unknown	$C_7H_5O_2^+$	0.39	84	9	7	0	0.033	0.78	0.034	0.54	0.034	0.51
unknown	$C_8H_7O_2^+$	NA	NA	NA	NA	NA	NA	NA	NA	NA	NA	NA
unknown	$C_{11}H_{13}O^+$	0.34	80	18	1	1	0.0072	0.17	0.0074	0.12	0.0074	0.11
unknown	$C_{16}H_{23}^+$	0.23	86	14	0	0	0.011	0.27	0.012	0.18	0.012	0.18
unknown	$C_{10}H_{11}O^+$	0.36	86	8	4	1	0.0091	0.22	0.0096	0.15	0.0096	0.14

unknown	$C_{20}H_{31}^+$	NA	NA	NA	NA	NA	NA	NA	NA	NA	NA	NA
unknown	$C_{15}H_{21}^+$	NA	NA	NA	NA	NA	NA	NA	NA	NA	NA	NA
unknown	$C_{18}H_{27}^+$	0.25	91	9	0	0	0.0061	0.14	0.0062	0.097	0.0063	0.094
unknown	$C_{19}H_{29}^+$	NA	NA	NA	NA	NA	NA	NA	NA	NA	NA	NA
unknown	$C_{17}H_{25}^+$	0.22	95	5	0	0	0.0078	0.18	0.0079	0.12	0.008	0.12
unknown	$C_{10}H_9O_3^+$	0.33	78	22	0	0	0.0054	0.13	0.0055	0.086	0.0056	0.084
unknown	$C_8H_5O_3^+$	NA	NA	NA	NA	NA	NA	NA	NA	NA	NA	NA
unknown	$C_8H_5O_2^+$	NA	NA	NA	NA	NA	NA	NA	NA	NA	NA	NA
unknown	$C_9H_7O_2^+$	1.1	68	8	24	0	0.013	0.31	0.014	0.22	0.014	0.21
unknown	$C_{14}H_{17}^+$	0.26	85	13	1	0	0.012	0.28	0.012	0.19	0.012	0.19
unknown	$C_{13}H_{15}^+$	NA	NA	NA	NA	NA	NA	NA	NA	NA	NA	NA
unknown	$C_{16}H_{21}^+$	0.23	94	6	0	0	0.0064	0.15	0.0065	0.1	0.0066	0.099
unknown	$C_{16}H_{19}^+$	0.3	89	11	1	0	0.0055	0.13	0.0057	0.089	0.0057	0.086
unknown	$C_{15}H_{17}^+$	NA	NA	NA	NA	NA	NA	NA	NA	NA	NA	NA
unknown	$C_{16}H_{17}^+$	0.29	92	8	0	0	0.0066	0.16	0.0068	0.11	0.0069	0.1
unknown	$C_{13}H_{11}O^+$	0.29	73	27	0	0	0.021	0.5	0.022	0.34	0.022	0.33

Table 4.7.4: Acute hazard assessment of select VOCs. Indoor concentrations are presented as time averages of measured living space concentrations for the periods that individual occupants are indoors at home.[a]

		Health guideline (ppb)		Max concentration (ppb)			Number of events exceeding a health guideline		
Ion formula	**Name**	**OEHHA REL**	**ATSDR MRL**	**H1 summer**	**H1 winter**	**H2 winter**	**H1 summer**	**H1 winter**	**H2 winter**
$C_3H_7O^+$	acetone		26000	61	23	4600	0	0	0
$C_2H_5O^+$	acetaldehyde	260		180	160	2400	0	0	3
$C_3H_5O^+$	acrolein	1.1	3	22	2.7	7.9	10	2	12
$C_3H_4N^+$	acrylonitrile		100	0.23	0.053	0.12	0	0	0
$C_3H_5O_2^+$	acrylic acid	2000		12	5.6	3.1	0	0	0
$C_6H_7^+$	benzene	8.5	9	2.9	2.2	1.5	0	0	0
CCl_3^+	chloroform	31	100	0.28	0.17	0.27	0	0	0
$C_6H_{15}O_2^+$	2-butoxyethanol	970	6000			0.39	NA	NA	0
$C_6H_5Cl_2^+$	1,4 dichlorobenzene		2000	0.055	0.034	0.055	0	0	0
CH_5O^+	methanol	21000		170	83	450	0	0	0
$C_4H_9O^+$	methyl ethyl ketone	4400		21	6.3	26	0	0	0
$C_6H_7O^+$	phenol	1500		1.7	1.5	1.1	0	0	0
$C_8H_9^+$	styrene	4900		0.9	0.29	1.3	0	0	0
$C_7H_9^+$	toluene	1300	2000	3.3	2.8	10.1	0	0	0
$C_8H_{11}^+$	xylene	5100	2000	1.6	0.75	1.2	0	0	0

[a] Reference exposure levels (OEHHA)[4] and minimal risk levels (ATSDR)[5] are presented for acute VOC exposures. OEHHA defines acute exposure levels using a 1-h averaging time. ATSDR defines acute exposures using a 1–14 day averaging time. OEHHA values were converted from mass per volume concentrations to mixing ratios by applying the ideal gas law and assuming standard conditions (298 K, 1 atm). All concentrations are reported in ppb.

4.7.5 Supporting Information References

[1] Liu, Y.; Misztal, P. K.; Xiong, J.; Tian, Y.; Arata, C.; Nazaroff, W. W.; Goldstein, A. H. Detailed investigation of ventilation rates and airflow patterns in a northern California residence. *Indoor Air* **2018**, *28*, 572–584.

[2] Liu, Y.; Misztal, P. K.; Xiong, J.; Tian, Y.; Arata, C.; Weber, R. J.; Nazaroff, W. W.; Goldstein, A. H. Characterizing sources and emissions of volatile organic compounds in a northern California residence using space- and time-resolved measurements. *Indoor Air* **2019**, *29*, 630–644.

[3] Cappellin, L.; Karl, T.; Probst, M.; Ismailova, O.; Winkler, P. M.; Soukoulis, C.; Aprea, E.; Märk, T. D.; Gasperi, F.; Biasioli, F. On Quantitative Determination of Volatile Organic Compound Concentrations Using Proton Transfer Reaction Time-of-Flight Mass Spectrometry. *Environ. Sci. Technol.* **2012**, *46*, 2283–2290.

[4] CalEPA, Office of Environmental Health Hazard Assessment (OEHHA). OEHHA Acute, 8-hour and Chronic Reference Exposure Level (REL) Summary. OEHHA, 2019. https://oehha.ca.gov/air/general-info/oehha-acute-8-hour-and-chronic-reference-exposure-level-rel-summary (accessed 2020-06).

[5] Agency for Toxic Substances and Disease Registry (ATSDR). MINIMAL RISK LEVELS (MRLS). ATSDR, 2020. https://www.atsdr.cdc.gov/mrls/pdfs/ATSDR%20MRLs%20-%20May%202020%20-%20H.pdf (accessed 2020-06).

Chapter 5

Intake Fractions for Volatile Organic Compounds in Two Occupied California Residences

This chapter is adapted from:

Lunderberg, D.M.; Liu, Y.; Misztal, P.K.; Arata, C.; Tian, Y.; Kristensen, K.; Nazaroff, W.W.; Goldstein, A.H. Intake Fractions for Volatile Organic Compounds in Two Occupied California Residences. *Environ. Sci. Technol. Lett.* **2021**, *8*, 386–391.

5.1 Abstract

Experimental estimates of residential intake fractions for indoor volatile organic compound (VOC) releases are scarce. We evaluated individual intake fractions (iF_i, mass inhaled by an individual per unit mass emitted) using $\sim$ five months of time-resolved VOC measurements acquired at two residences. First, we directly estimated iF_i using inert tracer gases that were released at fixed rates. Tracer gas iF_i values were generally consistent between occupants and comparable across seasons. Furthermore, iF_i for sources released on different floors of a residence were statistically indistinguishable, suggesting that source location within the living space was not strongly influential. Emissions from living space sources ($iF_i \sim 0.3\%$ = 3000 ppm) contributed to occupant exposures at rates 2–4 times higher than crawl space sources ($iF_i \sim 1000$ ppm) and >40 times higher than attic sources ($iF_i < \sim$70 ppm). Second, we indirectly estimated iF_i for 251 VOCs using net emission rates estimated by indoor-outdoor material balance. Although emission patterns varied between compounds, all VOC-specific iF_i estimates were clustered near the values of the living space tracer gases. These experimental observations substantiate the theoretical expectation that iF_i values are largely independent of analyte characteristics, a useful simplification for exposure assessments.

5.2 Introduction

Mitigation strategies for limiting adverse health effects of air pollution often focus on identifying the specific sources that contribute the most to exposures.[1, 2] One metric that can assist in such efforts is the intake fraction (iF), defined as a ratio: pollutant intake by a population (by inhalation, ingestion, or dermal absorption) normalized by total pollutant emissions from a given source or source category.[3] Intake fractions for air pollutants can vary by orders of magnitude.[4, 5] Typical intake fraction values for outdoor pollutant releases range from half of a ppm (i.e., 0.5 μg pollutant inhaled per g emitted) to a few hundred ppm.[4] Typical values for indoor pollutant releases are much larger, ranging from hundreds of ppm to a few percent (1% = 10,000 ppm). These high intake fractions for indoor releases mainly reflect the much lower rate of per-occupant pollutant removal by ventilation indoors as compared with the effective per-capita rate of pollutant transport by wind outdoors.[6]

Various forms of the intake fraction concept have been used in life cycle assessments (LCAs) to enable rapid evaluations of the magnitude of human exposure to pollutants in consumer and commercial products.[7–14] Indoor intake fractions have been estimated using material balance models.[5, 6, 14, 15] For volatile organic compounds (VOCs), these models indicate that intake fractions are principally controlled by air-change rates and by occupant behaviors.[5, 6] Empirical determinations of VOC intake fractions are scarce. One study of this type calculated intake fractions from surveys of air-change rates and activity pattern surveys[16] that assess time spent at home.[17] A critical untested conclusion of prior studies is that intake fractions of VOCs are independent of analyte temporal behavior, such as whether emissions are baseline dominated or spike dominated, and physical properties such as vapor pressure. While a few studies have utilized time-resolved experimental measurements to evaluate particulate matter intake fractions,[18–20] we were unable to identify any such experimental studies for VOC intake fractions in residences.

In this study, we report individual intake fractions (iF_i) via inhalation in two normally occupied residences in northern California as determined over three measurement campaigns. Intake fractions were assessed using chemical measurements from an online fast-response mass spectrometer, time-activity budgets from daily logs, and assumed standard breathing rates. To assess the importance of source location for non-reactive VOCs, we report iF_i for inert tracer gases that were released continuously at fixed rates in the living space, crawl space, and attic at each residence. To assess iF_i variability among diverse sources with different temporal behaviors and physical properties, we also report iF_i for 251 distinct VOCs sampled across three field campaigns using time-resolved emissions data derived by material balance. This study expands upon prior reports of speciated VOC emissions[21] (H1 only) and indoor exposures (H1 and H2).[22]

5.3 Materials and Methods

5.3.1 Site Description

The H1 and H2 monitoring campaigns have been extensively described;[21–24] a brief summary is provided here. Detailed measurements of airborne organic compounds and particulate matter were acquired at two normally occupied California residences in the East Bay region of the San Francisco Bay Area over three monitoring campaigns (H1 summer, H1 winter, H2 winter). The residences are single-family, wood-frame houses built in the late 1930s (H1) and early 1950s (H2) with approximately 180 m^2 of floor area each. The H1 site was a two-level residence, whereas the H2 site was a single-story house. The H1 and H2 residences were respectively occupied by two persons (adults designated H1M1 and H1F1) and four persons (two adults designated H2M1 and H2F1, a teenager, and an adult present only for a fraction of the campaign). During the campaigns, residents were encouraged to maintain their regular behavioral patterns with regard to indoor activities. Individual intake fractions were assessed for each of the two main adult occupants in each residence.

5.3.2 Study Design

This work focuses on VOC measurements acquired by a proton-transfer reaction time-of-flight mass spectrometer (PTR-ToF-MS)21-23 and daily occupant activity logs. At each residence, VOC concentrations were monitored at one outdoor and five indoor locations on a 5-minute rotating sample cycle yielding measurements at six locations once every 30 minutes. The five indoor locations were selected to characterize both the general living space (kitchen, bedroom hallway; living room for H2 only) as well as coupled unoccupied spaces (crawl space, attic; basement for H1 only). The H1 residence is constructed on two levels, with a kitchen, living room, and dining room situated toward the front (lower level) and a half flight of stairs connecting three bedrooms and two baths toward the back (upper level). The H1 basement is a single room beneath one bedroom. The remainder of the house has a crawl space beneath the floor. Both the H1 and H2 residences contain an attic above the main living space. The H1 and H2 floorplans with PTR-ToF-MS sampling locations have been reported previously.[22,23] Daily logs yielded basic time-activity information (‘awake’, ‘asleep’, ‘away’) with roughly 5-minute time resolution for each occupant.

Three non-reactive deuterated VOCs, propene-d6, propene-d3, and butene-d3 (“tracer gases”), were simultaneously released at fixed emission rates at different locations within the residences. The release of tracer gases served 1) to estimate time-resolved ventilation rates and indoor airflow patterns and 2) to simulate the release of continuous indoor sources in different indoor zones. Two tracer gas release schemes were used over the three monitoring campaigns. In the first scheme, the three tracer gases were emitted into the crawl space, the living space, and the attic at the H1 and H2 site to study air-change rates and interzonal flows throughout the entire residence. In the second scheme, the tracer gases were deployed in the crawl space, lower living space, and upper living space (H1) or the crawl space, kitchen

and living room (H2) to investigate interzonal transport and mixing within coupled living spaces.

5.3.3 Analysis and Calculations

In this work, we assess the individual intake fraction (iF_i), i.e. the ratio of pollutant mass inhaled by a single occupant to pollutant mass emitted. Inhalation masses were estimated using chemical measurements from an online fast-response mass spectrometer (30-minute time resolution), time-activity budgets from daily logs (5-minute time resolution), and age-bracket-specific standard breathing rates taken from the United States Environmental Protection Agency Exposure Factors Handbook.[26]

Emitted masses were determined using both direct and indirect experimental designs. First, we use the known emission rates of tracer gases as "direct estimates." These can be interpreted as surrogates for general inert emission sources released at constant rates in the living space, crawl space, and attic of the respective residences. Based on the direct estimate approach, we report iF_i estimates with daily time resolution in this study. Second, we use a material balance model21 to determine net indoor VOC emissions for 251 compounds with different temporal behavior and physical properties at 2-hour time resolution as "indirect estimates." A representative subset of compounds spanning orders-of-magnitude in vapor pressure is reported in Table 5.7.1. We report campaign-average iF_i values in this study design. A limitation of both study designs is that concentrations were measured in stationary locations as opposed to human breathing zones. As such, proximity effects, especially during occupant activities such as cooking, may produce actual individual intake fractions that are underestimated for some compounds.25 The magnitude of the proximity effect is expected to be unimportant for continuously released sources due to efficient mixing in the residence living space.23 A detailed description of our approach is reported in the supporting information.

5.4 Results and Discussion

We report iF_i values for the H1 summer, H1 winter, and H2 winter monitoring campaigns (Figs. 5.4.1, 5.7.1, 5.7.2). For each campaign, we report direct estimates of iF_i for tracer gases that were released at fixed rates in the living space, crawl space, or attic of the studied residences (Table 5.4.1). These values represent direct iF_i estimates for continuously released sources and can be interpreted as proxies for a generic source release in those locations. We also estimated indoor emission rates for the 251 unique VOCs observed over the three monitoring campaigns. Using these emissions data, we report campaign-averaged indirect iF_i estimates for all 251 VOCs (Figure 5.4.2).

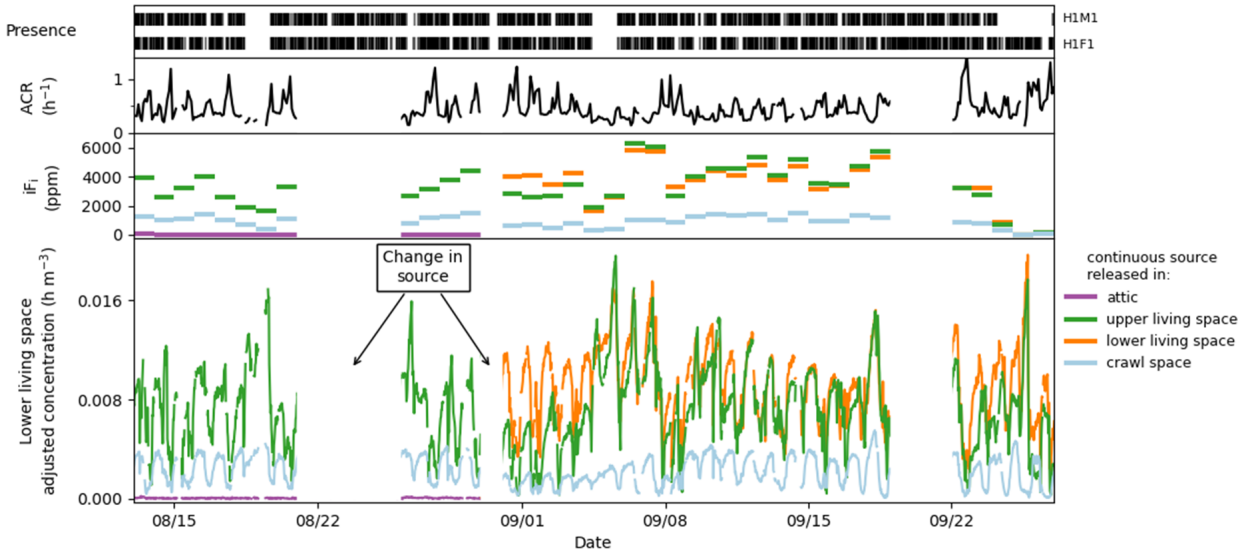

Figure 5.4.1: Time series of experimental data from study site H1 during the summer monitoring campaign. Times when occupants are present at the residence are marked in black in the uppermost panel. Time-resolved air-change rates are shown for the living space in the second panel. Daily individual intake fraction (iF_i) values for the continuously released tracer gas sources are shown for the H1M1 occupant in the third panel. The adjusted living room concentration (raw concentration [$\mu g\ m^{-3}$] divided by the mass release rate [$\mu g\ h^{-1}$]) of the continuously released tracer gas sources is shown in the bottommost source panel. Data proximate with changes to the tracer gas sources (location or release rate) are excluded.

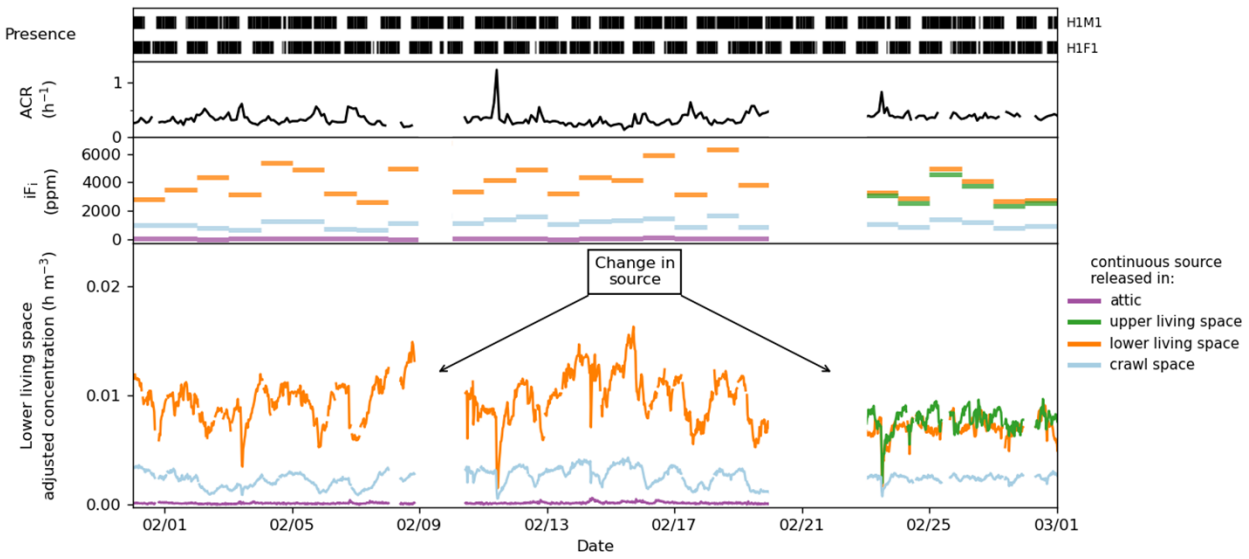

Figure 5.4.2: Mean individual intake fraction (iF_i) values for all observed VOCs during the H1 summer (217 compounds), H1 winter (170 compounds), and H2 winter (205 compounds) measurement campaigns are summarized in violin plots for two occupants in each house (H1M1, H1F1, H2M1, H2F1). The expected value as determined experimentally by continuous tracer-release is shown in red. Values corresponding to $C_7H_4ClF_2$, a compound of predominantly outdoor origin, are not shown.

Table 5.4.1: Summary statistics (mean ± standard deviation) of daily individual intake fractions (iF_i) for tracer gases released in different locations during the H1 summer, H1 winter, and H2 winter campaigns.[a]

	H1 summer			**H1 winter**			**H2 winter**		
Source released in:	**sample size (days)**	**H1M1 iF_i (ppm)**	**H1F1 iF_i (ppm)**	**sample size (days)**	**H1M1 iF_i (ppm)**	**H1F1 iF_i (ppm)**	**sample size (days)**	**H2M1 iF_i (ppm)**	**H2F1 iF_i (ppm)**
crawl space	$n = 36$	900 (± 400)	800 (± 200)	$n = 25$	1100 (± 300)	900 (± 200)	$n = 27$	1300 (± 400)	900 (± 300)
living space[b]	$n = 24$	3500 (± 1500)	3100 (± 900)	$n = 25$	3900 (± 1100)	3200 (± 800)	$n = 27$	2400 (± 800)	1700 (± 700)
upper living space	$n = 36$	3300 (± 1500)	2800 (± 900)	$n = 6$	3400 (± 900)	3000 (± 500)	-	-	-
attic	N/A [c]	<30	<30	N/A [c]	< 80	< 70	N/A [c]	< 70	< 60

[a] The number of daily determinations for each category is n.

[b] The "living space" refers to the "lower living space" at the two-level H1 residence and the "general living space" at the single story H2 residence.

[c] An upper bound campaign-average iF_i value is reported in place of summary statistics for daily iF_i values.

5.4.1 Direct Individual Intake Fraction Estimates via Controlled Emissions

Concentration time series of tracer sources, daily iF_i values, and time-resolved air-change rates are shown in Figure 5.4.1 for the H1M1 occupant during the H1 summer campaign. Similar data are shown for the H1 winter and H2 winter seasons in the SI (Figs. 5.7.1, 5.7.2). Changes in the concentration time series of the inert tracer gases are primarily associated with ventilation patterns, which are influenced by interzonal flows and the living zone air-change rate. The air-change rate is influenced by the extent to which doors and windows are open, indoor-outdoor temperature differences, and outdoor wind speed.[23] In the summer, a diurnal pattern is observed with enhanced ventilation during daytime periods leading to decreased tracer concentration. During summer nights periods, indoor/outdoor temperature differences are smaller, and doors and windows are more commonly closed, leading to enhanced tracer concentrations. The increase in iF_i from enhanced nighttime tracer concentrations is partially mitigated during sleeping hours owing to lower occupant breathing rates. Considering time varying ventilation rates and the occupants' time-activity patterns, daily iF_i for the living space and crawl space tracer releases spanned factors of 7 and 6 in range, respectively.

In total, iF_i for living space sources were largely independent of source location, season, and occupant behavioral patterns. We highlight that iF_i for two sources released on different levels of the two-level H1 residence were statistically indistinguishable due to high rates of internal mixing (Table 5.4.1). This finding suggests that source location within the general living space is not a key determinant for occupant exposures at the H1 site, where all interior doors were intentionally left open during the monitoring campaigns. Similarly, we note that iF_i values were comparable between occupants at the H1 site and occupants at the H2 site. Male iF_i values were slightly larger than female iF_i values, primarily due to larger assumed inhalation rates. Male iF_i values are statistically indistinguishable from female iF_i values when identical inhalation rates are assumed. We stress that these results were obtained at only two sites with four occupants. If generalizable to the broader population, these findings suggest that temporal differences in occupant behavior may not be key determinants of iF_i values. Estimated iF_i values for the two living space sources were slightly higher in the H1 winter season than in the H1 summer season, largely due to lower air-change rates during the winter period.[23] Estimated iF_i of living space sources for the H2 winter season were slightly lower than those observed at the H1 summer and H1 winter seasons. While mean ventilation rates were comparable between the two sites (H1 summer = 160 $m^3\ h^{-1}$, H1 winter = 120 $m^3\ h^{-1}$, H2 winter = 170 $m^3\ h^{-1}$), ventilation rates during periods of occupancy were higher during the H2 winter campaign, leading to the discrepancy.

Emissions into the general living space were considerably more impactful for occupant exposures than emissions in hidden coupled spaces. At the H1 and H2 sites, sources released in living spaces (iF_i = 1700–3900 ppm) reached human receptors at average rates 2–4 times higher than crawl space sources (700–1300 ppm) and >40 times higher than attic sources (iF_i < ∼70 ppm, season dependent). The attic tracer was often near or below the limit

of detection (defined as 3.3 sigma of blank measurements). During calculations of iF_i, we replaced non-detect measurements with the limit of detection value; attic iF_i values therefore represent an upper bound estimate. Although the air-change rate during occupancy was higher at the H2 site than at the H1 site, the H2 crawl space source entered the living space at higher efficiency leading to a minor increase in iF_i for crawl-space emissions at H2 as compared to H1.

To contextualize iF_i values reported in this work, we note that the time-averaged population intake fraction for distributed ground-level outdoor pollutant releases in the San Francisco Bay Area is estimated to be 38 parts per million.[4] That value, which accounts for inhalation intake of non-reactive airborne pollutants by the entire urban population, is roughly 100 times smaller than iF_i values reported in this work for inhalation intake by individuals for pollutant releases within the normally occupied space of their residences. As theoretically anticipated,[1, 2] indoor pollutant releases contribute much more to exposures than do outdoor pollutant releases per unit mass emitted.

We also highlight that first-order approximations are comparable to the time-resolved estimates provided in this work.[5] Using mean ventilation rates for the H1 summer (160 m^3 h^{-1}), H1 winter (120 m^3 h^{-1}), and H2 winter (170 m^3 h^{-1}) campaigns, age-specific daily breathing rates of 14.2 m^3 d^{-1} (H1) and 15.7 m^3 d^{-1} (H2),[26] and a population average of 69% time spent in a residence,[16] the first-order estimate of iF_i values at the three residences would be 2600 ppm, 3400 ppm, and 2700 ppm, respectively. These estimates based on theoretical expectations are within 30% of the direct experimental estimates determined from controlled tracer release. We note that the mean ventilation rates for this analysis were derived via material balance of the same time-resolved tracer gas concentrations as the "direct estimate" approach. Therefore, the resemblance between the time-resolved "direct estimate" approach and the time-averaged "first-order approximation" approach is partially attributable to methodological overlap.

5.4.2 Indirect Individual Intake Fraction Estimates for VOCs

Time-resolved indoor emission rates were evaluated by material balance for 251 distinct VOCs observed in the H1 summer, H1 winter, and H2 winter campaigns. These VOCs originated from diverse source processes, including continuous emissions from the building and its contents, episodic emissions from occupants and their activities such as cooking, cleaning, use of personal care products,21 and indoor chemistry,[27] resulting in substantial variability in mean concentration, temporal variability, and analyte physical properties. The emissions data were used to estimate the iF_i values as summarized graphically in Figure 5.4.2. The iF_i values tended to cluster and were comparable to values more directly estimated by tracer release.

A key assumption in some exposure assessment methods is that intake fraction values are largely analyte independent, as theory predicts.[5] Assuming that this assumption is correct, exposures in microenvironments with known emission patterns can be estimated using compound-independent intake-fraction values. In congruence with theoretical expec-

tations, our results provide direct empirical evidence that the temporal behavior of a source (as for instance, a continuously released emission from the building or an episodically released emission from an occupant activity) does not strongly affect iF_i for a broad suite of mainly organic compounds measured by PTR-ToF-MS (Figure 5.7.3). Limitations of this work include that it did not conduct personal monitoring or consider the influence of variable occupant breathing rates beyond a binary awake/asleep distinction. The approach used in this work would also underestimate emissions for strongly sorbing compounds or for compounds that undergo chemical degradation at fast time scales in the indirect experimental design, resulting in an overestimate of the respective iF_i value. These latter influences are expected to be minor. Another important consideration is the small sample size — only two households and four occupants were considered in this study. Additional work is needed to demonstrate applicability of the results to larger populations.

This study reports individual intake fraction (iF_i) values in two normally occupied residences via time-resolved VOC measurements. We find that iF_i values for VOC sources within the living space were consistent with past estimates and largely independent of source location, occupant behavioral patterns, and season. However, iF_i values for sources in the crawl space and especially for sources in the attic were smaller. Ultimately, this work corroborates theoretical expectations that indoor inhalation intake fractions are principally influenced by the ventilation patterns and generally independent of analyte characteristics.

5.5 Acknowledgements

The H1 and H2 occupants gave informed consent for this study, which was conducted under a protocol approved in advance by the Committee for Protection of Human Subjects for the University of California, Berkeley (Protocol #2016 04 8656). The authors thank the H1 and H2 occupants for cooperation in allowing their homes to be studied and in maintaining daily log sheets of occupancy and activities. We thank Robin Weber for technical assistance. This work was supported by the Alfred P. Sloan Foundation Program on Chemistry of Indoor Environments via Grants 2016-7050 and 2019-11412. D. L. acknowledges support from the National Science Foundation (Grant No. DGE 1752814). K. K. acknowledges support from the Carlsberg Foundation (Grant No. CF16-0624). The authors declare no competing financial interests.

5.6 References

[1] Evans, J. S.; Wolff, S. K.; Phonboon, K.; Levy, J. I.; Smith, K. R. Exposure efficiency: an idea whose time has come? Chemosphere 2002, 49, 1075–1091.

[2] Smith, K. R. Fuel Combustion, Air Pollution Exposure, and Health: The Situation in Developing Countries. *Annu. Rev. Energy Environ.* **1993**, *18*, 529–566.

[3] Bennett, D. H.; McKone, T. E.; Evans, J. S.; Nazaroff, W. W.; Margni, M. D.; Jolliet, O.; Smith, K. R. Defining Intake Fraction. *Environ. Sci. Technol.* **2002**, *36*, 206A–211A.

[4] Apte, J. S.; Bombrun, E.; Marshall, J. D.; Nazaroff, W. W. Global Intraurban Intake Fractions for Primary Air Pollutants from Vehicles and Other Distributed Sources. *Environ. Sci. Technol.* **2012**, *46*, 3415–3423.

[5] Nazaroff, W. W. Inhalation intake fraction of pollutants from episodic indoor emissions. *Build. Environ.* **2008**, *43*, 269–277.

[6] Lai, A. C. K.; Thatcher, T. L.; Nazaroff, W. W. Inhalation Transfer Factors for Air Pollution Health Risk Assessment. *J. Air Waste Manage. Assoc.* **2000**, *50*, 1688–1699.

[7] Hellweg, S.; Demou, E.; Bruzzi, R.; Meijer, A.; Rosenbaum, R. K.; Huijbregts, M. A. J.; McKone, T. E. Integrating Human Indoor Air Pollutant Exposure within Life Cycle Impact Assessment. *Environ. Sci. Technol.* **2009**, *43*, 1670–1679.

[8] Hodas, N.; Loh, M.; Shin, H.-M.; Li, D.; Bennett, D.; McKone, T. E.; Jolliet, O.; Weschler, C. J.; Jantunen, M.; Lioy, P.; Fantke, P. Indoor inhalation intake fractions of fine particulate matter: review of influencing factors. *Indoor Air* **2016**, *26*, 836–856.

[9] Huang, L.; Ernstoff, A.; Fantke, P.; Csiszar, S. A.; Jolliet, O. A review of models for near-field exposure pathways of chemicals in consumer products. *Sci. Total Environ.* **2017**, *574*, 1182–1208.

[10] Jolliet, O.; Ernstoff, A. S.; Csiszar, S. A.; Fantke, P. Defining Product Intake Fraction to Quantify and Compare Exposure to Consumer Products. *Environ. Sci. Technol.* **2015**, *49*, 8924–8931.

[11] Li, L.; Westgate, J. N.; Hughes, L.; Zhang, X.; Givehchi, B.; Toose, L.; Armitage, J. M.; Wania, F.; Egeghy, P.; Arnot, J. A. A Model for Risk-Based Screening and Prioritization of Human Exposure to Chemicals from Near-Field Sources. *Environ. Sci. Technol.* **2018**, *52*, 14235–14244.

[12] Ring, C. L.; Arnot, J. A.; Bennett, D. H.; Egeghy, P. P.; Fantke, P.; Huang, L.; Isaacs, K. K.; Jolliet, O.; Phillips, K. A.; Price, P. S.; Shin, H.-M.; Westgate, J. N.; Setzer, R. W.; Wambaugh, J. F. Consensus Modeling of Median Chemical Intake for the U.S. Population Based on Predictions of Exposure Pathways. *Environ. Sci. Technol.* **2019**, *53*, 719–732.

[13] Rosenbaum, R. K.; Meijer, A.; Demou, E.; Hellweg, S.; Jolliet, O.; Lam, N. L.; Margni, M.; McKone, T. E. Indoor Air Pollutant Exposure for Life Cycle Assessment: Regional Health Impact Factors for Households. *Environ. Sci. Technol.* **2015**, *49*, 12823–12831.

[14] Wenger, Y.; Li, D.; Jolliet, O. Indoor intake fraction considering surface sorption of air organic compounds for life cycle assessment. *Int. J. Life Cycle Assess.* **2012**, *17*, 919–931.

[15] Shin, H.-M.; McKone, T. E.; Bennett, D. H. Intake Fraction for the Indoor Environment: A Tool for Prioritizing Indoor Chemical Sources. *Environ. Sci. Technol.* **2012**, *46*, 10063–10072.

[16] Klepeis, N. E.; Nelson, W. C.; Ott, W. R.; Robinson, J. P.; Tsang, A. M.; Switzer, P.; Behar, J. V.; Hern, S. C.; Engelmann, W. H. The National Human Activity Pattern Survey (NHAPS): a resource for assessing exposure to environmental pollutants. *J. Exposure Anal. Environ. Epidemiol.* **2001**, *11*, 231– 252.

[17] Ilacqua, V.; Hänninen, O.; Kuenzli, N.; Jantunen, M. F. Intake fraction distributions for indoor VOC sources in five European cities. *Indoor Air* **2007**, *17*, 372–383.

[18] Cao, C.; Gao, J.; Wu, L.; Ding, X.; Zhang, X. Ventilation improvement for reducing individual exposure to cooking-generated particles in Chinese residential kitchen. *Indoor Built Environ.* **2017**, *26*, 226–237.

[19] Gao, J.; Cao, C.; Xiao, Q.; Xu, B.; Zhou, X.; Zhang, X. Determination of dynamic intake fraction of cooking-generated particles in the kitchen. *Build. Environ.* **2013**, *65*, 146–153.

[20] Gao, J.; Jian, Y.; Cao, C.; Chen, L.; Zhang, X. Indoor emission, dispersion and exposure of total particle-bound polycyclic aromatic hydrocarbons during cooking. *Atmos. Environ.* **2015**, *120*, 191–199.

[21] Liu, Y.; Misztal, P. K.; Xiong, J.; Tian, Y.; Arata, C.; Weber, R. J.; Nazaroff, W. W.; Goldstein, A. H. Characterizing sources and emissions of volatile organic compounds in a northern California residence using space- and time-resolved measurements. *Indoor Air* **2019**, *29*, 630–644.

[22] Lunderberg, D. M.; Misztal, P. K.; Liu, Y.; Arata, C.; Tian, Y.; Kristensen, K.; Weber, R. J.; Nazaroff, W. W.; Goldstein, A. H. High-resolution exposure assessment for volatile organic compounds in two California residences. Manuscript submitted.

[23] Liu, Y.; Misztal, P. K.; Xiong, J.; Tian, Y.; Arata, C.; Nazaroff, W. W.; Goldstein, A. H. Detailed investigation of ventilation rates and airflow patterns in a northern California residence. *Indoor Air* **2018**, *28*, 572–584.

[24] Kristensen, K.; Lunderberg, D. M.; Liu, Y.; Misztal, P. K.; Tian, Y.; Arata, C.; Nazaroff, W. W.; Goldstein, A. H. Sources and dynamics of semivolatile organic compounds in a single-family residence in northern California. *Indoor Air* **2019**, *29*, 645–655.

[25] McBride, S. J.; Ferro, A. R.; Ott, W. R.; Switzer, P.; Hildemann, L. M. Investigations of the proximity effect for pollutants in the indoor environment. *J. Expo. Anal. Environ. Epidemiol.* **1999**, *9*, 602–621.

[26] Chapter 6 – Inhalation Rates. Exposure Factors Handbook 2011 Edition (Final Report); EPA/600/R-090/052F; U.S. Environmental Protection Agency: Washington, DC, 2011.

[27] Liu, Y.; Misztal, P. K.; Arata, C.; Weschler, C. J.; Nazaroff, W. W.; Goldstein, A. H. Observing ozone chemistry in an occupied residence. *Proc. Natl. Acad. Sci. U. S. A.* **2021**, *118*, e2018140118.

5.7 Supporting Information

5.7.1 Calculation of Individual Intake Fractions

The individual intake fraction is the ratio of pollutant mass inhaled (M_{inh}) to the pollutant mass emitted (M_{emit}) for an individual occupant (Eq. 5.1.

$$\text{iF}_\text{i} = \frac{M_{\text{inh}}}{M_{\text{emit}}} \tag{5.1}$$

We define the function $P(t)$ to account for the time when the occupant is present within the indoor space.

$$P(t) = \begin{cases} 1 & \text{if occupant present at time } t \\ 0 & \text{otherwise} \end{cases} \tag{5.2}$$

Then, M_{inh} can be estimated as the integral of the airborne pollutant concentration ($C(t)$), the occupant breathing rate ($QB(t)$), and $P(t)$. For continuous pollutant releases, M_{emit} can be estimated as the integral of the emission rate $E(t)$ over some time interval of duration T.[1] Substitution of both expressions into Equation 5.1 yields Equation 5.2.

$$\text{iF}_\text{i} = \frac{\int_0^T C(T) \times Q_B(T) \times P(t)dt}{\int_0^T E(t)dt} \tag{5.3}$$

For continuously released tracer gases with fixed emission rates, we calculated iF_i on each calendar day from midnight to midnight (T = 24 h). An unavoidable uncertainty in this approach is that pollutants emitted during the final hours of each calendar day could be inhaled during the first few hours of the following day. The general consistency of conditions at midnight (since, for example, occupants tended to be sleeping) limits the error caused by this estimation detail. Also, the living space air-change rate during the three monitoring campaigns typically varied in the range 0.3–0.5 h^{-1}, with corresponding residence times of 2–3 hours. Because T = 24 h is much larger than the pollutant residence time and because airborne pollutant concentrations were moderately stable, especially when the occupants were inactive, the associated errors are expected to be small ($< 10\%$). For observed VOCs with estimated net emission rates, we calculated iF_i over the full monitoring period (T = duration of campaign).

True experimental determinations of M_{inh} would require airborne concentrations to be measured directly in the breathing zone of the occupant. That approach isn't compatible with PTR-based sampling in an observational study. In this work, we used the living space sampling location ("kitchen" at H1, "living room" at H2) during occupant waking hours and the stationary bedroom hallway sampling location during occupant sleeping hours as proxies for measurements of breathing zone concentrations. Occupant time budgets were determined using daily logs, with time resolution of approximately 5 minutes. Due to proximity effects, we expect moderate biases for strong episodic sources, such as those originating from cooking.[2] However, we expect any such biases to be minor for continuous indoor sources

based on the similarity of measurements of tracer gases released in different locations of the occupied space.[3] During the H1 campaigns, the bedroom doors were always left open such that the bedroom hallway measurement was an appropriate proxy of breathing zone concentrations during sleeping periods. However, during the H2 winter campaign, bedroom doors were closed during sleeping hours, which created a partially decoupled space. Therefore, there may be some uncharacterized biases in the H2 "direct estimate" results when using the bedroom hallway concentrations as a proxy for nighttime breathing zone concentrations. For the "indirect estimate" approach at H2, we use only the living room sampling location to estimate breathing zone concentrations due to small data gaps in the bedroom hallway sampling location. Concentration measurements in the bedroom hallway and living room were largely comparable during periods of co-measurement. In all cases, we use adjusted indoor concentrations (indoor concentration minus outdoor concentration) when calculating inhaled masses to avoid incorporating the influence of outdoor sources. For most VOCs, the indoor concentrations were markedly higher than those outdoors, so correcting for outdoor air contributions does not introduce much uncertainty.

We used two separate approaches to determine the emission rate $E(t)$. First, in the "direct estimate" study design, the emission rate is known as the experimentally controlled tracer release rate. Second, in the "indirect estimate" study design, we used VOC-specific emission rates that were previously reported at two-hour time resolution for the H1 site[4] and calculated in this work for H2 using the same procedure. To briefly summarize this method, tracer gases were used to estimate time-resolved air-change rates in the living space.[3] Then, after assuming non-reacting physicochemical behavior and well-mixed conditions, time-resolved estimates of net VOC emissions were prepared at 2–hour time resolution.[4] These net VOC emission rates were interpolated to the same 5-minute time resolution as occupant presence data to calculate campaign-average iF_i values. Time periods when air-change rates could not be reported or when researchers influenced indoor air concentrations were not considered in the analysis.

The material balance approach only accounts for loss from indoor air by means of ventilation. For most VOCs, loss rates by other mechanisms are expected to be small when compared to loss rates from indoor-to-outdoor transport. If any loss process beyond ventilation occurred, such as pollutant removal by a range hood during cooking, chemical degradation, or sorption to surfaces, the net emission rate as calculated by the "indirect estimate" approach will be underestimated. In turn, this would lead to overestimates of iF_i. While pollutant removal by a range hood is an effective source-control measure that reduces exposures, both chemical degradation and surface sorption may interfere with interpretation of iF_i as health-relevant byproducts are created and surfaced-sorbed pollutants can be re-emitted in later periods. Net deposition to surfaces was sometimes observed during large concentration spikes. We assumed that deposited VOCs would be re-emitted in the near future. Therefore, only positive net emission rates were considered during calculation of intake fractions to avoid double counting. The assumption was rarely impactful. In the absence of loss processes, we expect the largest uncertainties to originate from determination of the house volume and estimation of variable occupant breathing rates using standard reported

values in place of real values. The volume of each residence was estimated by direct measurement of room dimensions with subtractions for occluded spaces (cabinets, closets) and major furniture. Because the volume of occluding objects is small relative to the house volume, we estimate that volume uncertainties are no greater than 10% at H1. Uncertainties in the effective (well-mixed interior) house volume are larger at H2 due to variable door positions.

For both experimental designs, we estimate occupant breathing rates for principal occupants using values from the USEPA Exposure Factors Handbook.[5] At conclusion of the study, occupants H1M1 and H1F1 were in the 61–70 years age bracket, while occupants H2M1 and H2F1 were in the 51–60 years age bracket. Accordingly, we assumed inhalation rates of 0.35, 0.26, 0.33, and 0.26 $m^3\ h^{-1}$ for the four respective occupants during sleeping hours. We assumed that waking hours corresponded to light-intensity activity levels. Accordingly, we assumed inhalation rates of 0.83, 0.71, 0.86, and 0.70 $m^3\ h^{-1}$, respectively.

5.7.2 Figures and Tables

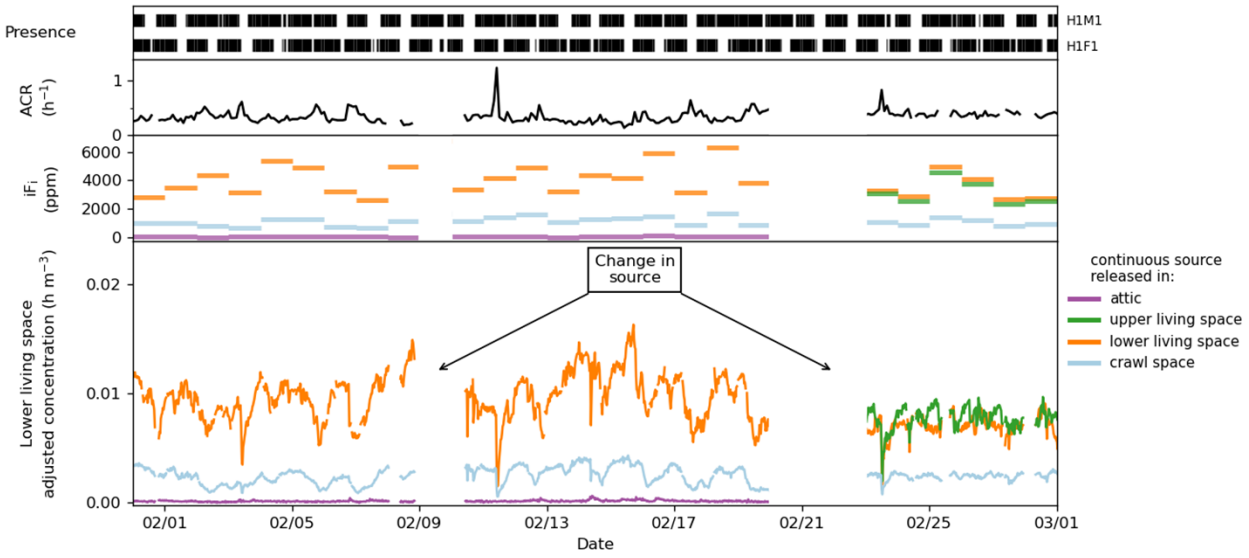

Figure 5.7.1: Time series of experimental data from study site H1 during the winter monitoring campaign. Times when occupants are present at the residence are marked in black in the uppermost panel. Time-resolved air-change rates are shown for the living space in the second panel. Daily iF_i values for the continuously released tracer gas sources are shown for the H1M1 occupant in the third panel. The adjusted living room concentration (raw concentration [$\mu g\ m^{-3}$] divided by the mass release rate [$\mu g\ h^{-1}$) of the continuously released tracer gas sources is shown in the bottommost source panel. Data coincident with changes to the tracer gas sources (location or release rate) are not shown.

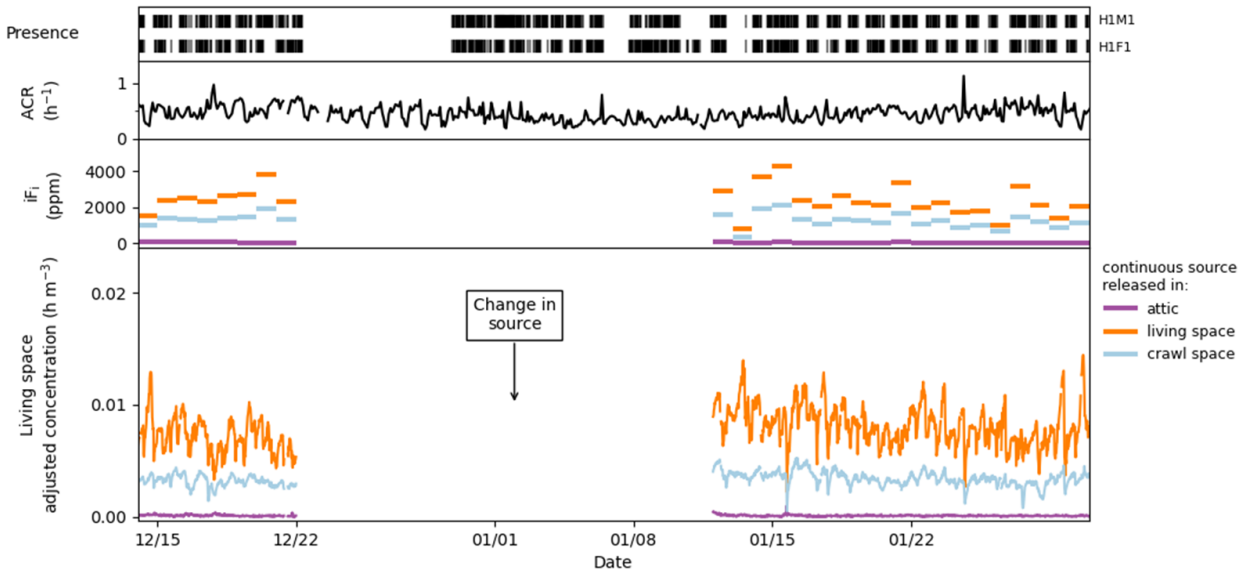

Figure 5.7.2: Time series of experimental data from study site H2 during the winter monitoring campaign. Times when occupants are present at the residence are marked in black in the uppermost panel. Time-resolved air-change rates are shown for the living space in the second panel. Daily iF_i values for the continuously released tracer gas sources are shown for the H2M1 occupant in the third panel. The adjusted living room concentration (raw concentration [μg m^{-3}] divided by the mass release rate [μg h^{-1}]) of the continuously released tracer gas sources is shown in the bottommost source panel. Data coincident with changes to the tracer gas sources (location or release rate) are not shown. Data from an additional multiweek period where indoor measurements were made only in the kitchen are not shown.

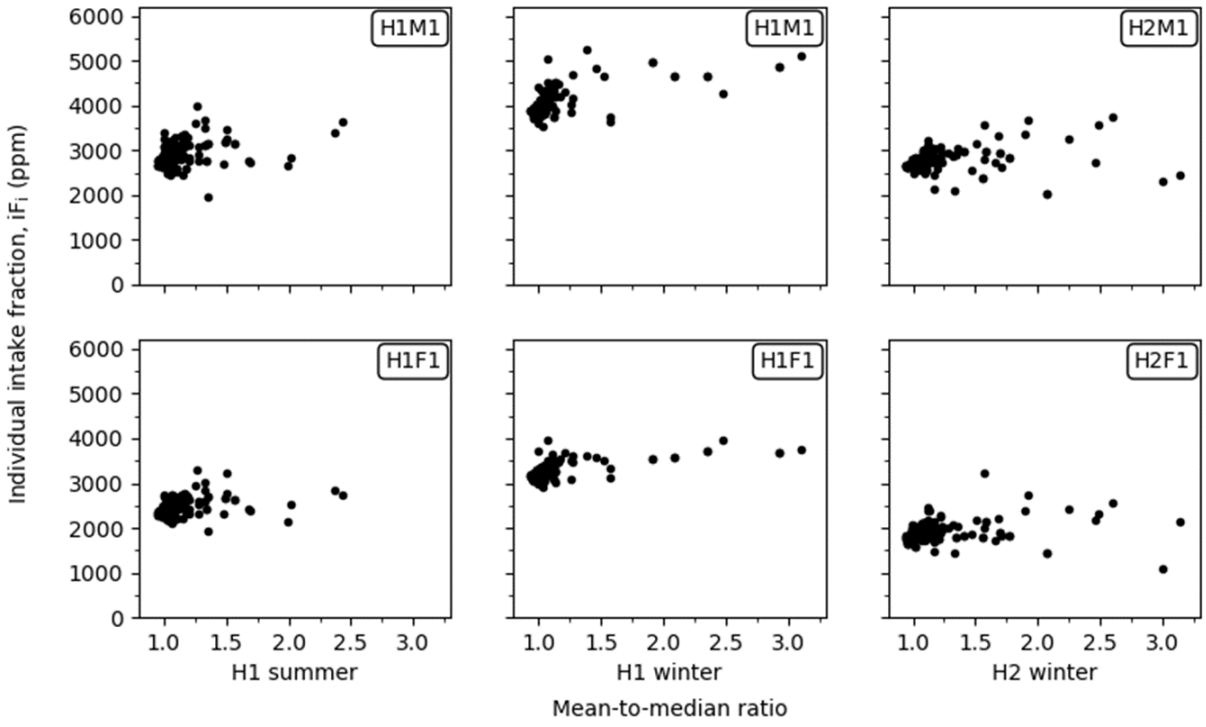

Figure 5.7.3: Mean iF_i values for all major VOCs observed during the H1 summer, H1 winter, and H2 winter campaigns are compared against the mean-to-median ratio of each VOC's concentration time series, a proxy for episodic emissions. Both the H1 summer and H1 winter campaigns have excluded a non-impactful x-axis outlier. Data in temporal proximity to changes in VOC source behavior (change in source location or source release rate) are not shown.

Table 5.7.1: Physicochemical properties (T = 298 K) and individual intake fractions (iF_i) of selected compounds.[a]

					H1 summer			H1 winter			H2 winter		
Class	**Ion**	**Name**	**log Koa**	**log P (atm)**	**MMR**	**H1M1**	**H1F1**	**MMR**	**H1M1**	**H1F1**	**MMR**	**H2M1**	**H2F1**
						iF_i (ppm)	**iF_i (ppm)**		**iF_i (ppm)**	**iF_i (ppm)**		**iF_i (ppm)**	**iF_i (ppm)**
alcohol	CH_5O^+	methanol	2.88	-0.78	1.02	2990	2520	1.06	4170	3390	1.24	2940	2050
alcohol	$C_2H_7O^+$	ethanol	3.25	-1.11	2.37	3410	2850	2.47	4280	3950	3.39	3610	1840
aromatic	$C_6H_7^+$	benzene	2.78	-0.9	1.06	2840	2450	1.06	4290	3340	1.1	2870	2060
aromatic	$C_8H_{11}^+$	xylene + ethyl benzene[b]	3.79	-1.94	1.08	2790	2430	1.08	4130	3220	1.08	2780	1960
aromatic	$C_6H_7O^+$	phenol	6.33[d]	-3.34	1.01	2830	2440	1.03	4130	3300	1.02	2730	1960
aromatic	$C_4H_6N^+$	pyrrole	3.88[d]	-1.96	2.43	3640	2750	1.39	5260	3610	1.91	3660	2750
carbonyl	$C_2H_5O^+$	acetaldehyde	2.22[d]	0.07	1.28	3080	2610	1.26	4020	3500	2.48	3570	2300
carbonyl	$C_3H_5O^+$	acrolein	2.29[d]	-0.44	1.08	2880	2470	1.05	4080	3320	1.12	2750	1940
carbonyl	$C_6H_{13}O^+$	hexanal + isomers	4.41	-1.83	1.03	2930	2500	1.05	4070	3320	1.04	2900	2030
carboxylic acid	$C_2H_5O_2^+$	acetic acid + isomers	4.31	-1.68	1.01	2890	2450	1.02	4040	3240	1.04	2650	1850
carboxylic acid	$C_3H_5O_2^+$	acrylic acid	5.17[d]	-2.28	1.11	2850	2420	1.07	4060	3330	1.11	2870	2030
carboxylic acid	$C_8H_{17}O_2^+$	octanoic acid + isomers	7.52[d]	-5.31	1.03	2650	2310	1	3700	3040	1.03	2670	1890
furanoid	$C_5H_5O_2^+$	furfural	4.22[d]	-2.54	1	2950	2480	1.06	4100	3270	1.04	2710	1980
halogen	CCl_3^+	chloroform	2.8	-0.59	1	3380	2730	0.99	4410	3720	1	2760	1910
nitrile	$C_2H_4N^+$	acetonitrile	2.31	-0.93	1.07	3230	2750	1.12	4430	3490	1.07	2610	1770
organosulfurs	CH_5S^+	methanethiol	6.08[d]	0.3	1.17	3200	2710	1.17	4200	3530	2.6	3750	2560
siloxane	$C_8H_{25}O_4Si_4^+$	D4 siloxane	3.98[d]	-2.86	1.09	3000	2440	1.09	4120	3220	1.17	2120	1470
siloxane	$C_{12}H_{37}O_6Si_6^+$	D6 siloxane	5.86[d]	-4.65	1.99	2650	2140	1.57	3750	3140	1.2	2710	1860
other	$C_5H_9^+$	isoprene	2.06	-0.14	1.06	3130	2600	1.06	4320	3410	1.08	2980	2120
other	$C_{10}H_{17}^+$	monoterpenes[c]	4.45[d]	-2.69	1.36	3150	2700	1.91	4950	3560	1.58	2960	2130
					mean (± st. dev.)	3020 (± 260)	2540 (± 170)		4230 (± 350)	3400 (± 210)		2930 (± 400)	2020 (± 270)

[a] Octanol-air partition coefficients (Koa) and vapor pressures (P) acquired directly from PubChem unless otherwise stated. Last accessed on 25 March 2021.

[b] Physicochemical properties reported for the para-xylene isomer.

[c] Physicochemical properties reported for the limonene isomer.

[d] Direct reports of Koa not available from PubChem. Koa was calculated via octanol-water partition coefficients (Kow) and Henry's law constants (KH) available from PubChem, where $[\log(K\text{oa}) = \log(K\text{ow}) + \log(K\text{H} \times RT)]$.

5.7.3 Supporting Information References

[1] Nazaroff, W. W. Inhalation intake fraction of pollutants from episodic indoor emissions. *Build. Environ.* **2008**, *43*, 269–277.

[2] McBride, S. J.; Ferro, A. R.; Ott, W. R.; Switzer, P.; Hildemann, L. M. Investigations of the proximity effect for pollutants in the indoor environment. *J. Expo. Anal. Environ. Epidemiol.* **1999**, *9*, 602–621.

[3] Liu, Y.; Misztal, P. K.; Xiong, J.; Tian, Y.; Arata, C.; Nazaroff, W. W.; Goldstein, A. H. Detailed investigation of ventilation rates and airflow patterns in a northern California residence. *Indoor Air* **2018**, *28*, 572–584.

[4] Liu, Y.; Misztal, P. K.; Xiong, J.; Tian, Y.; Arata, C.; Weber, R. J.; Nazaroff, W. W.; Goldstein, A. H. Characterizing sources and emissions of volatile organic compounds in a northern California residence using space- and time-resolved measurements. *Indoor Air* **2019**, *29*, 630–644.

[5] Chapter 6 – Inhalation Rates. *Exposure Factors Handbook 2011 Edition (Final Report)*; EPA/600/R-090/052F; U.S. Environmental Protection Agency: Washington, DC, 2011.

Chapter 6

Conclusions

6.1 Summary

The first half of this dissertation reports some of the first high-time resolution measurements of SVOCs in indoor residences. Specific focus on airborne concentrations and gas-particle phase partitioning of phthalate diesters is given in Chapter 2. Concentrations of gaseous phthalates were modulated by temperature, while concentrations of diethyl hexyl phthalate (DEHP), a compound with variable gas-particle phase partitioning, was strongly linked to airborne particle mass concentration. It is inferred that airborne particles were indirectly stimulating emissions of DEHP by aiding mass transport from condensed-phase surface reservoirs to bulk air. Similarly, the gas-particle phase partitioning of DEHP was observed to be related to both particle mass concentration and temperature. Increases in particle mass concentration and decreases in temperature were associated with higher particle-phase fractions. While phthalate diesters are just one class of compounds of public-health interest among thousands of observed chemicals, the results are a useful case study and many findings will generalize to SVOCs with similar physicochemical properties, such as vapor pressure or octanol-air partitioning coefficients. Key findings specific to phthalates from Chapter 2 were generalized to other compounds and SVOC in total in Chapter 3. SVOC were aggregated into bins of similar volatility based on retention time. Predominantly gaseous SVOC with vapor pressures similar corresponding to the C13 – C23 alkanes were strongly linked with temperature. Observed temperature dependences were largely comparable to expectations from theoretical models. Similarly, predominantly particle-phase SVOC with vapor pressures corresponding to the C25 – C31 alkanes were strongly linked to particle mass concentration. Siloxanes released in a major emission event were also observed to deposit on surfaces before re-emission into bulk air during subsequent particle loading events.

The second half of this dissertation focuses on human exposure to VOCs. In Chapter 4, a high-resolution exposure assessment was conducted. The analysis used multi-month high-time resolution VOC measurements collected from three intensive monitoring campaigns to (a) conduct a source apportionment analysis, (b) conduct a risk-based prioritization analysis,

and (c) assess how well high-time resolution measurements correspond to simulated results from traditional exposure analyses. A key finding is the discovery that for >90% of observed VOCs, the predominant contributor to chronic exposures originated from the building and its static contents rather than outdoor-to-indoor infiltration or episodic activities such as cooking. While some compounds such as acrolein, acetaldehyde, and acrylic acid were observed to exceed health guideline values, it was noted that ∼90% of compounds did not have associated toxicity data for comparison and were unable to be analyzed. In Chapter 5, continuously released inert tracer gases were used to simulate static pollutants. By linking occupant activity logs with real-time concentration data, the first experimental estimates of intake fractions (ratio of mass inhaled versus mass emitted) were reported. Intake fractions for pollutants released in different levels of the living space were indistinguishable at the H1 residence, where interior living space doors were intentionally left open. Pollutants released in the crawlspace yielded intake fractions roughly 2–4 times smaller than that of living space, while pollutants released in the attic were >40 times smaller than living space sources. Intake fractions are generally assumed to be compound independent. The study also provided the first experimental evidence to verify this key assumption, but estimating emissions and thereby intake fractions for >200 VOCs observed within the residence.

6.2 Future work

This dissertation represents an advancement in the state of knowledge on organic chemicals in indoor air. Significant knowledge gaps remain. Several additional opportunities for further study are considered below.

1. Advances in offline analytical instrumentation provide significant opportunities for additional survey-based study designs. Existing survey studies often use a targeted-analysis approach where quantification is limited to pre-selected analytes of interest. Many of these compounds are selected on the basis of public-health interest. However, in outdoor atmospheric chemistry, two dimensional gas chromatography time-of-flight mass spectrometry has been able to resolve thousands of unique organic chemicals in non-targeted analyses. Similar studies in indoor air would prove highly informative. While it is important to study compounds of public-health interest, it is also important to understand the underlying principles that govern abundances of organic chemicals indoors. A cross-sectional analysis that quantifies thousands of chemicals in hundreds of residences and simultaneously provides information about polarity and volatility would be of immense value in studying these principles. Additionally, identifying associations between compounds found among residences may also yield new insights into surface-oxidation chemistry and gas-particle-surface phase partitioning.

2. While high-resolution exposure assessments were conducted for VOCs, similar analyses have yet to be conducted for SVOCs. SVOCs originate from a variety of sources, including static sources related to the building and its contents, episodic activities such

as cooking related to occupant behavior, and external sources related to outdoor-to-indoor ventilation. Similar to VOCs, our preliminary findings suggest that gaseous SVOC exposures are largely related to the building and its static contents. However, exposures to low-volatility SVOCs that are predominantly bound to particles are generally attributed to episodic emission events such as cooking. An absence of high-time resolution SVOC concentration data exists in the literature and further effort is needed to explore what factors influence airborne exposures to SVOCs.

3. The results from these studies focus on two normally occupied residences and one test house. Our findings, while informative, may not fully generalize to the larger building stock or to other occupants with different behavioral patterns. It will be important to continue conducting intensive studies of residences with fundamentally different parameters to determine how well these findings generalize to other locations. The residences characterized in this study were older single family wood-framed homes with no recent history of remodeling, refurnishing, or smoking. Identifying homes for study with different key parameters, for instance a multi-family apartment complex that has been recently remodeled, would be of high value.